600277074

WATER QUALITY MONITORING IN DISTRIBUTION SYSTEMS

by

Nina I. McClelland
National Sanitation Foundation
Ann Arbor, Michigan 48106

and

K. H. Mancy
The University of Michigan
Ann Arbor, Michigan 48109

Contract No. 68-03-0043

Project Officer

James M. Symons
Water Supply Research Division
Municipal Environmental Research Laboratory
Cincinnati, Ohio 45268

MUNICIPAL ENVIRONMENTAL RESEARCH LABORATORY
OFFICE OF RESEARCH AND DEVELOPMENT
U.S. ENVIRONMENTAL PROTECTION AGENCY
CINCINNATI, OHIO 45268

DISCLAIMER

This report has been reviewed by the Municipal Environmental Research Laboratory, U.S. Environmental Protection Agency, and approved for publication. Approval does not signify that the contents necessarily reflect the views and policies of the U.S. Environmental Protection Agency, nor does mention of trade names or commercial products constitute endorsement or recommendation for use.

FOREWORD

The Environmental Protection Agency was created because of increasing public and government concern about the dangers of pollution to the health and welfare of the American people. Noxious air, foul water, and spoiled land are tragic testimony to the deterioration of our natural environment. The complexity of that environment and the interplay between its components require a concentrated and integrated attack on the problem.

Research and development is that necessary first step in problem solution and it involves defining the problem, measuring its impact, and searching for solutions. The Municipal Environmental Research Laboratory develops new and improved technology and systems for the prevention, treatment, and management of wastewater and solid and hazardous waste pollutant discharges from municipal and community sources, for the preservation and treatment of public drinking water supplies, and to minimize the adverse economic, social, health, and aesthetic effects of pollution. This publication is one of the products of that research; a most vital communications link between the researcher and the user community.

Concern for protecting the public health by assuring the quality of public drinking water supplies is apparent with passage of the Safe Drinking Water Act (Public Law 93-523), signed by the President on December 16, 1974. This is the first federal act dealing in depth with providing safe drinking water for public use. Through this project, the feasibility of measuring levels of drinking water contaminants *at the consumer's tap* has been demonstrated. Subsequent use of the mobile water quality monitoring laboratory will permit EPA to assure compliance with many of the maximum levels for inorganic chemicals proposed as national interim primary drinking water standards (CFR Vol. 40, No. 51—Friday, March 14, 1975).

Francis T. Mayo, Director
Municipal Environmental Research
Laboratory

ABSTRACT

A mobile laboratory with 18 integrated, computer controlled parametric systems for monitoring potable water quality in distribution systems was developed and field evaluated at ten locations in four United States cities: Chicago, Illinois; Ann Arbor and Detroit, Michigan; and Philadelphia, Pennsylvania. Temperature, conductivity, pH, chloride, dissolved oxygen, free and total residual chlorine, turbidity, corrosion rate, free and total fluorides, alkalinity, hardness, nitrate, copper, cadmium, lead, and calcium carbonate deposition rate are measured using commercially available and newly developed sensor systems.

CONTENTS

		Page
Foreword		iii
Abstract		iv
List of Figures		vii
List of Tables		xi
Acknowledgments		xiii
Sections		
I	Conclusions	1
II	Recommendations	4
III	Introduction	5
	General	5
	Study Aims and Objectives	5
	Study Plan	6
IV	Prototype Monitor	8
	General	8
	Theory	8
	Performance Characteristics	8
	SRM-Housed Systems	14
	General	14
	Electronics	15
	Recorder	18
	Sensors	18
	Interpretation of Hardness and Nitrate Data	19
	Commercial Systems	24
	Free and Total Residual Chlorine	24
	General	24
	Theory	24
	Experimental	27
	Results and Discussion	31
	Turbidity	33
	General	33
	Experimental	33
	Corrosion Rate	33
	General	33
	Theory	36
	Experimental	39
	Results and Discussion	40

		Page
	Other Systems	41
	Calcium Carbonate Deposition Test	41
	General	41
	Theory	41
	Experimental	50
	Results and Discussion	54
	Field Experience	59
	Alkalinity	62
	General	62
	Theory	62
	Experimental	70
	Results and Discussion	72
	Special Case Study	75
	Free and Total Fluorides	75
	General	75
	Theory	76
	Experimental	77
	Results and Discussion	78
	Automated System	87
	Continuous Fluoride Monitor	106
	Field Studies	111
	Trace Metals	121
	General	121
	Theory	123
	Experimental	126
	Results and Discussion	130
	Special Study	130
V	Mobile Laboratory	140
	General	140
	Physical Description	140
	Instrumentation	141
	Organization	141
	Computer System	142
	Field Studies	149
VI	References	168
VII	Project Publications	172
VIII	Appendices	174

FIGURES

No.		Page
1	NSF/EPA Mobile Water Quality Monitoring Laboratory	7
2	Schematic Arrangement of Schneider Robot Monitor	14
3	Schematic Diagram of SRM Flow Cell Cubicle, Top View	16
4	Schematic Illustration of Sensor Positions and Overall Arrangement of SRM-Housed Systems	17
5	Typical Strip Chart Recorder Output of Hardness Data	21
6	Conductivity Correction Nomogram	23
7	Distribution of Hypochlorous Acid and Hypochlorite Ion in Water at Different pH Values and Temperatures (2)	26
8	Schematic Illustration of Residual Chlorine Analyzer	29
9	Schematic Illustration of Cl_2 Analyzer	30
10	Free and Total Residual Chlorine Variations at Gulf Oil, Philadelphia	32
11	Schematic Illustration of Turbidity System	34
12	Schematic Illustration of Turbidimeter in the Mobile Laboratory	35
13	Schematic Illustration of Corrosion Rate Monitor in the Mobile Laboratory	40
14	Fluid Flow in the Rotating Electrode System	45
15	Concentration Profile at Electrode Surface under Steady State Conditions, in the Absence of $CaCO_3$ Film	47
16	Oxygen Current - Time Curves during $CaCO_3$ Deposition	49
17	Stability Index Monitor for Saturation Equilibrium Measurement	51
18	PIR Rotator - Electrode System	53
19	CCDT System in the Mobile Laboratory	53
20	Current versus Potential Sweep	55
21	Calcium Carbonate Deposition Test	56
22	Correlation of CCDT Slope with Ryzner Stability Index	57

No.		Page
23	CCDT versus Ryzner Stability Index	61
24	Effect of Caustic Feeder Cycling at Chicago CWFP on CCDT and pH Monitored at Site No. 1, Chicago/ Lehigh	63
25	$[H^+]$ versus CO_3^{2-} formality, given applying Equation 98	67
26	Experimental and Theoretical Relationships between Alkalinity and pH	68
27	Schematic Illustration of Alkalinity Monitor in the Mobile Laboratory	71
28	Good Quality Recording of Continuous Alkalinity Analysis	73
29	Alkalinity Calibration Curve	74
30	Characterization of Fluorides and Preparation of Buffers	79
31	Effect of pH on Fluoride Ion-Selective Electrode Measurement	80
32	Calibration Curves of Different Levels of pH	82
33	Effect of pH on Fluoride Ion Electrode Sensitivity	85
34	Complexometric Titrations of Fluoride with Aluminum	86
35	Aluminum Complexing Effect and Fluoride Recovery by Different Masking Agents	89
36	Rate of Fluoride Recovery with CDTA Masking Agent	90
37	Rate of Fluoride Recovery with Citrate Masking Agent	91
38	Schematic of Automated Sample Analysis for Free and Total Fluoride	92
39	Effect of Pump Surges on Reference Electrode	95
40	Effect of Flow Rate versus Response Time	97
41	Recorder Output for Calibration of Free and Total Fluoride (5 minutes)	98
42	Recorder Output for Calibration of Free and Total Fluoride (2 minutes)	99
43	Recorder Output for Calibration of Free and Total Fluoride (1 minute)	100
44	Calibration Curves for Automated Fluoride Electrode Measurement	102
45	Reproducibility of Fluoride Measurement in Absence of Complexing Cations	104

No.		Page
46	Reproducibility of Fluoride Measurement (1.0 mg/l) in Presence of Aluminum	105
47	Schematic Illustration of Free and Total Fluorides Monitor in the Mobile Laboratory	110
48	Fluoride System Output including a Calibration Series	112
49	Typical Calibration Curves for Fluorides, Prepared from Output in Figure 48	113
50	Special Fluoride Study at Chicago/Lehigh Station	118
51	Map Identifying Relative Locations of Monitoring Sites in Chicago	119
52	Output from Chicago Fluoride Monitor, recorded at Chicago/Greenleaf	120
53	Special Fluoride Study at Calumet Harbor	122
54	Plate-Strip Sequence for Differential Anodic Stripping Voltammetry	125
55	Schematic Diagram of DASV Flow Cell used in Mobile Laboratory System	128
56	Schematic Illustration of Trace Metals Monitor in the Mobile Laboratory	129
57	Typical Voltammograms of a Standard Solution and Tap Water Analyses	131
58	Sweep Rate Response	132
59	Household Trace Metals Survey, Cadmium	134
60	Household Trace Metals Survey, Lead	135
61	Household Trace Metals Survey, Copper	136
62	Schematic Illustration of Right Side Interior of Mobile Laboratory	143
63	Schematic Illustration of Left Side Interior of Mobile Laboratory	144
64	Photograph Showing Overview of Mobile Laboratory Interior	145
65	Relationship of Computer System to Analytical Sensor Systems	147
66	Computer System Software Relationships	148
67	Flowchart of INIT	150
68	Flowchart of NSFC	151
69	Flowchart of PUN	153
70	Flowchart of BELL	154

No.		Page
71	Flowchart of SMPL	155
72	Flowchart of FLOW	156
73	Flowchart of DAQ	157
74	Flowchart of Subroutine A (DAQ)	158
75	Flowchart of DATA	159
76	Normal Data Flow	162
77	Data from Main Flushing at Chicago/Calumet Harbor	165
78	Relative Locations of Philadelphia Monitoring Sites	166
79	$[H^+]$ as a Function of CO_3^{2-} and Cl_2 Formality	185
80	Experimental and Theoretical Relationships between Alkalinity and Potentials	186
81	ΔE versus $[Cl_2]$ in Alkalinity Determination	187
82	Potential versus Alkalinity Calibration Series	191

TABLES

No.		Page
1	Sensors in the Prototype Monitor	9
2	Electrochemical Sensors for Water Quality Monitoring	10
3	Performance Characteristics of Mobile Laboratory Sensor Systems	12
4	Summary of Data from Analyses of Test Solutions	58
5	Results of Field Studies	60
6	$[H^+]$ versus Alkalinity, applying Equation 98	69
7	Experimental and Theoretical Relationships between Alkalinity and pH	70
8	OH^- Selectivity Coefficients (K)	81
9	Shift in Intercept of Calibration Curves at Low pH Values	84
10	Aluminum Complexing Effect and Fluoride Recovery by Different Masking Agents	88
11	Iron Effect and Fluoride Recovery by Masking Agents	93
12	Reproducibility of Automated Measurements at Different Fluoride Levels in Presence and Absence of Aluminum	106
13	Fluoride and Iron Determinations in Water Samples (mg/l) from Jackson, Michigan, 2067	107
14	Characterization of Fluoride in Water Samples from Wyoming, Michigan, by the Manual and Automated Electrode Methods	108
15	Statistical Data Related to Manual and Automated Fluoride Electrode Measurements in Water Samples from Wyoming, Michigan	109
16	Characterization of Fluoride in Water Samples from Ann Arbor, Michigan (April 6, 1971)	115
17	Chronological Characterization of Fluoride in Water Distribution System of Ann Arbor, Michigan	116
18	Summary of Free and Total Fluoride Data (Chicago/Lehigh Station)	117
19	Electrode Deterioration	133

No.		Page
20	Electrode Response After Regeneration	133
21	Trace Metals Survey Sites	137
22	Summary of Raw Data from Household Trace Metals Survey	138
23	$[H^+]$ as a Function of CO_3^{2-} and Cl_2 Formality	188
24	Experimental and Theoretical Relationships between Alkalinity and Potentials	189
25	Theoretical Relationship between Alkalinity and Potential for Solutions with and without Free Residual Cl_2	189
26	Changes in Potential from Addition of 1.0 mg/l Free Residual Cl_2	190
27	Effect of Thiosulfate	192

ACKNOWLEDGMENTS

Sincere appreciation is expressed to the following persons who provided input to the project:

Gordon G. Robeck and James M. Symons, Ph.D., Director and Chief, Water Supply Research Division, respectively, who served as project officers. Through their efforts, continuation support was made available to equip the mobile laboratory and computerize monitoring operations. The merits of adding practical application to analytical feasibility are readily apparent. The overall guidance and support provided by both Mr. Robeck and Dr. Symons are greatly appreciated.

Further guidance and considerable constructive criticism were provided by members of the Advisory Committee. Their assistance, both individually and collectively, is also very much appreciated.

Commercially available instrumentation with potential applicability for the proposed monitoring system was evaluated early in the project. The cooperation of manufacturers who generously consigned equipment for this purpose is gratefully acknowledged:

Aqua Test Corporation
Capital Controls Company, Inc.
Hach Chemical Company
Schneider Instrument Company

During the various field assignments, personnel at each respective local water utility provided liason with NSF/EPA staff operating the mobile laboratory. Each of these persons responded willingly to needs of the permanent crew, and demonstrated enthusiastic support for the monitoring effort. Virtually every request was granted. Thanks is expressed on behalf of the entire project staff for their untiring assistance: Harvey Mieske, Ann Arbor; Richard A. Pavia, N. J. Davoust, Charles Halter, Ben F. Willey, and Green Whitney, Chicago; Carmen F. Guarino, Charles E. Vickerman, Joseph V. Radziul, Alan Hess, Charles Pierce, and David Gotshall, Philadelphia; and Gerald Remus and Albert Shannon, Ph.D., Detroit.

To assure smooth transfer of operations from NSF to EPA, three persons in EPA were assigned responsibility for operating the mobile laboratory: Marvin C. Gardels, Ph.D., Robert Thurnau, and Daniel F. Watkins. The EPA crew visited Ann Arbor to get

acquainted with NSF project staff, become familiar with systems in the mobile laboratory, and participate in the final meeting of the Advisory Committee. During the monitor's month-long visit to Philadelphia, the EPA crew rotated for one-week periods and accompanied the NSF operator to and from Philadelphia. EPA participation was scheduled to provide each operator with experience in shutting down, moving, and starting up in a new location. It was reassuring to observe the enthusiasm of the EPA crew for the task ahead. After more than four years of effort, the mobile laboratory and each of its systems were, themselves, like part of the project staff. A great deal of pride and effort went into their development. It is gratifying to know that future operations are in the hands of competent, concerned professionals.

Two weeks were scheduled to install - and develop software for - the on-board mini computer. The experts said it could not be done, but three dedicated people proved them wrong: William B. Everett, NSF; Charles A. Khuen, Ph.D. and James Seydel, Ph.D., The University of Michigan. These people met, assigned tasks, and agreed that the task was virtually impossible in the time available to them, then proceeded to ignore the clock and complete their assignments on schedule. For their initiative and persistence, sincere thanks to each of them for a job very well done.

Finally, the staff for this project worked tirelessly to achieve each of the expressed objectives. Their loyalty and dedication to the project through each phase of effort was indeed commendable. Special thanks are expressed to John R. Adams, who devoted many extra hours to operating the mobile laboratory on its various field assignments; Robert R. Wood; Warren K. Schimpff, Ph.D.; Thomas L. Schwenk, M.D.; Diane Daniel and Sue Buske, project secretaries, Nina I. McClelland, Ph.D. was project director, and K. H. Mancy, Ph.D. and Dr. McClelland, coprincipal investigators.

SECTION I
CONCLUSIONS

It is analytically feasible, using automated electrochemical techniques, to detect and measure changes in quality which do occur in potable water during transmission through distribution systems. A fully operational prototype drinking water quality monitor, with 18 integrated, computer controlled, parametric systems installed in a mobile laboratory was delivered by the National Sanitation Foundation to the National Environmental Research Center, Cincinnati, Ohio upon successful completion of the project, "Water Quality Monitoring in Distribution Systems." All systems were evaluated under actual field conditions by operating the mobile laboratory for two and a half months at remote sites on transmission lines in Ann Arbor and Detroit, Michigan; Chicago, Illinois; and Philadelphia, Pennsylvania.

The reliability and applicability of on-board systems in the mobile laboratory for detecting and measuring significant changes in quality at remote monitoring sites along distribution networks was clearly established. Because of relatively infrequent sampling schedules and time lapse between sampling and laboratory analysis, automated, onsite measurements are potentially more meaningful than data acquired from perimeter surveys. Widespread use of the NSF/EPA mobile laboratory and other similar systems could be expected to contribute significantly to diagnostic activities and preventive quality assurance programs consistent with surveillance and enforcement requirements of the Safe Drinking Water Act.

Correlation of data acquired by the mobile laboratory with measurements recorded at the water purification plant provides for calculation of residence times in the distribution system at periods of varying demand, indicates the need for flushing at or near deadends in the system, and assists the treatment plant operator in evaluating the need for-and effect of-changes in treatment plant operation.

Equipment design specifications developed early in the project were oriented principally to laboratory use. Computer control and mobile laboratory application became objectives only after the analytical feasibility of individual parametric systems was clearly established. Specific observations and analysis of data acquired during field operations suggest the following refinements in planning second generation equipment intended for field use; e.g.,

1. Computer capabilities can- and should- be greatly expanded. At the least, programs should be developed for better utilization of the automatic sampler; e.g., sampler operates when predetermined levels of specified parameters are exceeded; and on-board electronic data processing capability including computer graphics should be developed. In addition, either a cassette or magnetic tape system should be provided in lieu of the paper tape option purchased for this project. Selection was made on the basis of economy at the time of purchase; however, paper tape output is extremely difficult to handle in the field. Cassettes are attractive for ease in mailing from remote locations for additional processing on a larger computer away from the mobile laboratory.

2. The original DASV system was designed for laboratory operation. Its complex arrangement with switching/timing capability is unnecessary with the mini computer available. A commercial potentiostat is entirely adequate for DASV measurements, operational control should be a function of the computer. In addition, pH adjustment capability should be provided for the DASV monitor to extend its capability for measuring additional metals.

   A single Technicon pump could be used for all systems requiring reagent addition; i.e., DASV, alkalinity, and fluorides. Recurrent bubble entrapment problems in the fluoride systems should be eliminated. Further study of solution ground, peristaltic pump noise, and the role of organics with respect to the alkalinity monitor is indicated. Prepotentiometer electronics might be added to filter the signal.

3. Liquid junction ion-selective electrodes; i.e., hardness and nitrate should not be used when advanced electrode technology provides more reliable electrodes. Although it is unlikely that solid state probes will be feasible in the near future, improved bodies with better electrical shielding are promised by the manufacturers. Use of an electrode other than the divalent cation electrode for measuring hardness, and placing hardness outside of an SRM system should be considered. The overall usefulness of nitrate measurements in distribution system monitoring should be reviewed. It might be desirable to retain a nitrate electrode "for use as needed" and substitute routine monitoring of sodium or calcium.

4. Use of an electrode multiplexer should be considered. One multiplexer channel could be dedicated to bench measurements and calibrations while other channels are used for Technicon systems measuring special interest parameters. Linking multiplexer, potentiometer, and computer would reduce the number of potentiometers required in a mobile laboratory.

5. Better provision for external grounding, replacing the plastic adapter for intake water supply, and acquiring a pump for use in low line pressure areas in the field are recommended changes in the NSF/EPA mobile laboratory. Additional airconditioning capability is also a desirable improvement.

In developing a "second generation" mobile water quality monitoring laboratory, considerable savings in time and cost can be anticipated as a result of experience with this study.

SECTION II
RECOMMENDATIONS

1. The NSF/EPA mobile laboratory should be placed in regular service and made available to communities where water quality deterioration in the distribution system is known to occur. For systems in which the quality of water at the tap could be improved by modifying treatment plant operation, the mobile laboratory is an excellent diagnostic tool. It can be used to identify changes and, with continued monitoring, to assure the effectiveness of selected corrective measures.

2. The NSF/EPA mobile water quality monitoring laboratory should be made available to states for support of their new responsibilities, defined by the federal Safe Drinking Water Act (Public Law 93-523); and used routinely by EPA for public drinking water supply surveillance activities.

3. Additional mobile water quality monitoring laboratories should be constructed. This would provide for operation of two or more systems on the same transmission line as well as widespread, simultaneous monitoring capability. Federal, state, district, and large local water utility resources should be committed to this objective.

SECTION III
INTRODUCTION

General

The primary objective of any drinking water utility is to provide an adequate supply of high quality water to its users. The quality of water leaving the treatment plant is assured by routine analytical procedures at the local utility and periodic surveillance by state water supply agency personnel.

It is generally assumed, however, that quality of a treated water supply changes during transportation and delivery to the user's tap. These changes may occur as a result of: (1) physicochemical or biochemical transformations in the municipal- or household-pipeline; i.e., spontaneous changes in the water independent of pipeline characteristics; or (2) physicochemical interactions of the water with the municipal- or household-pipeline. Examples of these effects include "unstable" water which deposits calcium carbonate ($CaCO_3$) film as a function of its residence time in the piping system (a physicochemical transformation in the water itself), and uptake by the water of available metals from the piping system (a physicochemical interaction of water with the pipeline).

Regardless of the type of change which occurs during distribution, quality *at the user's tap* must be assured. In 1965 the Research Committee of the American Water Works Association (AWWA) recommended that instrumentation for measuring corrosion and stability be developed for distribution system monitoring applications. The research study, "Water Quality Monitoring in Distribution Systems," undertaken by the National Sanitation Foundation under grant and contract support from the U.S. Environmental Protection Agency, was a direct result of this recommendation.

Study Aims and Objectives

Principal objectives of the NSF study were to develop basic design criteria and operational specifications for a continuous monitoring system which could measure changes in water quality characteristics in distribution systems and provide for analytical quality control of water purification processes. Specific aims included: (1) establishing the analytical feasibility of commercially available sensor systems for potable water quality

monitoring applications, (2) developing new sensor systems as required, (3) assembling a prototype monitor, (4) establishing performance characteristics for each integrated parametric system in the prototype monitor, (5) installing the monitor in a mobile laboratory, and (6) operating the mobile laboratory at selected sites under actual field conditions.

The NSF/EPA mobile water quality monitoring laboratory, shown in Figure 1, was designed, constructed, and successfully operated at the municipal water treatment plant in Ann Arbor, Michigan; four sites in metropolitan Chicago; a remote distribution system site in Detroit; and four sites in Philadelphia. It was delivered to EPA/NERC, Cincinnati, Ohio in October 1973 for operation by EPA in future distribution system monitoring and research assignments.

Study Plan

Eleven persons with expertise in water utility management served as an advisory committee to establish priorities and provide overall guidance to the project staff. (The advisory committee membership is listed as Appendix A.) Parameters, selected by the advisory committee for inclusion in the prototype monitoring system, included temperature, conductivity, pH, chloride, dissolved oxygen, free and total residual chlorine, turbidity, corrosion rate, free and total fluorides, alkalinity, hardness, nitrate, copper, cadmium, lead, and calcium carbonate deposition rate.

Consistent with project aims and objectives, commercially available sensor systems were loaned to the project by their respective manufacturers. The analytical feasibility of including these systems in the prototype monitor was carefully evaluated in the laboratory. No effort was made to modify existing-or develop new-sensors when commercially available systems were shown to be applicable.

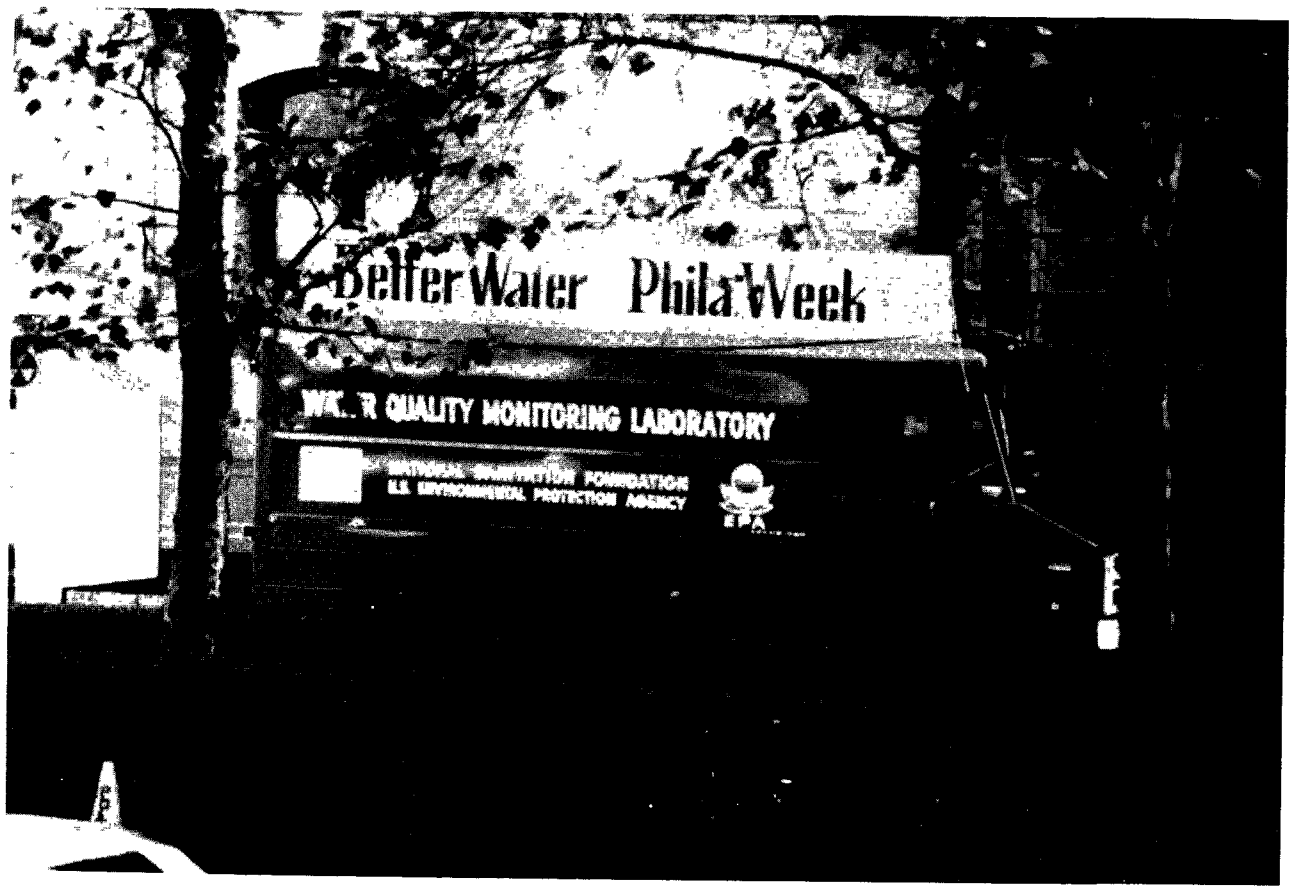

Figure 1. NSF/EPA mobile water quality monitoring laboratory.

SECTION IV
PROTOTYPE MONITOR

General

Eighteen parametric sensors are included in the prototype monitoring system developed during this study. Nine of these are commercially available and were used without modification. (See Table 1.) Five of the nine - temperature, conductivity, pH, chloride, and dissolved oxygen - are original equipment with the Schneider Robot Monitor(RM-25), an integrated instrument system designed for monitoring the quality of water in lakes and streams. These five sensors were shown to be highly reliable with no requirements for special timing sequence or preconditioning of the sample stream.

Other commercial sensors used without modification include free and total residual chlorine analyzers from Capital Controls (Models 871 and 872, respectively), a Hach CR low range light scatter turbidimeter (Model 1720), and an instantaneous corrosion rate monitor by Petrolite Corporation.

Orion ion-selective electrodes for fluoride, hardness, and nitrate are included in the prototype monitor. The fluoride system, which provides for both free and total fluoride measurements, requires preconditioning of the sample stream. Sensors for hardness and nitrate, though housed in Schneider modules, required development of support electronics and a flow interrupt timing/switching device.

Theory

Basic theoretical relationships describing electrochemical sensors for a number of parameters in the prototype monitor are summarized in Table 2. Theoretical considerations for other systems are described in greater detail in respective sections of the report.

Performance Characteristics

Performance characteristics of each sensor in the prototype system are described in Table 3. Terms are defined as follows:

Table 1 . SENSORS IN THE PROTOTYPE MONITOR

Parameter	Sensor Type	Unmodified Commercially Available System	Sample Pre-conditioned	Requires Special Timing Sequence
Temperature	Thermistor	√		
Conductivity	A-C Conductivity Cell	√		
pH	Glass Electrode	√		
Chloride	Solid State Ion Selective Electrode	√		
Dissolved Oxygen	Voltammetric Electrode	√		
Free Residual Chlorine	Galvanic Cell	√	√	
Total Residual Chlorine	Galvanic Cell	√	√	
Turbidity	Nephelometer	√		
Corrosion Rate	Polarization Admittance Technique	√		
Free Fluoride	Solid State Ion Selective Electrode		√	
Total Fluoride	Solid State Ion Selective Electrode		√	
Alkalinity	Potentionmetric Combination pH Electrode		√	
Hardness	Liquid Junction Ion Selective Electrode		√	√
Nitrate	Liquid Junction Ion Selective Electrode			√
Cadmium	Differential Anodic Stripping Voltammetry (DASV)		√	√
Lead	DASV		√	√
Copper	DASV		√	√
Calcium Carbonate Deposition Test	Potentiostatic Rotating Ring Disc Electrode			

Table 2. ELECTROCHEMICAL SENSORS FOR WATER QUALITY MONITORING

Sensor Type	Equation
Conductometric	$L = K_c \sum_i^n C_i \lambda_i z_i$ (1)
Potentiometric	$E_m = K + \frac{RT}{zF} \ln \left[a_i + K_J a_J^{z_i/z_j} \right]$ (2)
- Glass electrode (e.g., pH)	$pH = -\log a_{H^+}$ (3)
- Membrane electrodes (e.g., ion-selective electrodes)	
- cationic	$pM^+ = -\log a_{M^+}$ (4)
- anionic	$pA^- = -\log a_{A^-}$ (5)
Voltammetric Membrane Electrodes	$i_d = \left[z\ FAP_m \frac{1}{b} \right] a_{O_2}$ (6)

where:

L = specific conductance
K_c = cell constant
C_i = ionic concentration
λ_i = ionic equivalent conductance
z_i = ionic valency
E_m = measured electrode potential
F = Faraday constant
K_j = selectivity coefficient
i_d = diffusion current
A = electrode surface area
P_m = membrane permeability coefficient
b = membrane thickness

(1) *Detection limit* refers to the minimum detectable concentration of the parameter of interest. It is defined by the sensitivity of the sensor (the smallest change in the variable which causes a detectable change in instrument response). Detection limits shown in Table 3 refer to sensors in the mobile laboratory in continuous field operation. Under controlled laboratory conditions, most of these values are appreciably lower.

(2) *Range(s)* shown are the limits for which full scale response can be obtained either by electronic adjustments or by changing reagent ratios; e.g., alkalinity.

(3) *Selectivity coefficients* are constants in the Nernst relationship which account for the electrodes potential caused by interfering ions.

(4) *Precision* refers to the reproducibility of sensor measurements.

(5) *Temperature dependence* relates to sensor response to temperature as a function of its response to changes in levels of the species of interest; i.e., changes in the slope of a calibration curve which are attributed to changes in temperature. A thermistor can be included in the measurement circuit to compensate for this effect. Systems without temperature compensation circuits in the mobile laboratory are calibrated frequently; temperature of the sample stream between calibrations is assumed to be constant.

(6) *Ionic strength effect* refers to changes in the activity coefficient of the ions or molecules of interest which are attributable to changes in ionic strength of the sample stream. This effect is eliminated by reagent additions in a number of the mobile laboratory systems; i.e., the ionic strength of the sample stream is adjusted to a constant high value which does not vary significantly with the smaller changes in ionic strength of the sample.

(7) *Long-term stability, recalibration, and maintenance requirements* are listed together in Table 3. Long-term stability refers to change in sensor performance as a function of time; i.e., cumulative drift in electrode response does not result in measurement error greater than five percent. The frequency with which a sensor must be recalibrated or serviced is determined by its long-term stability. The schedule for electrode rejuvenation or replacement of membranes and filling solutions must be carefully followed to insure continuing stability of response.

A clear understanding of performance characteristics for each sensor in the monitoring system, careful attention to recalibration schedules and maintenance and service requirements, as well as operator alertness to clues of malfunction are critical to successful operation of the NSF/EPA mobile laboratory.

Table 3. PERFORMANCE CHARACTERISTICS OF MOBILE LABORATORY SENSOR SYSTEMS

Parameter	Detection Limit	Range(s)	Selectivity Coefficients or Interferences	Precision	Temperature Dependence	Applicable pH Range	Ionic Strength Effect	Long Term Stability, Recalibration and Maintainance Requirements
Hardness	10 mg/l equiv. $CaCO_3$	One Decade, e.g. 10—100 mg/l equiv. $CaCO_3$	Zn^{2+}=3.5 Mg^{2+}=1.0 Fe^{2+}=3.5 Ba^{2+}=0.94 Cu^{2+}=3.1 Sr^{2+}=0.56 Ni^{2+}=1.35 Na^{+}=0.15 Ca^{2+}=1.0 K^{+}=0.10	±5 mg/l @120—150 mg/l equiv. $CaCO_3$	Considered in calculation of hardness from divalent cation activity measurements	5.5 to 12	Considered in calculation of hardness from divalent cation activity measurements	These liquid junction ion selective electrodes have been shown to have stable potentials which permit continuous use for periods up to seven days without recalibration; however, due to the shape of the electrode tip, twice daily attention is required to insure that bubbles have not formed on the tips. Complete rejuvenation of the probes must be performed every 30 days.
Nitrate	1 mg/l	Two Decades, e.g. 1—100 mg/l	HCO_3^-=0.02 CO_3^{2-}=0.006 Cl^-=0.006	N.D.[1]	Thermistor Compensated	2—12	N.S.[2]	
Chloride	3.0 mg/l	0—240 mg/l	OH^-=0.013	±2 mg/l	Thermistor Compensated	2—12	N.S.	7 days; No known maintainance
Temperature	N.A.	0—120°F	None	±0.2°F	N.A.	N.A.	N.A.[3]	7 days; No known maintainance
Conductivity	N.A.	0—1200 0—2400 micro MHOS/cm	None	±5 micro MHO/cm	Thermistor Compensated	5—12	This parameter Measures Changes in ionic strength	7 days; Internal flow channel and electrode surfaces must be cleaned monthly
pH	N.A.	pH2—12	Na^+	±0.02 units	Thermistor Compensated	2—12	N.S.	7 days; No known maintainance
Dissolved Oxygen	0.1 mg/l	0—12 0—24 mg/l	None	± 0.1 mg/l	Thermistor Compensated	2—12	N.S.	7 days; Electrode must be rejuvenated every 30 days
Free Residual Chlorine	0.01 mg/l	0—1.0 0—2.0 0—3.0 mg/l	None	±0.01 mg/l	Thermistor Compensated	Sample pH adjusted to pH 4.5 by reagent addition	Ionic strength adjusted to constant value by reagent addition	Daily checking of calibrations by comparison with amperometric titration is required. Reagent reservoirs must be refilled every 7 days
Total Residual Chlorine	0.01mg/l							
Turbidity	0.01JTU	0—0.1 0—1.0 0—3.0 0—30 JTU	Air bubbles in sample stream must be removed by a bubble trap	±0.02 JTU	N.A.	N.A.	N.A.	7 days; Periodic cleaning of photocell windows maintains sensitivity. Light fouling of the windows does not effect accuracy within the 7 day calibration period

Continuation Table 3

Parameter	Detection Limit	Range(s)	Selectivity Coefficients or Interferences	Precision	Temperature Dependence	Applicable pH Range	Ionic Strength Effect	Long Term Stability, Recalibration and Maintainance Requirements
Free Fluoride	0.1 mg/l	0.1—2.0 mg/l	OH^-=0.7@[F^-]= 10^{-6} to 10^{-4}M OH^-=0.07@[F^-]= 10^{-4} to 10^{-3}M OH^-=0.05@[F^-]= 10^{-3} to 10^{-2}M	± 0.02mg/l	+0.17% increase in apparent signal for 1°C increase in temp. (Theoretical)	Sample pH adjusted to pH 5.0 — 5.4	Ionic strength adjusted to constant value by reagent addition	Daily introduction of standards maintains accuracy and demonstrates integrity of the flow system. Electrodes are known to be stable over very long periods of time. Reagent reservoirs must be refilled every ten days
Total Fluoride	0.1 mg/l							
Alkalinity	10mg/l	60mg/l span e.g. 20—80 mg/l equiv. $CaCO_3$	Residual chlorine interferes, but is eliminated by addition of thiosulfate to the sample stream	± 3mg/l equiv. $CaCO_3$	Unknown	N.A.	Ionic strength adjusted to constant value by reagent addition	Reagent reserviors must be refilled every four days. Recalibration must be performed for each new set of reagents
Cadmium	0.001mg/l	0—0.1mg/l	Trace organics can interfere by giving false peaks. Accurate identification of peak potential indicates the presence of interferences	N.D.	N.D.	Sample pH adjusted to pH 3	Ionic strength adjusted to constant value by reagent addition	Standards are analyzed automatically every six hours. DASV electrodes must be replated daily
Lead	0.001mg/l	0—0.1mg/l						
Copper	0.001mg/l	0—0.1mg/l						
CCDT	N.A.	N.A.	Unknown	N.A.	Unknown	Variation in pH results in variation in rate of film deposition	N.A.	Each analysis is discrete. Electrode must be rejuvenated between each run by cleaning with dilute nitric acid
Corrosion	N.A.	10 calibrated ranges from 0—0.1 MPY to 0—1000 MPY (Mils per yr.)	None	± 5% of range	Temperature variation results in change in corrosion rate	Variation in pH results in variation in rate of corrosion	N.A.	No calibration or maintainance requirements. Internal electronic standard demonstrates instrument integrity.

[1]N.D. = not determined; i.e., a specific relationship between the referenced characteristic and the parameter of interest was not determined for the mobile laboratory sensor system.

[2]N.S. = not significant; i.e., variations in ionic strength of tap waters in the U.S. would not produce more than ten percent variation in the apparent activity of the parameter of interest.

[3]N.A. = not applicable; i.e., the referenced characteristic is not related to the parameter of interest.

SRM-HOUSED SYSTEMS

General

The Schneider Robot Monitor (SRM) is a modular instrument system with three stacked sliding drawer cubicles (Figure 2). Sensors, flow cells, flow controlled valves (except the flow interrupt assembly for hardness and nitrate), inlet reservoirs, an outlet header, all interconnecting tubing and fittings, a splash protected terminal board for sensor connections, and a high pressure header and tubing designed for automatic sensor cleaning are housed in the bottom cubicle. (To facilitate visual inspection of the entire flow system, all tubing is transparent plastic, and flow cells, reservoirs and sample headers, machined from solid blocks of Plexiglas, are polished to be transparent and clear. There are no metal plumbing components in contact with the sample stream.)

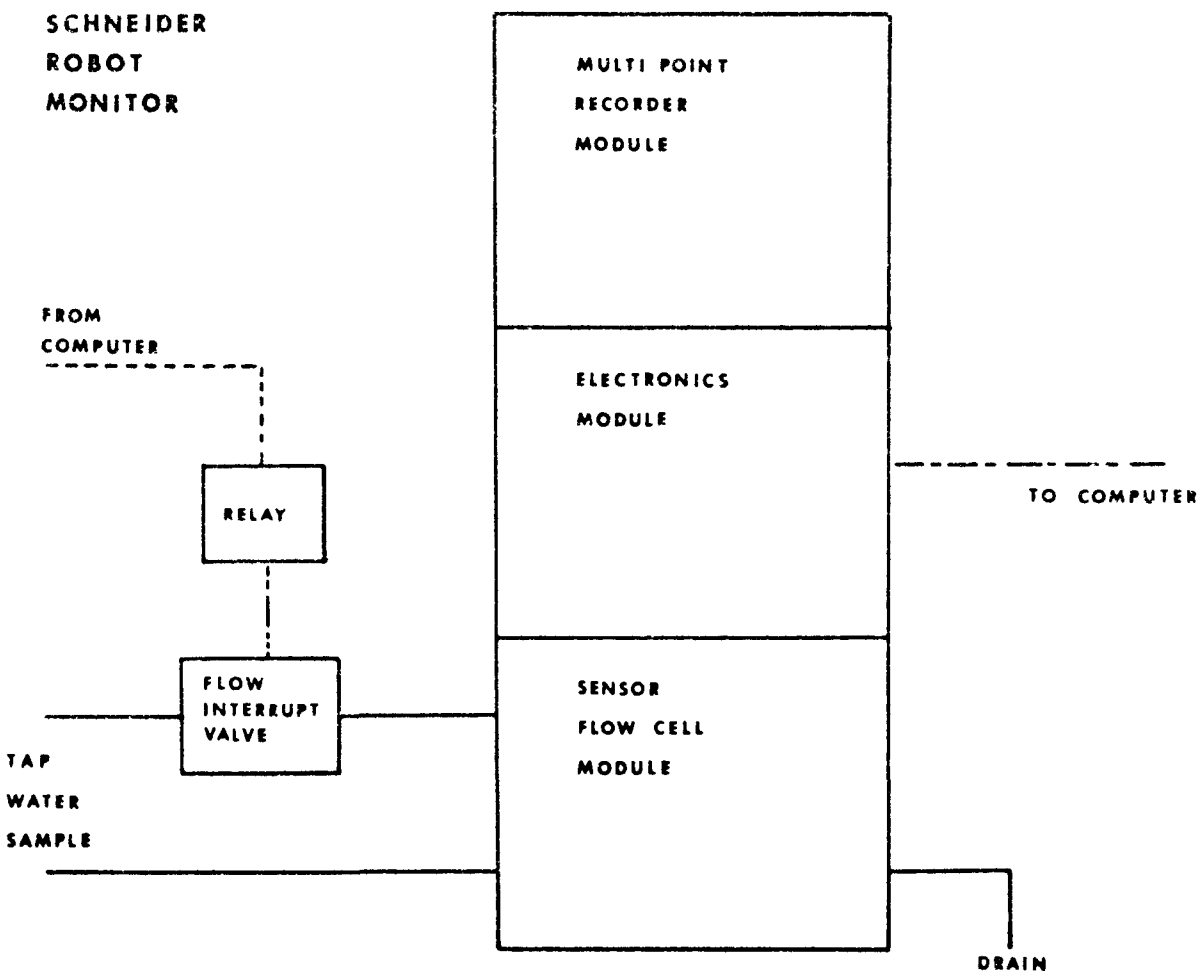

Figure 2. Schematic arrangement of Schneider Robot Monitor.

Flow through the cubicle is illustrated in Figure 3. The sample stream enters the cubicle through the inlet reservoir and is distributed evenly to all flow cells. To ensure adequate mixing and to facilitate cleaning, flow cells are funnel-shaped at the inside bottom. They are capped at the top by neoprene stoppers through which the sensor assemblies are inserted. Each flow cell is provided with an air bleeder hole to prevent air locking. The effluent from all flow cells is collected by the outlet header and discharged to a drain through a common effluent line.

Each individual SRM-housed sensor except temperature is installed in a separate flow cell. For convenience in calibrating the dissolved oxygen electrode, the temperature sensor is installed as part of the DO electrode assembly. In the prototype system, six flow cells are engaged and two positions open, as shown schematically in Figure 4.

Electronics

All sensor systems are wired to their respective electronic circuitry (analyzers) through the electrode terminal board in the flow cell cubicle. This board consists of 37 barrier strip terminals and four steatite insulated terminals for coax cable tie points. Individual sensor assemblies are provided with appropriate leads or terminals attached for lead connection.

The eight plug-in type modular electronic analyzers are housed in the middle cubicle. The panel-rack assembly is slide mounted as two separate drawers for easy access. The panel through which power is supplied to the analyzers and a test signal supply for the recorder are located in the analyzer cubicle.

A solid state operational amplifier is the active element in each analyzer system. This type of circuitry is particularly useful for stable amplification of small DC voltages and permits the use of ancillary items for temperature compensation, linearization of sensor characteristics, etc. A built-in calibration check and moisture sealed panel meter are provided with each analyzer module. Panel meters have individually calibrated hand drafted scales with an accuracy of ± 0.5 percent.

Outputs from the electrometers are used as inputs to a second stage operational amplifier. Offset is introduced in the second stage to give a proper zero scale, and provision is made for handling either polarity or measuring electrode input. Temperature compensation with a wide range of adjustment is accomplished with a thermistor in the input or feedback circuits of a third stage operational amplifier.

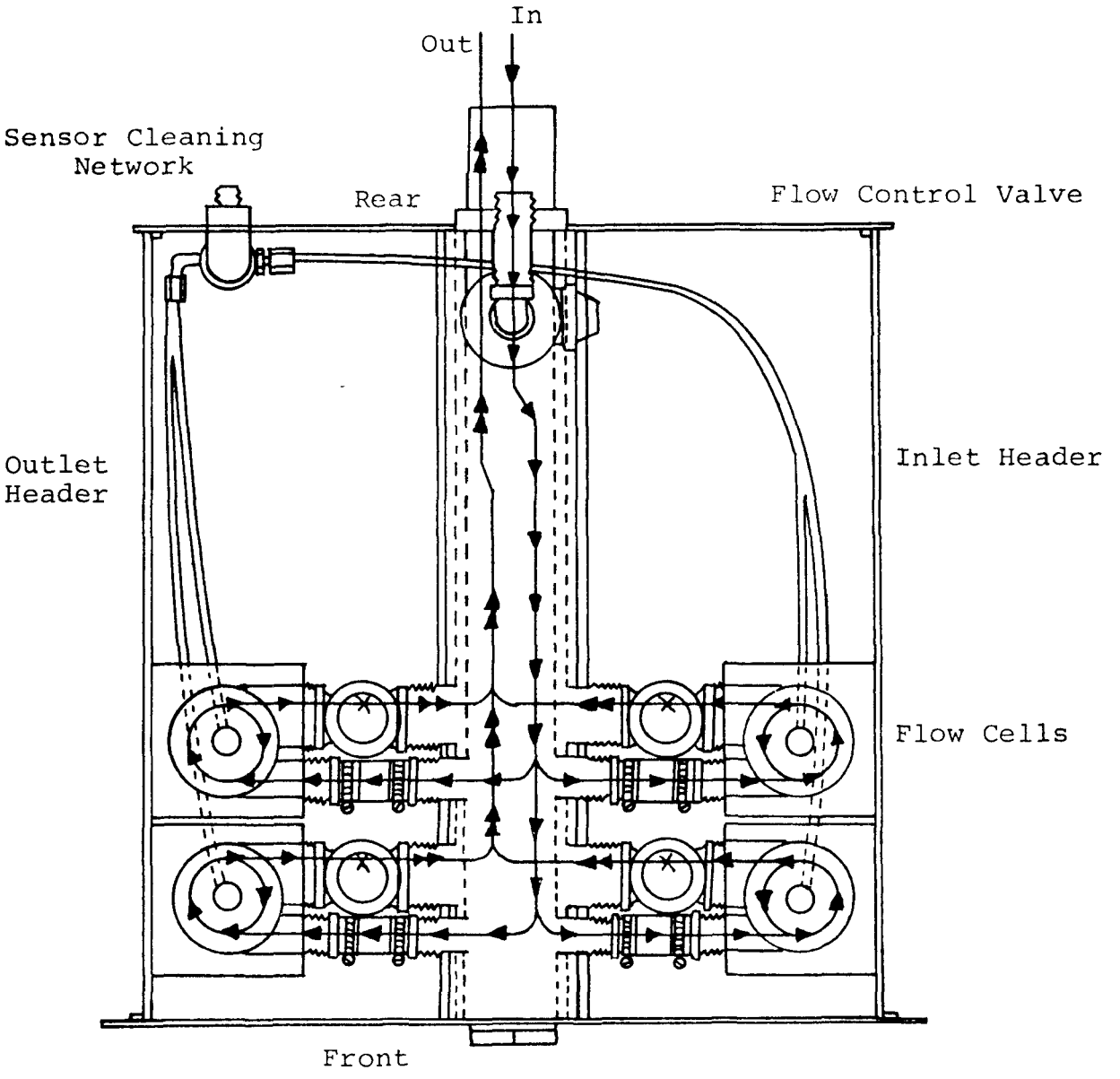

To flow cell

From flow cell

X Downward flow

Note: 4 to 8 flow cells may be used in the cubicle.

Figure 3. Schematic diagram of the SRM flow cell cubicle, top view.

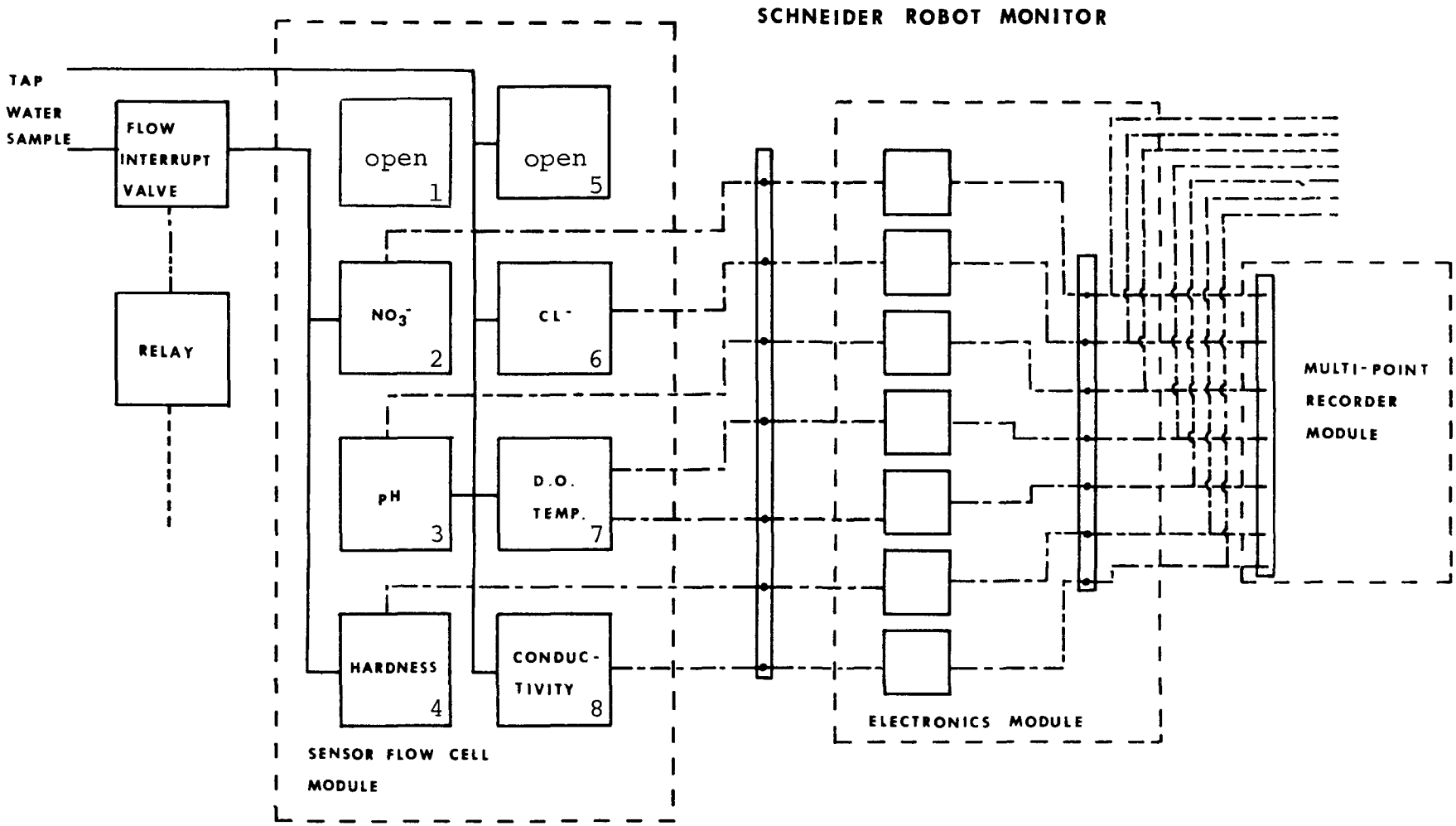

Figure 4. Schematic illustration of sensor positions and overall arrangement of SRM-housed systems.

Recorder

Sensor output from the SRM-housed systems is displayed (in addition to the analyzer panel meters) on an Esterline Angus 24-point servo recorder (Model E1124E), located in the upper cubicle. The recorder has a 50 millivolt range and is used with 60 seconds per point printing speed and one inch per hour chart drive.

Sensors

The five original SRM sensors - temperature, conductivity, pH, dissolved oxygen, and chloride - are operated and maintained in conformance with the manufacturer's instructions contained in manuals supplied with the mobile laboratory. They sense the species of interest, generally without interference from any other species which may be present in the test water. No reagents are added for their normal operation, but standard solutions are required weekly for calibration. In field operation, no unusual problems were observed with sensors for temperature, pH, and chloride. Very occasional erratic readout or discontinuities in strip chart data from the conductivity system were caused by bubble entrapment on the sensor surface. The dissolved oxygen sensor is flow sensitive. Short-term noncumulative drift in output was observed occasionally when flows dropped to critically low levels. In general, one gpm flow at 20 psi is maintained past the electrode. Long-term cumulative drifts in calibration indicate degeneration of electrode response and the need for rejuvenation.

Unique problems were addressed in developing operational systems for hardness and nitrate. Like the DO membrane electrode, the hardness and nitrate probes are flow sensitive; however, they produce stable output only under quiescent conditions. They must be *completely* isolated from hydrodynamic effects of the sample stream. A flow interrupt system, including chassis, power supply, and relay for switching AC voltage to a three-way solenoid valve was installed in the mobile laboratory. Test water passing through the valve goes either to waste (during interruption of flow) or to exchange the sample in the hardness and nitrate flow cells. The relay power assembly is activated by digital output from the computer through the program "FLOW," which sets a digital output bit high, waits 15 minutes, sets the bit off, waits 45 minutes, then begins the cycle again; i.e., test water flows through the sample cell for 15 minutes, then the flow cell is quiescent and the sample completely isolated from test water flowing to other sample cells for 45 minutes. During this interval, electrode response equilibrates and valid measurements of hardness and nitrate are recorded just prior to the time when samples are exchanged by new flow into the cells.

In addition to being flow sensitive, hardness and nitrate electrodes are, as a result of their design and construction, extremely subject to bubble entrapment and accumulation of static electricity. Bubbles are easily trapped in the concave bottom configuration of Orion liquid junction electrodes. To overcome this effect, box-shaped bubble traps constructed from heavy gauge, coarse-mesh stainless steel screen are attached to the hardness and nitrate electrodes by a plastic ring which fits tightly over the outside of the electrode body. The bottom of the trap is covered with a flat sheet of plastic to keep bubbles from reaching the electrode from the bottom, and the entire trap assembly is filled with glass beads into which the electrode is seated. The glass beads effectively prevent any movement of bubbles to the electrode while allowing completely free movement of test solution to the sensing surface.

An alternate electrode design (marketed by Corning) was also evaluated. Its flat bottom surface was an attractive feature, but exceptionally high impedance made it totally impractical for use in the prototype system. Although the Orion 92 series liquid junction electrodes have a tendency to accumulate static electrical charge, a new design with lower impedance and improved shielding has been announced. It is strongly recommended that, when they are available, the feasibility of substituting new liquid junction series electrodes in the mobile laboratory be evaluated by EPA.

The nitrate liquid junction ion-selective electrode is expected to give valid analytical results at nitrate activity somewhat less than ten mg/l of NO_3^-; however, chloride and bicarbonate ions interfere when they exceed the nitrate concentration by a factor of ten. The nitrate probe is calibrated over two decades of nitrate activity; i.e., 1.0 mg/l at the bottom of the scale, ten mg/l at midscale, and 100 mg/l of NO_3^- activity at full scale. Most United States tap waters contain less than 1.0 mg/l, and normal response of the electrode is near the bottom of the scale. As nitrate concentration in the test water increases, electrode response is proportional. If the nitrate concentration should increase to a dangerous level (e.g., 45 mg/l), the electrode can be expected to track the change with precision. Because of the logarithmic response of the probe, good precision is attainable at very low as well as high levels.

Preparation of reagents used with SRM-housed systems is described in Appendix B.

Interpretation of Hardness and Nitrate Data

In interpreting hardness and nitrate data, activity coefficients and complexation are important considerations. Physical characteristics of the liquid junction ion-selective electrode make it

difficult to design a sample flow cell without imposing pressure problems on the electrode; thus, it is impossible to add ionic strength buffers and masking agents vis-a-vis the fluoride monitoring system. (Addition of an ionic strength buffer would provide for measuring standards and sample at constant ionic strength giving direct measurement of ionic concentration; masking agents would free bound Ca^{2+} and Mg^{2+} from sulfate and bicarbonate for direct sensing by the electrode.) Electrode measurements are adjusted by applying constant factors, determined experimentally.

Two corrections must be applied: one for the activity coefficient and the second, for that percentage of the total amount of Ca^{2+} and Mg^{2+} which may be complexed. If the two factors are constant over the monitoring period, the equation for the correction of free uncomplexed species activity to total concentration is:

$$[M^{2+}]_T = \frac{(M^{2+})_F}{f_{M^{2+}}\ \alpha_{M^{2+}}} \qquad (7)$$

where:

$(M^{2+})_F$ = the monitored value

$f_{M^{2+}}$ = the partition coefficient or the fraction of the divalent metal ion concentration which is unbound

$\alpha_{M^{2+}}$ = the average activity coefficient for divalent metal ions in the monitor stream

Another factor to be considered in operating the hardness monitoring system is the effect of the flow interrupt device, which alternately causes flow/no flow in the system. Figure 5 is an example of typical strip chart recorder output for hardness data. Measurement points on half of the output are connected to better illustrate the nature of electrode response to the flow interrupt system. During the flow portion of the cycle, response of the electrode is erratic or noisy; when flow is stopped, the signal becomes quiet and quite stable. Hardness is measured after the signal has stabilized.

On the strip chart recording, shown in Figure 5, the divalent cation electrode is calibrated to read from 3.16×10^{-4}M $CaCl_2$ to 3.16×10^{-3}M $CaCl_2$ over the 12 inch scale. This places 1.0×10^{-3}M $CaCl_2$, or 100 mg/l of equivalent $CaCO_3$, at exactly midscale (60.0 recorder chart units). To properly analyze the data, electrode and EDTA titration data are compared to determine the fraction of hardness which is free to be sensed by the electrode. The complete procedure for converting strip chart recorder output for free divalent cation activity to total hardness concentration is as follows:

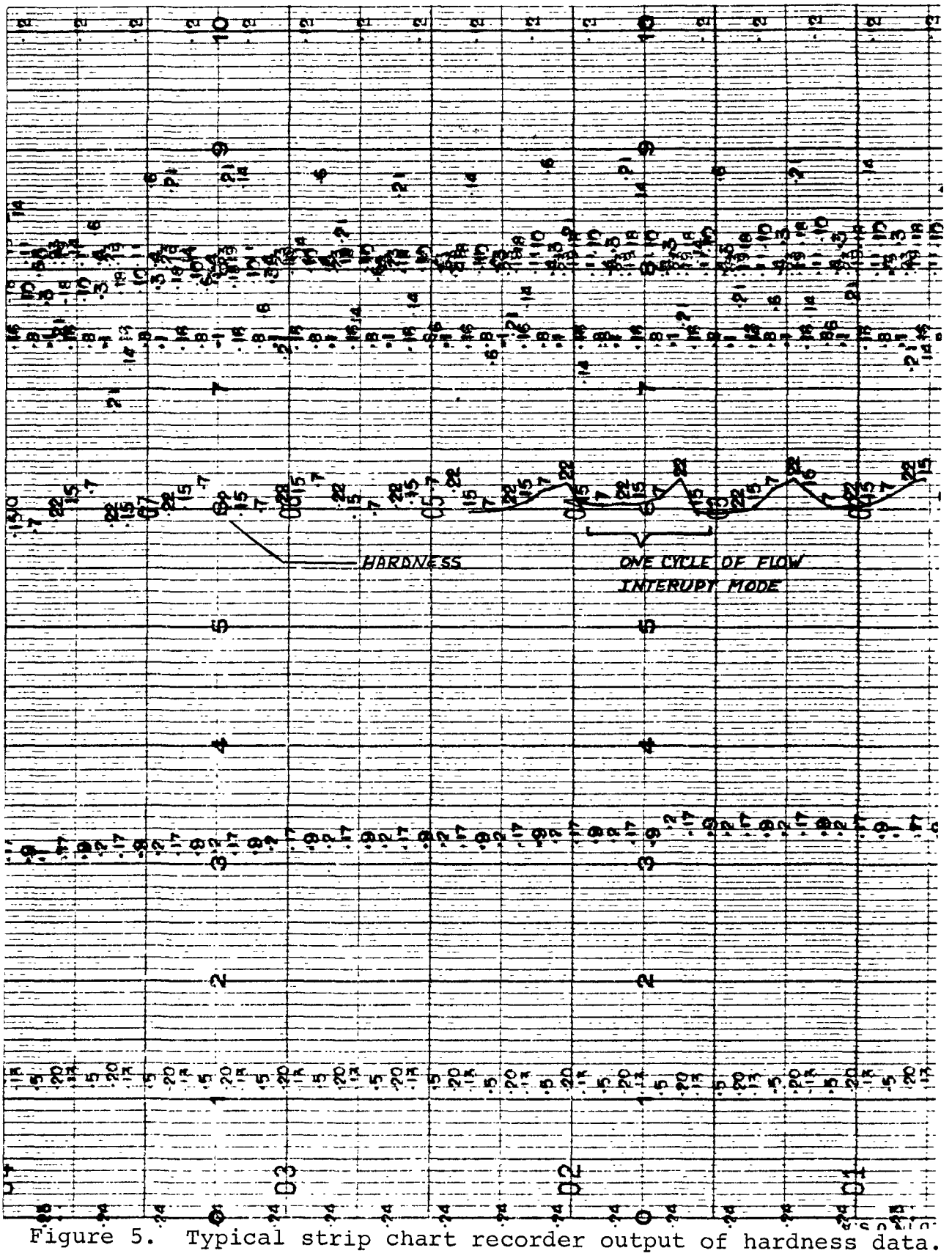

Figure 5. Typical strip chart recorder output of hardness data.

1. Determine the free divalent cation activity by comparing chart recorder output to a calibration curve.
2. Use the nomogram provided by the Orion Company (Figure 6) to convert activity to concentration measurements

   a. Determine free activity
   b. Determine conductivity
   c. Place a straightedge along a line through the free hardness activity and the measured specific conductance and read the percent correction for total hardness concentration where the straightedge crosses the third line.
   d. Correct the free hardness activity to free hardness concentration:

$$[Me^{2+}]_{electrode} = (Me^{2+})_{free} + C_f (Me^{2+})_{free} \quad (8)$$

3. Determine the fraction of the total hardness concentration which is complexed and unavailable to be sensed by the divalent cation electrode.

$$\frac{[Me^{2+}]_{electrode}}{[Me^{2+}]_{EDTA}} = f \quad (9)$$

4. Determine the total hardness concentration:

$$[Me^{2+}]_{total} = \left\{ \frac{(Me^{2+})_{free} + C_f (Me^{2+})_{free}}{f} \right\} \quad (10)$$

Example:

1. Free divalent cation activity = 100 mg/l equiv $CaCO_3$.
2. a. Free activity = 100 mg/l equiv $CaCO_3$.
   b. Conductivity = 320 μυ/cm.
   c. C_f = 5.5 percent or 0.055.
   d. $[Me^{2+}]_{free}$ = (100 mg/l)+0.55(100 mg/l)
      = 100 mg/l + 5.5 mg/l
      = 106 mg/l
3. $f = \frac{[Me^{2+}]_{electrode}}{[Me^{2+}]_{EDTA}} = \frac{106 \text{ mg/l}}{129 \text{ mg/l}} = 0.82$

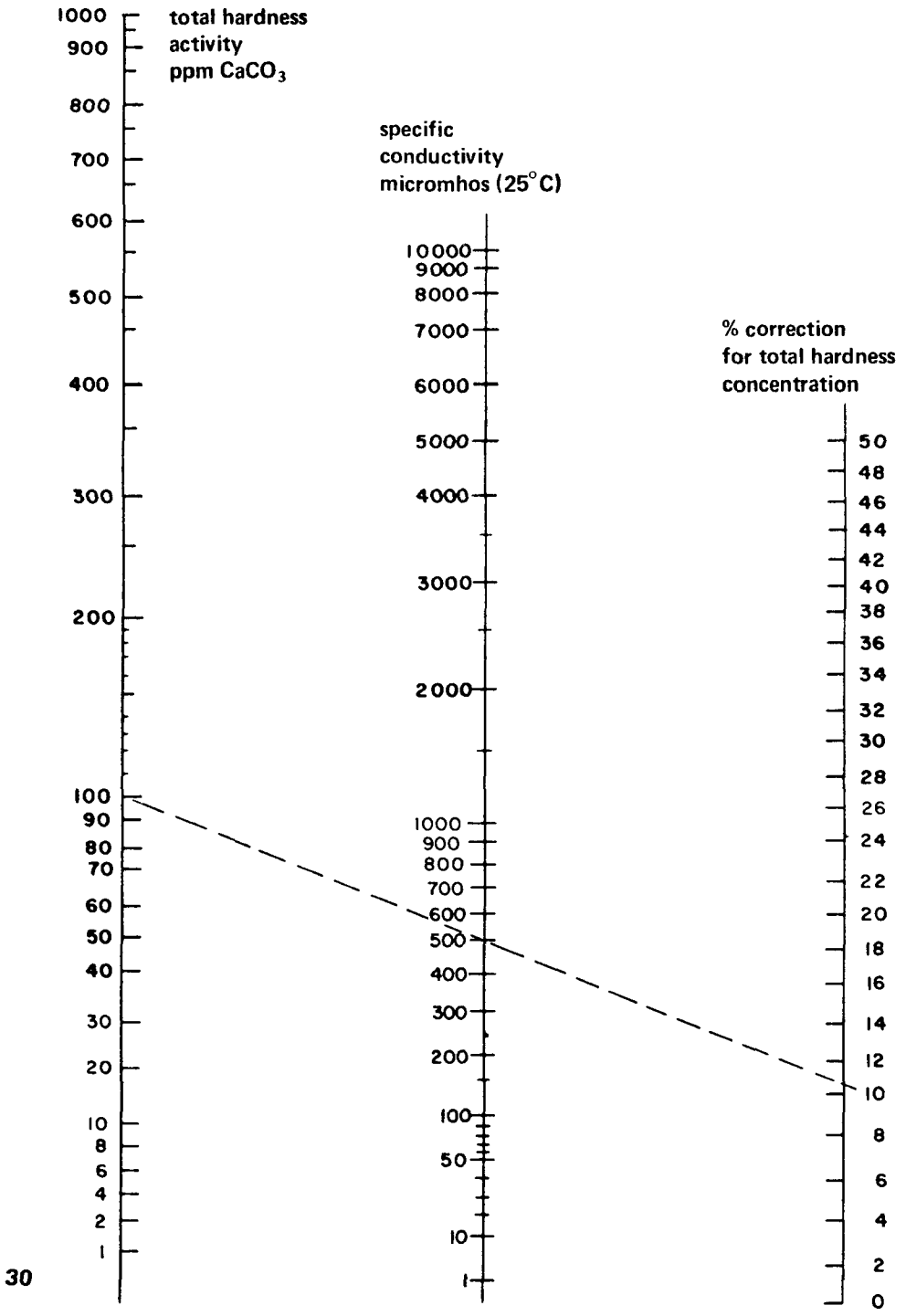

Figure 6. Conductivity correction nomogram.

4. $$[Me^{2+}]_{total} = \left\{ \frac{(100\ mg/l) + .055(100\ mg/l)}{0.82} \right\}$$

$$= 129\ mg/l\ of\ equiv\ CaCO_3$$

Nitrate measurements are not expected to require the degree of correction described for the hardness system. Nitrate is not found in a complexed state and its concentration usually need not be known with great accuracy, unless it is present near the maximum permissible level specified in the Drinking Water Standards (1). Unfortuantely, NSF cannot present any actual field data obtained from the nitrate sensing system; i.e., the mobile laboratory was not operated in an area where nitrate activity exceeded the detection limit of the sensor.

COMMERCIAL SYSTEMS

FREE AND TOTAL RESIDUAL CHLORINE

General

Residual chlorine is the single most important parameter in drinking water quality. Its presence in a finished water is generally considered to indicate that disinfection is complete, and the water is safe to drink.

At the water treatment plant, chlorine application is highly mechanized and carefully controlled. It must be added to the treated water at a level sufficient to accomplish disinfection but not sufficient to incite taste and odor complaints from the consumer. A total residual of 1.0 mg/l in water leaving the treatment plant is generally assumed to meet these objectives.

In traveling through the distribution system, it is entirely possible that the level and type of chlorine residual will change. These changes may occur as a function of other parameters which characterize the quality of the water itself, or as a result of conditions within the transmission pipeline. It is therefore desirable, if not necessary, that residual chlorine levels be monitored in the distribution system.

Theory

Regardless of the form in which chlorine is added, it reacts with the water to form hypochlorous acid or hypochlorite ion:

$$Cl_2 + H_2O \rightleftharpoons HOCl + H^+ + Cl^- \qquad (11)$$

gaseous chlorine — hypochlorous acid

$$Ca(OCl)_2 + H_2O \rightleftharpoons Ca^{2+} + 2\ OCl^- + H_2O \quad (12)$$

calcium hypochlorite — hypochlorite ion

$$NaOCl + H_2O \rightleftharpoons Na^+ + OCl^- + H_2O \quad (13)$$

sodium hypochlorite

The equilibrium condition of HOCl and OCl^- is described by Equation 14:

$$HOCl \rightleftharpoons OCl^- + H^+ \quad (14)$$

$$K_i = 2.5 \times 10^{-8}$$

Thus, the ratio of HOCl and OCl^- present following disinfection is determined by pH of the treated water:

$$\log \frac{[OCl^-]}{[HOCl]} = pH + \log K \quad (15)$$

The effect of pH on [HOCl]: $[OCl^-]$ species distribution is illustrated graphically in Figure 7. From this figure, it is apparent that a mixture of the two species exists in most United States drinking water supplies. In either form, it is referred to as "free residual chlorine."

The term "total residual chlorine" includes both free and "combined" forms. The most common combined chlorines are monochloramine and dichloramine, found in the presence of ammonia:

$$NH_3 + HOCl \rightarrow NH_2Cl + H_2O \quad (16)$$

monochloramine

$$NH_2Cl + HOCl \rightarrow NHCl_2 + H_2O \quad (17)$$

dichloramine

Trichloramine occurs in tap water only infrequently; e.g., with extreme pH or breakpoint chlorination:

$$NH_2Cl + HOCl \rightarrow NCl_3 + H_2O \quad (18)$$

trichloramine

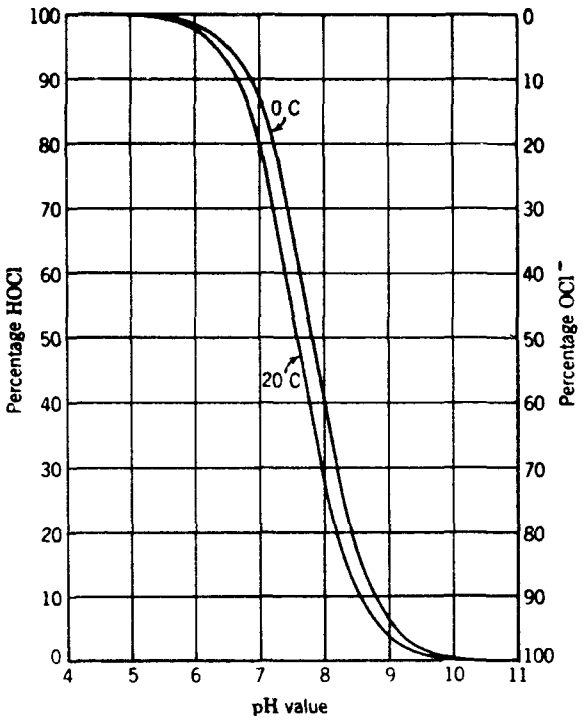

Figure 7. Distribution of hypochlorous acid and hypochlorite ion in water at different pH values and temperatures (2).

The rate at which the various forms of combined chlorine achieve disinfection is significantly less than that of free chlorine.

Nine analytical methods for measuring residual chlorine are described in Standard Methods (3). One of these, the amperometric technique, is used in the mobile laboratory in both the free and total residual chlorine analyzers, and in the manual titrator used to standardize the analyzers.

In the amperometric procedure, a galvanic cell is developed; i.e., a current flows between immersed electrodes when a free oxyhalogen acid; e.g., HOCl (hypochlorous acid), is present in the test water. Null point amperometric titration describes the principle of this method. Residual chlorine is quantitatively removed from solution by reaction with a titrated reducing agent; e.g., phenylarsine oxide. As reducing agent is added, current resulting from the presence of HOCl in the test water is reduced. Titrant is added until there is no further decrease in cell current. The titrant required to reach this end point (i.e., no further current decrease) is directly proportional to the level of residual chlorine present in the water.

Equation 19 describes the principle of electrolytic reduction of an oxyhalogen acid (HOX) at an inert cathode in the cell:

$$Cu^{\circ}|Cu^{2+}||X^{-}|HOX, Au \text{ (or Pt)} \quad (19)$$

$$\text{(or } Cu^{\circ}|Cu^{2+}||Cl^{-}|HOCl, Au \text{ (or Pt))} \quad (20)$$

Half reactions for Equation 20 include:

$$\text{Anodic:} \quad Cu^{\circ} = Cu^{2+} + 2e \quad (21)$$

$$E_a^{\circ} = -0.337 \text{ volts}$$

$$\text{Cathodic:} \quad HOCl + H^{+} + 2e = Cl^{-} + 2H_2O \quad (22)$$

$$E_c^{\circ} = 1.28 \text{ volts}$$

Combining Equations 21 and 22, the overall reaction is:

$$Cu^{\circ} + HOCl + H^{+} = Cl^{-} + Cu^{2+} + H_2O \quad (23)$$

and the standard cell emf will be,

$$E_{cell}^{\circ} = E_a^{\circ} + E_c^{\circ} = 0.94 \text{ volts} \quad (24)$$

Consequently, the cell potential at equilibrium, at 25°C, will be,

$$E_{cell} = 0.94 + 0.03 \log \frac{[Cu^{2+}][Cl^{-}]}{[HOCl][H^{+}]} \quad (25)$$

Thus, cell emf is a function of $[Cu^{2}]$, [HOCl], and $[H^{+}]$. The potential of the large surface area (nonpolarizable) copper anode is a constant (as $[Cu^{2+}]$ in the bulk of the test solution approaches zero) and is determined by the rate of dissolution of copper from its surface. In practice, $[H^{+}]$ is kept constant by the addition of pH 4.5 sodium acetate/acetic acid buffer. Cell emf, then, is determined by - and varies with - the level of HOCl in the testwater.

Experimental

Presently there are at least four amperometric-type residual chlorine analyzers which are commercially available. In two of the four systems, potential is measured across an extremely high resistance (rather than current flowing in the galvanic cell, measured across a low, fixed resistance). Three of the four systems use gold/copper electrode couples; the fourth, a platinum/copper couple. The gold or platinum electrode serves simply as an inert surface at which the HOX is reduced; thus, the theory of operation of each of the four instruments is essentially the same. Cell

geometry for each of the systems includes a large surface area copper cylinder (the anode), surrounding a wire or rod of the noble metal (cathode).

Cleanliness of the anode is vitally important. Fouling causes surface area variations and large drifts in potential over short time intervals. As a result, electrode cleaning devices are included with each instrument. One of the systems has the cell filled with plastic balls. A motorized arm drives the balls in the cell. Two of the units are filled with plastic pellets which abrade a rotating electrode. In the fourth unit, grit in the sample cleans the electrodes, agitated by velocity of the flowing sample stream.

It is also important to maintain constant ionic strength in the sample stream. Significant changes in total ionic strength (measured as total dissolved solids or as conductivity) result in HOX activity coefficient variations without changes in analytical concentration. The high strength sodium acetate/acetic acid buffer adjusts ionic strength in addition to controlling pH.

Signal variations resulting from temperature effects on cell emf require compensation. A typical galvanic residual chlorine analyzer is illustrated schematically in Figure 8. In this figure, R_2 is a variable resistance in parallel with the sensing electrode. It can be manually adjustable (assuming that temperature of the sample stream remains constant between calibrations), or a temperature dependent transducer (thermistor) can be used in which resistance varies automatically with changes in temperature.

Total residual chlorine is measured by adding potassium iodide to free combined residuals:

$$\underset{\text{mono-chlor-amine}}{NH_2Cl} + I^- \rightleftharpoons \underset{\text{mono-iod-amine}}{NH_2I} + Cl^- \tag{26}$$

$$\underset{\text{dichlor-amine}}{NHCl_2} + 2I^- \rightleftharpoons \underset{\text{diiod-amine}}{NHI_2} + 2Cl^- \tag{27}$$

Because iodamines are highly unstable in aqueous solutions, the reactions continue to produce hypoiodous acid, an oxyhalogen acid which is sensed by the galvanic cell:

$$NH_2I + H_2O \rightleftharpoons NH_3 + \underset{\text{hypo-iodous acid}}{HOI} \tag{28}$$

$$NHI_2 + H_2O \rightleftharpoons NH_2I + HOI \tag{29}$$

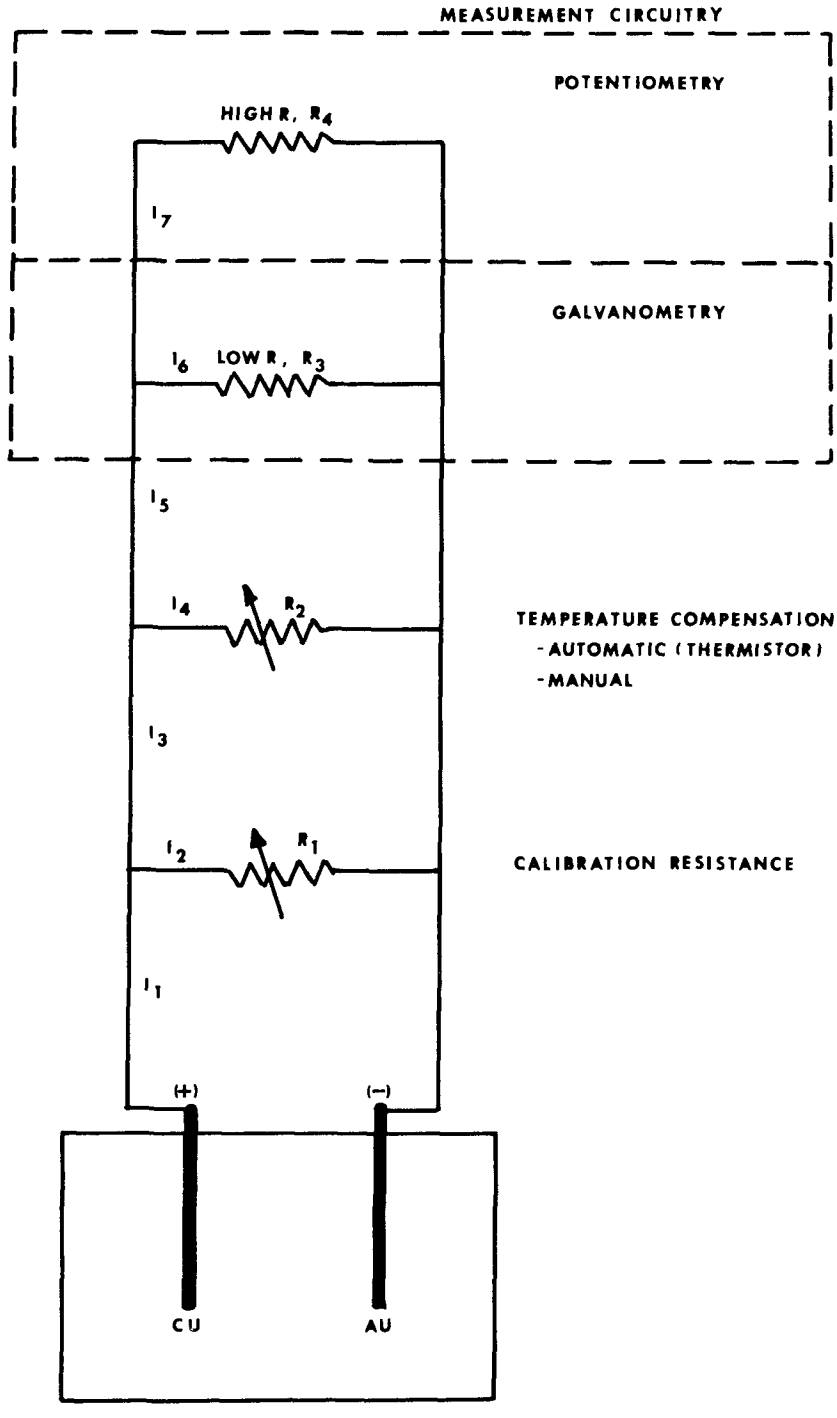

Figure 8. Schematic illustration of residual chlorine analyzer.

Two Capital Controls residual chlorine analyzers, Models 871 for free residual and 872 for total residual, and a Wallace and Tiernan (W&T) amperometric titrator, Series A-790, are used in the mobile laboratory. The Capital Controls analyzers are wall mounted galvanic units, operated continuously. The electrodes are cleaned by 200 polyvinylchloride (PVC) balls rotating in the test stream. A schematic illustration of these units is shown in Figure 9. The manual W&T titrator is used for daily calibration of the continuous analyzers.

Each continuous analyzer has a gold/copper couple. Chlorine is the active electrolyte and produces a current measured with a microammeter. Reagents are introduced to the analytical cell by a cam feeder which operates every ten seconds. Reagent reservoirs are two liter bottles with sufficient capacity for approximately seven days. In both units, a buffer addition adjusts pH of the test water to 4.5, and adjusts ionic strength. The free chlorine analyzer responds directly to free chlorine in the sample stream. A second reagent, potassium iodide, is added in the total chlorine analyzer as a masking agent to convert combined to free forms which can be sensed by the electrode. Preparation of reagents used for monitoring residual chlorine is described in Appendix B.

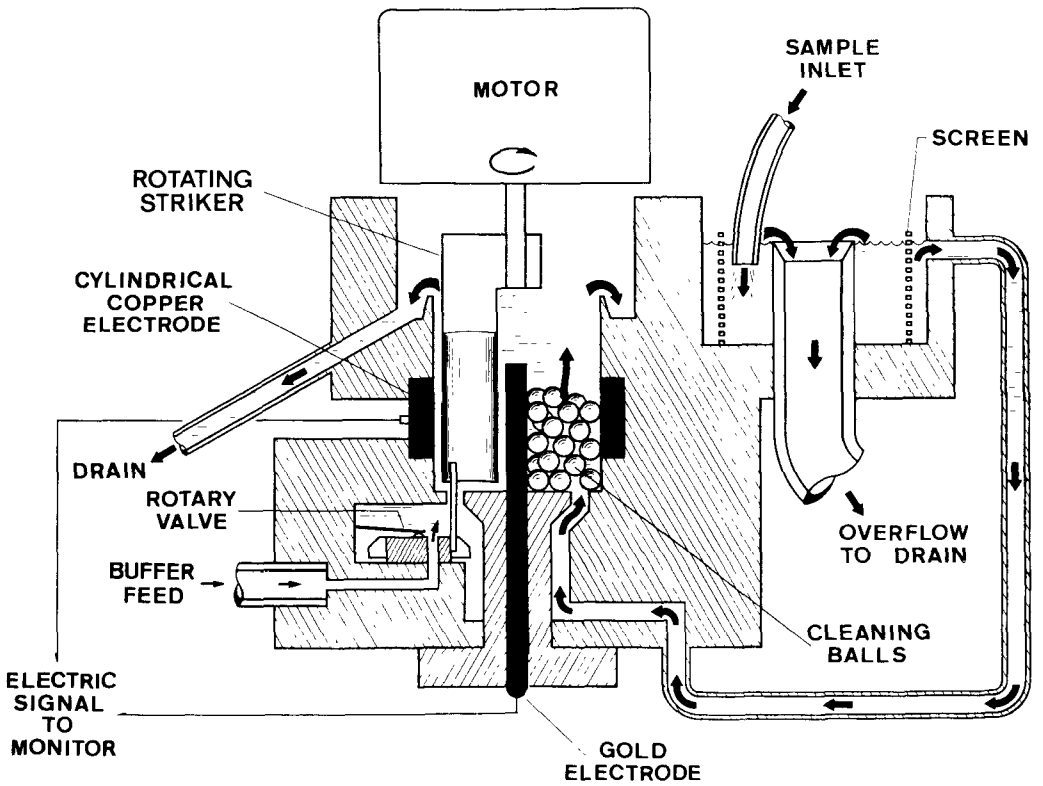

Figure 9. Schematic illustration of Cl_2 analyzer.

Results and Discussion

During more than three and a half months of continuous field operation and up to three years of intermittent operation in the laboratory, the residual chlorine analyzers operated with complete satisfaction. Maintenance was limited to routine weekly preparation of buffer and masking agent reagents and daily calibration.

In Chicago, the first two monitoring sites were on heavily used distribution mains where residence time was normally on the order of 15 to 20 hours, and total chlorine residuals, consistently in the range of 0.7 to 0.9 mg/l. Each of these sites was approximately ten miles from the filtration plant. At the third and fourth monitoring sites, Des Plaines and Calumet Harbor, the unit was located far out, near the ends of the distribution systems. At Des Plaines, the water had been transported nearly 20 miles through main transmission lines and the residence time was unknown. Free chlorine averaged 0.14 mg/l and total chlorine, 0.28 mg/l. At Calumet Harbor, the monitoring site was only eight miles from the water treatment plant, but near the end of a large main used mostly for industrial fire flows. As a result, residence time in the main was approximately 35 hours. Free chlorine at this site averaged 0.24 mg/l and total, 0.40 mg/l over a nine-day period of observation.

Changes in residual chlorine levels during a main flush at the Calumet Harbor site are described on pages 164 and 165.

At Philadelphia International Airport, there was opportunity to evaluate analyzer response to ammoniated samples. Free chlorine ranged from "not detectable" to 0.1 mg/l, and was generally <0.05 mg/l. With no apparent difficulty, the free chlorine analyzer differentiated between free chlorine and loosely combined chloramines. (At the operating pH; i.e., 4.5, the possibility of converting some combined forms to free chlorine was questioned (4).) This observation was confirmed by amperometric titration at pH seven.

At the fourth location in Philadelphia, the Gulf Oil Refinery, sudden variations in chlorine residual were observed. A portion of the recorder output from this site is shown in Figure 10. The capacity of these analyzers to detect sudden changes in both increasing and decreasing concentrations is clear from the output, confirmed by titration at the time of occurrence. The variations were attributed to the mixing of water from two different storage locations.

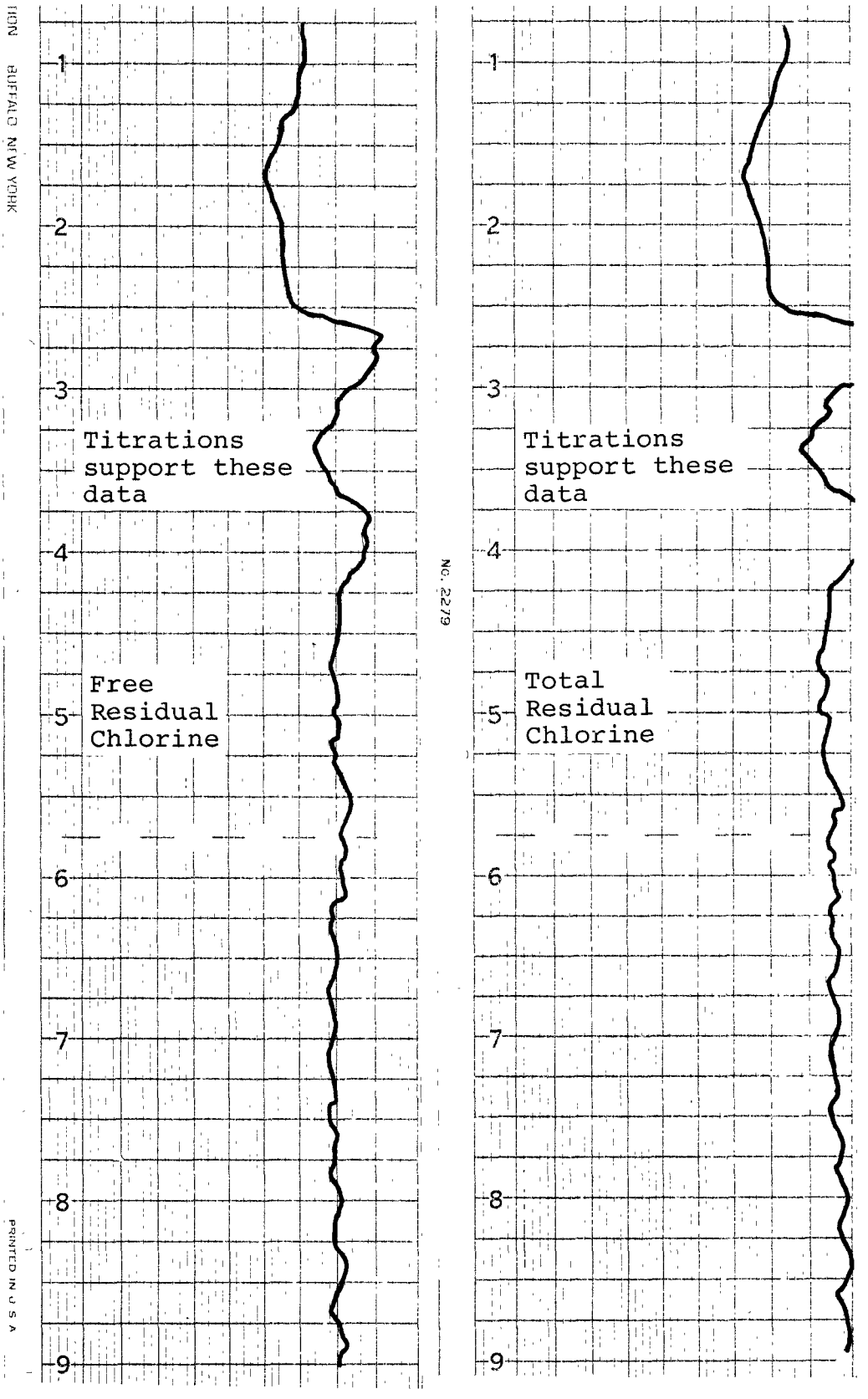

Figure 10. Free and total residual chlorine variations at Gulf Oil, Philadelphia.

TURBIDITY

General

Turbidity is defined as, "an expression of the optical property of a sample which causes light to be scattered and absorbed rather than transmitted in straight lines through the sample" (5). It is caused by the presence of suspended matter in the sample stream. The American Water Works Association has developed a goal of 0.1 Jackson Turbidity Units (JTU) for drinking water (6); the EPA standard is five JTU or less (1).

Experimental

The Hach CR low range turbidimeter, Model 1720, continuous flow nephelometer is used to measure turbidity in the mobile laboratory. The measurement is accomplished by passing a strong beam of light through the sample. Turbidity, present as fine particles, scatters a portion of the light beam which is measured by two photocells submerged in the sample. If the sample is free of turbidity, no light is scattered and no light reaches the measuring cells; conversely, the presence of turbidity in the sample results in light being scattered. Some of this light falls on the photocells, and is registered on the readout meter.

The meter is calibrated with a reflectance rod of 5.0 JTU. Schematic illustrations of the turbidity system and the turbidimeter in the mobile laboratory are shown in Figures 11 and 12.

This system was essentially trouble free throughout its use in the NSF project. Data acquired routinely during field assignments are reported in the respective reports of these activities (7,8,9).

CORROSION RATE

General

Corrosion is a serious-or potentially serious-problem in most potable water distribution systems. Taste, odor, and appearance problems resulting from corrosion of transmission lines may make water unacceptable to the consumer, and corrosion induced pipeline perforations may permit back siphonage of contaminated groundwater into the system.

A major investment of the water supply industry is the distribution network. Continuous effort to produce a water with no tendency toward pipeline corrosion is a principal treatment objective.

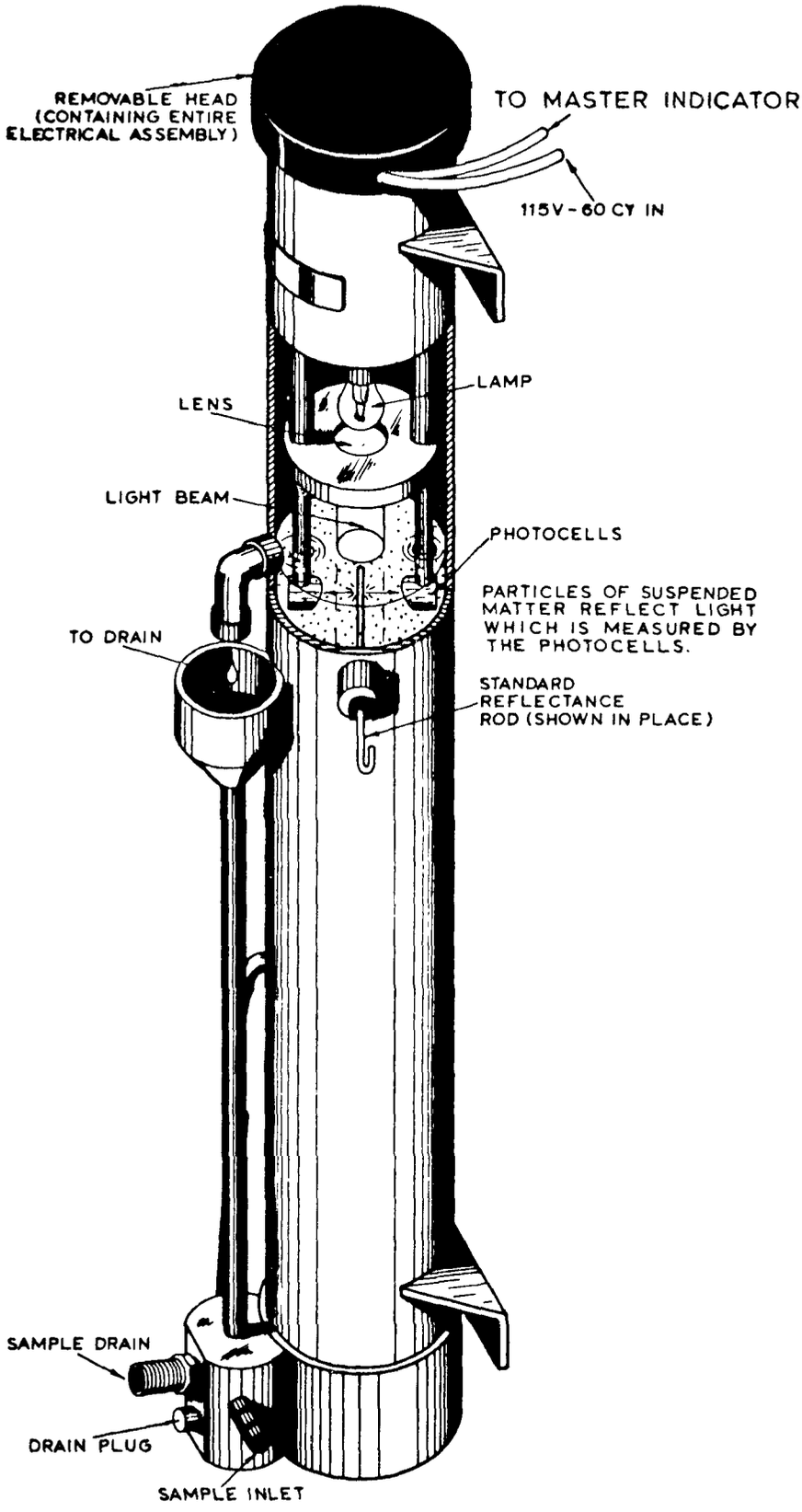

Figure 11. Schematic illustration of turbidity system.

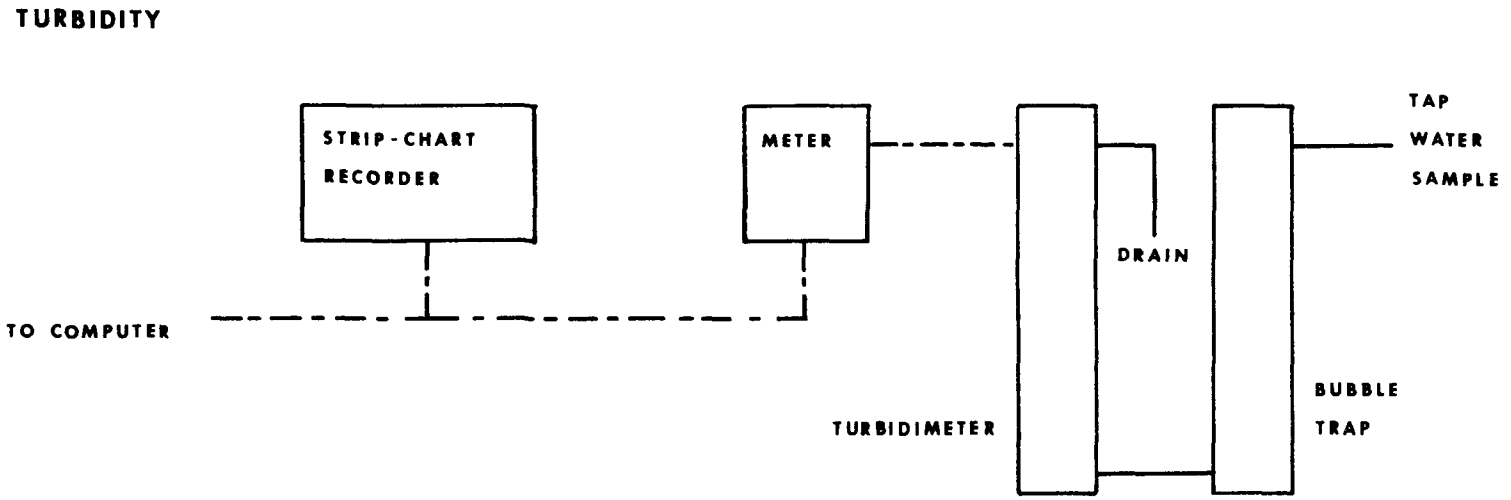

Figure 12. Schematic illustration of turbidimeter in the mobile laboratory.

Theory

Electrode potentials, expressed as intensity measurements of reversible equilibrium conditions, and the Butler equation for electrochemical kinetics, are basic considerations in describing the current-potential relationships associated with corrosion.

It is assumed that equilibrium conditions are maintained in the thermodynamic development of electrode potentials; i.e., there are both charge balance and mass balance in electrode reactions for a metal (electrode) in a solution of its ions:

$$M \rightleftharpoons M^{2+} + 2e^- \tag{30}$$

Thus, at equilibrium, the same velocity occurs regardless of the direction of the reaction. The electrode potential is determined by the metal ion activity, expressed by the Nernstian relationship:

$$E = E^\circ + \frac{RT}{2F} \ln \frac{[O_x]}{[Red]} \tag{31}$$

where:

E = measured electrode potential
E° = standard electrode potential

In corrosion, however, the anodic and cathodic reactions are usually different. Although there is charge balance, there is also mass flux. The anodic mass flux is, in fact, corrosion.

A typical corrosion cell is shown in the following series of equations:

Anodic: $Me \rightarrow Me^{2+} + 2e^-$ (32)

Cathodic: $2H^+ + 2e^- \rightarrow H_2$ (33)

or

$1/2O_2 + H_2O + 2e \rightarrow 4OH^-$ (34)

Thus, there is a net mass flux, hydrogen gas evolves from the system, and corrosion products are formed from metal dissolution. The metal is not at equilibrium potential (as it is in Equation 30). It exists in transient or steady state with its potential a function of the rate determining step in the reaction. If the rate determining step is the anodic process, the potential of the metal shifts in a positive direction; if it is cathodic, excess electrons will accumulate on the metal, causing a negative shift in potential. Because of the kinetic effect and the possibility that another cathodic reactant may be available, a corroding metal surface in neutral solutions rarely acquires equilibrium potential values.

In addition to the energetics of corrosion; i.e., the tendency of a reaction to proceed as measured by its thermodynamic properties, reaction kinetics are vitally important considerations. The basic equation for electrochemical kinetics is expressed as:

$$i_p = i_o \left\{ \exp\left[\frac{\alpha F}{RT}\eta\right] - \exp\left[\frac{(1-\alpha)F}{RT}\eta\right] \right\} \tag{35}$$

where:

i_p = polarization current density
i_o = exchange current density
α = charge transfer coefficient
η = polarization overvoltage

The overvoltage is defined by:

$$\eta = E_i - E_{eq} \tag{36}$$

where:

E_i = electrode potential with an impressed current, i, flowing through the cell
E_{eq} = electrode equilibrium potential (with no external current flowing through the cell)

The exchange current, i_o, represents the spontaneous rates at which the anodic and cathodic reactions are proceeding. Because these are not identical for corrosion conditions, i_o indicates the rate of metal dissolution for the anodic reaction and the rate of the cathodic reaction, whatever it might be.

Thus, i_o is an exact measure of the rate of reaction if the true current density relationship is known. It is difficult to measure because true surface area is not easy to determine. It is usually known within a factor of two, so use of *apparent* surface area in calculating i_o does not invalidate the results.

The effect of major current excursions on naturally corroding metal surfaces is important in measuring corrosion rate by polarization techniques. Once an electrode has been used for a complete polarization curve, its surface has changed irreversibly from its original freely corroding condition. If, however, only small increments of current or potential are applied to the electrode surface, the perturbation to the naturally occurring corrosion rate is small and might not affect the long term corrosion rate of the sample being measured.

Thus, the overvoltage of a reversible electrode reaction is a linear function of the applied current density for values of overvoltage only slightly different from the reversible potential.

This relationship can be developed from Equation 31, using, for small values of x, the approximation:

$$e^x = 1 + x \tag{37}$$

For small values of overvoltage, η, Equation 35 can be rewritten as:

$$i_p = i_o \left\{ \left[1 + \frac{\alpha F}{RT} \eta \right] - \left[1 + \frac{(1-\alpha)F}{RT} \eta \right] \right\} \tag{38}$$

$$i_p = \left(i_o \frac{F}{RT} \right)_{\eta \to o} \tag{39}$$

$$\left[\frac{d\eta}{di_p} \right]_{\eta \to o} = \frac{RT}{F} \cdot \frac{1}{i_o} \tag{40}$$

From the empirical Tafel relationship:

$$\eta = a + b \log i_p \tag{41}$$

where:

a and b = constants for a particular system

$i_p = i_a + i_c$

Equation 40 becomes:

$$\left[\frac{d\eta}{di_p} \right]_{\eta \to o} = \left[\frac{b_a \, b_c}{b_a + b_c} \right] \cdot \frac{1}{2.3 \, i_o} \tag{42}$$

where:

subscript "a" = anodic Tafel slope for b
subscript "c" = cathodic Tafel slope for b

The differential $d\eta/di_p$ is the polarization resistance, expressed as ohms. In corrosion measurements, the term i_o (the exchange current for reversible systems) is replaced by i_{corr}. The corrosion current, i_{corr}, per unit area represents the rate of the corrosion reaction and is directly proportional to weight loss (the classical method for measuring corrosion).

Simplifying Equation 42:

$$\frac{\Delta E}{\Delta I} = \frac{b_a \, b_c}{2.3(b_a + b_c) i_{corr}} \tag{43}$$

or,

$$\log \frac{\Delta E}{\Delta I} = \log \frac{b_a \, b_c}{2.3(b_a + b_c)} - \log i_{corr} \tag{44}$$

Plotting $\Delta E/\Delta I$ versus $\log i_{corr}$ produces a slope equal to -1. When the cathodic reaction is controlled by diffusion, b_c is approximated by infinity, and Equation 44 expressed as:

$$\frac{\Delta E}{\Delta I} = \frac{b_a}{2.3 i_{corr}} \tag{45}$$

or,

$$i_{corr} = \frac{b_a}{2.3} \cdot \frac{\Delta I}{\Delta E} \tag{46}$$

Experimental

A corrosion rate instrument, capable of monitoring the instantaneous corrosion rate of metals in their use-environment, is installed in the mobile laboratory (Figure 13). This instrument, manufactured by the Petrolite Division of Petreco Corporation, uses a "polarization of adjusted known surface area admittance" technique with three identical electrodes machined from the material of interest. In the measurement cycle, a current is imposed between the working electrode and an auxiliary counter electrode sufficient to polarize the test electrode ten millivolts with respect to the reference (third) electrode. The magnitude of the current required to effect the ten mv polarization is directly proportional to the corrosion rate, and is interpreted as mils per year of surface corrosion. In use, this instrument is set up with three active stations. Station one is an internal calibration device used to monitor correct operation of the instrument. Stations two and three are used for actual corrosion rate measurements. For station two, a set of freshly polished electrodes is installed in a flow cell, and corrosion rate measurements are initiated immediately. Data obtained with these electrodes over several days or weeks of monitoring are used to provide information about the rate of attainment of corrosion equilibrium in the test medium. For comparison, a second set of electrodes is sent ahead to a new monitoring site for advance exposure (passivated) to the test water. When the laboratory arrives, these electrodes are installed in the test cell to provide comparative equilibrium corrosion rate measurements.

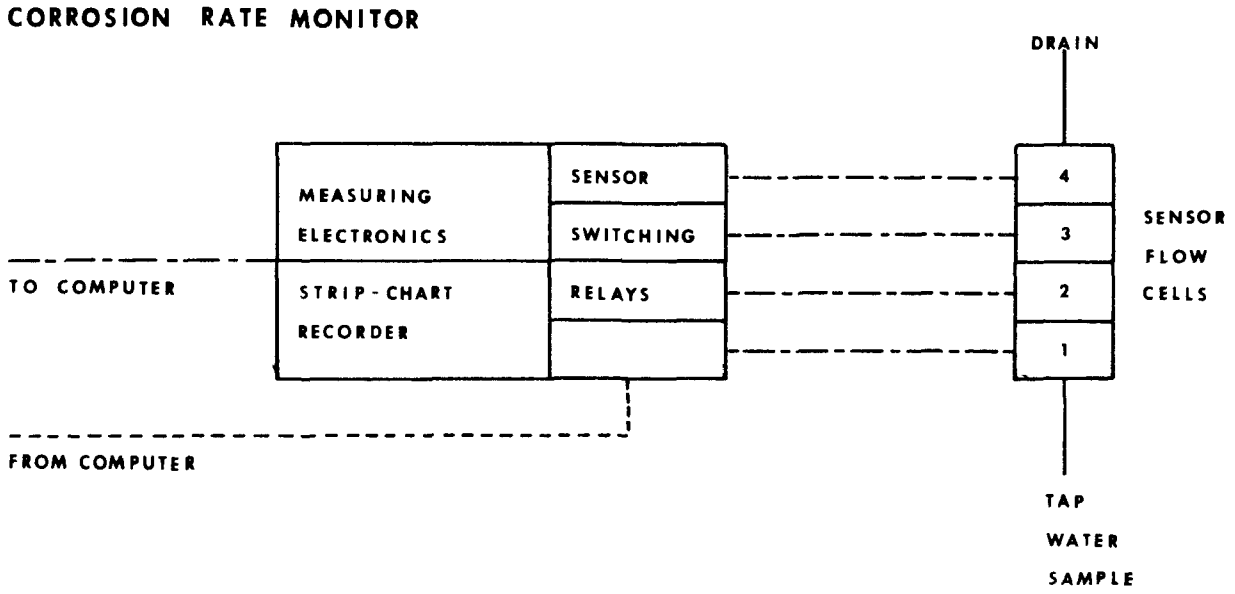

Figure 13. Schematic illustration of corrosion rate monitor in the mobile laboratory.

Results and Discussion

Mechanically, the corrosion rate monitor proved to be a trouble-free system in Chicago; however, significance of the Des Plaines data is questionable, because the electrodes were not passivated in the test waters.

The time required for passivation is a function of corrosion and deposition characteristics of the test water. In Grand Rapids, Michigan, for example, where water is heavily scale forming, passivation is accomplished in a matter of hours. In Ann Arbor, where water is corrosive, months are required.

New (repolished) electrodes were used at three of the four Chicago area test sites. Moving the van on a weekly basis (three of the four locations) precluded passivating and acquiring long-term data with the same electrode systems. In preparing for the Philadelphia trip, new electrodes were sent ahead for passivation in the water in which they were to be used. Because the corrosion rate monitor is a four channel system, passivated and new electrodes can be used simultaneously to develop both kinetic and long-term corrosion rate data.

Unfortunately, the Philadelphia trip produced no meaningful corrosion rate data. The Chicago data were meaningful; i.e., daily mean corrosion rates at the first location ranged from 2.2 to 3.0 mils per year, and at the second location, 2.0 to 2.2 mils

per year. These sites are served by water from the Central Water Filtration Plant (CWFP), where caustic is added for corrosion control. In Des Plaines, the daily mean ranged from 3.8 to 6.8 mils per year, reflecting different mix ratios of Chicago CWFP and Des Plaines treated supplies. At Calumet Harbor, the daily mean was 5.0 to 7.6 mils per year for water treated at Chicago's South Water Filtration Plant (SWFP) where no corrosion inhibitors are added in the treatment process.

These observations suggest that the Petrolite instrument has good potential for application in the water supply industry; however, improvement in its ruggedness and mechanical integrity are recommended.

OTHER SYSTEMS

CALCIUM CARBONATE DEPOSITION TEST

General

Calcium carbonate ($CaCO_3$) deposition is an important consideration in water utility operation. Excessive deposition in the transmission pipeline reduces carrying capacity; conversely, corrosion may occur when no protective film is formed. Either event results in serious economic losses to the community; thus, a practical objective of the water treatment operator is to produce a finished water which will deposit a light protective film in the distribution network.

Theory

Equilibrium Reactions

Water which is either over or undersaturated with respect to $CaCO_3$ tends to undergo chemical change and approach a state of equilibrium. Thermodynamically, this tendency can be expressed in terms of change of free energy (ΔG), as shown in the following reactions:

$$CaCO_{3(s)} \rightarrow Ca^{2+} + CO_3^{2-}$$

$$\Delta G = RT \ln \frac{[Ca^{2+}][CO_3^{2-}]}{K_s} \qquad (47)$$

$$CaCO_{3(s)} + H^+ \rightarrow Ca^{2+} + 2HCO_3^-$$

$$\Delta G = RT \ln \frac{[Ca^{2+}][HCO_3^-]}{K_s[H^+]} \qquad (48)$$

$$CaCO_{3(s)} + H_2CO_3^* \rightarrow Ca^{2+} + 2HCO_3^-$$

$$\Delta G = RT \ln \frac{[Ca^{2+}][HCO_3^-]^2 K_2}{K_1 K_s [H_2CO_3^*]} \tag{49}$$

where:

K_1 = first dissociation constant for $H_2CO_3^*$
K_2 = second dissociation constant for $H_2CO_3^*$
K_s = solubility product of $CaCO_3$
$[H_2CO_3^*]$ = $[H_2CO_3]+[CO_2]$

For oversaturated waters, ΔG is negative; for undersaturated waters, ΔG is positive.

It is common practice to characterize the degree of departure from calcium carbonate equilibrium conditions by calculating the hydrogen ion activity at which, without change in total alkalinity and calcium content, a water would be in equilibrium with solid calcium carbonate (3); i.e.,

$$[H^+]_{eq} = \frac{[Ca^{2+}]_{act}[HCO_3^-]_{act}}{K_s/K_2} \tag{50}$$

The H^+ activity of the test water is correlated with a hypothetical value for H^+. When $[H^+]_{meas} > [H^+]_{eq}$, the water is aggressive with respect to $CaCO_3$; when $[H^+]_{meas} < [H^+]_{eq}$, the water will deposit $CaCO_3$.

Langelier (10) proposed using the difference between measured pH and calculated equilibrium pH as a measure of "stability;" i.e., the tendency of a water to be scale forming or corrosive. He defined the term "saturation index" (SI) as follows:

$$SI = pH_{meas} - pH_{eq} \tag{51}$$

where pH_{eq} is defined from Equation 50 as:

$$pH_{eq} = \log(K_{s/K_2}) - \log[Ca^{2+}]_{act} - \log[HCO_3^-]_{act} \tag{52}$$

The concentration of HCO_3^- can be calculated from analytically measurable parameters; e.g.:

$$[HCO_3^-] = \frac{[Alk]_T - {}^{K_w}/_{[H^+]} + [H^+]}{(1 + {}^{2K_2}/_{[H^+]})} \tag{53}$$

and

$$[HCO_3^-] = X_1 C_T \tag{54}$$

where:

C_T = the analytical concentration for total carbonates

and

$$X_1 = \frac{[HCO_3^-]}{C_T} \tag{55}$$

Within the pH range of many natural waters (7.5 to 9.0), X_1 is close to unity and $[HCO_3^-] \simeq C_T$. Below pH 8.3,

$$[HCO_3^-] = [Alk]_T \tag{56}$$

Larson and Buswell (11) added an ionic strength correction (μ):

$$pH_{eq} = \log(K_s/K_2) - \log [Ca^{2+}]_{act} - \log[Alk]_T + 9.30 + \frac{2.5\sqrt{\mu}}{5.5\mu + 5.3\sqrt{\mu} + 1} \tag{57}$$

Accordingly, from Equation 51, a positive saturation index indicates a scale forming water; a negative index indicates a scale dissolving water.

Another parameter, the "stability index" (S), proposed by Ryzner (12), refers also to equilibrium pH:

$$S = 2pH_{eq} - pH_{meas} \tag{58}$$

According to Ryzner, whose work was principally empirical and based on weight changes of coupons in a test water, waters with a stability index of ≤ 7.5 are scale forming; waters with indices >7.5 are increasingly scale dissolving.

Kinetic Considerations

Calculation of the calcium carbonate stability index, using either Equation 51 or 58, has been widely applied in the water treatment industry; however, there are a number of limitations to this procedure. The calculated index provides information about the extent of departure from equilibrium only; i.e., the directional tendency of a water to deposit or dissolve a calcium carbonate film. Kinetic aspects of water stabilization or rates of attainment of equilibrium are not considered; thus, the rate

and amount of calcium carbonate deposited or dissolved cannot be predicted. It has been demonstrated experimentally that, in the absence of crystallization nuclei, oversaturated solutions of calcium carbonate may remain oversaturated for years (13,14,15). In addition, the presence of Mg^{2+}, polyphosphates, or dissolved organic matter (present in most water supplies) may significantly influence the rate of calcium carbonate precipitation or dissolution. This effect is not necessarily pH dependent.

The effect of Mg^{2+} on the rate of calcium carbonate nucleation was studied by Pytkowicz (13). These studies indicate that magnesium-free artificial seawater yields much shorter times of nucleation (in order of minutes) than natural seawaters (in the order of several hours). Enrichment of water samples with magnesium was found to significantly decrease the rate of calcium carbonate nucleation. This was explained as a result of formation of magnesium carbonate complexes, which are highly stable with higher alkalinities. These complexes are very effective in inhibiting calcium carbonate crystal formation.

Polyphosphates and trace organics interfere with the rate of calcium carbonate deposition because of their tendency to form complexes. This causes a sequestering effect which keeps the calcium ions in solution. This effect can be demonstrated by comparing results of Ca^{2+} determinations using a calcium ion-selective electrode and the EDTA titration technique. The former measures free Ca^{2+} and the latter, total Ca^{2+} concentration. If EDTA titrations are greater than ion-selective electrode measurements, all of the calcium present in the water supply is not in the free ionic form. It is distributed between the free form and a fraction which exists as solubilized complexes, generally organo- or phospho- in nature.

McClanahan (16) studied the role of dissolved oxygen and the mechanism of $CaCO_3$ film formation with respect to cast iron corrosion using a three electrode system, the rotating ring disc electrode.

In the iron corrosion process, the metal undergoes anodic dissolution at iron starved regions (Equation 59), and oxygen is cathodically reduced to hydroxide at oxygen rich regions (Equation 60). The occurrence of hydroxide raises the pH in the vicinity of the corroding metal surface and may cause the ion product of $CaCO_3$ to surpass the solubility limits, depositing $CaCO_3$ on the corroding metal surface:

$$Fe_{(s)} \rightarrow Fe^{2+}{}_{(aq)} + 2e^- \tag{59}$$

$$1/2\ O_2 + H_2O + 2e^- \rightarrow 2OH^- \tag{60}$$

$$2Ca^{2+} + 2HCO_3^- + 2OH^- \rightarrow 2CaCO_{3\,(s)} + 2H_2O \tag{61}$$

Thus, it is clear that a water which is undersaturated with $CaCO_3$ may deposit $CaCO_3$ regardless of its Langlier Index; i.e., in theory, any pipe material capable of supplying electrons may cause $CaCO_3$ to deposit from waters which contain both calcium and carbonate ions.

Rotating Ring Disc Electrode

The rotating ring disc electrode is a voltammetric system with rigorously defined hydrodynamic transport. Consider a flat disc rotating with uniform angular velocity about an axis perpendicular to the plane of the electrode. Because of the centrifugal force acting upon it, the layer of adjacent solution adheres to the disc and acquires a radial flow. The radial flow displacement is accompanied by an axial flow from the bulk of the test solution to the surface of the electrode (17). Figure 14 is a schematic illustration of fluid flow in the rotating electrode system.

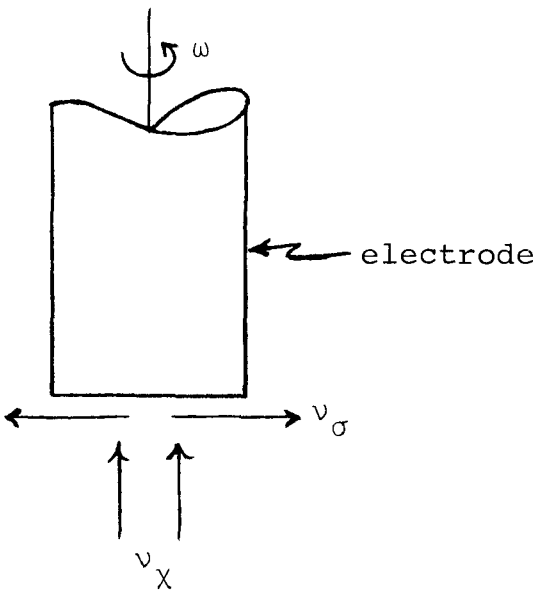

Figure 14. Fluid flow in the rotating electrode system.

Under constant rates of rotation, the thickness of the hydrodynamic boundary layer is a function of the angular velocity of the rotating disc (ω) and the kinematic viscosity of the test solution (ν) (18); thus, mass transport to the electrode surface depends solely on the rate of rotation of the disc electrode.

It is assumed, based on the Nernst diffusion layer theory, that a major part of the concentration gradient occurs across a stagnant liquid layer, the Nernst diffusion layer (S_n)(19). The hydrodynamic boundary layer (S_H) can be equal to or greater than S_n.

The rate of mass transport; e.g., molecular oxygen in CCDT, in the χ direction, normal to the electrode surface, can be expressed as follows:

$$\frac{\partial C}{\partial t} = D \frac{\partial^2 C}{\partial \chi^2} - \nu\chi \frac{\partial C}{\partial \chi} \tag{62}$$

where:

C = dissolved oxygen concentration
t = time
D = oxygen diffusivity coefficient
$\nu\chi$ = axial liquid velocity

Under steady state conditions:

$$\frac{\partial C}{\partial t} = 0 \tag{63}$$

and

$$\nu\chi \frac{\partial C}{\partial \chi} = D \frac{\partial^2 C}{\partial \chi^2} \tag{64}$$

If the rotating disc electrode is maintained at a potential at which the following reaction will proceed:

$$O_2 + 2H_2O + 4e^- \rightarrow 4OH^- \tag{65}$$

the concentration profile shown in Figure 15 will prevail in the vicinity of the electrode.

Because electrolytic reduction of molecular oxygen at the electrode surface (Equation 65) is more rapid than oxygen mass transport, the concentration of oxygen at the surface of the electrode approaches zero ($C_o = C_{\chi \to o}$). In addition, a linear concentration gradient is assumed to exist within the Nernst diffusion layer (Figure 15).

The current flowing in the electrode is proportional to the concentration gradient at the electrode surface, $\left(\left(\frac{\partial C}{\partial \chi}\right)_{\chi \to o}\right)$,

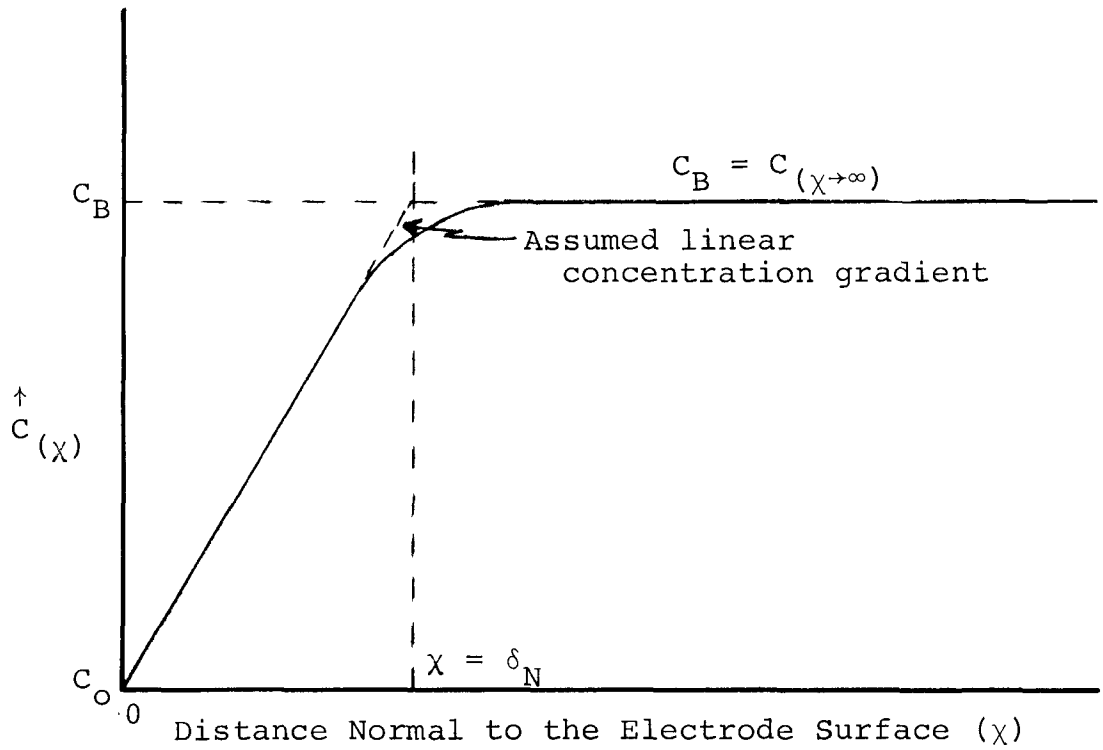

Figure 15. Concentration profile at electrode surface under steady state conditions, in the absence of $CaCO_3$ film.

and can be expressed as:

$$i = nFAD\left(\frac{\partial C}{\partial \chi}\right)_{\chi \to o} \tag{66}$$

where:

- i = diffusion current
- n = number of electrons transferred per mole of reactant
- F = the Faraday constant
- D = diffusion coefficient
- C = concentration of electroactive species
- χ = distance to the electrode surface

Under steady state conditions:

$$\left(\frac{\partial C}{\partial \chi}\right)_{\chi \to o} = \frac{C_B - C_o}{\delta_N} \tag{67}$$

where:

C_B = bulk concentration
C_o = concentration at the electrode surface
δ_N = diffusion layer thickness

If $C_o = 0$, the limiting current is:

$$i_\ell = nFAD \frac{C_B}{\delta_N} \tag{68}$$

The thickness of the diffusion layer can be estimated from (64):

$$\delta_N = kD^{1/3}\omega^{-1/2}\nu^{1/6} \tag{69}$$

Combining Equations 68 and 69:

$$i = K\ nFAD^{2/3}\omega^{1/2}\nu^{-1/6}C_B \tag{70}$$

Thus, according to Equation 70, the current is limited by diffusion in an interfacial Nernst layer, the thickness of which is solely dependent on the angular velocity of the rotating disc. The theory of rotating ring disc electrodes is discussed in much greater detail in the literature (18,20,21,22).

Calcium Carbonate Film Formation

The steady state current for the electrolytic reduction of dissolved oxygen at the surface of the rotating disc electrode remains constant with respect to time, as shown in Curve 1, Figure 16. This is true if P_{O_2}, temperature, and the speed of rotation are constant, and the test solution contains no Ca^{2+}. The oxygen limiting current decreases with time in the presence of Ca^{2+}, and the rate of decrease is directly proportional to the concentration of Ca^{2+}, as shown in Curves 2 through 5, Figure 16. This decrease in current is attributed to the formation of $CaCO_3$ film on the surface of the electrode, according to the following reactions:

$$O_2 + 2H_2O + 4e^- \rightarrow 4OH^- \tag{71}$$

$$OH^- + HCO_3^- \rightleftharpoons CO_3^{2-} \tag{72}$$

$$Ca^{2+} + CO_3^{2-} \rightleftharpoons CaCO_3\downarrow \tag{73}$$

Formation of $CaCO_3$ film on the electrode starts at the center of the disc and grows radially. This observation is compatible with the hydrodynamic regime prevailing at the surface of the electrode. The rate of film growth is proportional to the change of oxygen diffusion current with time. Curves 2 through 5 (Figure 16)

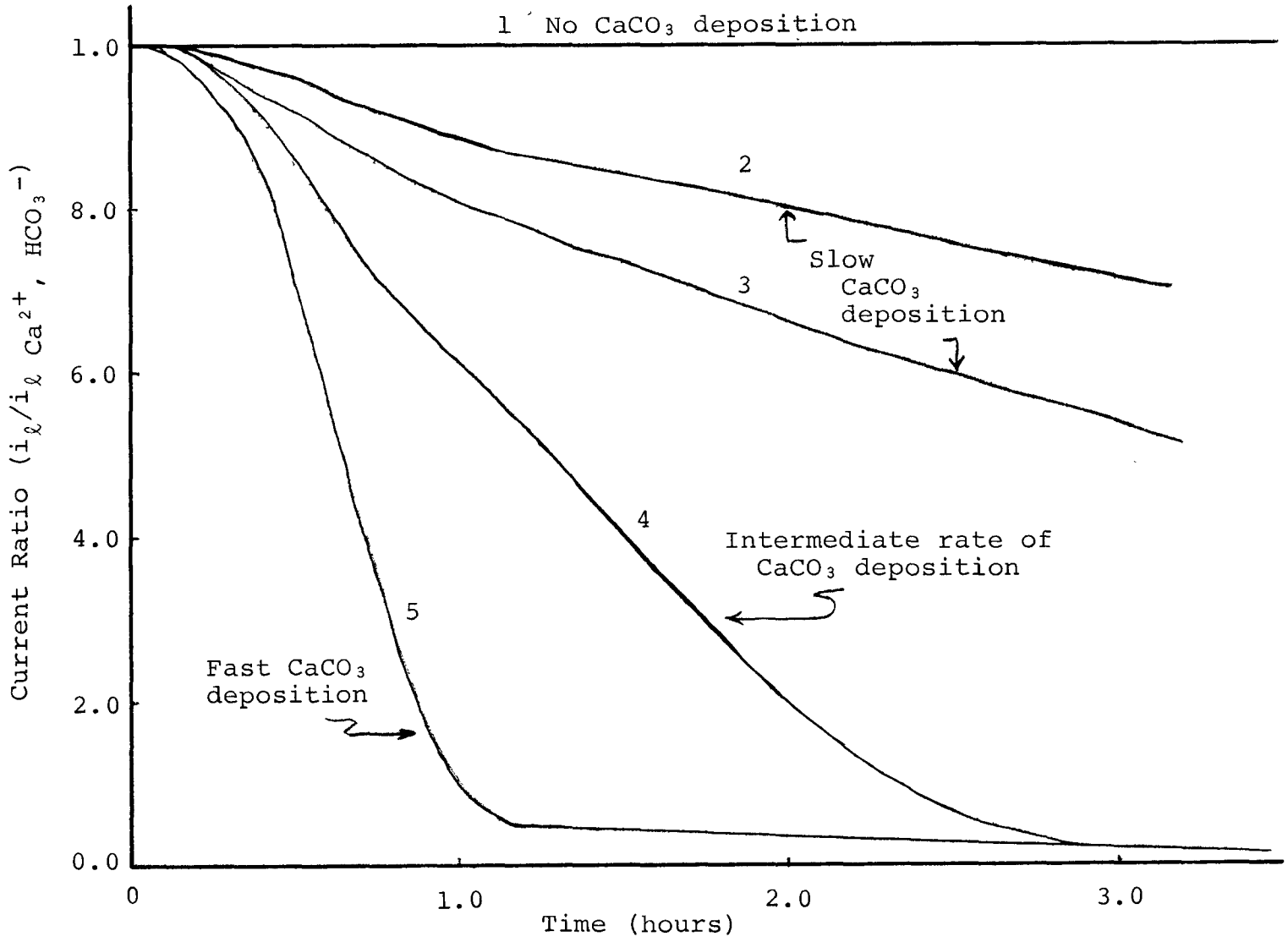

Figure 16. Oxygen current - time curves during $CaCO_3$ deposition.

exhibit an initial transient change in current followed by a steady state or linear decrease, and finally the current reaches a minimum limiting value. At minimum current values, the electrode surface is assumed to be completely covered by $CaCO_3$ film. Acidification or addition of a sequestering agent to the test solution solubilizes the $CaCO_3$ film, returning the current to its original value. The equation for diffusion current in the presence of $CaCO_3$ film is:

$$i = nFA(P_m/\delta_F)C_B \tag{74}$$

where:

P_m = coefficient of $CaCO_3$ film permeability to molecular oxygen
δ_F = thickness of $CaCO_3$ film

It is interesting to note that after the $CaCO_3$ film is formed, both P_m and δ_F are independent of system hydrodynamics. Permeability of the film to molecular oxygen is the limiting step in transfer of oxygen to the electrode surface, and P_m depends only on $CaCO_3$ crystallinity.

Experimental

Column Studies

In 1939, Enslow proposed a "continuous stability indicator" (23,24). A stream of water was slowly but continuously passed through a column of powdered chalk. The pH and titratable alkalinity were measured before and after contact in the column. Changes in these parameters were related to the corrosivity or scale forming capacity of the test water. A contact time of two hours was considered sufficient for the water to be in complete equilibrium with calcium carbonate.

Early in the NSF project, an apparatus similar to Enslow's column was constructed from a 24-inch length of three-inch ID plastic pipe. (See Figure 17.) Test water was recirculated through the column using a peristaltic pump. The column was packed either with marble (calcium carbonate) chips or powdered calcium carbonate. Ion-selective electrodes were used to measure influent and effluent hardness. Changes in pH, even with low flows and high recirculation rates, were very small, never approaching the hypothetical pH_{eq}. Changes in hardness were negligible. It soon became apparent that very long contact times were required for the water to come into equilibrium with calcium carbonate.

A second study was designed to demonstrate the rate of attaining calcium carbonate equilibrium in various waters in contact with different forms of calcium carbonate. In a batch system, waters

Monitored Differences Between Influent and
Effluent pH and Hardness Determines
Stability Index

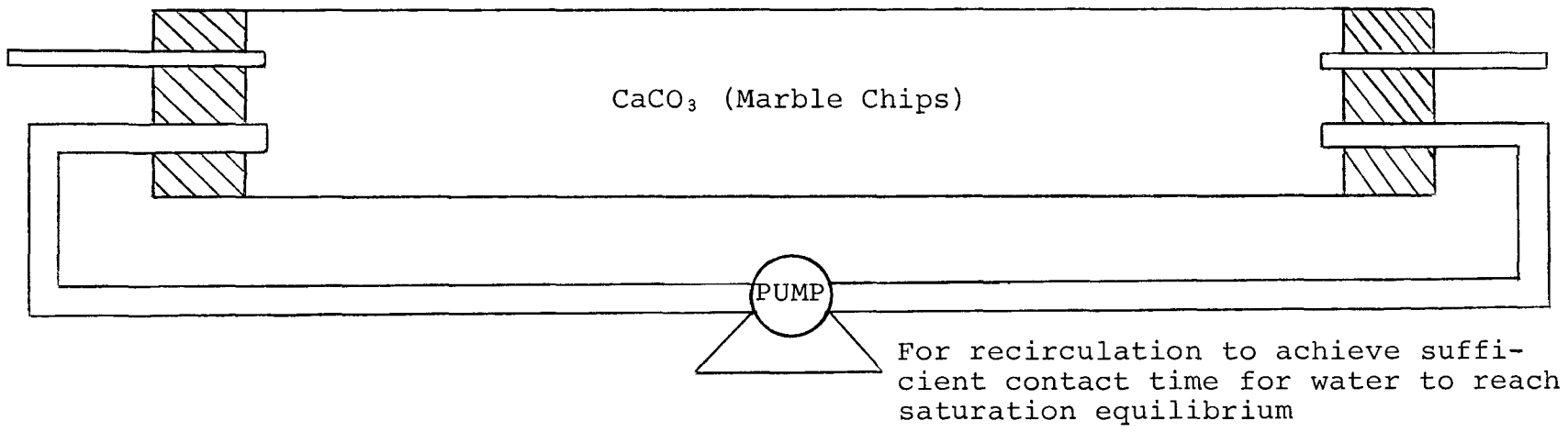

Figure 17. Stability index monitor for saturation equilibrium measurement.

of defined chemical characteristics were mixed at constant rates with marble chips or pure powdered calcium carbonate. Temperature of the test samples was controlled in a water bath at 25 $\pm 0.2°C$. Hardness and pH were measured with respect to time using a glass pH electrode and an Orion divalent cation selective electrode. Attainment of equilibrium was shown to be asymptotic, and pH changes did not closely coincide with changes in $[Ca^{2+}]$. The time required to reach reasonably steady values of pH and $[Ca^{2+}]$ was in the order of 30 to 60 hours.

Calcium Carbonate Deposition Test (CCDT)

Need for a short-term test for measuring the rate of calcium carbonate deposition from a treated water was clearly apparent. The theory of $CaCO_3$ film formation and application of the rotating ring disc electrode provide the basis for CCDT. The rate of $CaCO_3$ film formation is determined from the slope of the linear portion of current-time curves. Calcium hardness, alkalinity, and pH are the basic water quality characteristics concerned with deposition or dissolution of $CaCO_3$.

Instrumentation

Instrumentation for the CCDT includes a Heath potentiostat and current measuring bridge, polarography module Model EU-401-B; a Heath operational amplifier, Model EU19-B; and Heath operational amplifier stabilizer, Model EU19-4. Output is recorded on a Heath, Model EU20-V multi-speed, multi-range strip chart recorder. The electrode/rotator system, shown in Figure 18, is from Pine Instrument Company. A circular flat gold working electrode, the disc (cathode), is surrounded by a thin gold ring, the counter electrode (anode). The electrode system is encased in a molded rod of teflon, carefully machined to eliminate vibration at high rotational velocities. Constant velocity is maintained by the PIR rotator, belt driven by a synchronous motor. The electrode is held in position by the rotator spindle. Both electrode and spindle are electrically insulated from the rotator frame. Electrical connections for potential control and current measurement are made to ring and disc through carbon brushes on brass rotating rings. Different sized pulleys are used to set the rotator speed. The CCDT instrument assembly is illustrated schematically in Figure 19.

Procedure

For discrete samples of tap or formulated water, one liter is placed in a 1.5 liter beaker and covered with Plexiglas. The beaker is placed on a jack stand and raised to the electrodes, placed through carefully dimensioned holes in the cover. PCO_2

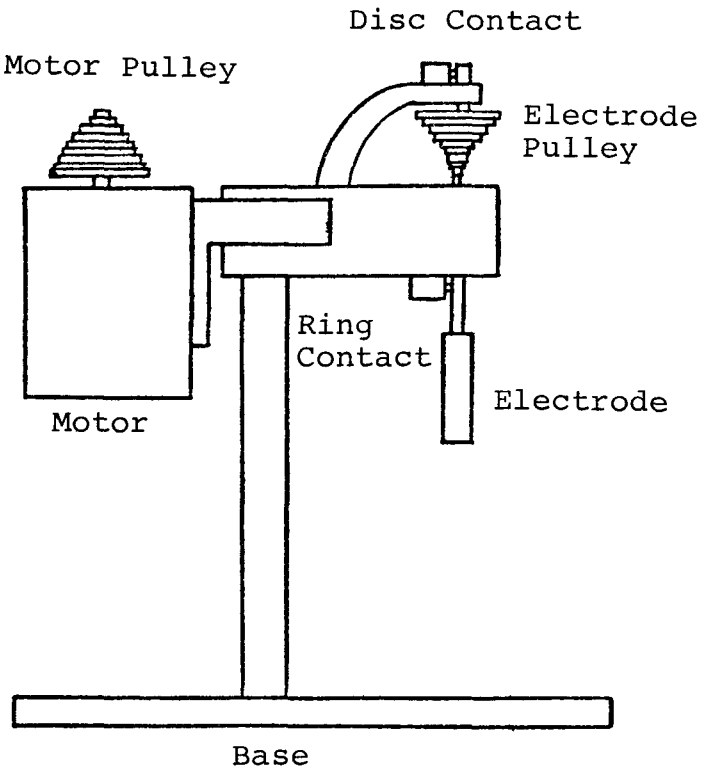

Figure 18. PIR rotator - electrode system.

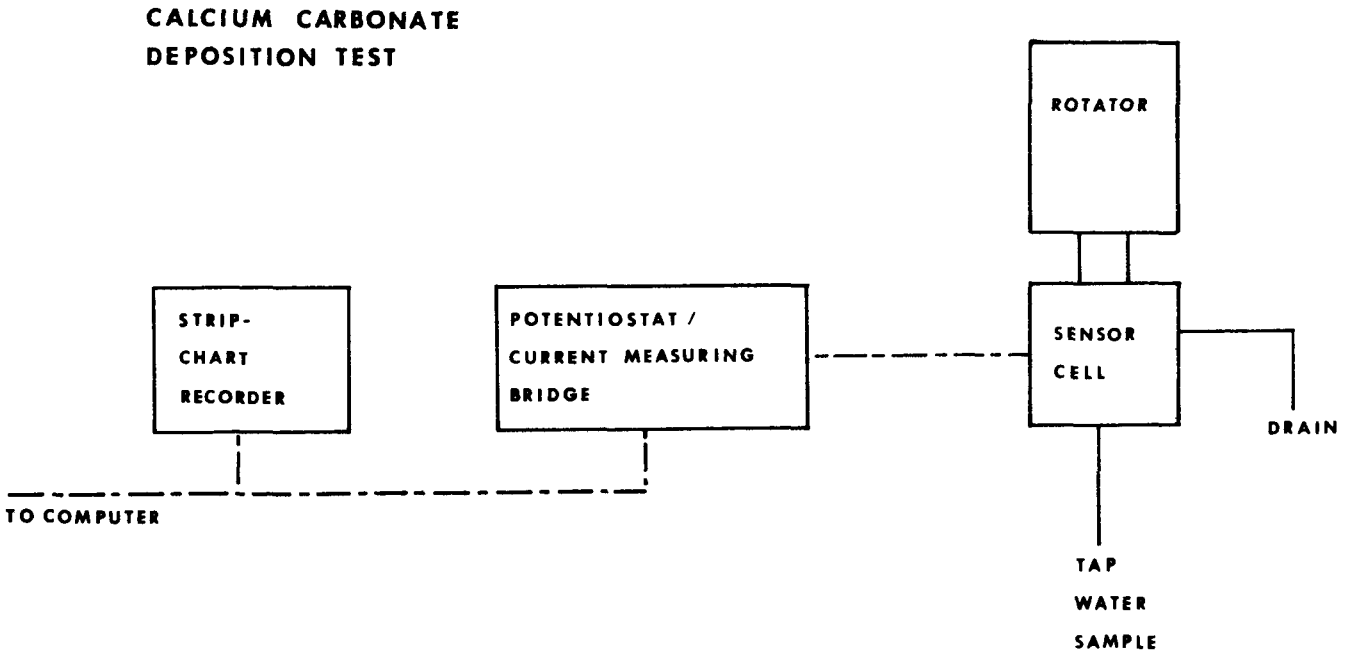

Figure 19. CCDT system in the mobile laboratory.

is controlled by mixing CO_2 with air - from which CO_2 has been scrubbed by bubbling through a solution of concentrated NaOH - in a Matheson 665 gas proportioner, and monitoring pH with a glass electrode system inserted in the sample cell.

When the test is initiated, 100 ml of the test water is immediately withdrawn from the sample cell for analysis of hardness, calcium, alkalinity, and pH.

Rotational speed of the electrode is 1600 rpm. This speed was selected as a compromise between the needs for maintaining constant hydrodynamic conditions at the surface of the electrode and mixing in the bulk of the solution, and the turbulence associated with high rotational velocities. At 1600 rpm, there is little turbulence in the test solution. Speeds greater than 1600 rpm provide no additional increase in diffusion current attributable to changes in mass transport of oxygen to the electrode surface.

The potential at which the cathode is controlled, -0.9 V versus S.C.E., is the potential at which the smallest change in current is observed over the largest region of change in potential. A recording of current as a function of potential sweep, used to determine the operating potential, is shown in Figure 20. The test is continued for a period sufficient to establish the linear portion of the current decay curve. CCDT is reported as the slope of the linear portion of the curve, in microamps per minute.

During field operation of the mobile laboratory, CCDT was measured in a covered continuous flow cell in which the test water entered at the bottom and overflowed through a port at the top. pH control is not required in the continuous flow system.

Results and Discussion

Plots of diffusion current versus time for a series of formulated water samples are shown in Figure 21. Chemical characteristics of each of these samples are shown in Table 4. Curves 1 and 5 in Figure 21 were obtained from waters with Ryzner Stability Indices (S)=6.92 and 6.95 and CCDT values of 10.08 and 11.32 μamps/min, respectively. These waters are expected to be scale forming. Curve 2 is from a water with S=8.76 and CCDT=0.8 μamps/min, a water expected to be corrosive to $CaCO_3$. Curves 6, 7, and 8 are from waters with moderate scale forming characteristics, as shown by their significant values of CCDT.

CCDT versus S for each of the formulated water samples is plotted in Figure 22. The utility of CCDT as a rapid technique for measuring scale forming tendency is clearly demonstrated by the high correlation of these data.

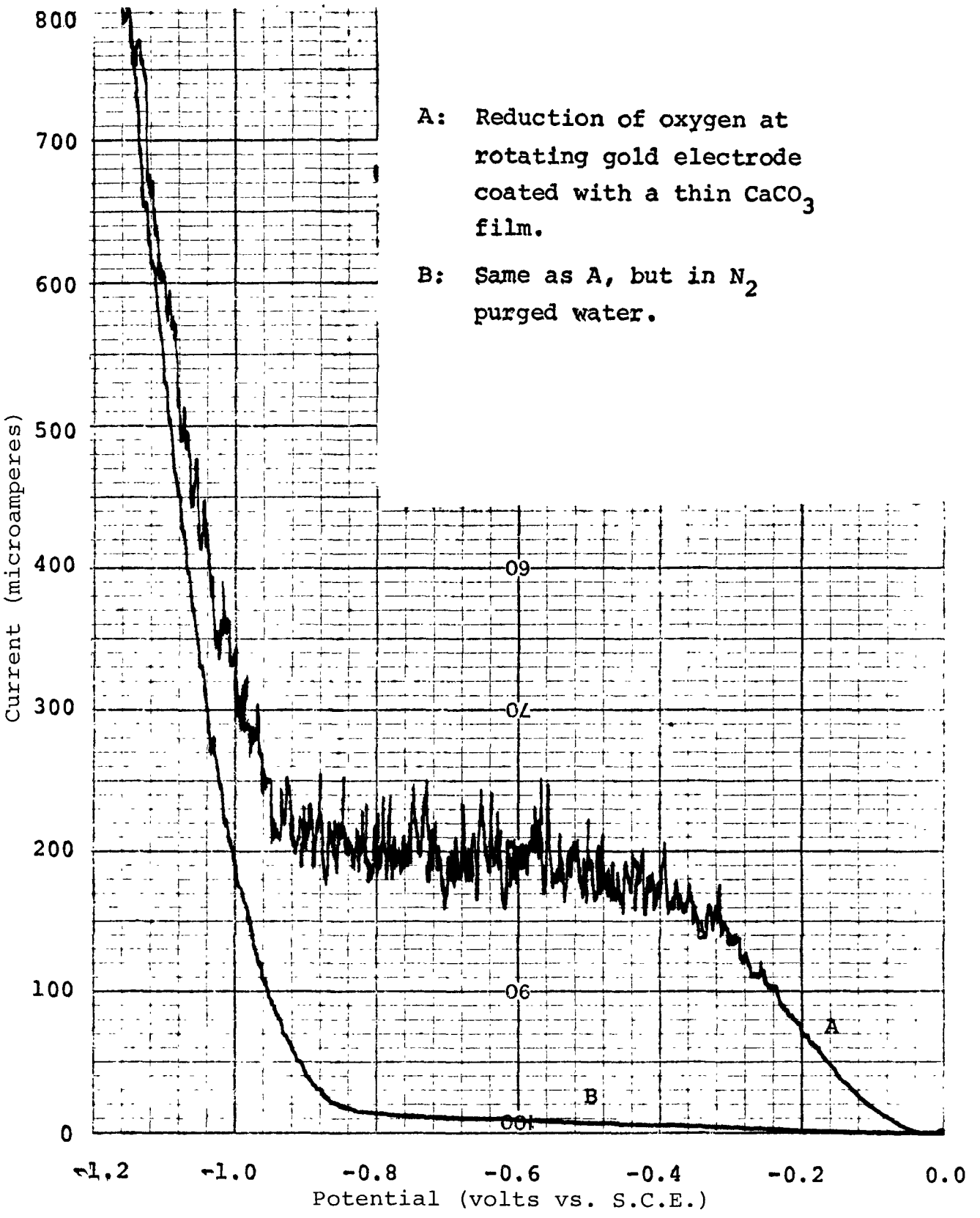

Figure 20. Current versus potential sweep.

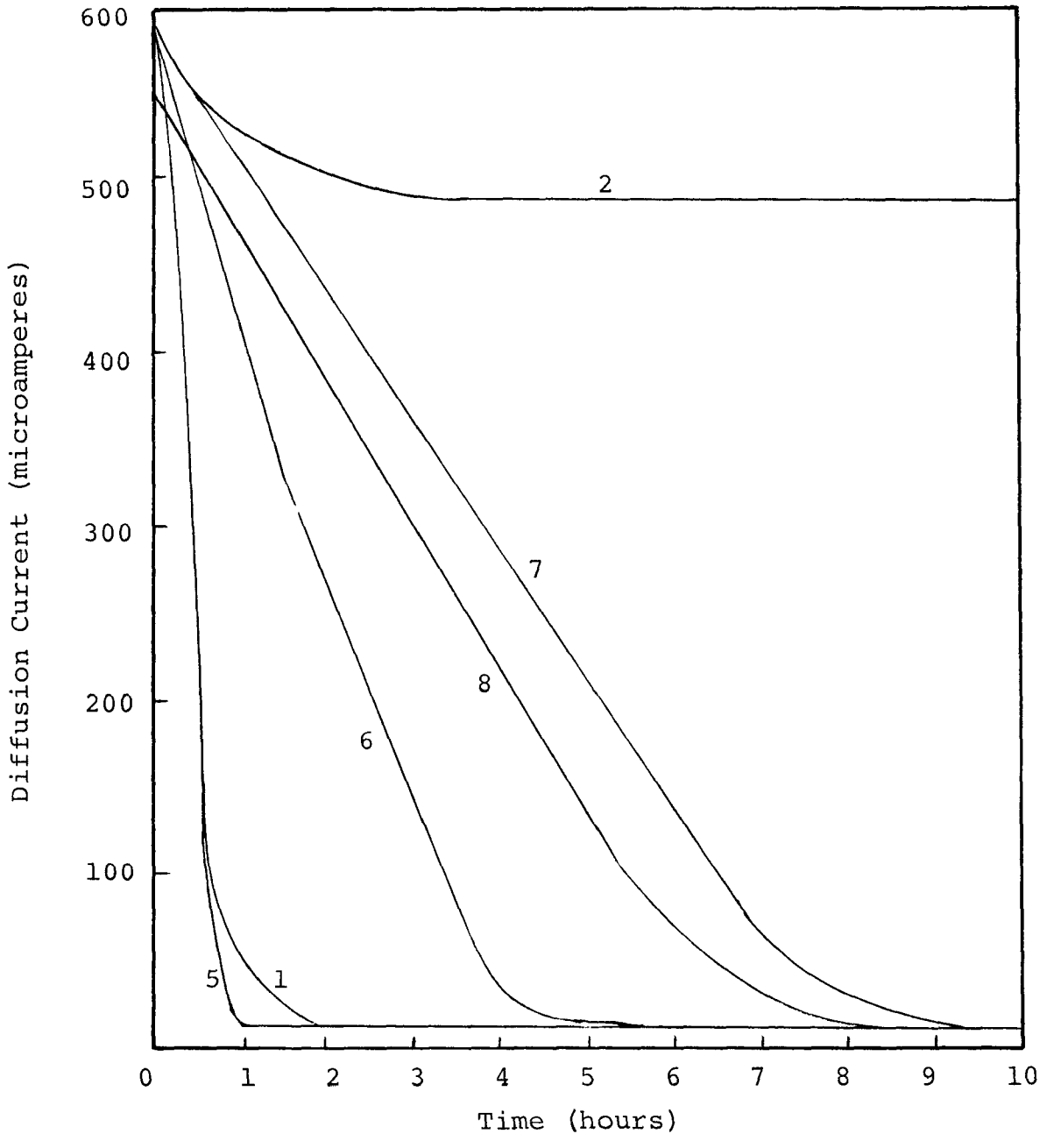

Figure 21. Calcium carbonate deposition test. Effect of initial solution composition on rate of film formation.

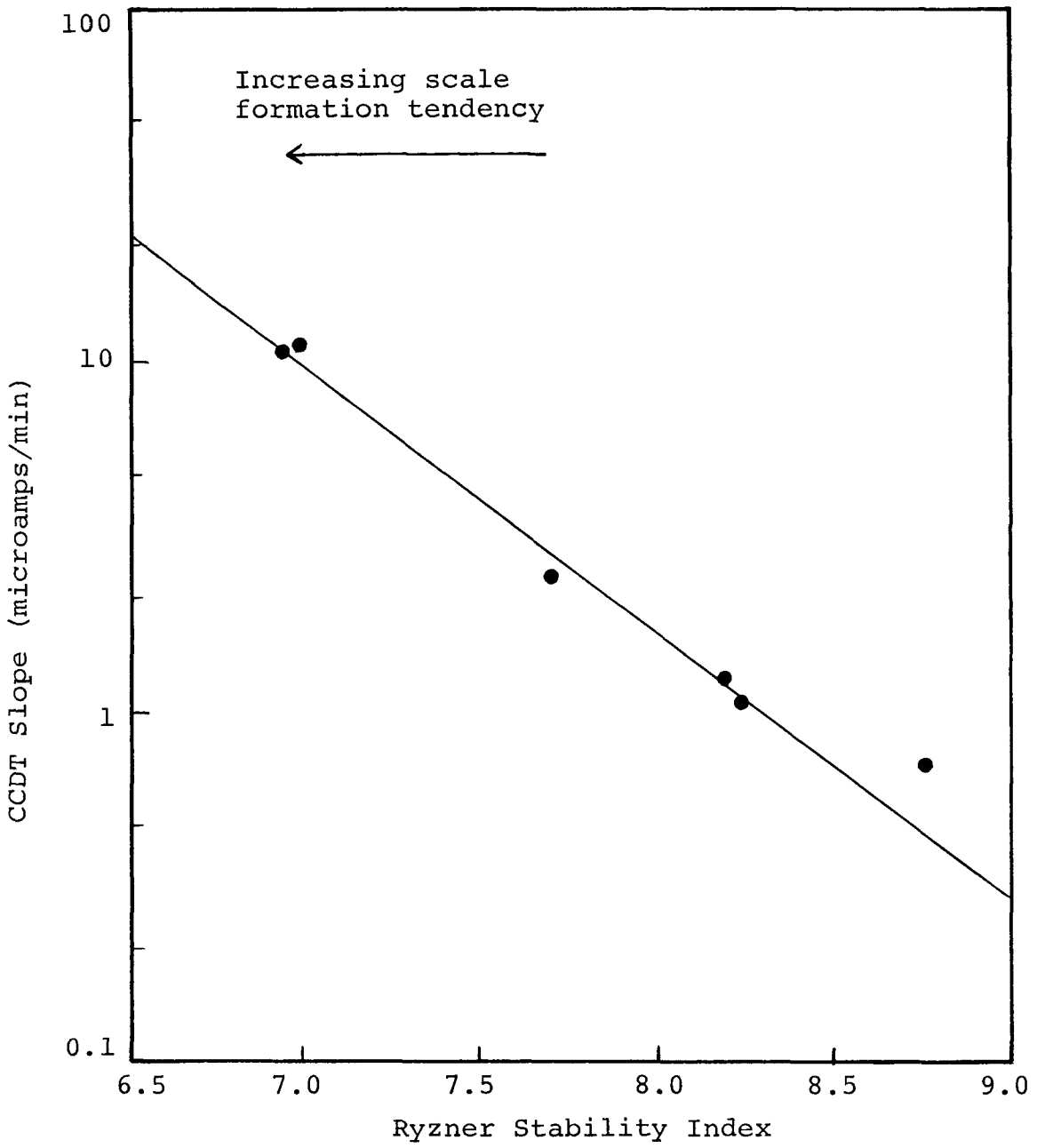

Figure 22. Correlation of CCDT slope with Ryzner stability index.

Table 4. SUMMARY OF DATA FROM ANALYSES OF TEST SOLUTIONS

Curve Identification (Figure 2.)	Hardness (mg/l as C_aCO_3	Calcium (mg/l)	Total Alkalinity (mg/l as C_aCO_3	Solution pH Measure	Langelier pHs	Langelier Saturation Index (SI)	Ryzner Stability Index (S)	Diffusion Current Slope (μamps/minute)
1	221	88.5	59.0	8.22	7.92	+0.65	6.92	10.08
2	230	92.0	14.5	7.56	8.52	-0.60	8.76	0.87
5	174	69.5	65.0	8.31	7.99	+0.68	6.95	11.32
6	192	77.0	34.4	8.03	8.22	+0.17	7.70	2.25
7	88	35.2	40.4	8.08	8.49	-0.06	8.20	1.24
8	123	49.2	35.2	7.92	8.40	-0.13	8.18	1.43

The effect of pH and levels of calcium and bicarbonate ions on CCDT was evaluated with solutions of $Ca(HCO_3)_2$ at pH=6.5, 7.5, and 8.3. In each of these solutions, bicarbonate concentration was four times greater than the levels of calcium. The solutions were prepared by mixing $CaCl_2$ and $NaHCO_3$, and bubbling with a mixture of oxygen, nitrogen, and carbon dioxide. Bubbling was continued throughout the test to maintain a constant pH. Results of these analyses, plotted in Figures 21 and 22, demonstrate that relationships do exist between CCDT and pH, Ca^{2+}, and HCO_3^- levels in a test water.

Tap water samples, brought to the laboratory from a number of Michigan cities as well as those included in the mobile laboratory field assignments, showed a wide variety of scaling characteristics, measured by CCDT. These data with pertinent chemical characteristics of each test water are shown in Table 5. CCDT values for each of the 18 samples in Table 5 are plotted versus S as semilogarithmic coordinates in Figure 23. The numbers circled in Figure 23 coincide with sample numbers assigned in Table 5. Dotted lines in Figure 23 separate the grid into regions representing varying degrees of scale formation. With CCDT values >3, waters are known to form films which reduce carrying capacities of transmission lines. From CCDT >0.75 but <3.0, films may be deposited which will, in time, affect carrying capacities; however, small amounts of inhibitors added to the water will significantly reduce the problem. Waters with CCDT values between 0.2 and 0.75 can be expected to produce thin hard films of $CaCO_3$ which will effectively protect against corrosion.

The most apparent departure between observed and predicted scaling using the Ryzner Index occurred at pH >9; i.e., lime softened waters designated 4, 6, 8, and 9, and a Zeolite softened water, sample 1. The Zeolite treated water has high pH and high alkalinity; thus, S was low although calcium hardness was reduced to 15 mg/l. This water was not scale forming and no CCDT slope was observed, but $S \simeq 6.6$ predicted excessive scale formation. The occurrence of S values overpredicting scale formation; i.e., S indicates excessive scaling when none is observed, is not uncommon for finished waters with high pH.

Field Experience

During field assignment of the mobile laboratory in the metropolitan Chicago area, unique opportunity was provided to evaluate the responsiveness of CCDT to water quality changes in the distribution system. Caustic is added routinely at the Central Water Filtration Plant (CWFP) for corrosion control. For the 24-hour period beginning at 1200 hours on May 30, 1973, caustic feeders were taken out of service. The mobile laboratory was operating at a four year old fire station, 10.5 miles from the CWFP. Two continuous flow CCDT measurements were made each day.

Table 5. RESULTS OF FIELD STUDIES

	Total Hardness	Calcium	Magnesium	Total Alkalinity	pH	pHs	CCDT	LSI	RSI	PO_4 Addition
Howell, MI	38.3	15.	0.	322.	8.60	7.59	None	+1.01	6.58	N
Saline, MI	350.0	79.	37.	296.	7.65	7.57	4.80	+0.12	7.49	N Sample Before PO_4^{3-}
Jackson, MI	385.0	106.	29.	340.	7.45	7.38	18.50	+0.07	7.31	N
Ann Arbor, MI	128.0	30.	13.	46.	9.74	8.91	None	+0.83	8.08	Y After PO_4
Detroit, MI	105.0	31.	7.	80.	8.45	8.55	.53	-0.10	8.65	N
Ypsilanti, MI	102.0	33.	5.	32.	10.25	8.91	None	+1.34	7.57	Y
Grand Rapids, MI	133.0	34.	12.	93.	8.20	8.44	1.22	-0.24	8.68	N
Adrian, MI	125.0	26.	15.	38.	10.05	8.98	.17	+1.06	7.91	N
Lansing, MI	84.0	18.	10.	36.	9.47	8.72	None	+0.75	7.97	?
Ann Arbor Twp., MI	393.0	99.	36.	312.	7.50	7.36	17.50	+0.14	7.22	N
Petersburg, MI	420.0	110.	40.	182.	7.30	7.64	4.70	-0.34	7.98	N
Chicago, IL (CWFP)*	124.0	33.	10.	106.	8.09	8.39	.54	-0.30	8.69	N
Chicago, IL (SWFP)*	119.0	34.	8.	101.	7.93	8.41	.32	-0.48	8.89	N
Philadelphia, PA*	112.0	33.	7.	49.	8.75	8.73	.22	+0.02	8.71	N
YSH No. 8	167.0	36.	18.	222.	7.30	7.38	1.45	-0.08	7.46	N
YSH, comp	119.0	26.	13.	196.	7.59	7.57	.90	+0.02	7.55	N
Ann Arbor, MI (T.P.)	101.0	23.	11.	50.	9.87	8.48	.26	+1.39	7.09	N Sample taken at treatment plant before additon of PO_4
Saline, MI	350.0	91.	30.	298.	7.38	7.12	.40	+0.26	6.86	Y Sample after PO_4^{3-}

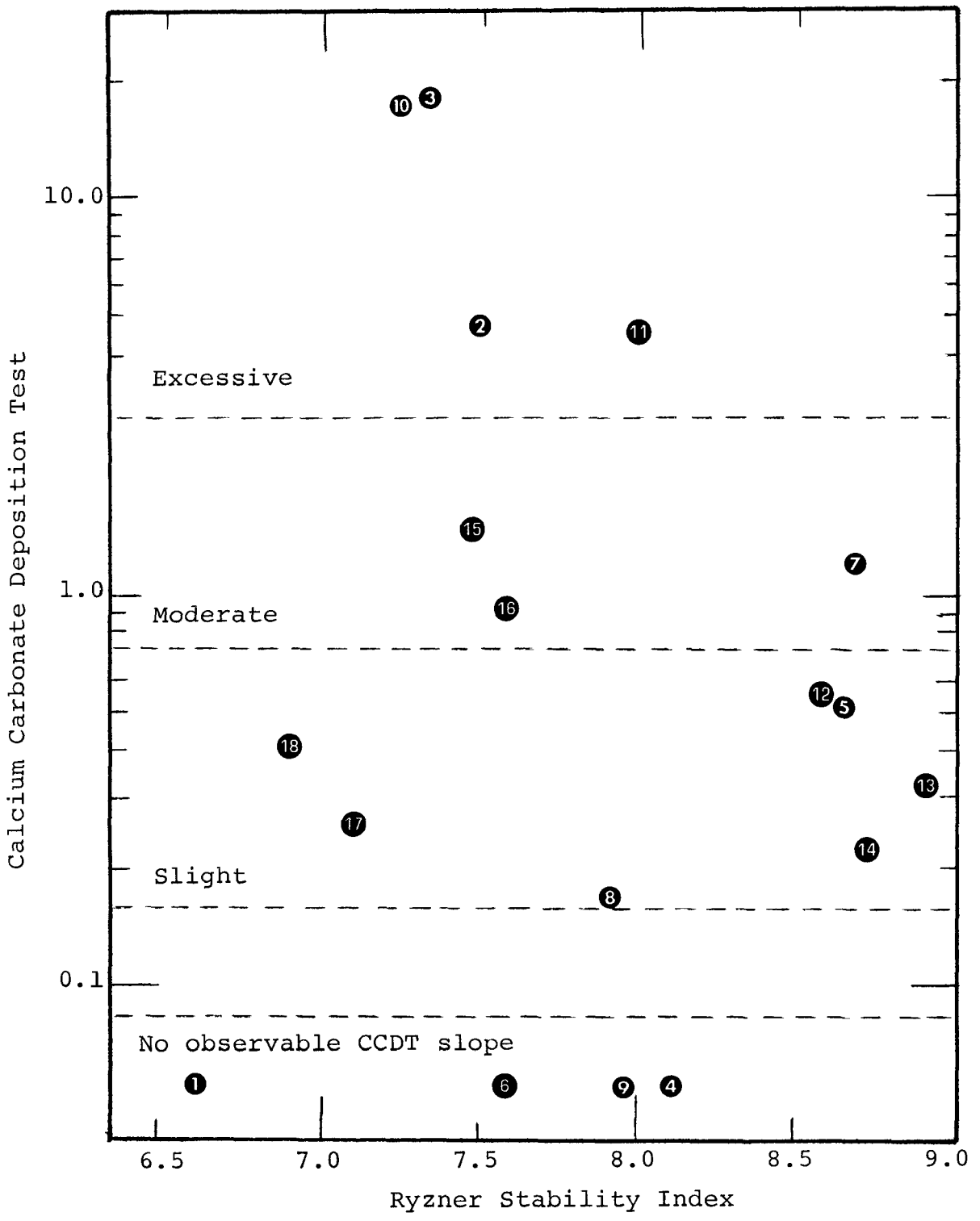

Figure 23. CCDT versus Ryzner stability index.

Arrival of the distributed caustic-free water at the mobile lab was marked by changes in observed levels of pH and CCDT. Mean CCDT for the previous day (May 29) was 0.52. The lowest daily mean CCDT, 0.26, occurred on May 31. On June 3, a mean CCDT of 0.47 indicated that water with caustic had returned to the area. At CCDT ≈ 0.50, light hard protective film formation is assured. The low mean CCDT (0.26) indicated that more corrosive water was present in the lines. These data are plotted in Figure 24.

In extensive laboratory and field applications of CCDT, this test was shown repeatedly to be capable of accurately predicting, without respect to the metallic corrosion reaction, whether or not films of $CaCO_3$ would form on the surface of distribution system pipelines.

ALKALINITY

General

An automated potentiometric technique for measuring total alkalinity in tap water was developed in this study. The method was fully evaluated in the laboratory and used successfully in the mobile laboratory during field assignments. As a result of apparent faulty operation on Cincinnati tap water which has high levels of residual chlorine, detailed theoretical relationships were developed and the procedure slightly modified.

Theory

A linear relationship exists between the resultant pH of a suitably selected phthalate buffer solution (KHP) and the total carbonate formality of a test water. Theoretical aspects of this relationship are described using an example test water. Assume the alkalinity of the test water is in the range 30 to 60 mg/l as $CaCO_3$ ($3(10)^{-4}$ to $6(10)^{-4}$ F CO_3^{2-}). It has been shown experimentally that five parts of the test water and one part stock phthalate buffer produce the linear relationship between resultant pH and sample alkalinity. Initial formalities of the buffer are:

$$KHP = 0.050$$
$$HCl = 0.019$$

and of the test water:

$$Na_2CO_3 = 6/5\ C$$

and final formalities for the mixture (buffer:sample = 1.5) are:

$$KHP = 8.33(10)^{-3}$$

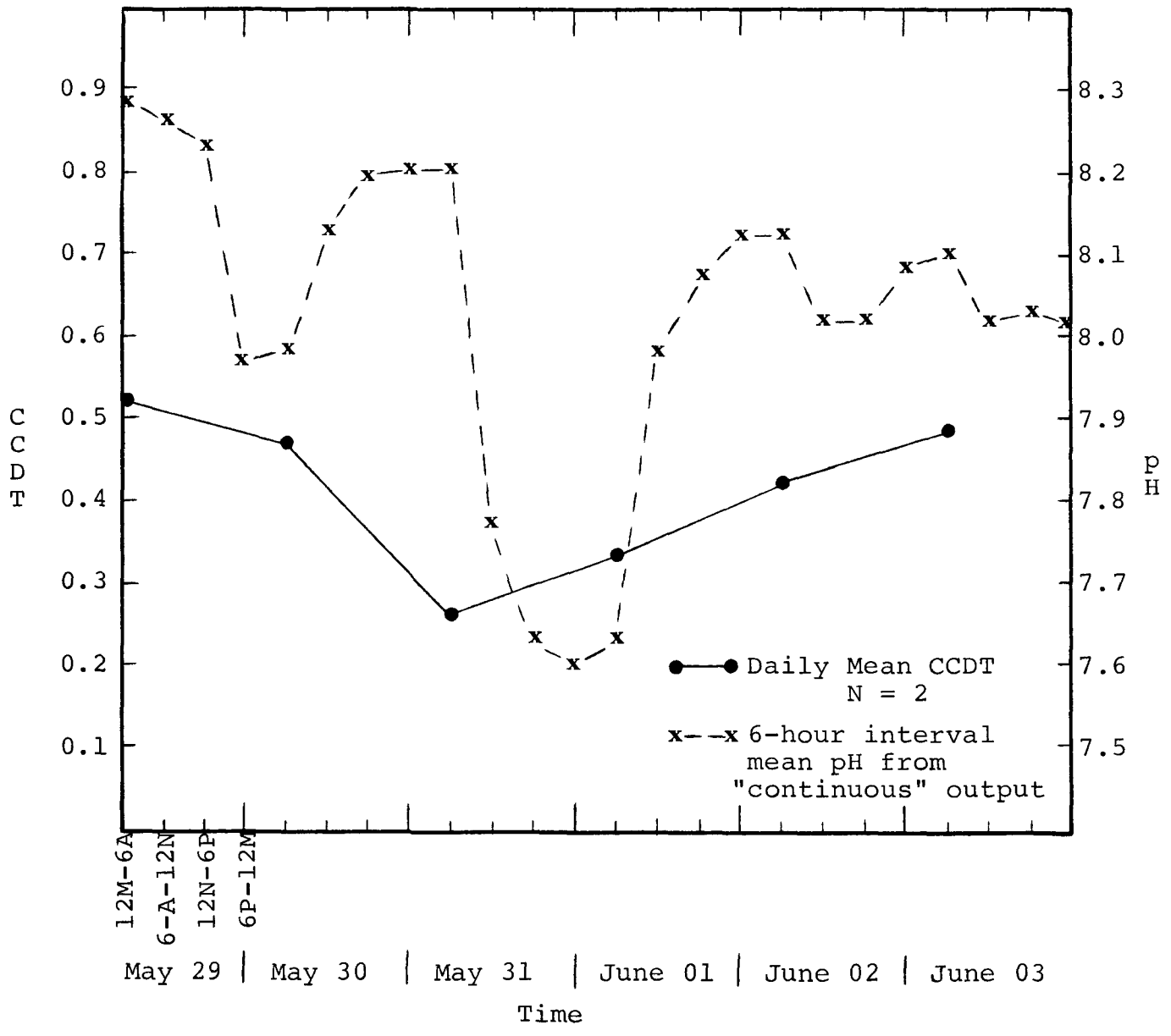

Figure 24. Effect of caustic feeder cycling at Chicago CWFP on CCDT and pH monitored at Site No. 1, Chicago/Lehigh.

$$HCl = 3.17(10)^{-3}$$
$$Na_2CO_3 = C$$

$[H^+]$ can be calculated as a function of C, applying the following series of known relationships:

$$K_1 = \frac{[H^+][HP^-]}{[H_2P]} = 1.3(10)^{-3} \quad (75)$$

$$K_2 = \frac{[H^+][P^{2-}]}{[HP^-]} = 3.9(10)^{-6} \quad (76)$$

$$K_3 = \frac{[H^+][HCO_3^-]}{[H_2CO_3]} = 4.6(10)^{-3} \quad (77)$$

$$K_4 = \frac{[H^+][CO_3^{2-}]}{[HCO_3^-]} = 4.4(10)^{-11} \quad (78)$$

$$K_W = [H^+][OH^-] = 10^{-14} \quad (79)$$

$$[Cl^-] = 3.17(10)^{-3} \quad (80)$$

$$[K^+] = 8.33(10)^{-3} \quad (81)$$

$$[Na^+] = 2\ C \quad (82)$$

$$[H_2CO_3] + [HCO_3^-] + [CO_3^{2-}] = C \quad (83)$$

$$[H_2P] + [HP^-] + [P^{2-}] = 8.33(10)^{-3} \quad (84)$$

$$[H^+]+[Na^+]+[K^+] = [OH^-]+[Cl^-]+[HP^-]+ 2[P^{2-}]+[HCO_3^-]+ 2[CO_3^{2-}] \quad (85)$$

By assuming $[CO_3^{2-}] = 0$, $[P^{2-}] = 0$, and $[OH^-] = 0$, derivations can be stated as follows:

from Equation 77:

$$[H_2CO_3] = \frac{[H^+]}{K_3}[HCO_3^-] \quad (86)$$

from Equation 75:

$$[H_2P] = \frac{[H^+]}{K_1}[HP^-] \quad (87)$$

from Equations 83 and 86:

$$[HCO_3^-]\left\{\frac{[H^+]}{K_3} + 1\right\} = C \quad (88)$$

and

$$[HCO_3^-] = \frac{4.6(10)^{-3}\ C}{[H^+] + 4.6(10)^{-3}} \tag{89}$$

from Equations 84 and 87:

$$[HP^-] \left\{ \frac{[H^+]}{K_1} + 1 \right\} = 8.33(10)^{-3} \tag{90}$$

and

$$[HP^-] = \frac{1.083(10)^{-5}}{[H^+] + 1.3(10)^{-3}} \tag{91}$$

from Equations 79, 81, 82, 85, 89, and 91:

$$[H^+] + 2\ C + 8.33(10)^{-3} = 3.17(10)^{-3} + \frac{1.083(10)^{-5}}{[H^+] + 1.3(10)^{-3}} + \frac{4.6(10)^{-3}C}{[H^+] + 4.6(10)^{-3}} \tag{92}$$

then:

$$\text{L.C.D.} = \left\{[H^+] + 1.3(10)^{-3}\right\} \left\{[H^+] + 4.6(10)^{-3}\right\} \quad [H^+]^2 + 5.9(10)^{-3}[H^+] + 5.98(10)^{-6} \tag{93}$$

where:

L.C.D. ≡ lowest common denominator

$$[H^+]^3 + 2C[H^+]^2 + 5.16(10)^{-3}[H^+]^2 + 5.9(10)^{-3}[H^+]^2 + 1.18(10)^{-2}C[H^+] + 3.044(10)^{-5}[H^+] + 5.98(10)^{-6}[H^+] + 1.196(10)^{-5}C + 3.086(10)^{-8} - 1.083(10)^{-5}[H^+] - 4.982(10)^{-8} - 4.6(10)^{-3}\ C[H^+] - 5.98(10)^{-6}C = 0 \tag{94}$$

$$[H^+]^3 + \left\{1.106(10)^{-2} + 2C\right\} [H^+]^2 + \left\{2.559(10)^{-5} + 7.2(10)^{-3}C\right\} [H^+] - 1.896(10)^{-8} + 5.98(10)^{-6}C = 0 \tag{95}$$

neglect the $[H^+]^3$ term and solve with quadratic equation:

$$[H^+] = \frac{-2.559(10)^{-5} - 7.2(10)^{-3}C + \sqrt{\{2.559(10)^{-5} + 7.2(10)^{-3}C\}^2 - 4\{1.106(10)^{-2} + 2C\}\{-1.896(10)^{-8} + 5.98(10)^{-6}C\}}}{2.212(10)^{-2} + 4C} \quad (96)$$

$$[H^+] = \frac{-2.559(10)^{-5} - 7.2(10)^{-3}C + \sqrt{6.548(10)^{-10} + 5.184(10)^{-5}C^2 + 3.685(10)^{-7}C + 8.388(10)^{-10} - 2.646(10)^{-7}C + 1.517(10)^{-7}C - 4.784(10)^{-5}C^2}}{2.212(10)^{-2} + 4C} \quad (97)$$

$$[H^+] = \frac{-2.559(10)^{-5} - 7.2(10)^{-3}C + \sqrt{4(10)^{-6}C^2 + 2.556(10)^{-7}C + 1.489(10)^{-9}}}{2.212(10)^{-2} + 4C} \quad (98)$$

The relationship between hydrogen ion concentration and carbonate formality given in Equation 98 is shown to be linear by the data in Table 6 and Figure 25. This linearity extends to the relationship between resultant pH and carbonate formality, as shown in Figure 26. In addition, results of an actual experiment are compared with theoretical predictions in Figure 26. These data are shown in Table 7.

Thus, when the initial pH and total carbonate formality of a test water are known, concentrations of the species of interest can be calculated as follows:

$$K_1 = \frac{[H^+][HCO_3^-]}{[H_2CO_3]} = 4.6(10)^{-3} \longrightarrow [H_2CO_3] = \frac{[H^+]}{K_1}[HCO_3^-] \quad (99)$$

$$K_2 = \frac{[H^+][CO_3^{2-}]}{[HCO_3^-]} = 4.4(10)^{-11} \longrightarrow [CO_3^{2-}] = \frac{K_2}{[H^+]}[HCO_3^-] \quad (100)$$

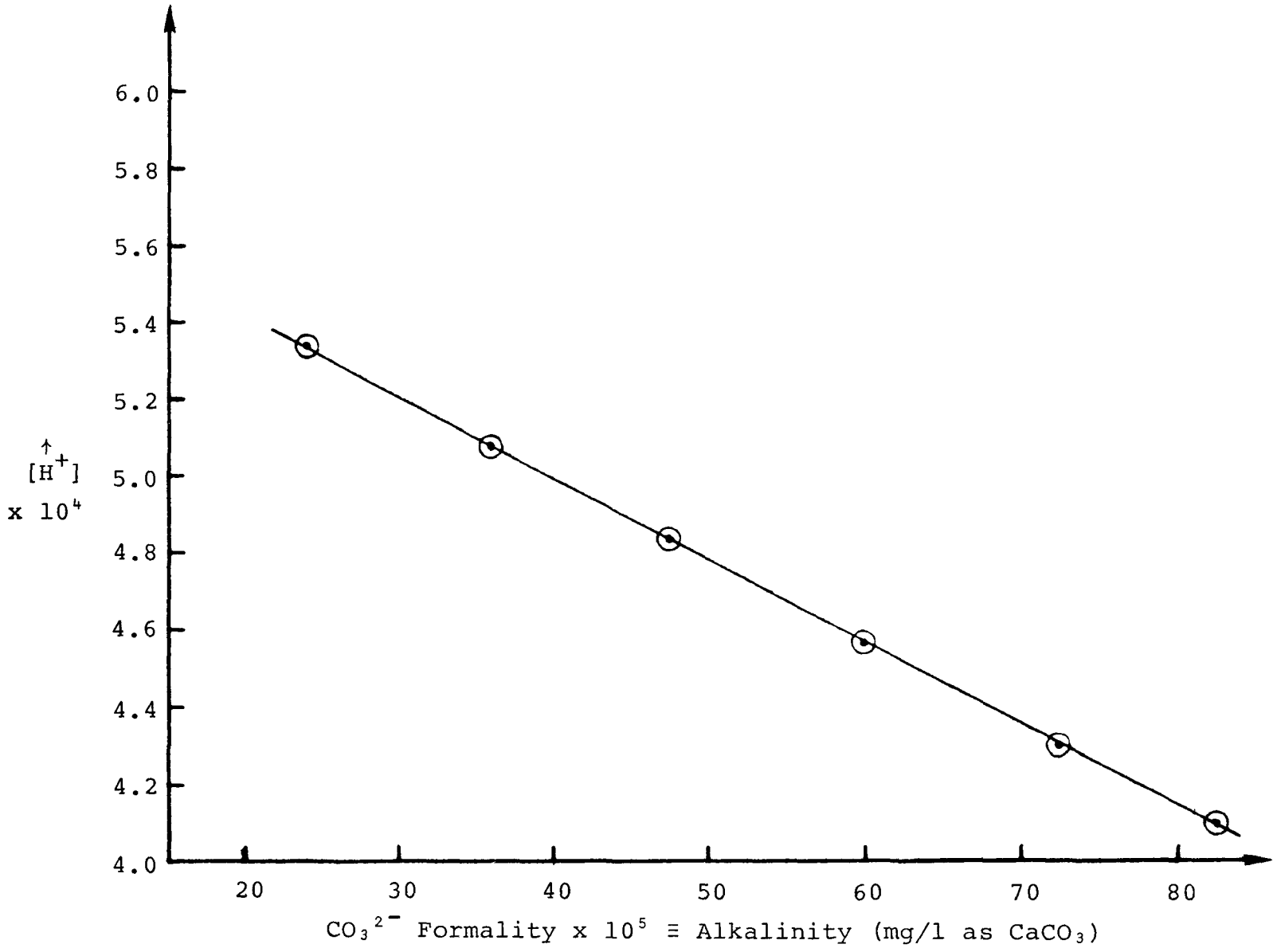

Figure 25. $[H^+]$ versus CO_3^{2-} formality, given applying Equation 98.

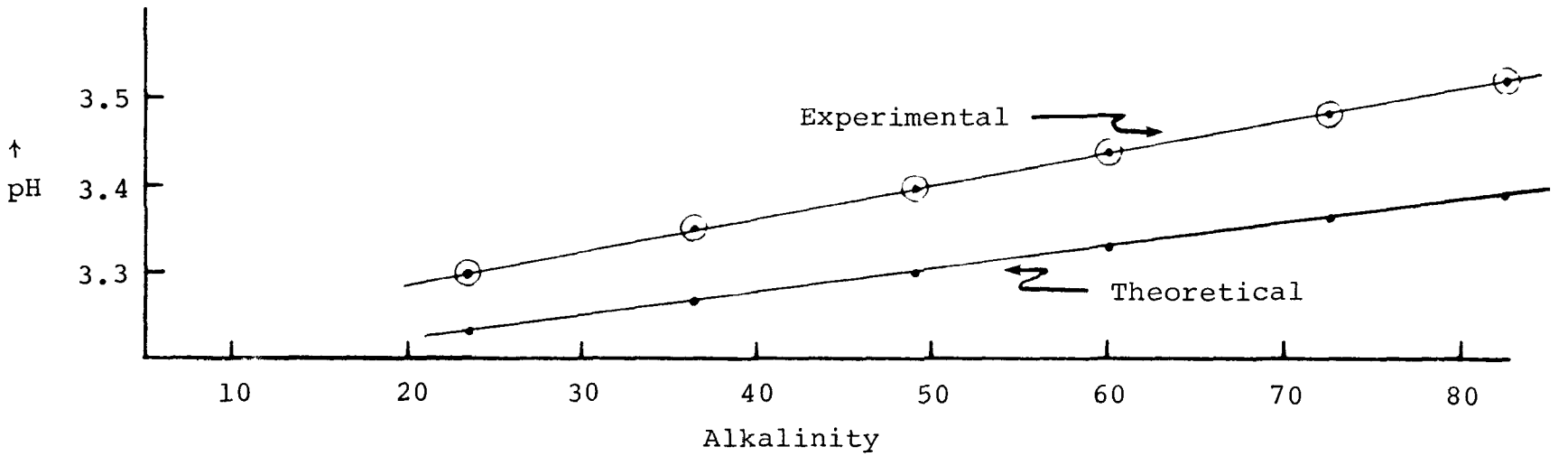

Figure 26. Experimental and theoretical relationships between alkalinity and pH.

$$[H_2CO_3] + [HCO_3^-] + [CO_3^{2-}] = C \tag{101}$$

Substitution of Equations 99 and 100 into 101 gives:

$$[HCO_3^-] = \left\{ \frac{[H^+]}{K_1} + C + \frac{K_2}{[H^+]} \right\} = C \tag{102}$$

$$[HCO_3^-] = \frac{K_1 [H^+] C}{[H^+]^2 + K_1 [H^+] + K_1 K_2}$$

Table 6. $[H^+]$ VERSUS ALKALINITY, APPLYING EQUATION 98

Alkalinity (mg/l as $CaCO_3$)	$[H^+]$ (molarity)
24	$5.33(10)^{-4}$
36	$5.07(10)^{-4}$
48	$4.82(10)^{-4}$
60	$4.57(10)^{-4}$
72	$4.34(10)^{-4}$
84	$4.11(10)^{-4}$

*(CO_3^{-2} formality) x 10^5 = Alkalinity in mg/l as $CaCO_3$

Linear regression:

$$[H^+] = \{57.9133 - 0.237515*ALK\}(10)^{-5}$$

Table 7. EXPERIMENTAL AND THEORETICAL RELATIONSHIPS BETWEEN ALKALINITY AND pH

Alkalinity (mg/l as $CaCO_3$)	pH	
	Experimental	Theoretical
24	3.303	3.273
36	3.347	3.295
48	3.391	3.317
60	3.434	3.340
72	3.476	3.362
84	3.519	3.386

Experimental

The sensing element in the alkalinity monitor is a combination glass pH/reference electrode with a ground glass collar. The electrode fits directly into a glass flow cell. Instrumentation includes a Corning Model 101 digital pH/mv meter; Honeywell Electronik 194 multi-speed, multi-range servo recorder for signal conditioning; and an analog output to the computer. A Technicon II peristaltic pump is used for reagent/sample proportioning. A Valcor series SV-72 three-way miniature dri solenoid valve switches between baseline and sample solutions. AC line voltage is switched to the valve by computer controlled relay. A schematic illustration of the system is shown in Figure 27.

The Corning Model 101 is especially suited for use in the alkalinity system because of its exceptionally quiet operation and its provision for a solution ground. The alkalinity measurement is read from approximately 20 millivolts variation in a signal with a total magnitude of only 200 millivolts; thus, the need for quiet operation is apparent. The peristaltic action of the pump controlling flow through the system produces an electrical signal. This peristaltic noise is reduced by a solution ground placed in the sample line. Many ground configurations were studied. The most successful provides for contact with the solution at two points - in the influent sample line, just before the pump; and after the debubbler, just before the sensor cell. These two grounds are connected together and terminate at the solution ground terminal in the pH meter.

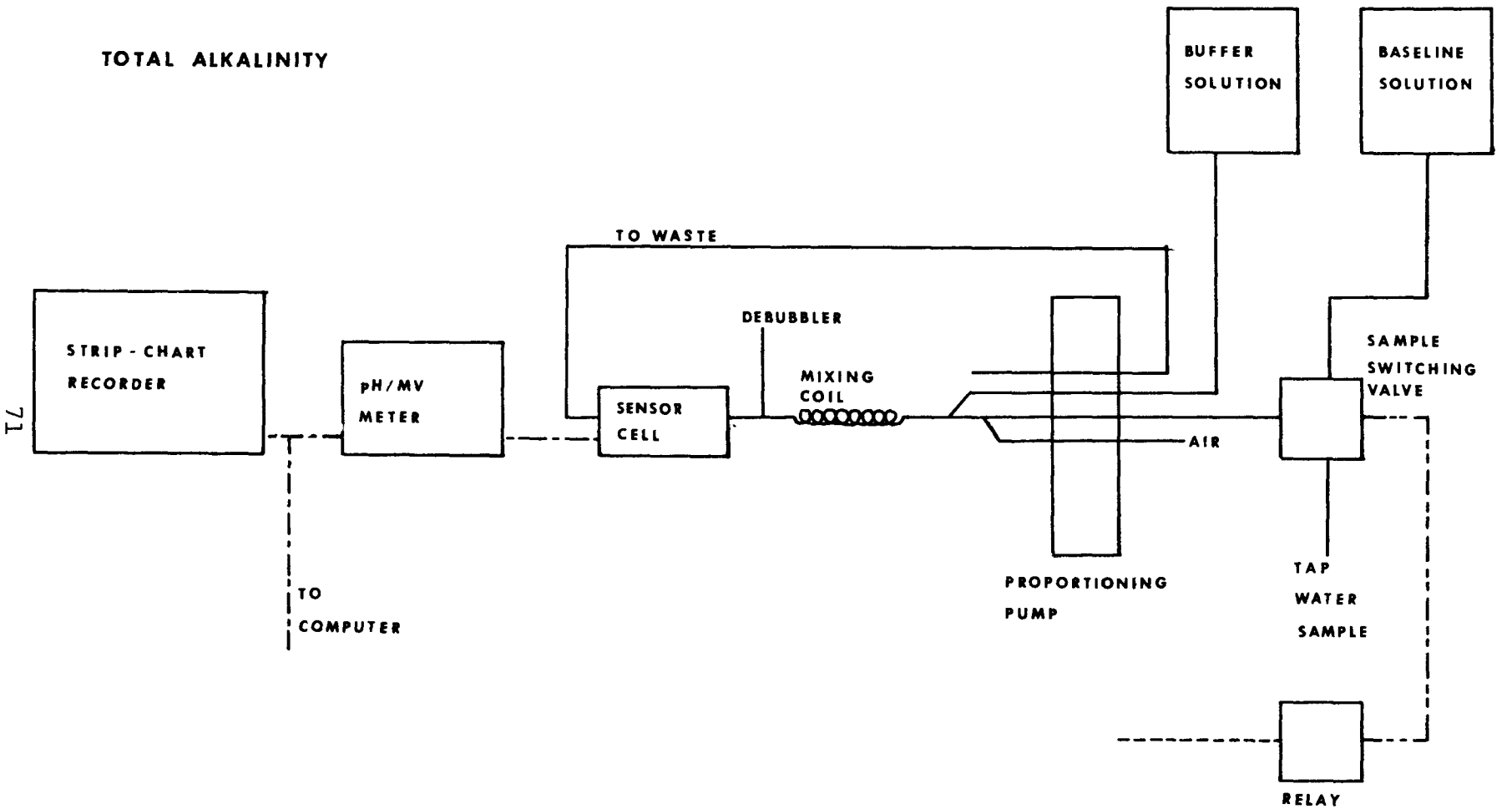

Figure 27. Schematic illustration of alkalinity monitor in mobile laboratory.

Because of the acid nature of solutions used in the system, it is not uncommon for the ground wire to become coated with corrosion products and lose contact with the solution. Whenever signal quality degenerates, the grounds are simply replaced.

The system operates on a 26-minute cycle controlled by the computer. At initiation of the cycle, the relay is switched to the "on" position and the three-way valve is connected to the baseline solution. For the next 13 minutes, baseline solution is drawn into the system. Air bubbles are introduced beyond the pump to separate the sample stream into discrete samples. The buffer is added and a three-inch glass mixing coil provides mixing and reaction time before the sample reaches the electrode system. The sample stream is debubbled just before it enters the sensor flow cell. The bubble stream goes to waste under siphon while the remainder of the sample is drawn past the sensors, then to waste. At the end of the 13-minute period, the computer sets the relay to "off" and the three-way valve is open to the test water stream. A complete cycle of 26 minutes is required to read both baseline and test water samples.

Preparation of reagents used with the alkalinity monitor is included in Appendix B.

Results and Discussion

A good quality recording of "continuous" alkalinity analyses is shown in Figure 28. The analytical region of the curve is from the tip of "drop" to the center of the equilibrated signal from the sample. Greatest precision is achieved by measuring peak height immediately after initial leveling off. The computer begins its measurement after switching from baseline to sample and continues to seek equilibrated signal for a period of six minutes. In Figure 28, the height of the measured peak is 27.0 chart units (C.U.). Measurement of peak height to the nearest 0.5 C.U. and reading alkalinity from a calibration curve produces data with an accuracy of ± 2 mg/l, essentially the same as that which is stated in Standard Methods (3) for potentiometric titration of alkalinity.

A calibration series of five or six standards is run for each combination of newly prepared baseline or buffer solution. Peak heights in C.U. are plotted on the abscissa and concentration on the ordinate. A typical calibration curve is shown in Figure 29. To ensure accuracy of the data, the standards are checked by potentiometric titration and the continuous output compared with a potentiometric titration of a tap water sample.

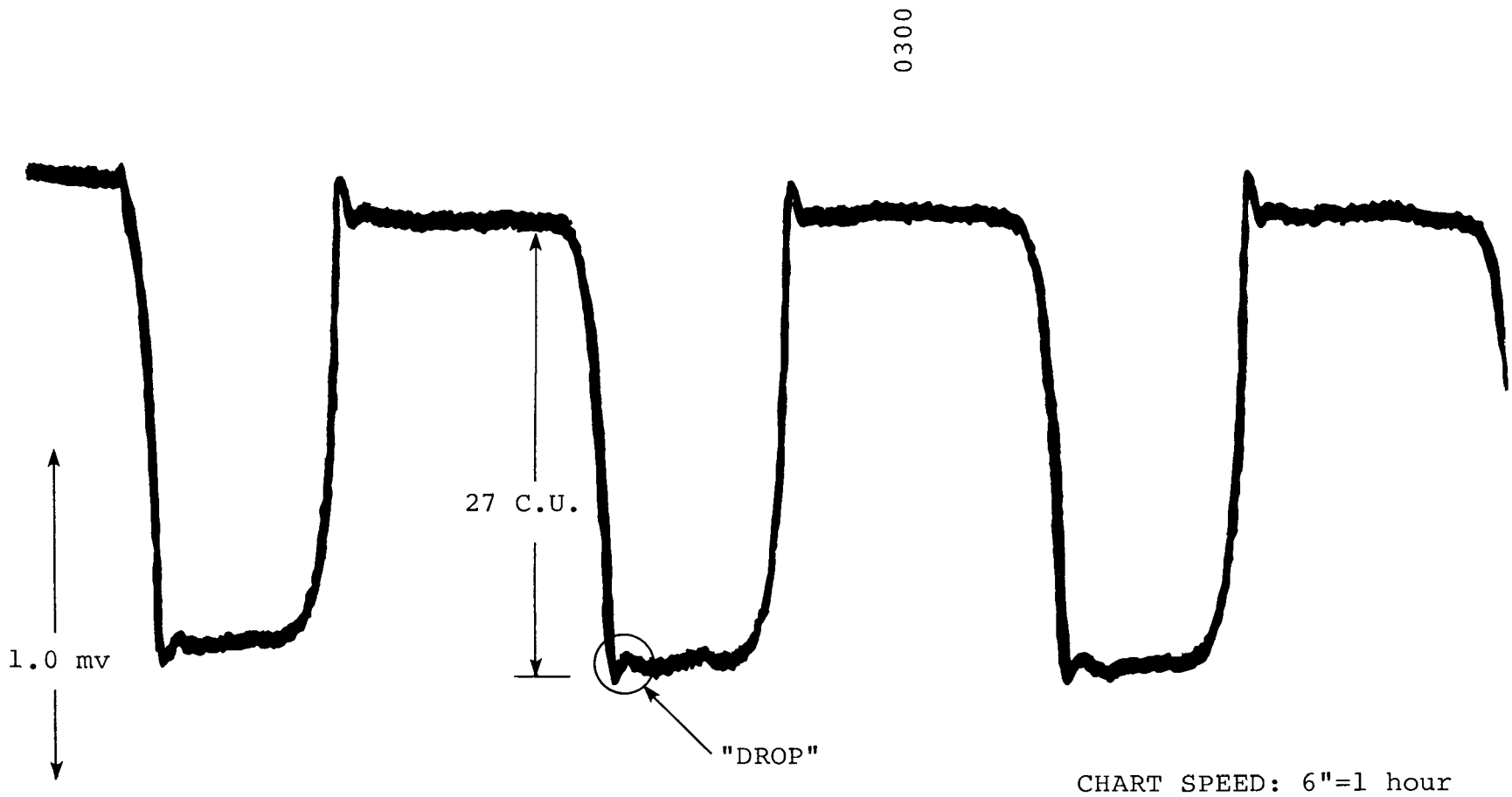

Figure 28. Good quality recording of continuous alkalinity analysis.

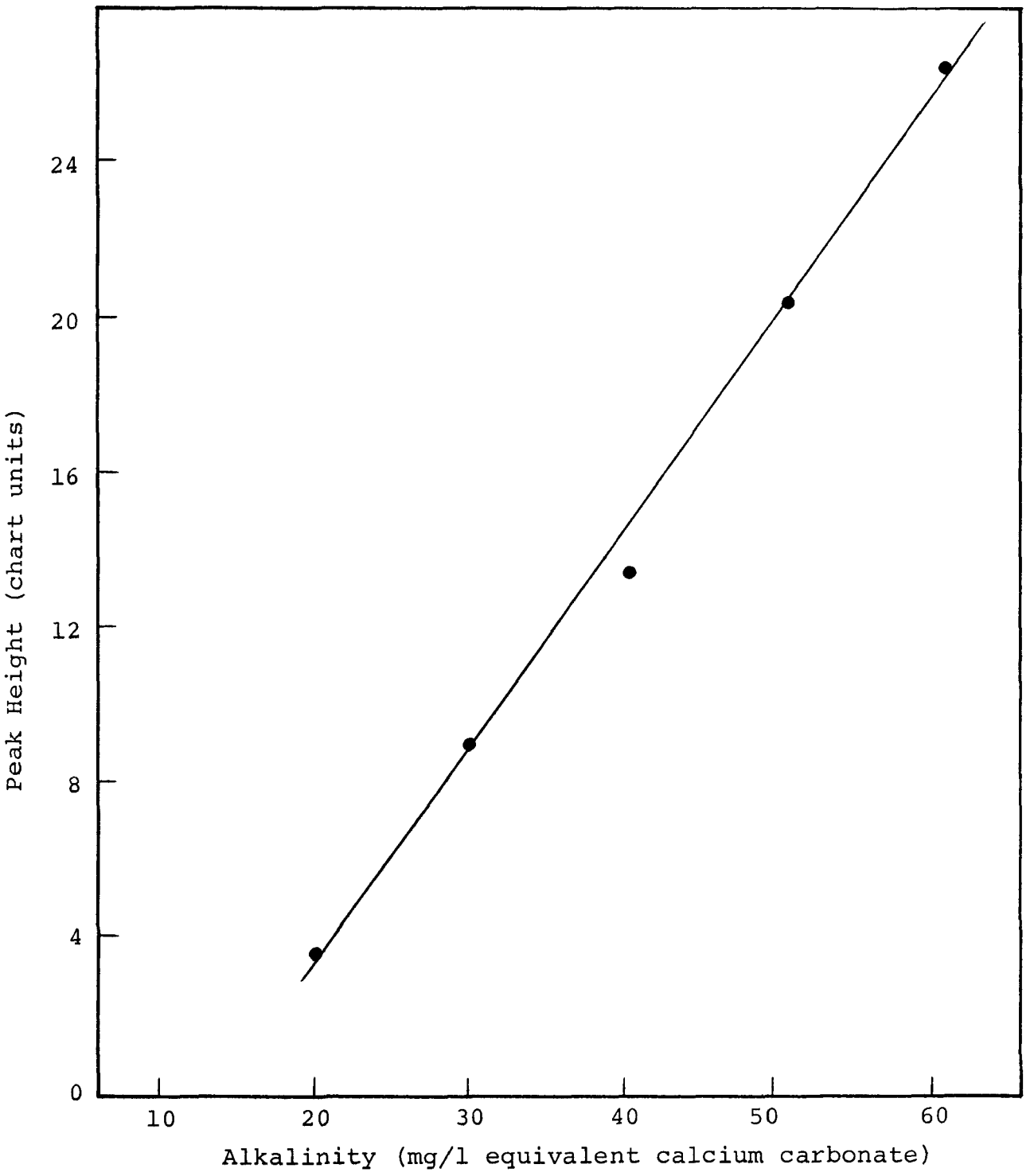

Figure 29. Alkalinity calibration curve.

Special Case Study

Following delivery of the mobile laboratory to the EPA/NERC facility in Cincinnati, hookup was made to monitor Cincinnati tap water. For some time, the alkalinity system did not produce data which was equivalent to that reported by NSF during most periods of field assignment; i.e., the basic relationship between final pH and alkalinity could not be reproduced. Titrations with quiescent solutions allowed to equilibrate, stirred solutions at equilibrium, and stirred solutions read at constant time intervals produced apparently randomly scattered data points. High levels of free residual chlorine were thought to be contributing to this anomalous behavior. The phenomenon had been observed on two previous occasions - once when the laboratory was located immediately adjacent to the water treatment plant in Ann Arbor, Michigan, and once in the Calumet Harbor area of metropolitan Chicago.

To quantify the role of free residual chlorine in potentiometric measurement of alkalinity, an experiment was proposed and results of the experiment calculated theoretically. The protocol and related calculations are presented in detail in Appendix C. Experimental data closely approximated the theoretical results and established the anomaly could not be attributed to the presence of chlorine alone. The apparent interference was eliminated by adding thiosulfate (five mg/l) to the buffer solution, suggesting that chlorine may have contributed to the problem, perhaps synergistically with an unidentified organic present in the test water. The problem has not recurred since EPA substituted a combination electrode with a calomel reference for the silver chloride reference-combination electrode in the original equipment.

FREE AND TOTAL FLUORIDES

General

Fluorides are added to treated water supplies as sodium fluosilicate (Na_2SiF_6), commonly referred to as sodium silica fluoride; fluosilicic acid (H_2SiF_6); or sodium fluoride (NaF), each of which dissociates to release free fluoride ions (F^-). Prior to this study, it was generally assumed that fluorides reached the consumer in this form; i.e., as free ions, and that those which were added during treatment were not different from those which may be present in natural waters. This assumption is invalid. In most chemically treated finished waters, fluorides are complexed with polyvalent cations, such as aluminum or iron, which are commonly added as coagulants or may be present as natural constituents of the raw water.

In a survey of public water supplies in the 100 Largest Cities in the United States (25), residual aluminum and iron in distri-

bution systems were reported to be as high as 1.5 and 1.7 mg/l, respectively.

Fluoride is an important parameter of drinking water quality. In high concentrations it may have a toxic effect; at low levels it is beneficial; i.e., an effective preventer of dental caries (26,27,28,29). Chemical reactions between F^- and tooth enamel are postulated as follows:

$$\underset{\text{hydroxylapatite}}{Ca_{10}(PO_4)_6(OH)_2} + 2F^- \rightarrow \underset{\text{fluorapatite}}{Ca_{10}(PO_4)_6F_2} + 2OH^- \qquad (103)$$

or

$$\underset{\text{hydroxylapatite}}{Ca_{10}(PO_4)_6(OH)_2} + 20F^- + 8H^+ \rightarrow \underset{\text{calcium fluoride}}{10CaF_2} + 6HPO_4^{2-} + 2H_2O \qquad (104)$$

Reaction 103 is generally favored at low levels of fluoride; i.e., in fluoridated waters; reaction 104 occurs in the presence of high concentrations of F^-; e.g., dentifrices (30).

The recommended level for fluoride in drinking water is less than 1.7 mg/l (1); thus, analytical detection methods must be accurate at this level. In the NSF project, the potentiometric ion-selective electrode technique was studied in detail, and automated for measuring both free and total fluorides in the mobile laboratory.

Theory

The potentiometric membrane electrode selective for F^- can be described schematically as follows:

Internal Reference Electrode	Internal Reference Solution $[XF]_r$	Membrane	External Solution $[YF]_t$	External Reference Electrode
Ag/AgCl	$AgCl_{(s)}$, Cl^-, F^-	LaF_3	Test Solution	Saturated Calomel Electrode (S.C.E.)

where:

vertical lines represent boundaries or liquid junctions between components of the cell.

The basis for ion-selective electrode measurements is the Nernst equation:

$$E_m = E_o - \frac{RT}{zF} \ln \left[a_{F^-} + \sum_i K a_i^{a_i/a_{F^-}} \right] \qquad (105)$$

where:

E_m = measured potential

E_o = a constant equal to the sum of the potentials at the Ag/AgCl electrode, the saturated calomel electrode, the liquid junction potential between the test solution and the reference electrode, and the potential across the membrane when F^- activity in the test solution is = 1.0

R = gas content

T = absolute temperature

z = number of electrons involved in the electrode reaction

a_{F^-} = activity of F^-

a_i = activity of ith interfering ion

K^i = selectivity coefficient of interfering ion with respect to F^-.

Activity (a) is related to concentration (c) as shown in the following empirical expression:

$$a = \alpha c \tag{106}$$

where:

α = activity coefficient

At 25°C, the slope of the line described by Equation 105 is approximately 60 mv; however, in practice measurements are usually read from calibration curves. In calibrating ion-selective electrodes, changes in total ionic strength of the test solution must be considered. With the fluoride electrode, OH^- is the only species which interferes with F^- measurements. The effect is apparent when the level of OH^- is greater than one-tenth the level of F^- present in the test water (31,32). Other anions commonly found in drinking water; i.e., Cl^-, SO_4^{2-}, HCO_3^-, NO_3^-, and PO_4^{3-} do not interfere even when they are present at levels 1,000 times the level of F^- (31,33,34,35,36).

It is important to differentiate between OH^- interference and the complexing effect of certain cations; e.g., H^+, Al^{3+}, Fe^{3+} (31,34). Fluoride combined with these cations cannot be sensed by the electrode, but this effect is different from the interference of OH^-.

Experimental

Equipment used in studying and optimizing the fluoride ion-selective electrode measurement technique included an Orion digital pH/mv meter, Model 801; Orion solid state fluoride ion-selective electrodes, Model 94-09; saturated calomel reference electrodes;

and polyethylene containers to minimize loss of F^- by adsorption onto glassware. A Corning digital electrometer, Model 101, was substituted for the Orion 801 early in the study. The Corning meter proved to be a much more reliable instrument, and with its activity mode, appreciably simpler to use. Calibration was set so the upper limit read "100" for 5×10^{-5}M F^- and the lower limit, "20" for 10^{-5}M F^-; thus, percent recovery of F^- in the test solution could be read directly.

In studying the effect of pH, a stock solution of sodium fluoride was prepared from which suitable dilutions were made. pH was varied by addition of strong acids and bases, and ionic strength was maintained at 0.5M by addition of appropriate volumes of concentrated sodium nitrate ($NaNO_3$) solution. Potentials were measured after equilibrium was established. At low fluoride and high pH levels, more than 15 minutes were required to reach equilibrium.

Complexometric titration techniques were used to characterize aluminum-fluoride complexes. pH was controlled by an acetate buffer. Solubility of the complexes was suppressed with ethanol.

In measuring total fluorides, a masking agent is added to complex Al^{3+} more strongly than F^-, liberating bound fluoride for sensing by the electrode. The relative efficiencies of four masking agents was studied: EDTA (disodium salt of ethylenediaminetetraacetic acid), CDTA (cyclohexanediaminetetraacetic acid), oxalate, and citrate.

Equipment in the free and total fluoride monitoring system installed in the mobile laboratory included the Orion digital pH/mv meter, Model 801 (for total fluorides) and a Leeds and Northrup expanded scale pH/mv meter, Model 7415-EO (for free F^-); two Orion solid state fluoride ion-selective electrodes, Model 94-09; Ag/AgCl (total) and calomel (free) reference electrodes; an Esterline Angus dual pen strip chart recorder; a Technicon Pump II for reagent/sample proportioning; and Valcor three-way miniature dri solenoid valves, series SV-72, for switching between baseline and standard solutions. AC line voltage was switched to the valves by computer controlled relays.

A schematic procedure for measuring free and total fluorides with ion-selective electrodes is shown in Figure 30. Preparation of reagents is described in Appendix B.

Results and Discussion

pH Effect

The effect of pH on fluoride electrode measurements is shown in Figure 31. The OH^- interference effect is apparent when the

SAMPLE

Free Fluoride, A	Total Fluoride, B
- Add free fluoride buffer (FFB)* to sample, 1:1	- Add total fluoride buffer (TFB)+ to sample, 1:1
- Potentiometric measurement	- Potentiometric measurement

Complexed Fluoride, C = B-A

Preparation of Buffers:

To about 700 ml double distilled water add:

	*Free fluoride buffer, FFB	+Total fluoride buffer, TFB
Acetic acid	5.7 ml (0.1 M)	11.4 ml (0.2 M)
Sodium nitrate	84.99 g (1.0 M)	59.5 g (0.7 M)
Sodium citrate	None	58.8 g (0.2 M)

Adjust the pH to 5.2 with concentrated solution of sodium hydroxide, and the volume to 1.0 liter.

Figure 30. Characterization of fluorides and preparation of buffers.

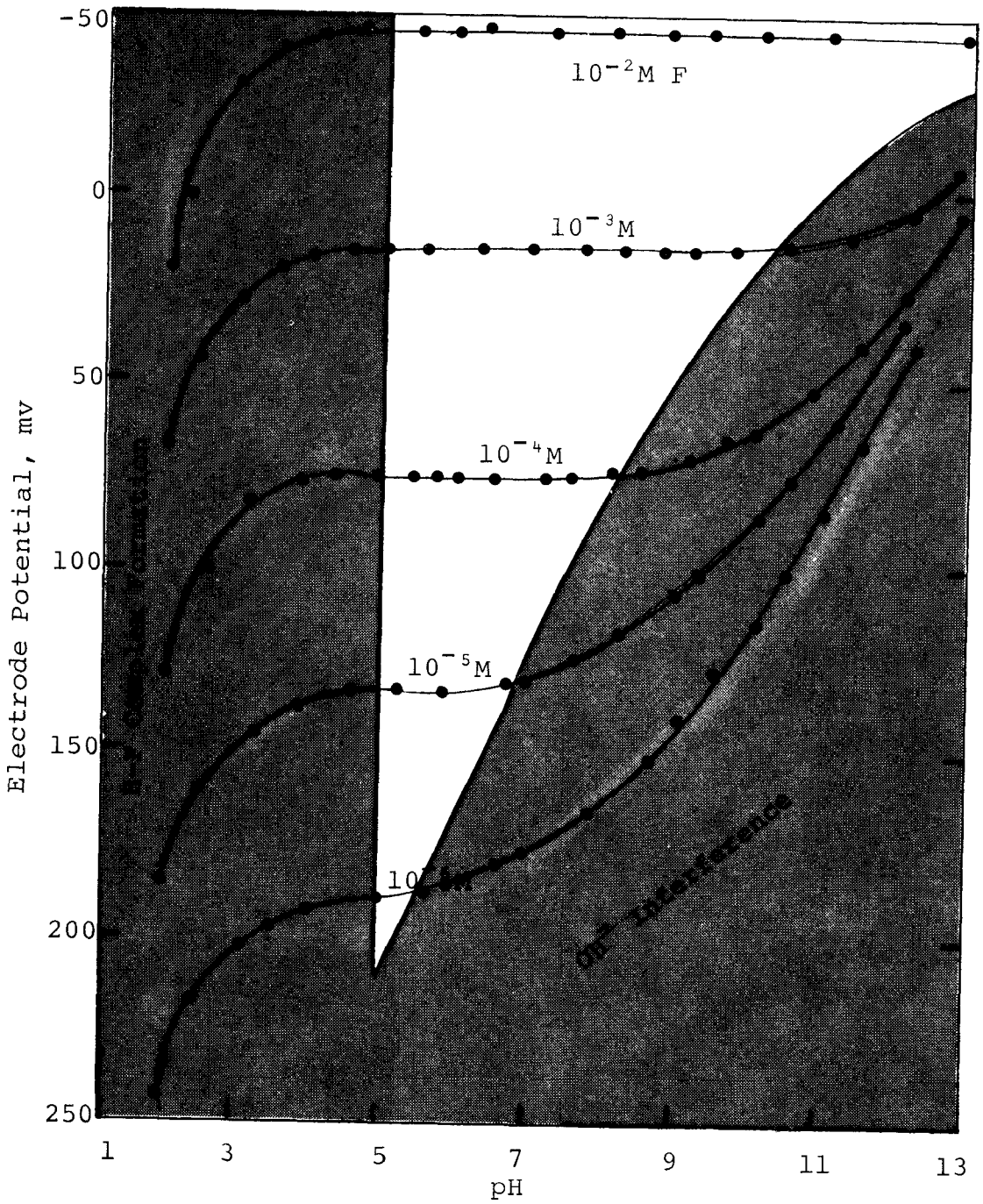

Figure 31. Effect of pH on fluoride ion-selective electrode measurement.

curves in Figure 31 show a nonlinear relationship and shift toward more negative potentials. Because F^- and OH^- have similar changes and ionic radii (31), the electrode senses both (but to varying degrees); thus, a false increase in apparent F^- activity may occur at high levels of OH^-.

The effect of H-F complexation is also apparent in Figure 31. Hydrogen ions combine with fluoride ions to form hydrogen fluoride (HF) and bifluoride ions (HF_2^-), neither of which are sensed by the electrode (37,38).

According to the literature (31,32), the fluoride electrode can be used for measurements in drinking water at pH five to eight; however, data from this study indicate a much more restrictive pH range (Figure 31). At 10^{-6}M F^-, the optimum range is 5.0 to 5.4; thus, pH 5.2 is used in the NSF fluoride monitor and is recommended for all ion-selective electrode measurements of fluorides in water supplies.

The selectivity coefficient (K) of OH^- with respect to F^- can be calculated as follows:

$$E = E_o - \frac{RT}{F} \ln [(F^-) + K(OH^-)] \qquad (107)$$

Using the data from Figure 31, estimated values for K are shown in Table 8. Note that K increases as the level of F^- decreases; i.e., the interference effect of OH^- is more predominant at lower concentrations of F^-. At levels of F^- commonly found in drinking waters, values of K are on the order of 0.70. By calculation, using Equation 107, it can be shown that at 10^{-6}M F^-, the OH^- interference effect is significant only at pH > 5.4.

A further illustration of OH^- interference is shown in Figure 32 in which calibration curves at various levels of pH are plotted as electrode potential versus concentration of F^-. Nonlinear electrode response is greater as fluoride concentration decreases and pH increases. At low pH, electrode response follows the classical Nernstian relationship. Linearity was extended to 10^{-6}M F^- at pH values of two and three. The parallel shift in

Table 8. OH^- SELECTIVITY COEFFICIENTS (K)

F^- Concentration	K
10^{-6}M - 10^{-4}M	0.70
10^{-4}M - 10^{-3}M	0.07
10^{-3}M - 10^{-2}M	0.05

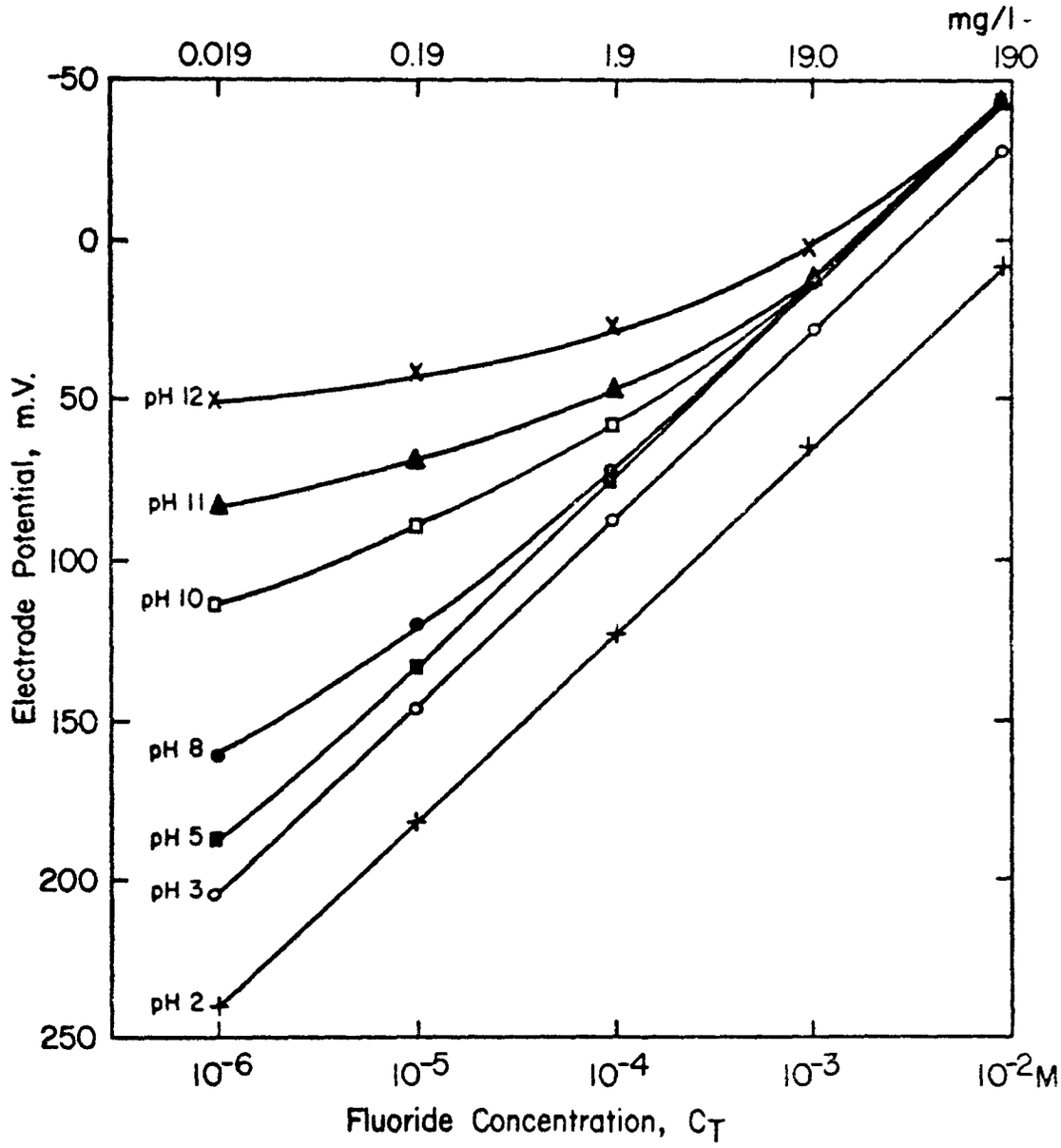

Figure 32. Calibration curves of different levels of pH.

the intercept of the calibration curves below pH five can be explained in terms of H^+ complexation (37):

$$(F^-)(H^+) \rightarrow K_1(HF)_{pK_1 = 2.9} \tag{108}$$

$$(HF)(F^-) \rightarrow K_2(HF_2^-)_{pK_2 = 0.77} \tag{109}$$

where:

K_1 = first dissociation constant
K_2 = second dissociation constant

and:

$$C_T = 2(HF_2^-) + (HF) + (F^-) \tag{110}$$

where:

C_T = total concentration of fluoride

For solutions of fluoride more dilute than 0.05M, (HF_2^-) can be neglected and Equation 107 rewritten as (39):

$$C_T = (HF) + (F^-) \tag{111}$$

Combining Equations 108 and 111 and solving for F^-:

$$(F^-) = C_T \frac{K_1}{K_1 + (H^+)} \tag{112}$$

Then, substituting Equation 112 into the Nernst equation and rearranging:

$$E = E_o - \frac{RT}{F} \ln \frac{K_1}{K_1 + (H^+)} - \frac{RT}{F} \ln C_T \tag{113}$$

where the term $- RT/F \ln K_1/K_1 + (H^+)$, the "shift term," is constant for given pH and temperature and independent of fluoride concentration. At pH > 5, (H^+) is relatively small, the ratio $K_1/K_1 + (H^+)$ approaches 1.0, and the shift term = 0; i.e., no shift in intercept occurs. At pH < 5, (H^+) is large, and the shift term is positive and increases with decreasing pH. Experimentally determined values for shift in intercept at 25°C correlate closely with calculated values, as shown in Table 9.

Table 9. SHIFT IN INTERCEPT OF CALIBRATION CURVES AT LOW pH VALUES

pH Range	Calculated	Experimental
2-3	36. mv	40. mv
3-5	14. mv	15. mv

It follows, then, that at constant pH, H^+ complex formation is constant at all levels of fluoride and has no effect on the slope of the calibration curve; i.e., at constant pH, changes in the slope of a calibration curve developed within sensitivity limits of the electrode are the result of OH^- interference only. The effect of pH on electrode sensitivity is shown in Figure 33.

Divalent Cation Effect

Both calcium (Ca^{2+}) and magnesium (Mg^{2+}) ions form insoluble or sparingly soluble salts of fluoride. High levels of these cations (145 mg/l Ca^{2+} and 120 mg/l Mg^{2+} as $CaCO_3$), the principle hardness ions, are commonly found in distributed finished waters (23). Even in much higher concentrations than those reported for treated waters, neither Ca^{2+} or Mg^{2+} showed any effect on fluoride electrode measurements. Recovery of 5×10^{-5}M F^- was complete in the presence of 10^{-2}M Ca^{2+} and Mg^{2+}; i.e., >400 mg/l Ca^{2+} and >240 mg/l Mg^{2+}. At these levels, any CaF_2 or MgF_2 which is formed is well below their respective solubility products; i.e., K_s = 10.4 and 8.15, respectively.

Trivalent Cation Effect

Trivalent cations; e.g., Al^{3+} and Fe^{3+}, rapidly complex with fluoride. The extent of complexation is a function of pH and relative levels of F^- and complexing species in the test solution.

Water which is treated by alum coagulation may contain from 3.3 to 1,500 mg/l aluminum (25). Over the period March 1970 to February 1971, aluminum levels in Ann Arbor, Michigan tap water varied from <20 to 500 mg/l, measured by emission spectroscopy. The Al-F complex was characterized by potentiometric (ion-selective electrode) titration. Results are shown in Figure 34. Addition of acetate buffer (Curve II) to maintain pH 5.2 significantly improved end point detection. With no pH control (Curve I), addition of Al^{3+} titrant lowered the pH of the test solution resulting in further $H^+ + F^-$ complexation. Addition of ethanol (Curve III) also significantly improved the titration. Both ethanol and buffer added to the test solution (Curve IV) produced the

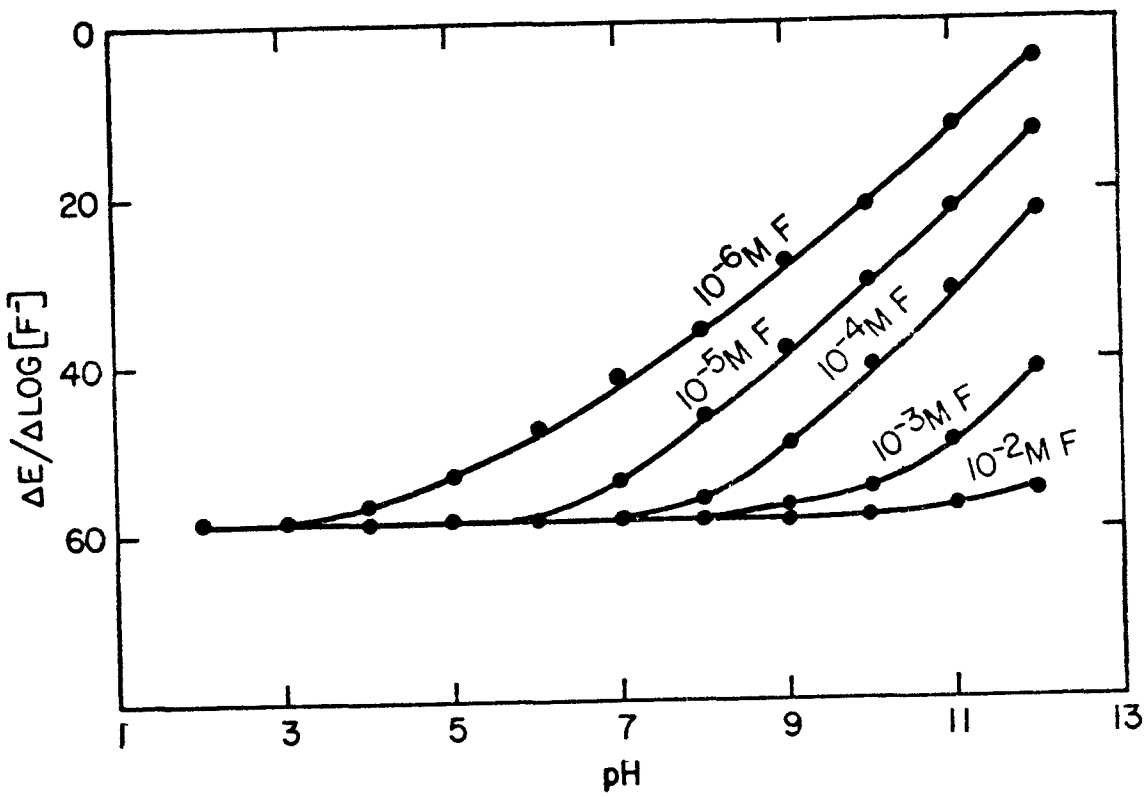

Figure 33. Effect of pH on fluoride ion electrode sensitivity.

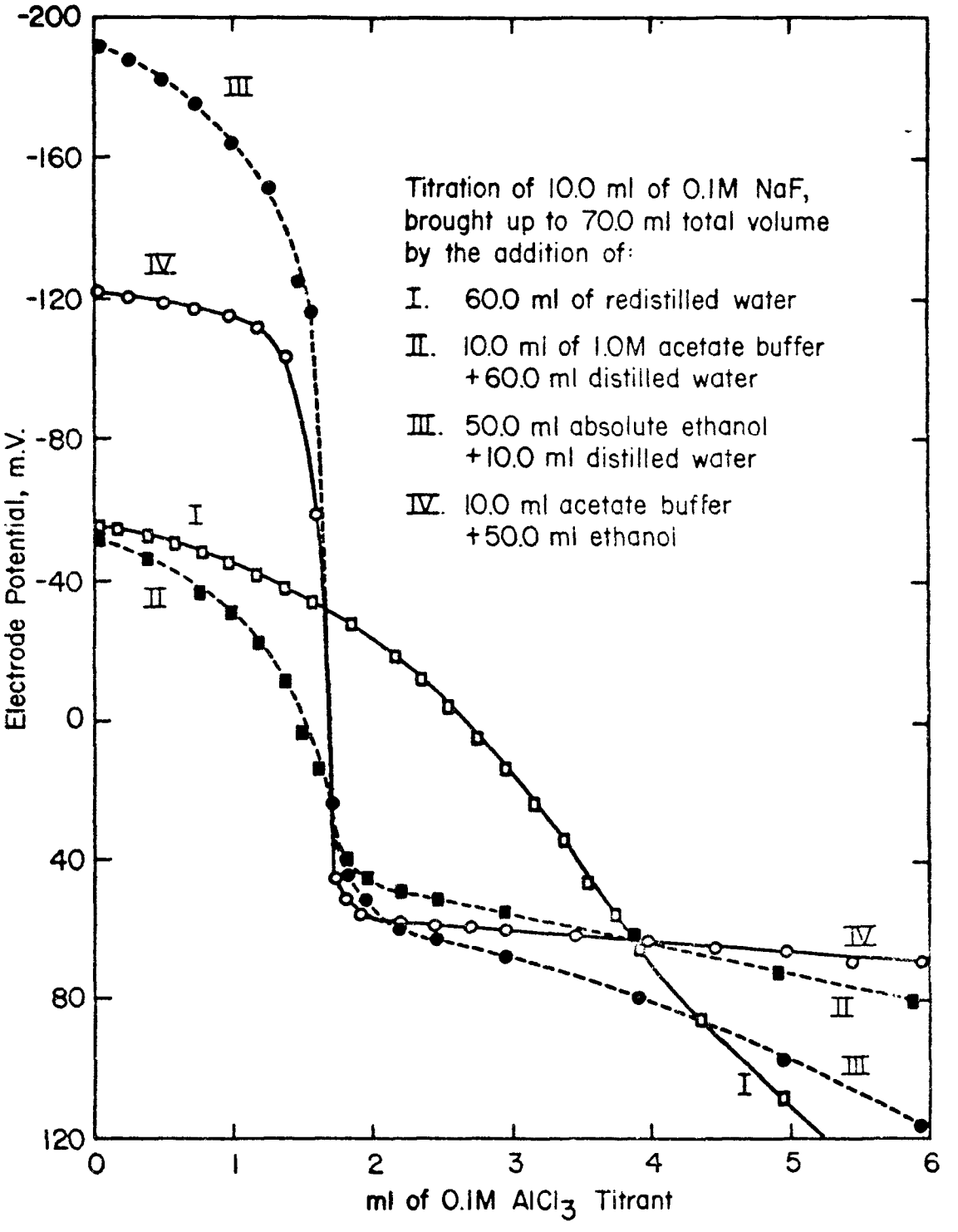

Figure 34. Complexometric titrations of fluoride with aluminum.

optimum condition for titration. Stoichiometric calculation of the complex coordination number using the data from Figure 34 identified the complex as $(AlF_6)^{3-}$.

A number of masking agents have been proposed for potentiometric measurement of total fluorides (40,41,42). Frant and Ross (40) added citrate to total ionic strength adjustment buffer (TISAB); Crosby, et al (41) changed the composition of TISAB and added EDTA; and Harwood (42) used CDTA. Four separate masking agents were studied early in the NSF project: oxalate, citrate, EDTA, and CDTA. Solutions of each were made from corresponding equivalent weights. Increments of aluminum were added to standard solutions of 5×10^{-5}M or 1.0 mg/l F^-. When complexation was complete, a masking agent was added and percent recovery of F^- calculated. Electrode measurements were made in the presence of 1.0M acetate buffer (pH = 5.2) with constant ionic strength (1.0M $NaNO_3$). Results are shown in Table 10.

EDTA, CDTA, oxalic and citric acids have respective stability constants with aluminum as follows: 16.1(43), 17.6(43), 14.6 (44), and 20.0 (45). EDTA and oxalate did not yield high recovery rates. Despite its relatively high stability constant, Al-EDTA complex formation is too slow for EDTA to be an effective masking agent in the measurement of fluoride. Heating or standing overnight showed no improvement. The solubility of oxalate in TISAB buffer solution was limited. At 6.0 meq/l, CDTA yielded the highest recovery, but higher levels of CDTA had no further effect on recovery rates (Figure 35). At higher concentrations of any masking agent, citrate yielded highest recoveries. As shown in Table 10 and Figure 36, 60 meq/l citrate provided good recoveries. At 600 meq/l citrate (0.2M), 100 percent recovery at 0.5 mg/l Al^{3+} occurred after 6.5 minutes; at 0.1 mg/l Al^{3+} recovery was complete after three minutes. (See Figure 37.) Averaged additive effects with no synergism or potentiation were observed when two or more of the masking agents were mixed.

Iron frequently occurs in drinking water in higher concentrations than aluminum; i.e., levels from two to 1,700 mg/l are reported in the 100 Largest Cities in the United States (25). The effect of Fe^{3+} - F^- complex formation was also studied. Results, shown in Table 11, indicate that iron does not form stable complexes with fluoride. Nearly 100 percent recovery occurred with acetate buffer alone. At Fe^{3+} >2.0 mg/l, competitive complexing effects were observed. Complete F^- recovery at very high concentrations of Fe^{3+} occurred with citrate and, to a lesser extent, with CDTA.

Automated System

A schematic illustration of the automated free and total fluoride measurement system is shown in Figure 38. This system was operated in the laboratory to establish performance characteristics;

Table 10. ALUMINUM COMPLEXING EFFECT AND FLUORIDE RECOVERY BY DIFFERENT MASKING AGENTS

		% Recovery of Fluoride							
Aluminum	meq/l	0.0	0.006	0.012	0.024	0.06	0.12	0.6	1.2
Concentration	mg/l	0.0	0.054	0.108	0.216	0.54	1.08	5.4	10.8
Acetate	0.1M	100	94	90	80	56	28	5	3
Buffer	1.0M	100	95	92	83	62	48	15	10
	meq/l								
EDTA	6.	101	98	94	88	81	69	24	15
	30.	100	97	92	86	80	69	25	16
	60.	100	97	90	85	79	68	27	15
Oxalate	6.	100	99	96	94	89	85	54	32
	30.	102	100	97	96	93	91	82	67
CDTA	6.	102	101	99	97	95	92	86	73
	30.	101	100	97	95	91	87	85	73
	60.	100	100	97	94	89	85	82	73
Citrate	6.	101	100	100	99	95	92	67	53
	30.	101	100	100	100	100	99	89	83
	60.	102	101	101	100	101	100	95	91

Buffered masking agents added to standard solutions containing 5×10^{-5}M fluoride, (0.95 mg/l), and variable aluminum concentration

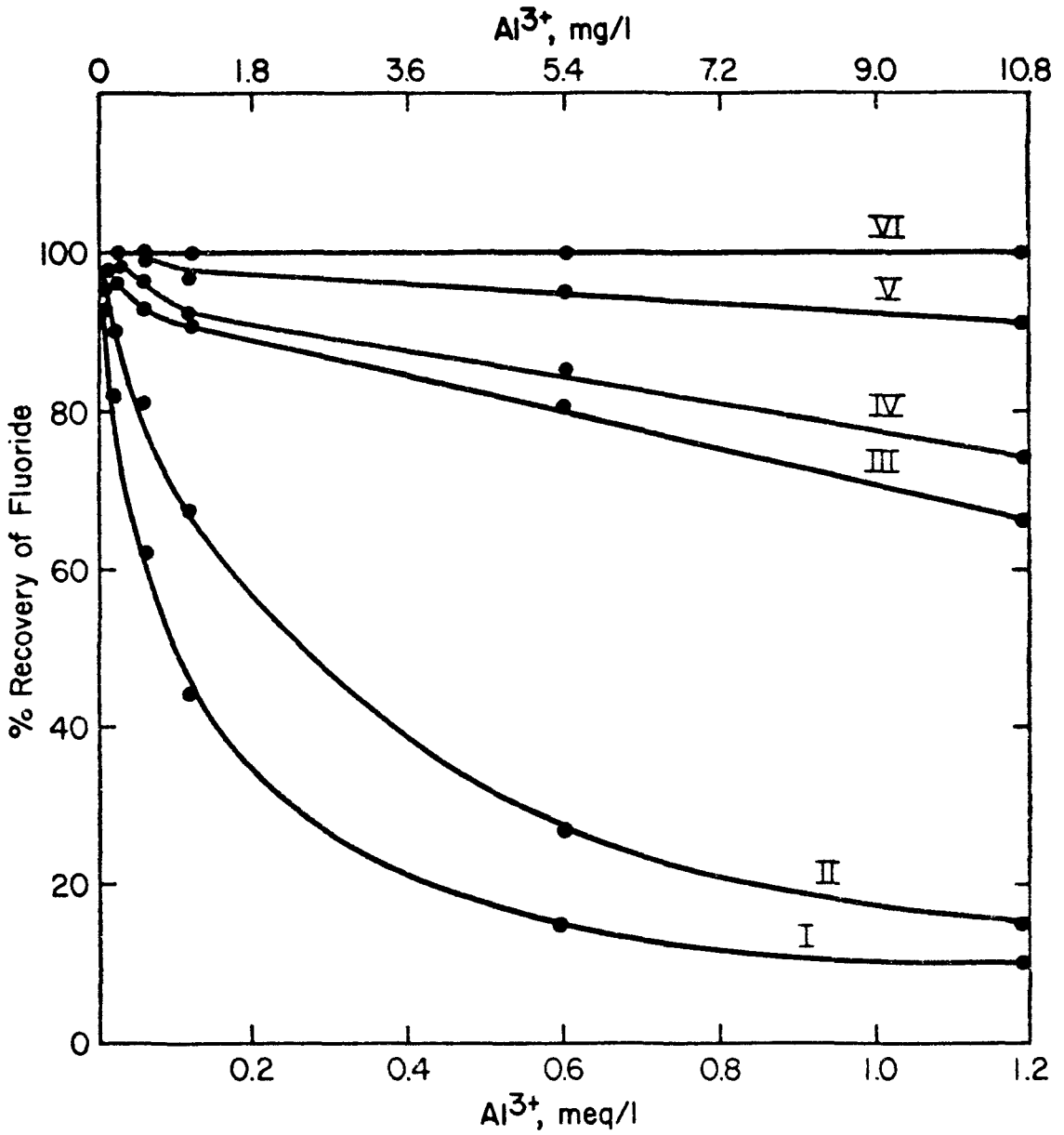

I	Acetate buffer, 1.0M	IV	CDTA, 60 meq/l
II	EDTA, 60 meq/l	V	Citrate, 60 meq/l
III	Oxalate, 30 meq/l	VI	Citrate, 200 meq/l

Figure 35. Aluminum complexing effect and fluoride recovery by different masking agents.

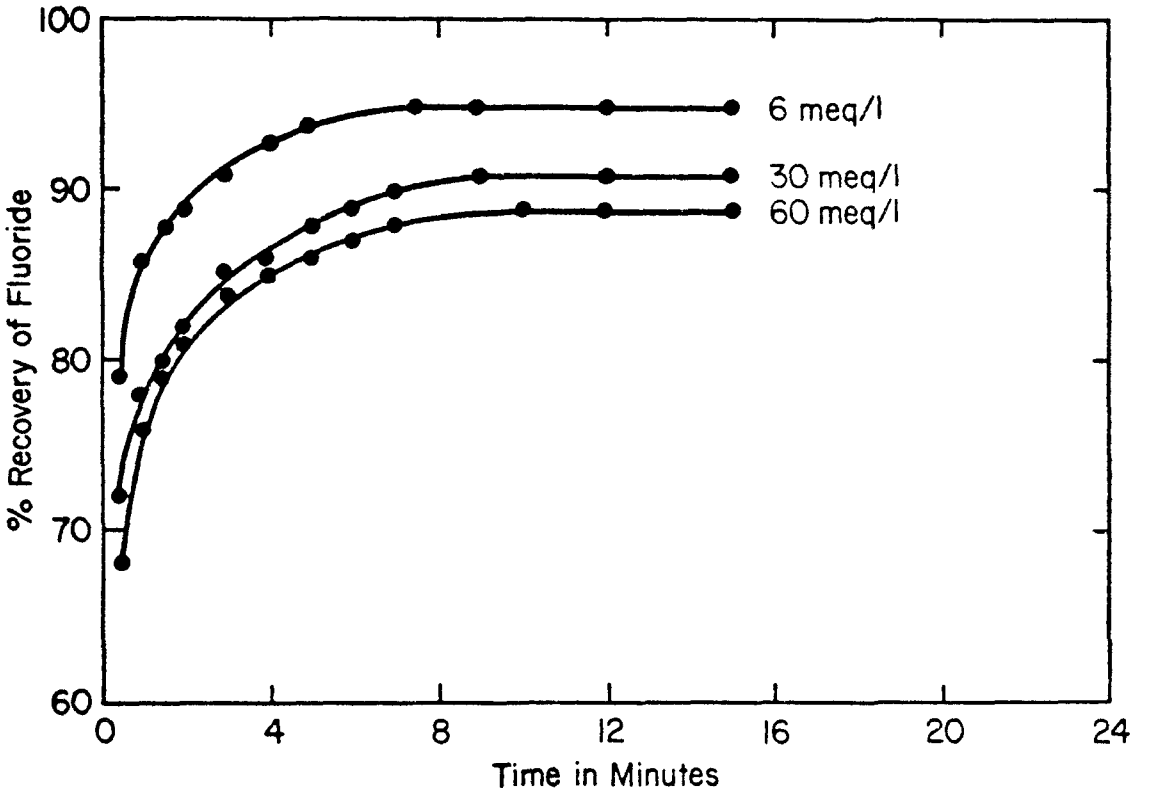

Standard solutions contain 1.0 mg/l fluoride and 0.5 mg/l aluminum.

Figure 36. Rate of fluoride recovery with CDTA masking agent.

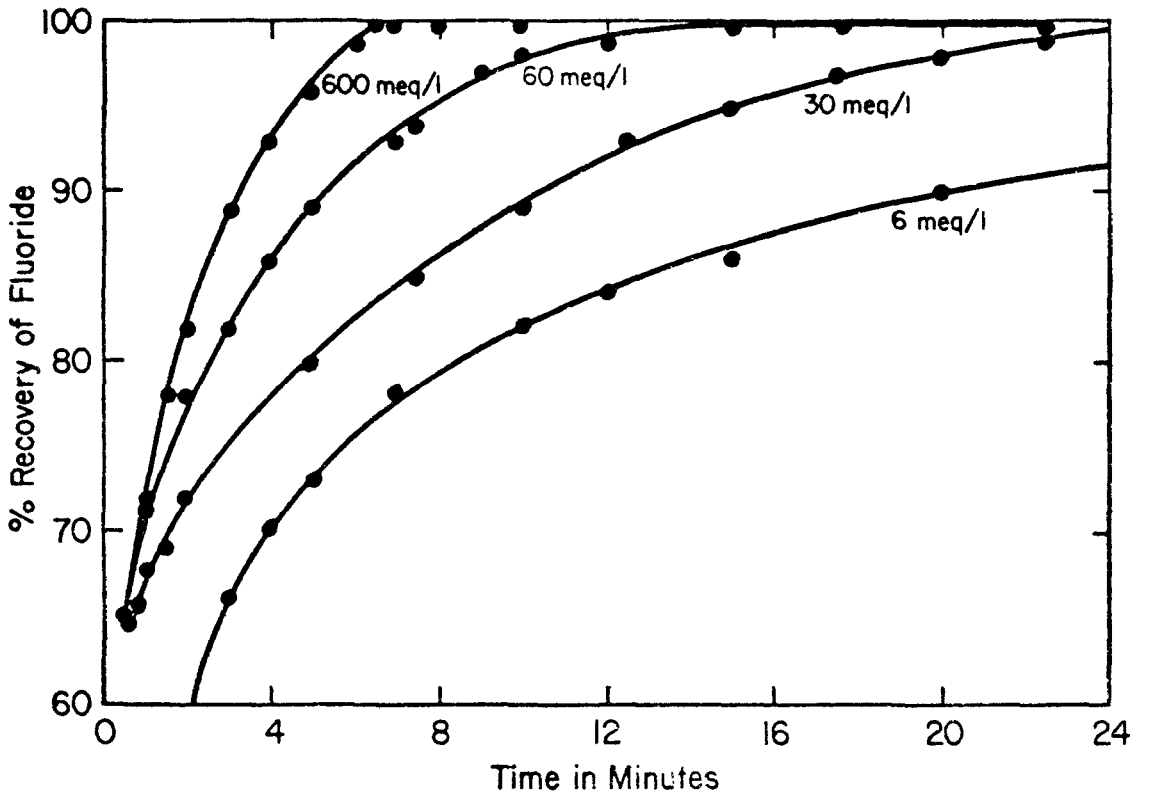

Standard solutions contain 1.0 mg/l fluoride and 0.5 mg/l aluminum.

Figure 37. Rate of fluoride recovery with citrate masking agent.

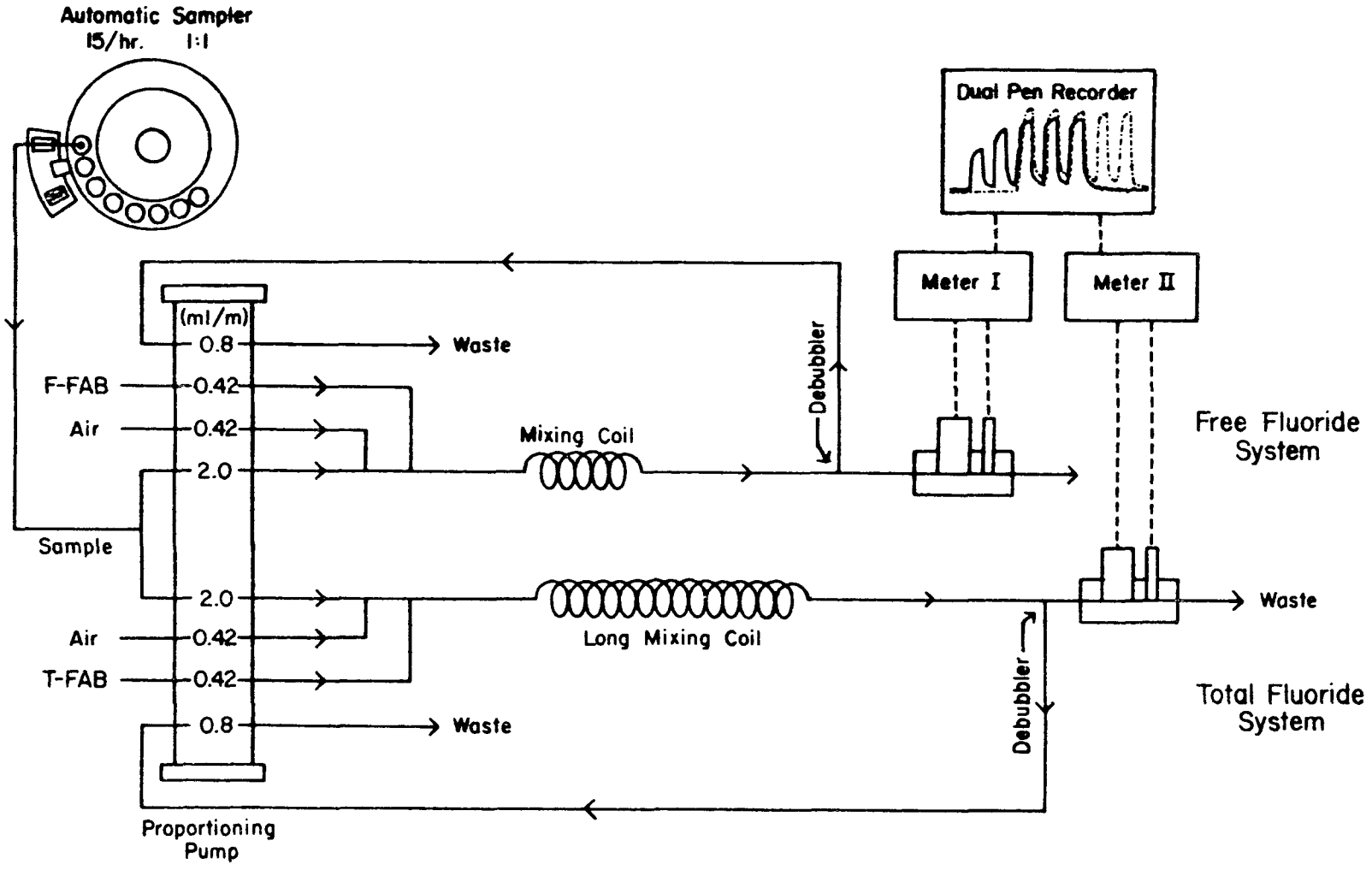

Figure 38. Schematic of automated sample analysis for free and total fluoride.

Table 11. IRON EFFECT AND FLUORIDE RECOVERY BY MASKING AGENTS

		% Recovery of Fluoride								
Iron	meq/l	0.0	0.006	0.012	0.024	0.06	0.12	0.6	1.2	2.4
Concentration	mg/l	0.0	0.11	0.22	0.45	1.12	2.23	11.17	22.34	44.68
Acetate Buffer	1.0 M meq/l	100	101	101	100	100	99	98	95	84
CDTA	30.	100	100	100	100	100	100	100	99	98
Citrate	6.	100	100	100	100	100	100	100	100	97
	30.	100	100	100	100	100	100	100	100	99
	60.	100	100	100	100	100	100	100	100	100

i.e., buffer to sample ratio, flow rates, mixing times, etc. required for design of the "continuous" fluoride monitor. Flow rates for each reagent/sample stream are expressed numerically in the schematic. Standard solutions and samples are placed in individual sampler cups. Automatic sampling is initiated after stable baselines are established for reagents flowing through the two flow cells. The sample- or standard- is withdrawn, segmented with air, and mixed with buffer in a mixing coil. The sample stream is debubbled; i.e., the segmented air and a portion of the test solution are pumped to waste. Residual test solution is passed through the flow cell for sensing by the electrode.

Sensed potentials for standards or samples from each electrode system appear as output peaks from the recorder, one each for free and total fluoride. Calibration curves are used to read the respective peak heights as fluoride concentrations. Complexed fluoride is reported as the difference between total and free.

The Nernstian semilogarithmic relationship has an important effect on automated measurements; i.e., it precludes the use of zero concentration fluoride as baseline solution in the measurement system. A fluoride standard solution must be used as the wash between samples and standards. A concentration of 0.1 mg/l F^- is used for the wash/baseline solution. This level of F^- is well above the lower limit of detection for the electrode, is in the linear range of electrode response, and is a level at which the electrode response rate is relatively fast. Fluoride levels higher than the baseline concentration; i.e., F^- >0.1 mg/l appear as positive peaks (above the baseline), and F^- <0.1 mg/l appear as negative peaks (below the baseline).

Effect of Pump on Reference Electrode

Early in the study, electrode potentials fluctuated in regular rhythmic sequence with surges of the proportioning pump. This effect is shown in Figure 39. These fluctuations were assumed to be related to variation in junction potential of the reference electrode, resulting from movement of the solution boundary at the porous electrode junction. The effect was overcome by shifting the location of the pump to the debubbling line ahead of the flow cell, and placing the reference electrode slightly downstream after the fluoride sensing electrode. With these two changes, the surging effect of the pump was suppressed and a smooth curve obtained as recorder output (Figure 39).

Buffer: Sample Ratio

Electrode response is appreciably faster at high- than at low-levels of fluoride; thus, buffer is added to the sample in small amounts. If, for example, the fluoride concentration in a test

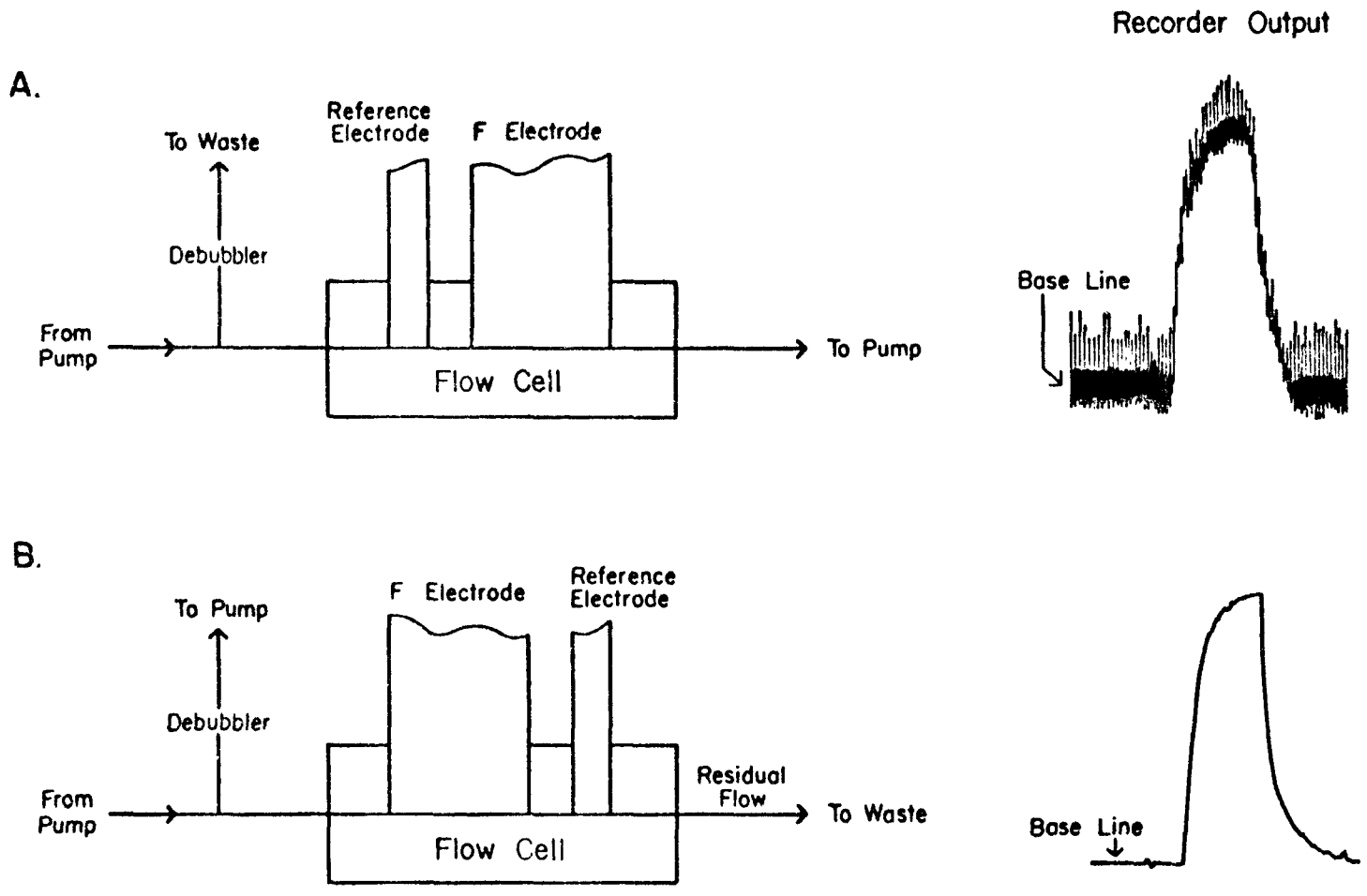

Figure 39. Effect of pump surges on reference electrode.

water is 1.0 mg/l and the buffer to sample ratio is 1:1, 1:2, or 1:5, the final concentration of fluoride in the sample stream is 0.5, 0.67, or 0.83 mg/l, respectively. In addition, simple dilution might lower the level of fluoride beyond minimum detection of the electrode or the linear range of electrode response. A buffer to sample ratio of 1:5 was used throughout this study.

Flow Rates

Early in the study, a net flow rate of 0.95 ml/minute through the flow cell was used. Electrode response was significantly improved when the flow rate was increased to 2.04 ml/minute. This effect is shown in Figure 40. Higher flow rates resulted in no further improvement.

Mixing Time

Coils are used to mix reagents with test waters in the fluoride system, and to provide sufficient lag time to allow reaction kinetics to proceed to completion. A two-minute coil is adequate for the free fluoride system, but a longer coil is required for the masking agent to react with Al-F complexes in the total fluoride system. At Al^{3+} = 1.5 mg/l, recovery of fluoride at one mg/l is 92.5 percent complete with a six-minute coil, and 100 percent complete with a nine-minute coil. A 12-minute coil is used for higher levels of complexes in the test water.

Concentrations of Buffer and Masking Agent

In the automated system, double concentration buffers, F-FAB and T-FAB, are used with buffer:sample = 1:5. This maintains the citrate at an effective level for masking aluminum and provides for rapid kinetics.

Adsorption Effect

Adsorption of F^- on glass coils was effectively minimized by aging (rinsing) new coils in a solution of 0.5 mg/l F^- for 24 hours prior to their use in the system. Polyethylene and teflon coils interfered with the passage of regular segments of air in the sample stream.

Sample and Wash Times

It was expected that time equivalent to the time required for an electrode to fully respond to a level of F^- in the test solution would be required to remove the response. Figures 41, 42, and 43

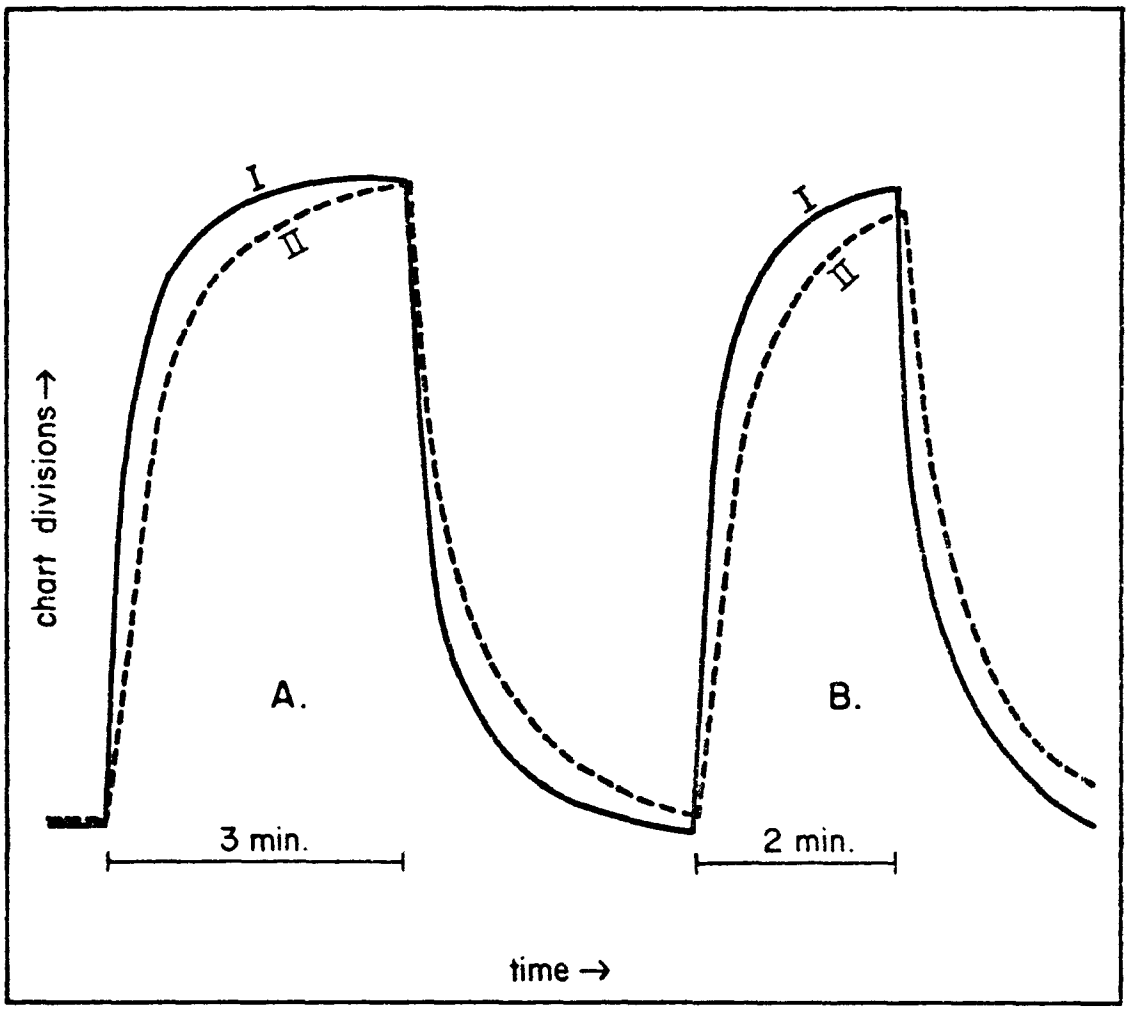

Sample and Wash Time: A - 3 minutes
B - 2 minutes

Flow Rate: I - 2.04 ml/minute
II - 0.95 ml/minute

Figure 40. Effect of flow rate versus response time.

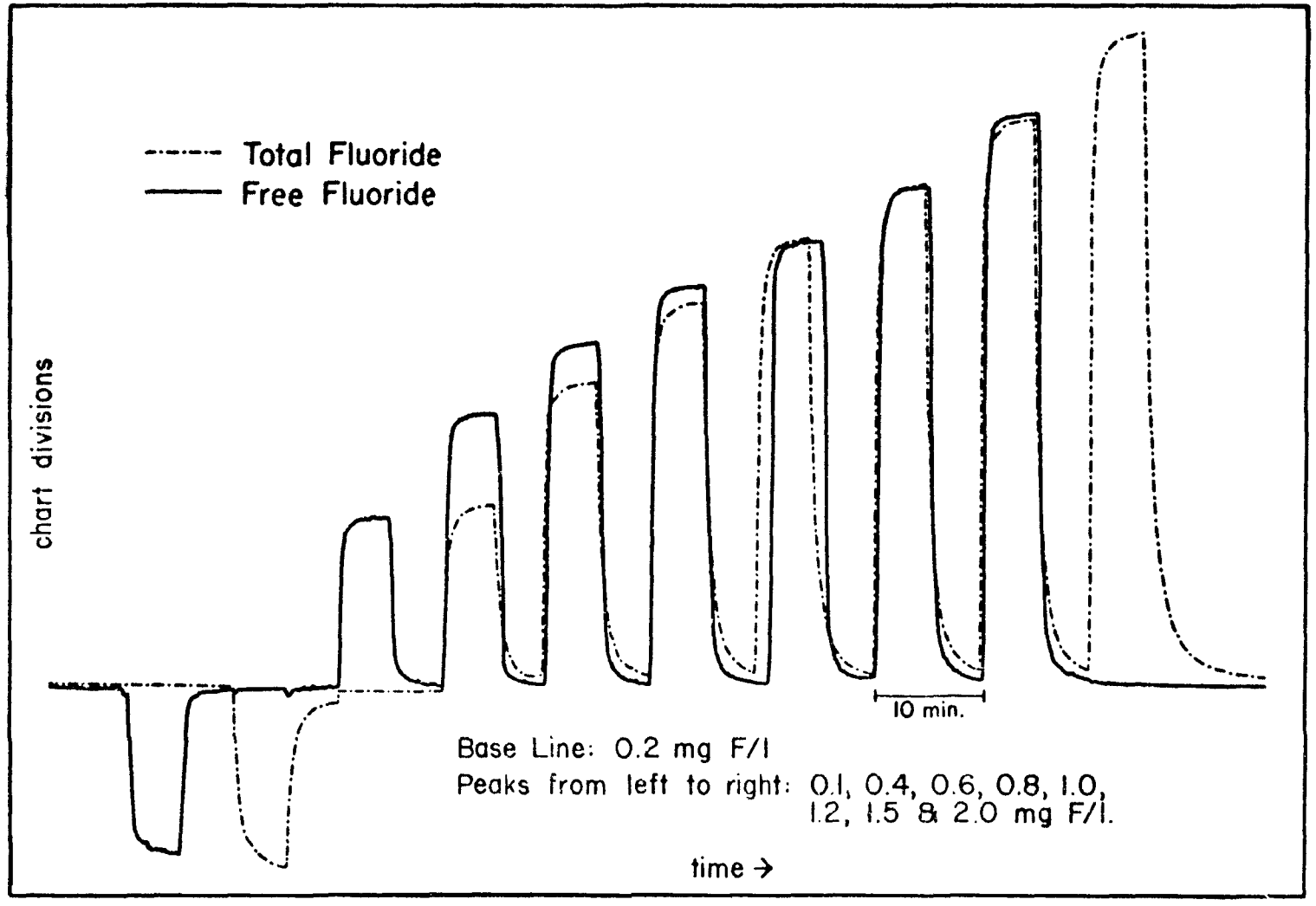

Figure 41. Recorder output for calibration of free and total fluoride. Sample and wash time, 5 minutes each.

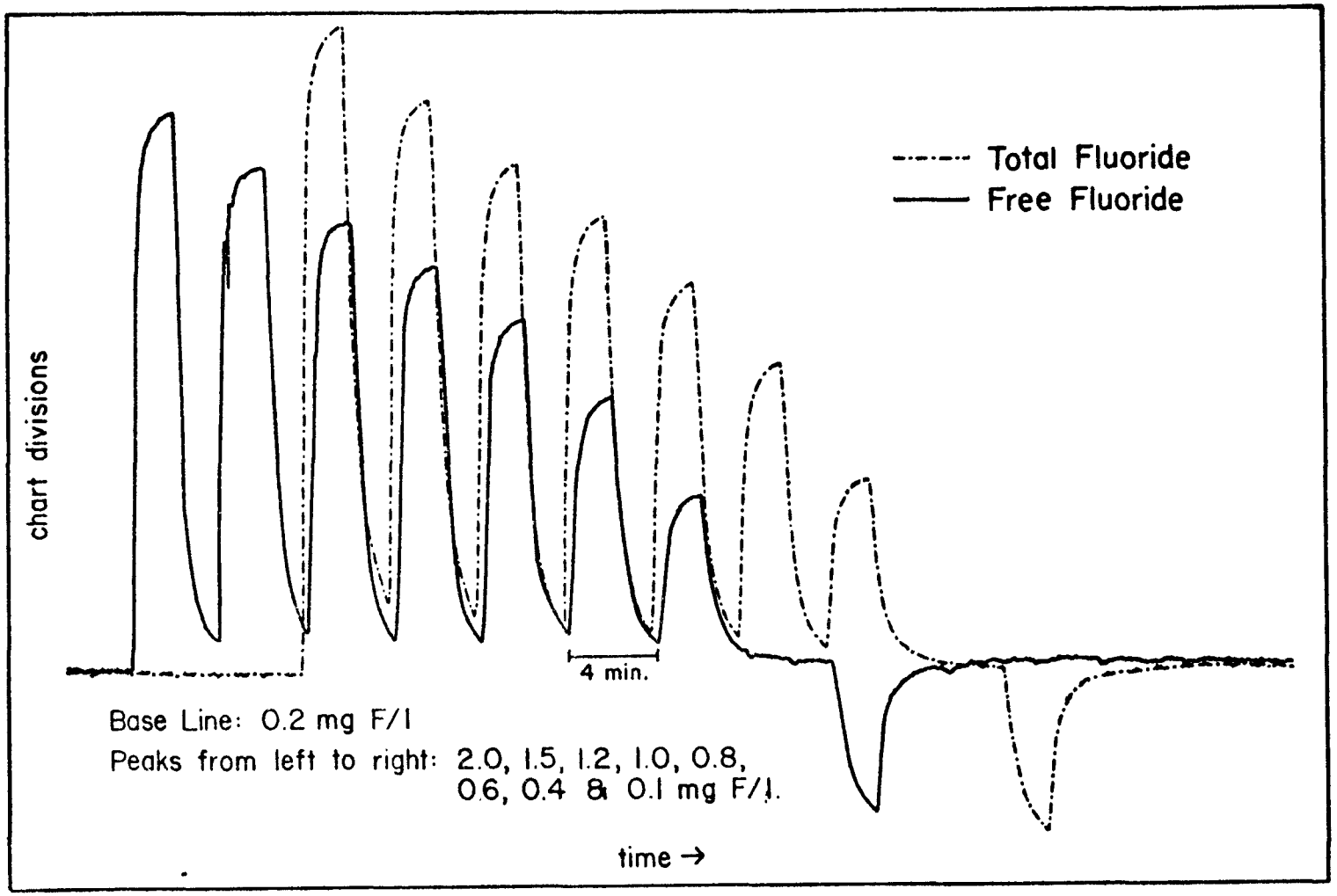

Figure 42. Recorder output for calibration of free and total fluoride. Sample and wash time, 2 minutes each.

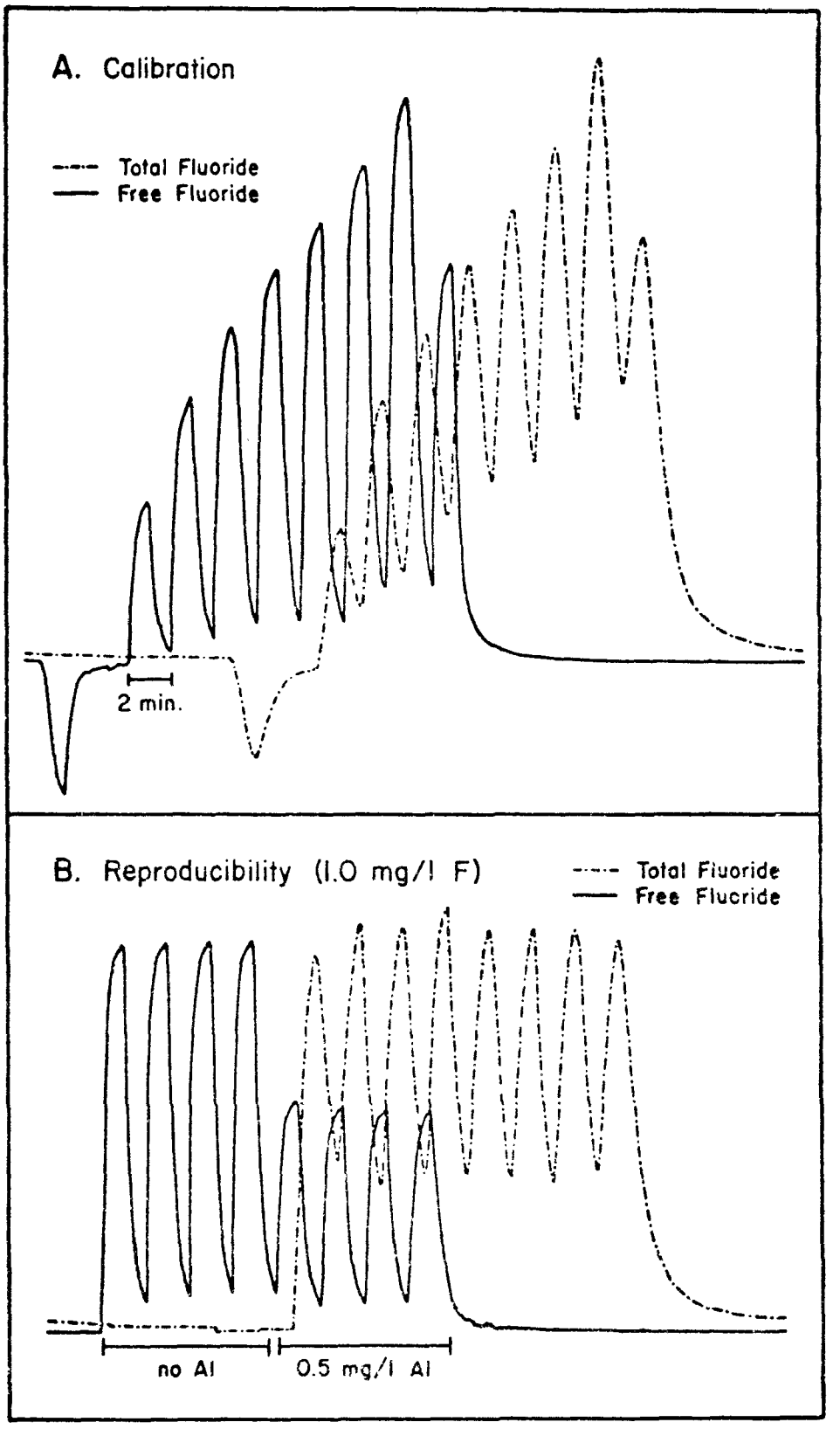

Figure 43. Recorder output for calibration of free and total fluoride. Sample and wash time, 1 minute each.

show calibration curves made at five, two, and one minute sample/wash times, respectively. At one minute, reproducibility was poor, with or without aluminum present (Figure 43). A sample/wash time of two minutes each; i.e., 15 samples/hour, was highly reproducible and adequate for automation.

Calibration

Recorder outputs for the calibration procedure with sample/wash times of two minutes each are shown in Figure 42. Fluoride standards with increments from 0.1 to 2.0 mg/l were used. Each standard is represented by two peaks, one for free and one for total fluoride. Calibration curves drawn from corresponding peak heights versus fluoride concentrations are shown in Figure 44. A linear relationship was shown to exist for samples to 200 mg/l or $>10^{-2}$M F^-, but this level is much greater than any level expected to occur in drinking water measurements.

Precision

Precision of the automated system was evaluated by calculating the deviation (S), in mv, from peak heights and determining the corresponding S in concentration from the following relationships:

$$E_1 = E_o - 2.3 \frac{RT}{F} \log A_1 \tag{114}$$

and:

$$E_2 = E_o - 2.3 \frac{RT}{F} \log A_2 \tag{115}$$

where:

E_1 = potential of fluoride concentration C_1
A_1 = activity of fluoride concentration C_1
E_2 = potential of fluoride concentration C_2
A_2 = activity of fluoride concentration C_2

$$E_1 - E_2 = 2.3 \frac{RT}{F} (\log C_2 - \log C_1) \tag{116}$$

$$\frac{\Delta E}{\text{slope}} = \log C_2 - \log C_1 \tag{117}$$

Thus, with the potential difference resulting from fluoride measurements, the slope, and original concentration (C_1) known, C_2 and ΔC can be calculated; and the difference in concentration (ΔC_x) at any other fluoride level (C_x) resulting from a potential variation (ΔE_x) can be expressed as:

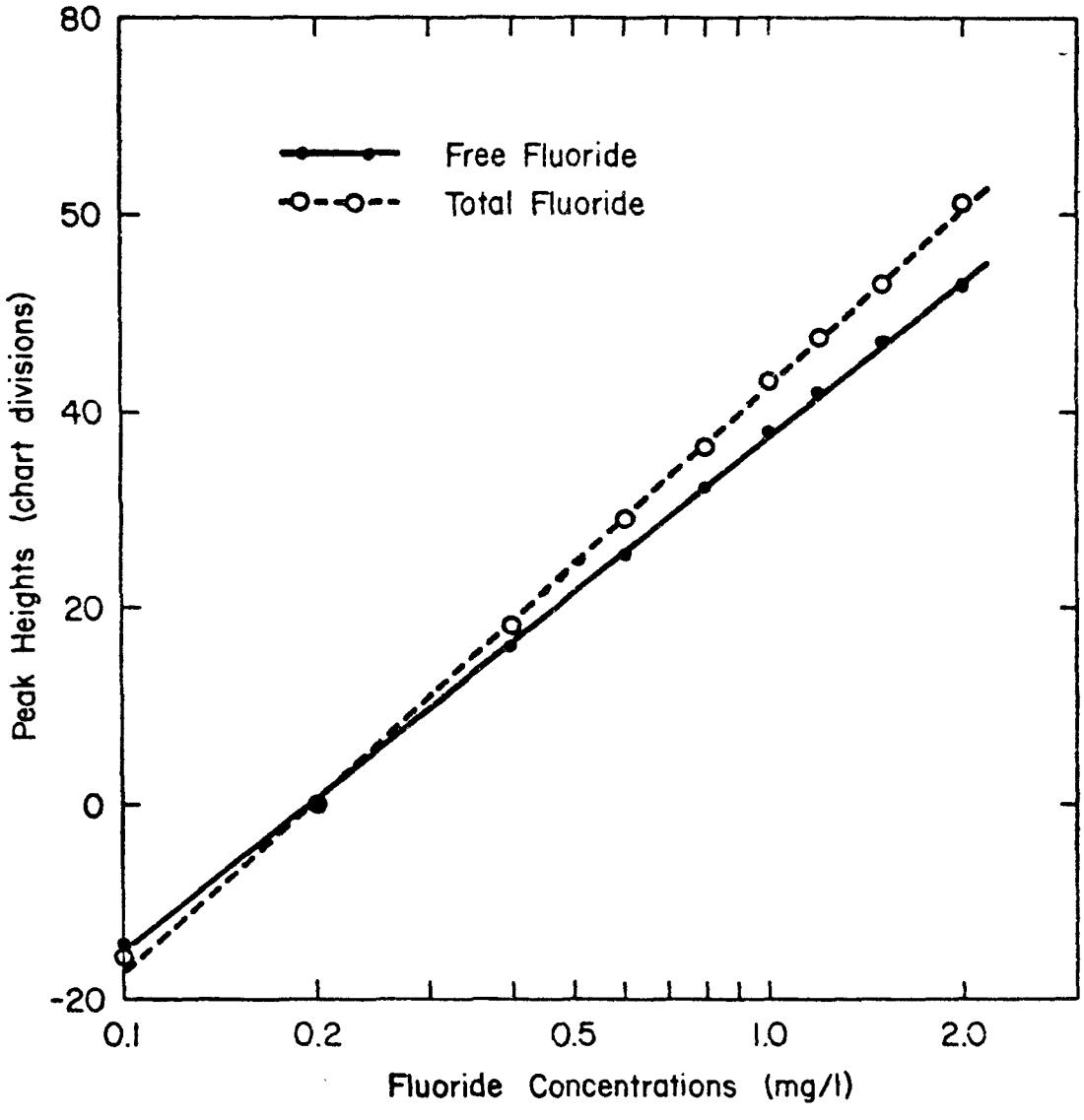

Figure 44. Calibration curves for automated fluoride electrode measurement.

$$\Delta C_x = \frac{\Delta C}{C_1} C_x \Delta E_x \tag{118}$$

i.e., at 25°C, F^- = one mg/l, and the slope is ≃ 60 mv, the effect of a one mv potential variation is:

$$\frac{1}{60} = \log C_2 - 0 \tag{119}$$

or:

$$C_2 = 1.04 \text{ mg/l} \tag{120}$$

and:

$$\Delta C = 1.04 - 1.0 = 0.04 \text{ mg/l} \tag{121}$$

Reproducibility of fluoride measurements at various levels of fluoride and no complexing agents is shown in Figure 45. The reproducibility with fluoride of 1.0 mg/l and various levels of aluminum is shown in Figure 46. Standard deviations and coefficients of variation for peak heights in Figures 45 and 46 are shown in Table 12. The high precision of the method is clear from the low standard deviations and coefficients of variation. The concentration effect ranged from coefficients of 0.17 to 0.63 percent with a mean of 0.37 percent in the absence of aluminum, and from 0.35 to 0.99 percent (1.0 mg/l F + 1.5 mg/l Al) with a mean of 0.67 percent with aluminum present. The peak height coefficient of variation is generally smaller than the concentration coefficient, but increases as peak height decreases; thus, concentration coefficients are better measurements of precision.

Accuracy

Accuracy is measured by mean error ($\bar{E}$), which is defined as the difference between the actual mean of all data ($\bar{X}$) and the true mean (T.V.); i.e.,

$$\bar{E} = \bar{X} - \text{T.V.} \tag{122}$$

and:

$$\text{R.E.} = \frac{\bar{X} - \text{T.V.}}{\text{T.V.}} \times 100 \tag{123}$$

where:

R.E. = relative error

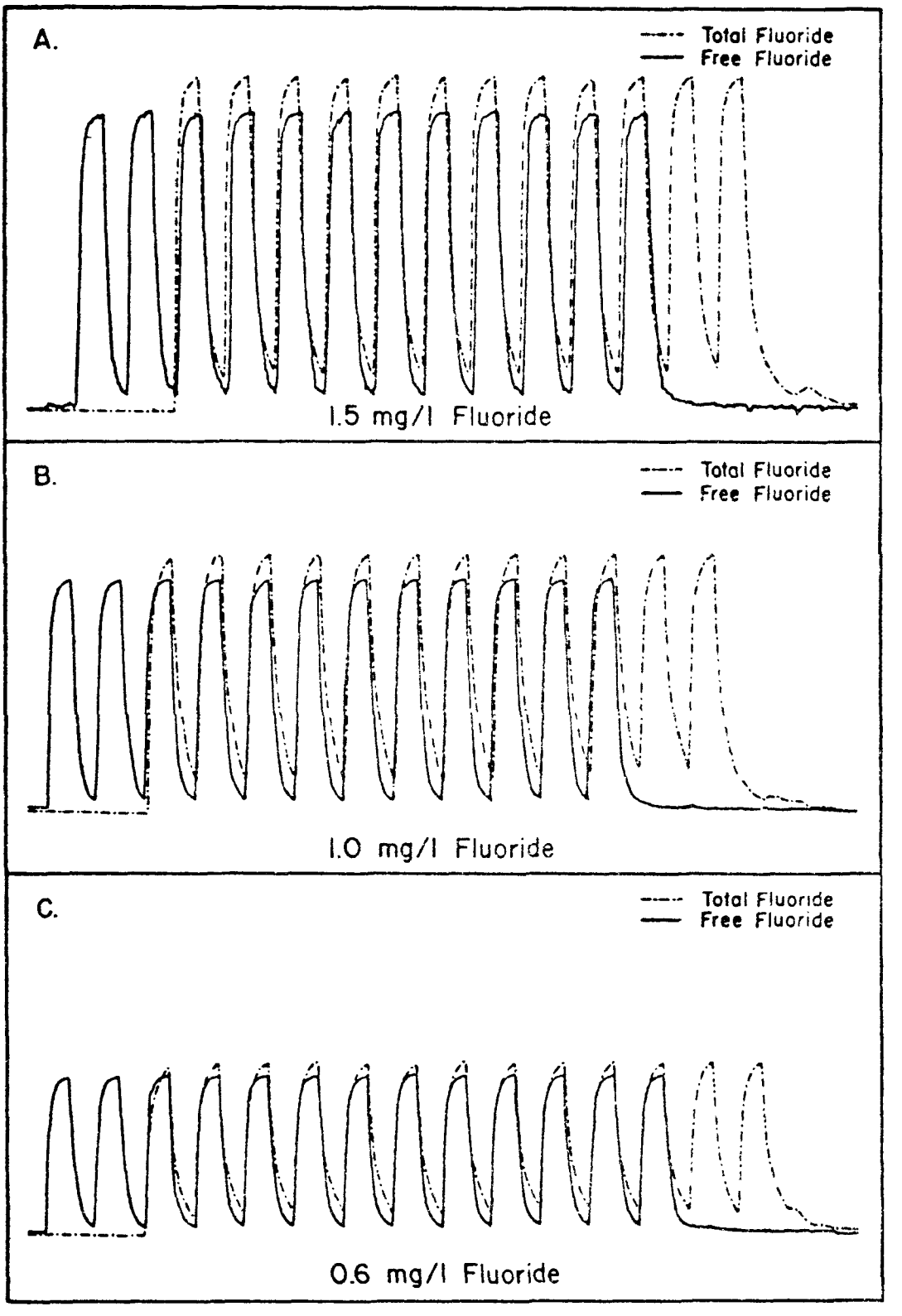

Figure 45. Reproducibility of fluoride measurement in absence of complexing cations.

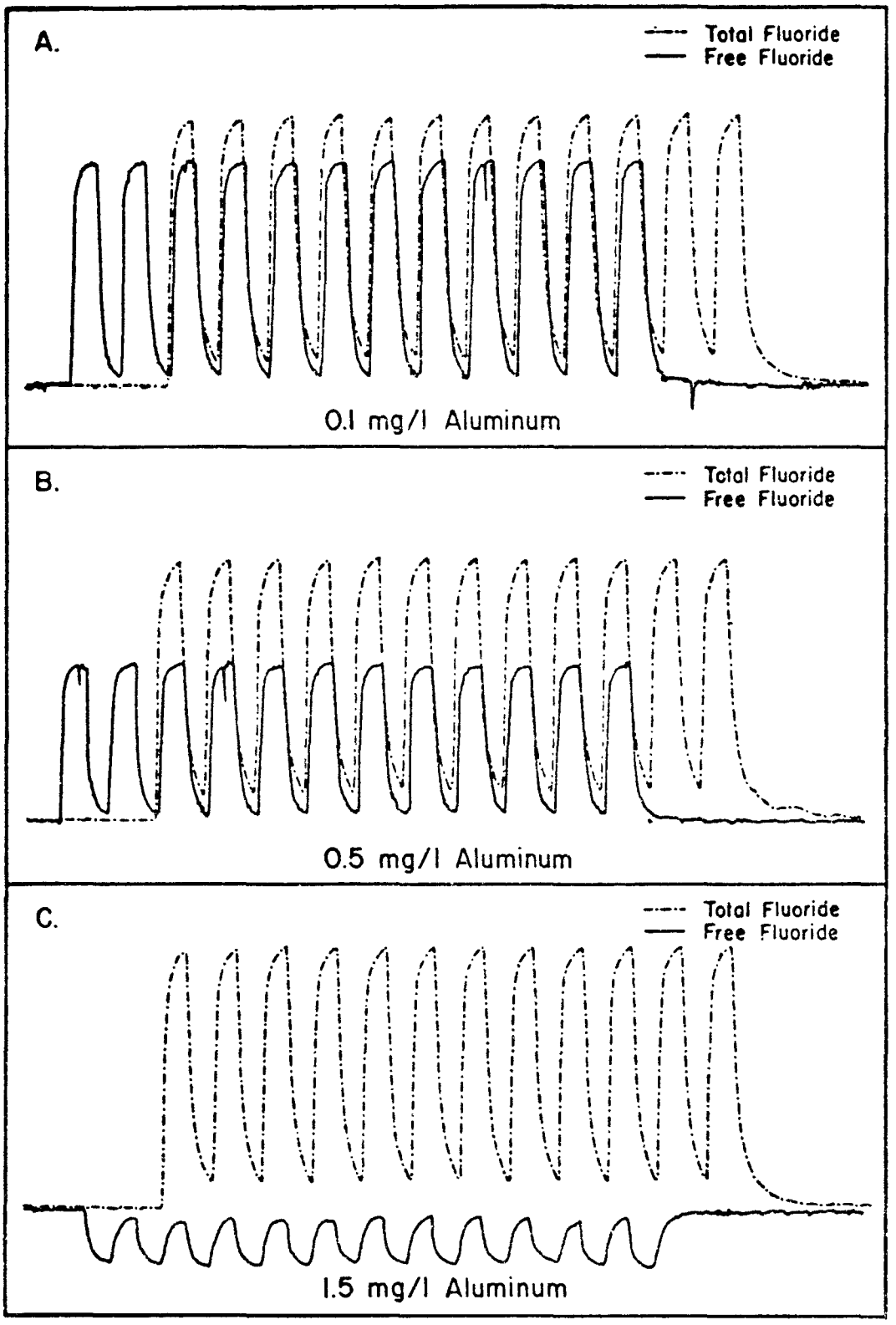

Figure 46. Reproducibility of fluoride measurement (1.0 mg/l) in presence of aluminum.

Table 12. REPRODUCIBILITY OF AUTOMATED MEASUREMENTS AT DIFFERENT FLUORIDE LEVELS IN PRESENCE AND ABSENCE OF ALUMINUM

Original Conc.(mg/l) F + Al	Fluoride Form	Fluoride Measured Mean Value		Standard Deviation		Coefficient Variation	
		Peak Height (Chart division)	F.Conc. (mg/l)	Peak Height	F.Conc.	Peak Height (%)	F.Conc. (%)
1.5 + 0.0	Free	47.97	1.50	.065	.004	.14	.27
	Total	54.59	1.50	.158	.009	.29	.63
1.0 + 0.0	Free	38.28	1.00	.101	.004	.26	.40
	Total	43.30	1.00	.074	.003	.17	.30
0.6 + 0.0	Free	25.99	.60	.030	.001	.12	.17
	Total	28.18	.60	.118	.003	.42	.47
1.0 + 0.1	Free	36.52	.92	.188	.008	.51	.75
	Total	43.61	1.02	.185	.007	.42	.73
1.0 + 0.5	Free	24.58	.58	.104	.002	.42	.35
	Total	42.9	.98	.119	.005	.28	.50
1.0 + 1.5	Free	-9.26	.12	.247	.001	2.66	.99
	Total	43.32	1.00	.178	.005	.411	.71

In establishing the accuracy of the fluoride automated system, data were correlated with SPADNS data for the same samples, expressed as T.V. Actual data obtained for test waters from two Michigan cities using both SPADNS and the automated technique are shown in Tables 13, 14, and 15 (pages 107, 108, and 109, respectively).

Continuous Fluoride Monitor

Figure 47 is a schematic illustration of the complete fluoride monitoring system installed in the mobile laboratory. The system operates on a 26-minute cycle, controlled by the computer. At initiation of the cycle, the relay is switched to the "on" position and the three-way valve is connected through to the baseline solution. For the next 13 minutes, baseline solution is drawn into the system. Ahead of the pump, a Y-connector separates the sample and sends it to both the free and total

Table 13. FLUORIDE AND IRON DETERMINATIONS IN WATER SAMPLES (mg/l) FROM JACKSON, MICHIGAN, 2067

Sample Number	Location	Free Fluoride, Electrode (mg/l)	Total Fluoride (mg/l)		Iron, Phenan-throline (mg/l)	Emission Spectroscopy	
			Electrode	SPADNS		Aluminum (mg/l)	Iron (mg/l)
1	Well raw water	0.22	0.22	0.28	1.45	0.03	1.35
2	Plant effluents, N. pump	0.25	0.25	0.30	1.24		
3	Plant effluent, composite of N. E25 pumps	1.10	1.11	1.09	1.20	0.03	1.15
4	Moby Dick Restaurant	0.29	0.30	0.37	0.27		
5	Miller Eng. Co.	0.47	0.48	0.51	0.94		
6	Elec. Maint. & Supply Co.	0.29	0.30	0.33	1.03		
7	City Hall	0.99	1.00	1.01	1.98		
8	Fire Station No. 1	0.70	0.70	0.70	2.00		
9	Union Gas Station	1.11	1.11	1.10	1.26		
10	Residential house	0.79	0.79	0.81	0.62		
11	Laundry	0.79	0.78	0.79	N.D.*		
12	Shell Station	0.72	0.73	0.75	0.32		

*Not detectable

Table 14. CHARACTERIZATION OF FLUORIDE IN WATER SAMPLES FROM WYOMING, MICHIGAN BY THE MANUAL AND AUTOMATED ELECTRODE METHODS

Location	Sample Number	Free Fluoride (mg/l)		Total Fluoride (mg/l)		Complexed* Fluoride (%)	Aluminum (mg/l)	Iron (mg/l)
		Manual	Automated	Manual	Automated			
Well raw water	1–A+	.11	.12	.11	.13	–	–	–
	2–B+	.11	.11	.11	.12	–	.02	.100
Plant effluent	3–A	.79	.75	1.07	1.06	26.2	–	–
	4–B	.75	.72	1.06	1.03	29.2	.40	.015
Hudsonville	5–A	.87	.83	1.04	1.05	16.4	–	–
	6–B	.72	.68	1.06	1.05	32.1	–	–
Georgetown	7–A	.92	.88	1.08	1.11	14.8	.10	.020
	8–B	.76	.74	1.06	1.05	28.3	.30	.020
Geron	9–A	.87	.87	1.04	1.05	15.6	–	–
	10–B	.80	.73	1.06	1.05	24.5	–	–
Kentwood	11–A	.89	.85	1.06	1.06	16.0	–	–
	12–B	.77	.71	1.06	1.06	27.4	–	–
City Hall	13–A	.87	.83	1.06	1.05	17.9	–	–
	14–B	.81	.75	1.06	1.06	23.8	–	–
Pyron-Porter	15–A	.88	.85	1.05	1.06	16.2	–	–
	16–B	.79	.72	1.05	1.05	24.8	–	–
Nogel-Albers	17–A	.87	.86	1.06	1.08	17.9	–	–
	18–B	.70	.72	1.06	1.07	33.3	.40	.015

+ A: grab sample (July 22, 1971); B: Composite (15–22 July, 1971)

* Calculated from the manual electrode measurement.

Table 15. SOME STATISTICAL DATA RELATED TO MANUAL AND AUTOMATED FLUORIDE ELECTRODE MEASUREMENTS IN WATER SAMPLES FROM WYOMING, MICHIGAN

Parameter	Free–F Measurement		Total–F Measurement	
	Manual	Automated	Manual	Automated
Mean, $\bar{x}$ *	0.737 mg/l	0.704 mg/l	0.952 mg/l	0.955 mg/l
Std. Deviation, S	0.2367	0.2252	0.3065	0.3034
Correlation coefficient, r	0.9931		0.9989	
Degrees of freedom, d.f.	34		34	
t–value	0.4436		0.0240	
Statistical difference	N.S.†		N.S.	

*All the 18 samples were included.

†Not significant – no difference could be established.

fluoride systems. Beyond the pump, an air bubble is introduced to separate the sample stream into many discrete samples and the appropriate buffer reagent is added. Next, a mixing coil provides mixing and reaction time before sample reaches the sensors. Mixing coil length is especially important in areas where free fluoride is significantly different than total. The sample stream is debubbled just before it enters the sensor flow cells. The bubble stream goes to waste under siphon while the remainder of the sample is drawn by a fourth pump line past the sensors, then to waste. At the end of the 13-minute period, the computer sets the relay to "off" and the three-way valve is open to the tap water sample stream. A complete cycle of 26 minutes is required to read both baseline and tap water samples. Prepared reagents are sufficient for ten days to two weeks, depending on system downtime.

Fluoride sensor flow cells are constructed from glass, not plastics. As new cells are required, they are aged (placed in service for 24 hours to reach equilibrium with fluorides in the test stream) to prevent loss of fluoride from adsorption. Other glass components; e.g., mixing coils, are similarly aged.

Normal daily maintenance of the fluoride system includes careful examination of the recorder output to assure that the signal is of high quality. Bubbles which become trapped in the flow cells and on the surface of the electrode sensing element are the most frequent problem. They are removed by briefly pinching off the

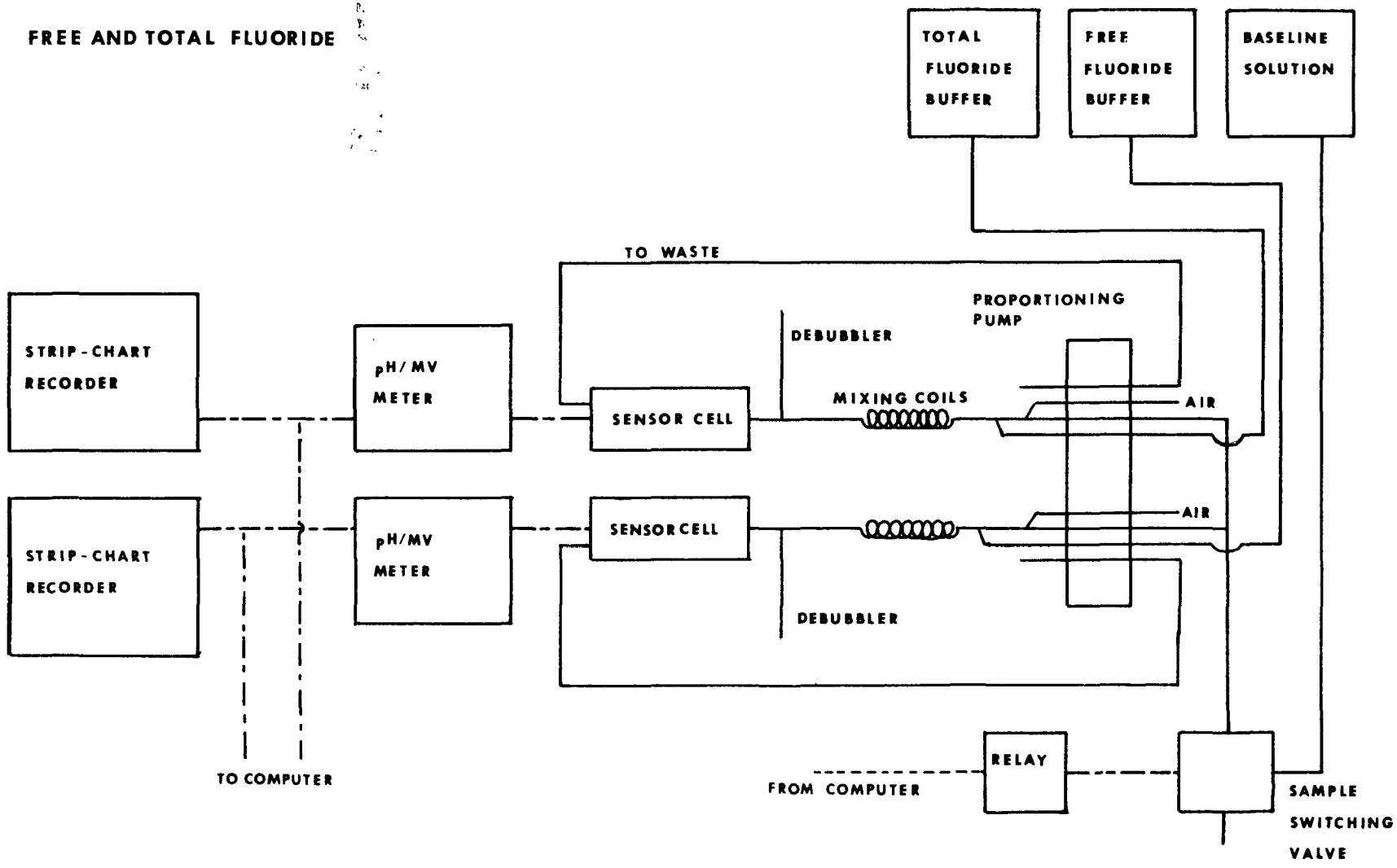

Figure 47. Schematic illustration of free and total fluorides monitor in the mobile laboratory.

flow cell outlet and releasing it quickly, causing a flow surge in the cell. Persistent bubbles are dislodged by removing the electrode from the flow cell and replacing it immediately. The millivolt meter is in the standby mode during this operation.

Standard solutions used for calibration of the strip chart and computer output are 0.2, 0.5, and 1.0 mg/l fluoride in distilled water. Peak heights are measured in chart units (or mv) and plotted on semilogarithmic graph paper, with peak height on the linear scale and concentration on the log scale. Figure 48 is an example of fluoride system output and includes a calibration series. Figure 49 is the calibration curve prepared from this recording.

	Peak Height (C.U.)	
$[F^-]$ (mg/l)	Free	Total
0.1	0.0	0.0
0.2	25.0	17.0
0.5	53.5	36.5
1.0	78.0	52.5

Fluoride concentrations in tap water are determined by measuring peak heights and comparing them with the calibration charts. It is important to note that the three or more points describing the calibration curve may not be linear, particularly as electrodes age. It is not uncommon to observe a decreasing slope with decreasing concentrations of fluoride.

Field Studies

The fluoride system was used to acquire data from several special field studies. Samples from Jackson, Wyoming, and Ann Arbor, Michigan were analyzed in the laboratory prior to installing the fluoride monitor in the mobile laboratory.

Jackson, Michigan

Raw water for the City of Jackson, Michigan is drawn from deep wells (380 to 400 feet) in rock. Treatment includes chlorination and fluoridation only. Fluoride is added as sodium silica fluoride. Polyethylene bottles were used to collect 12 grab samples from the well field, the water treatment plant, and a number of sites along a principal distribution system pipeline.

Fluoride in these samples was measured in the NSF laboratory by ion-selective electrode and SPADNS; and iron, by phenanthroline. Results are shown in Table 13. Iron levels ranged from 0.27 to

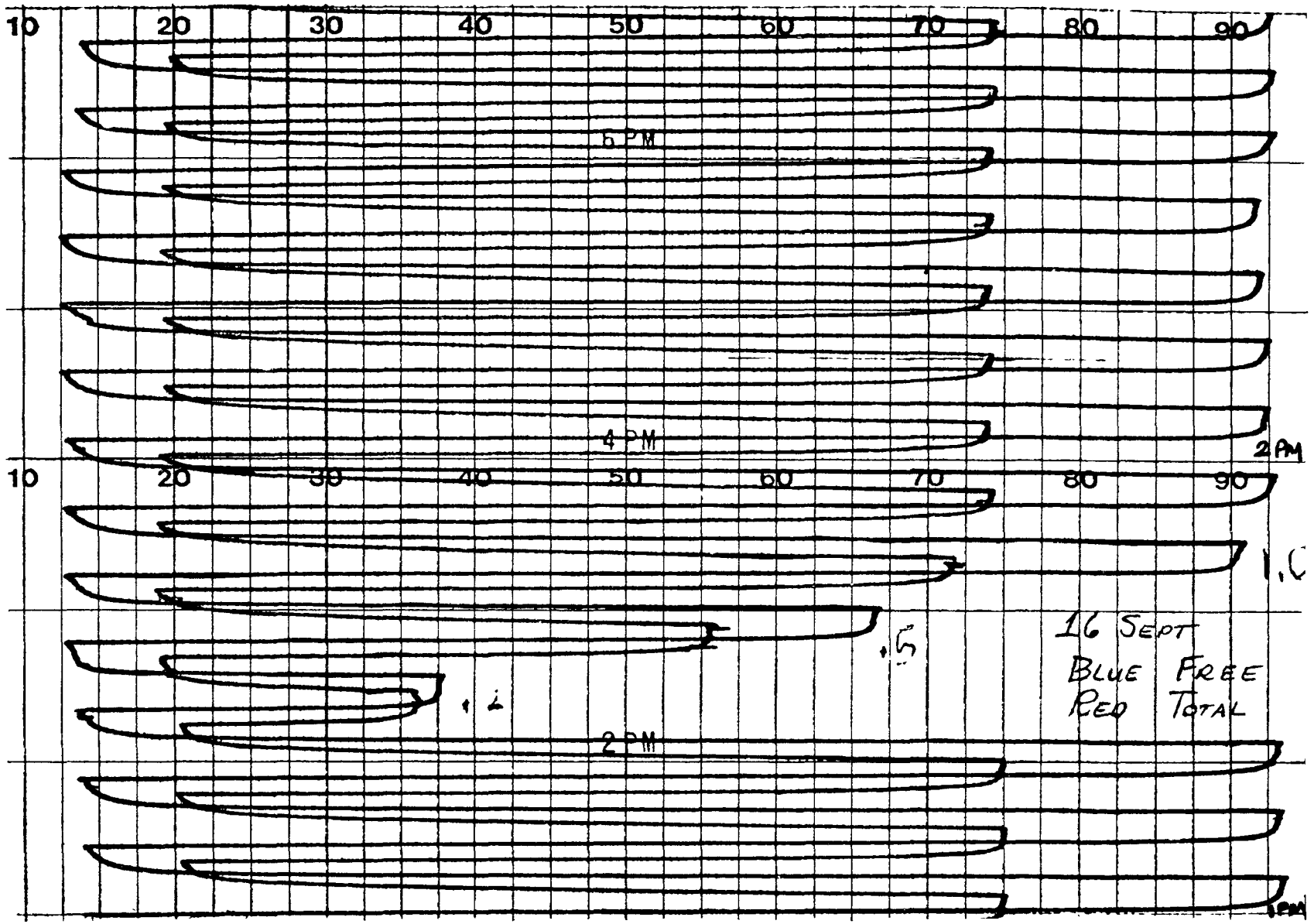

Figure 48. Fluoride system output including a calibration series.

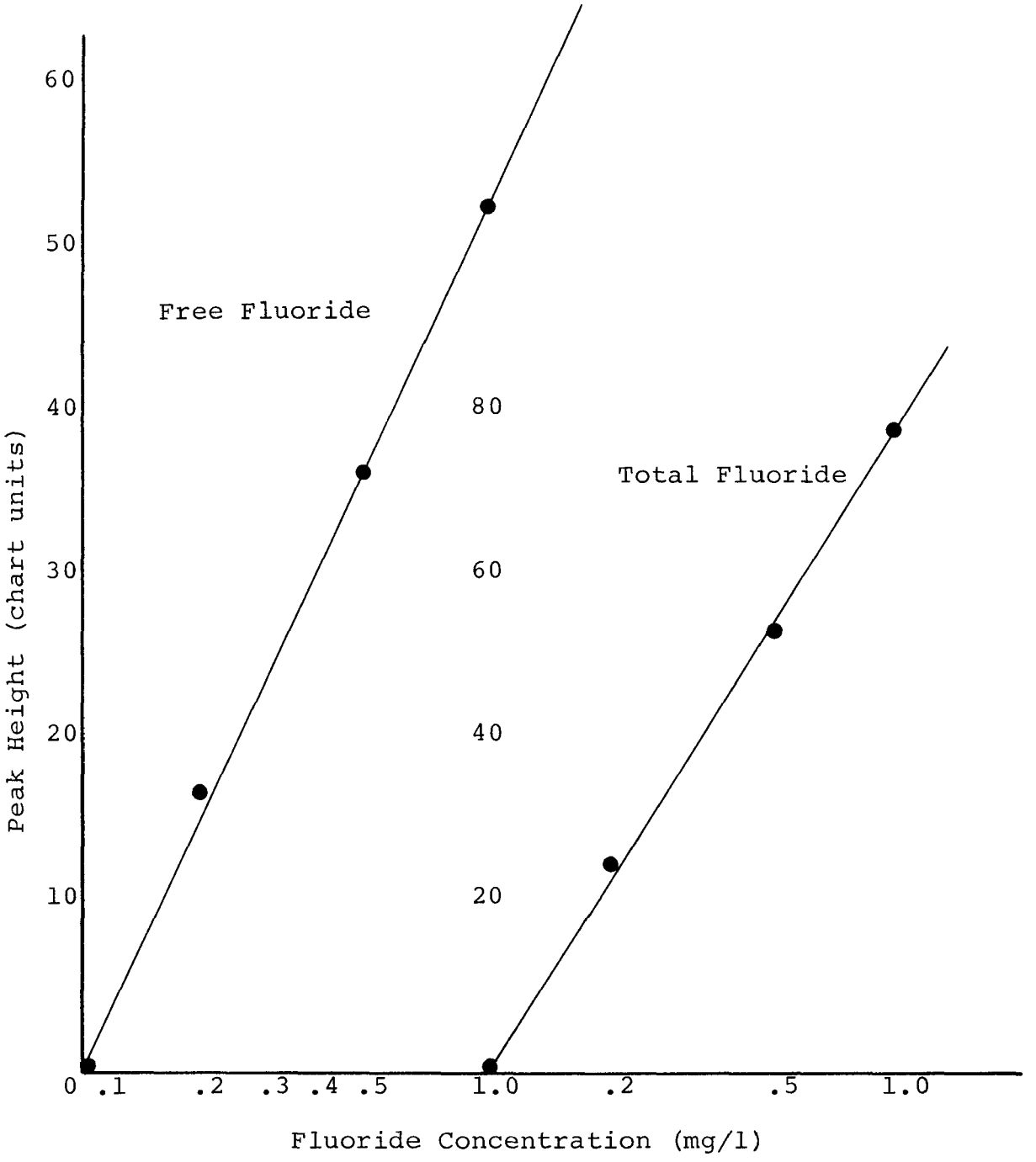

Figure 49. Typical calibration curves for fluorides, prepared from output in Figure 48.

2.0 mg/l, with a mean of 1.12 mg/l. (The laundry, sample no. 11, apparently used iron removal procedures to protect against stains. This sample was excluded from the mean.) Comparison of the data for free versus total measured fluorides indicated no significant complex formation at these levels of iron. This is consistent with previous laboratory observations. The wide variations in fluoride levels were attributed to inefficient mixing as the water was fluoridated. Sodium silica fluoride is mixed as a paste and fed to the water in pulses, creating a nonhomogeneous mixture of fluoride and treated water.

The fluoride data acquired by ion-selective electrode and that from SPADNS were highly correlated; i.e., correlation coefficient equal to 0.994 and student's t equal to 0.1975, indicating there was no statistically significant difference between the two methods.

Wyoming, Michigan

The population of Wyoming is 78,000. Raw water is drawn from 380 to 400 feet deep wells in rock. Treatment includes alum flocculation, filtration, phosphate addition for corrosion control, chlorination, and fluoridation. Both grab and weekly composite samples were analyzed in the laboratory. Results are shown in Table 14.

Levels of complexed fluoride were clearly significant in the Wyoming treated water supply. In the distribution system, they ranged from 14.8 to 33.3 percent of the total fluoride. Key samples were also analyzed for aluminum and iron by emission spectroscopy (Table 14). There was close correlation between aluminum levels and fluoride complexation (correlation coefficient = 0.96). The data from manual and automated measurement of fluorides in Wyoming samples are compared statistically in Table 15. Again, the two methods were not significantly different.

Ann Arbor, Michigan

Ann Arbor has a population of 84,000 and takes 80 percent of its raw water supply from the Huron River, and 20 percent from wells in drift, 35 to 56 feet deep. Treatment includes alum flocculation, lime softening, filtration, phosphate addition for corrosion control, chlorination, and fluoridation. Data from 15 locations sampled on April 6, 1971 are shown in Table 16. Most of the Ann Arbor area is represented in three samples. Aluminum in these samples was <0.02 mg/l; and iron, <0.1 mg/l. No complexing effects occur at these levels; i.e., free and total fluoride levels are essentially the same. It is further suggested by the data in Table 16, that fluoride levels are similar throughout the distribution system; i.e., they are not affected by length of pipeline or main residence times.

Table 16. CHARACTERIZATION OF FLUORIDE IN WATER SAMPLES FROM ANN ARBOR, MICHIGAN (APRIL 6, 1971)

Sample Number	Location	Free Fluoride (mg/l)	Total Fluoride (mg/l)
1	River raw water	.14	.14
2	Well raw water	.30	.30
3	Plant finished effluent	.96	.97
4	Shell station, 1251 N. Maple	.94	.95
5	Fire station, 2130 W. Huron	.95	.96
6	Standard station, 1336 S. Main	.96	.96
7	Lakewood School, 344 Gray Lake	.95	.94
8	Residency, 2250 S. Seventh	.98	.98
9	Water Department Distribution Center, S. Industrial Highway	.98	.98
10	Main fire station, 219 E. Huron	.95	.96
11	Northside School, 912 Barton	.93	.93
12	Bolgos Farms Store, 3601 Plymouth Road	.96	.94
13	Concordia College, 4090 Geddes	.96	.97
14	Mary D. Mitchell School, Pittsview Drive	.96	.97
15	Newport Elementary School, 2776 Newport Road	.98	.99

Average values of fluoride analyses from different locations in Ann Arbor at various times during the period 1970 to 1972 are shown in Table 17. During 1970, fluoridation was inadequate. Fluoride concentrations were considerably below the optimum level.

Table 17. CHRONOLOGICAL CHARACTERIZATION OF FLUORIDE IN WATER DISTRIBUTION SYSTEM OF ANN ARBOR, MICHIGAN

Date	Free Fluoride* (mg/l)	Total Fluoride* (mg/l)	Complexed Fluoride Percent
July 28, 1972	0.98	.99	NS
April 3, 1972	0.98	1.00	NS
January 20, 1971	1.08	1.10	NS
September 16, 1971	1.11	1.11	NS
April 6, 1971	0.96	0.97	NS
March 22, 1971	0.97	0.98	NS
March 9, 1971	0.94	0.94	NS
November 6, 1970	0.43	0.50	14.0
October 4, 1970	0.59	0.64	7.8
October 15, 1970	0.29	0.33	9.1
October 5, 1970	0.49	0.53	7.5

*Values presented are mean values of >10 samples

Aluminum analyses showed variations from <0.02 to 0.5 mg/l, and iron varied from <0.015 to 0.9 mg/l during that period. Fluoridation has improved since early 1971. Levels now approach 1.0 mg/l, the optimum level. Aluminum is generally below 0.05 mg/l; and iron, below 0.3 mg/l.

Chicago, Illinois

Raw water for the City of Chicago is entirely of surface origin. It is drawn from Lake Michigan and treated in one of two plants, the Central- or the South- Water Filtration Plants. The combined rated pumping capacity from these two plants is nearly three billion gallons per day. Distribution is made through more than 4,000 miles of tunnels and mains to all of Chicago and 72 suburban communities. Treatment at both plants includes alum-lime flocculation, high rate filtration, chlorination, and fluoridation. Caustic for corrosion control is added at the Central Plant.

During its first month's assignment in the Chicago area, the mobile laboratory was located at a fire station, 10.5 miles from the Central Plant. Average daily mean, high, and low free and total fluoride levels recorded on coincident days of normal opera-

tion are summarized in Table 18. Although aluminum is not measured in the mobile laboratory, the water treatment plant laboratory reported a level of 0.16 mg/l in routine quarterly distribution system samples from the north district. It is apparent that complexed fluorides are important in the Chicago water supply.

Table 18. SUMMARY OF FREE AND TOTAL FLUORIDE DATA (CHICAGO/LEHIGH STATION)

Total Fluoride, (mg/l)				Free Fluoride, (mg/l)			
High	Low	Average Daily Mean	n	High	Low	Average Daily Mean	n
1.10	.66	.90	15	.90	.47	.71	15

Beginning at 1200 hours on May 25, 1973, fluoride feeders at the Central Plant were taken out of service. The purpose of this operational change was to observe the capability of the fluoride monitor in the NSF/EPA mobile laboratory to detect the change, and to determine residence times in the distribution system. Results are reflected by a reduction in total fluoride levels recorded from 1200 to 2000 hours.

This study was repeated on May 29th and 30th with fluoride feeders cycled in- and out-of-service two times at four-hour intervals. The first out-of-service period was from midnight May 28th to 0400 hours May 29th. Results are plotted separately in Figure 50. The data show that transmission time to the Lehigh location during periods of low demand is 17 $\pm$ 1 hours. This is apparent from the first recorded drop in total fluoride. When the feeders were placed back in service, recovery was incomplete because of the low demand period and mixing in the distribution system. Also as a result of these factors, the second decrease was significantly lower than the first, and lasted until demand increased during the morning hours.

The City of Chicago operates a high purity aluminum electrode fluoride monitor (Fisher Porter) at another fire station 8.5 miles from the Central Filtration Plant. The relative locations of these stations are shown in Figure 51. Data recorded by the Chicago monitor during the May 29th-May 30th period are shown in Figure 52. The actual levels of fluoride are not expressed on the recorder output, but it is interesting to note the relative

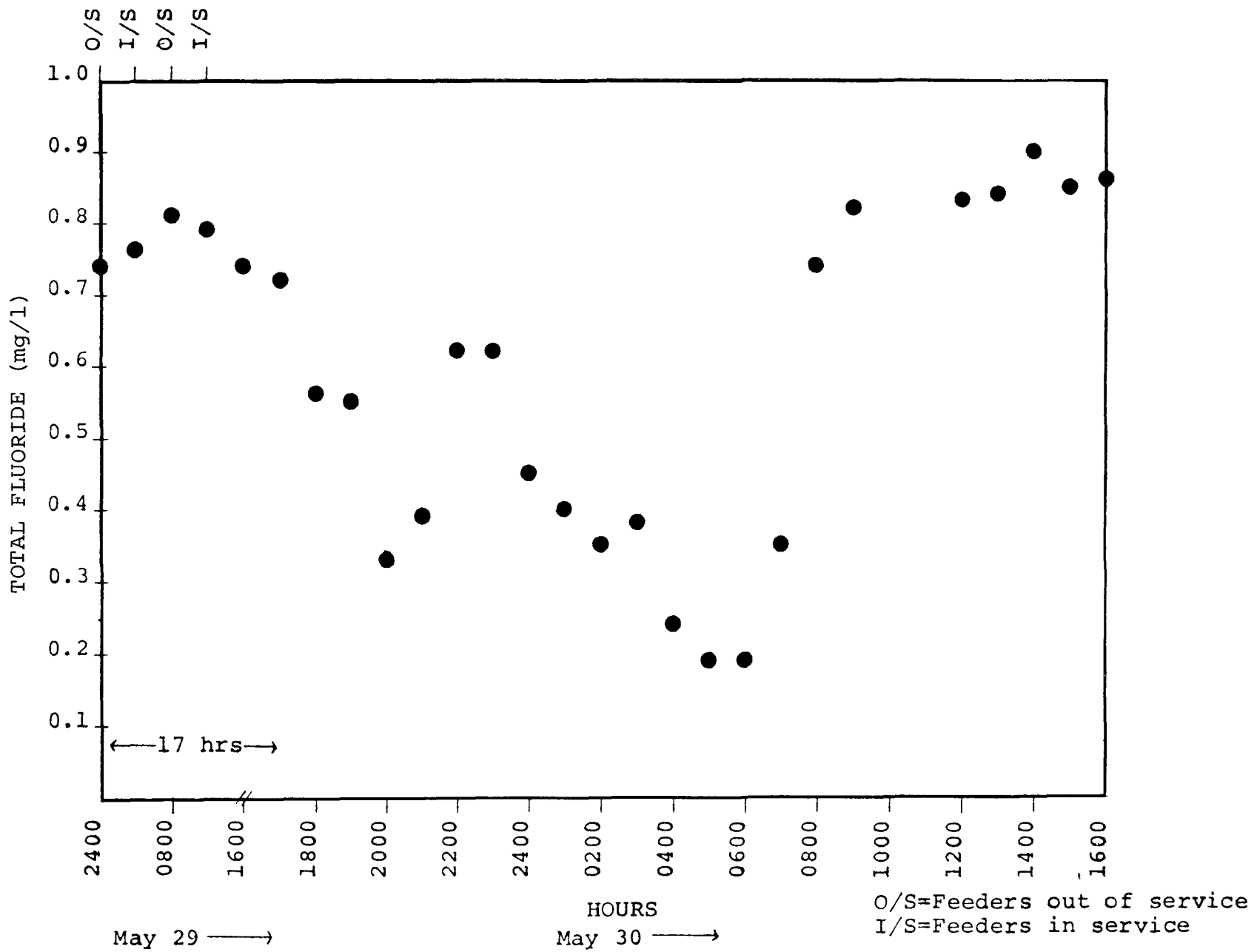

Figure 50. Special fluoride study at Chicago Lehigh station.

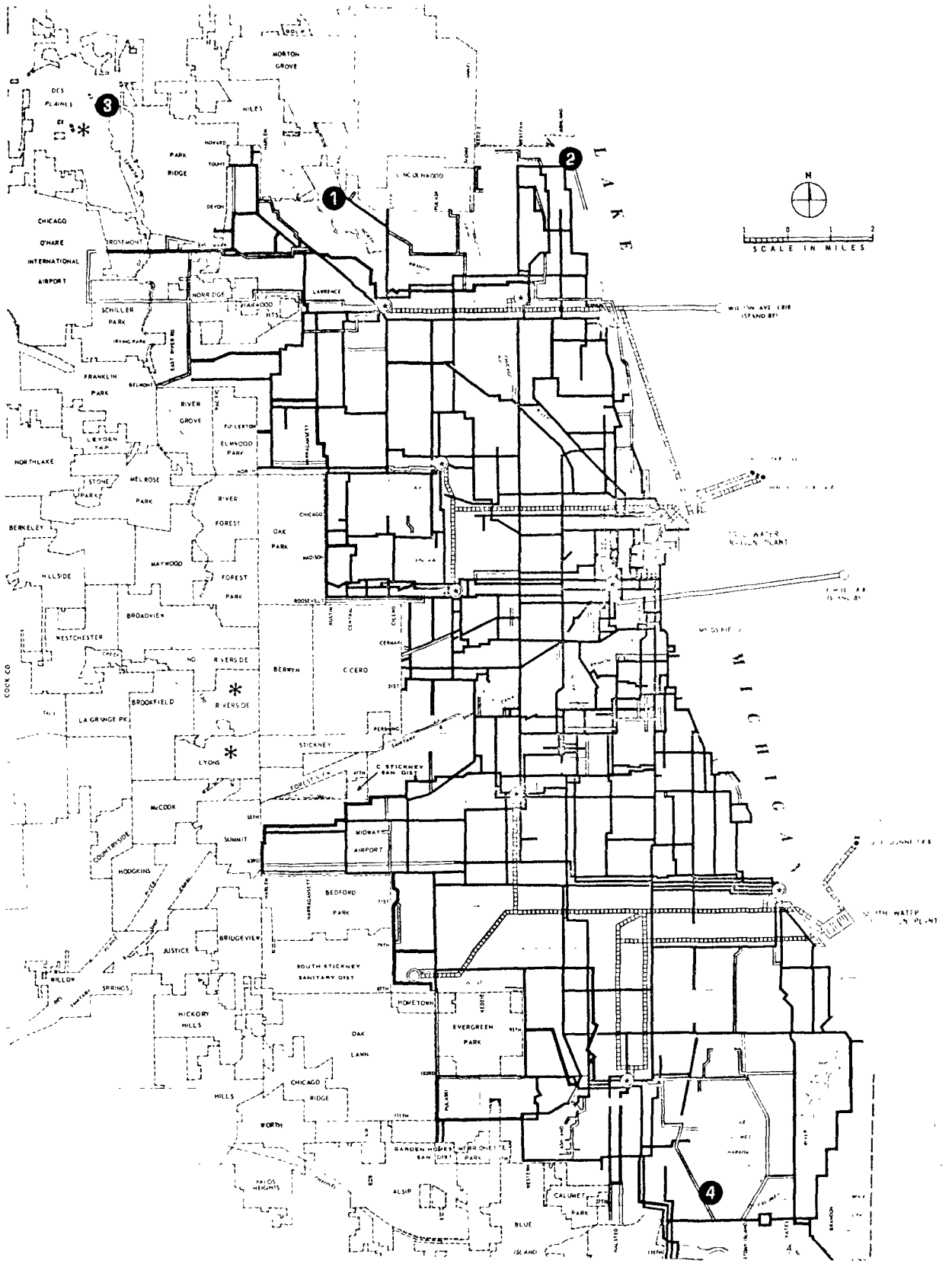

Figure 51. Map identifying relative locations of monitoring sites in Chicago.

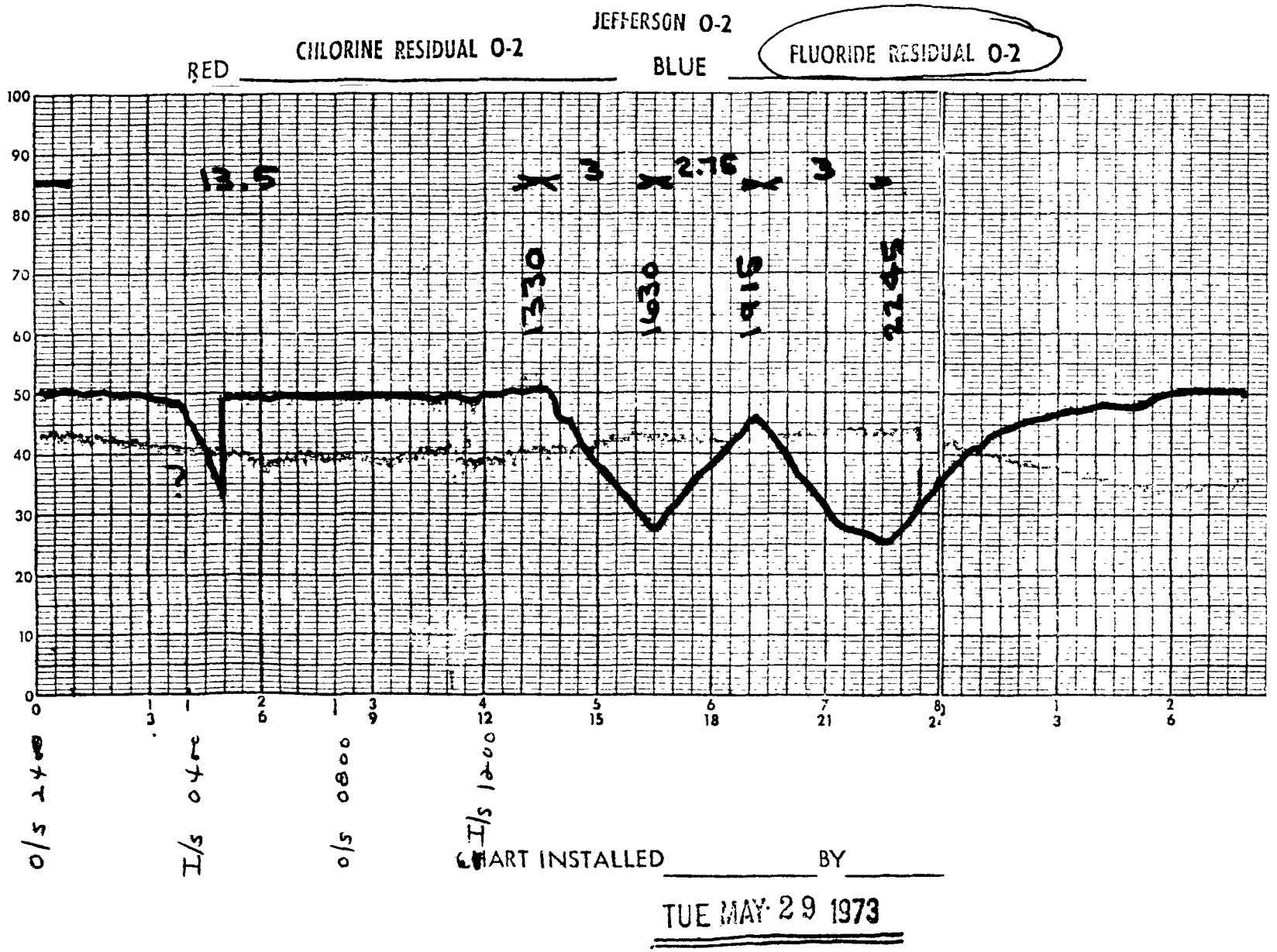

Figure 52. Output from Chicago fluoride monitor, recorded at Chicago/Greenleaf.

times at which peaks were recorded by the Chicago monitor versus those by the NSF monitor:

	1st minimum	Crest	2nd minimum
Chicago Monitor	1650	1915	2250 (May 29)
NSF Monitor	2000	2200	0600 (May 30)

(Reference to Figure 51 indicates more direct transmission to the Chicago monitor than to the NSF mobile laboratory.)

A subsequent fluoride detection study occurred at the mobile laboratory's fourth location in the Chicago area, Calumet, which receives its water from the South Water Filtration Plant. Beginning at 1000 hours on June 25, 1973, fluoride feeders were interrupted twice, with two consecutive on-off cycles. These data are plotted in Figure 53. Note that times of recorded changes at the South Plant outlet are shown in this figure. The first change at the treatment plant outfall was detected 5-1/4 hours after the feeders were taken out of service. The first minimum level was recorded at the plant outlet 9-3/4 hours after the feeders were out-of-service. This level was recorded by the NSF monitor after 31 hours.

TRACE METALS

General

Trace metals in public water supplies are of special concern because of their potential long-term chronic effects on the consumer. Surface and ground supplies vary in types and quantities of metals constituents but, in general, both are significantly lower than EPA Interim Primary Drinking Water Standards (1).

Metals are not removed by conventional water treatment processes. In addition to their occurrence in raw waters, they may be introduced to treated waters as impurities in chemicals used in the treatment process, or as products of corrosion in municipal distribution systems or individual household plumbing.

Simple analytical methods for detecting and measuring trace metals in water supplies are not generally available. Except for neutron activation analysis (NAA) and anodic stripping voltammetry (ASV), direct measurement of trace metals cannot be made without concentration of the test solution; i.e., separation, digestion with acid, and concentration, which frequently modifies the physicochemical characteristics of the species of interest.

Although activation analysis offers the high sensitivity required for trace analysis, its use is limited by availability of reactor facilities. Further, it is an elemental analysis procedure that

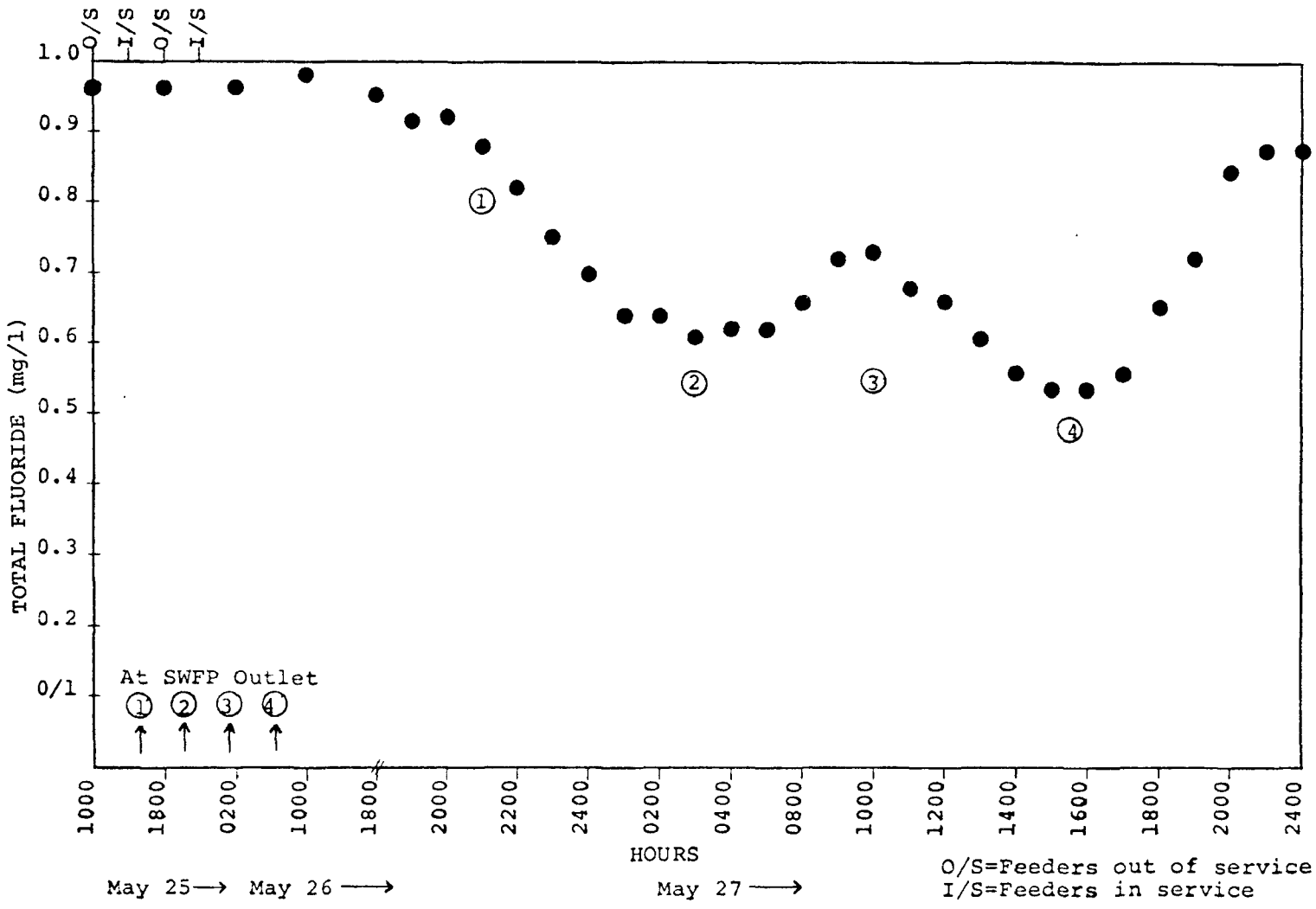

Figure 53. Special fluoride study at Calumet Harbor.

provides no information about oxidation state or degree and type of complexation.

The analytical feasibility of anodic stripping voltammetry for trace metals analysis in natural and wastewaters has been established (46). In addition to its high sensitivity, simplicity, and portability, ASV has the unique capability of characterizing free versus complexed trace metals.

Theory

ASV consists of: (1) a preconcentration (preelectrolysis, cathodic deposition, or plating) step, in which the metal ion (or ions) of interest is reduced by controlled potential electrolysis and deposited as an amalgam on the surface of a composite mercury graphite electrode (CMGE), and (2) anodic dissolution (reverse electrolysis, or stripping), in which the metal is oxidized and returned to solution. ASV is, therefore, a nondestructive method of analysis.

The plating step is carried out under reproducible conditions so that concentration onto the electrode is quantitative (total plating), or a reproducible fraction of the desired component is deposited from solution (partial plating). By controlling the potential during this process, the more easily electrolyzed constituents can be separated; thus, the plating step is achieved by applying to the electrodes a potential which is cathodic of the polarographic half-wave potential by approximately 0.3 to 0.4 volts (where the current has its limiting value), and maintaining this potential for a given period of time under reproducible conditions of stirring, type, and area of the microelectrode, and composition of the medium. After a short rest period (which allows the solution to become quiescent, the stripping process is initiated.

The stripping process is performed by a voltammetric scanning procedure which produces a response proportional to the amount of material deposited. The resulting "stripping voltammogram" produces peaks, the heights of which are proportional to the concentrations of corresponding electroactive metal ions, and the potentials, a qualitative indication of the nature of the species present in the solution. Thus, the important characteristics of the voltammogram are: the heights of the peaks (peak current, i_p, in microamperes), peak width at 1/2 i_p (W 1/2 in volts or millivolts), and peak potential (E_p, in volts). These characteristics are affected by the type of microelectrode used, and by the rate of voltage change (sweep rate, ν, millivolts per second) employed in the stripping process.

Three electrodes are used in conventional ASV: reference (Ag/AgCl), counter (a platinum wire), and test or working (mer-

cury-graphite) electrodes. Test electrodes are made by plating a thin film of mercury onto a polished, wax impregnated graphite rod. Because oxygen is an interference in trace level analyses, the flow cell has provision for nitrogen deaeration. The analytical curve (voltammogram) includes peaks for background current as well as for metals being measured.

Differential ASV (DASV) is a four electrode system. A second working electrode is used to subtract extraneous background signals from the voltammogram, significantly improving the sensitivity of the technique. The fourth electrode is identical to the working electrode except that it is excluded from the plating step. During the stripping procedure, the background current signal from the fourth electrode is subtracted from the analytical current signal producing only current peaks for the metals of interest. The special DASV plating-stripping sequence is diagrammed in Figure 54.

In the voltammogram, the peak value of the current is proportional to the concentration of the reduced species, the area and thickness of the electrode, and the potential scan rate, as shown in Equation 124:

$$i_p = (ZFAl \frac{\phi}{e} \nu)C_R \qquad (124)$$

where:

i_p = peak current
Z = number of electrons transferred
F = the Faraday
A = electrode surface area
l = thickness of mercury film
$\phi = \frac{ZF}{RT}$
ν = potential scan rate
e = Naperian logarithm
C_R = concentration of reduced species

Film thickness is determined by controlled electrolysis of the mercury onto a graphite electrode. The value of i_p varies nearly proportionally to the scan rate for very thin mercury films; however, it varies significantly with film thickness at higher sweep rates. For lower values of one, i_p varies only slightly with film thickness.

Equation 125 expresses peak position:

$$E_p = E_o + \frac{e}{\phi} \log \frac{\delta l \nu \phi}{D} \qquad (125)$$

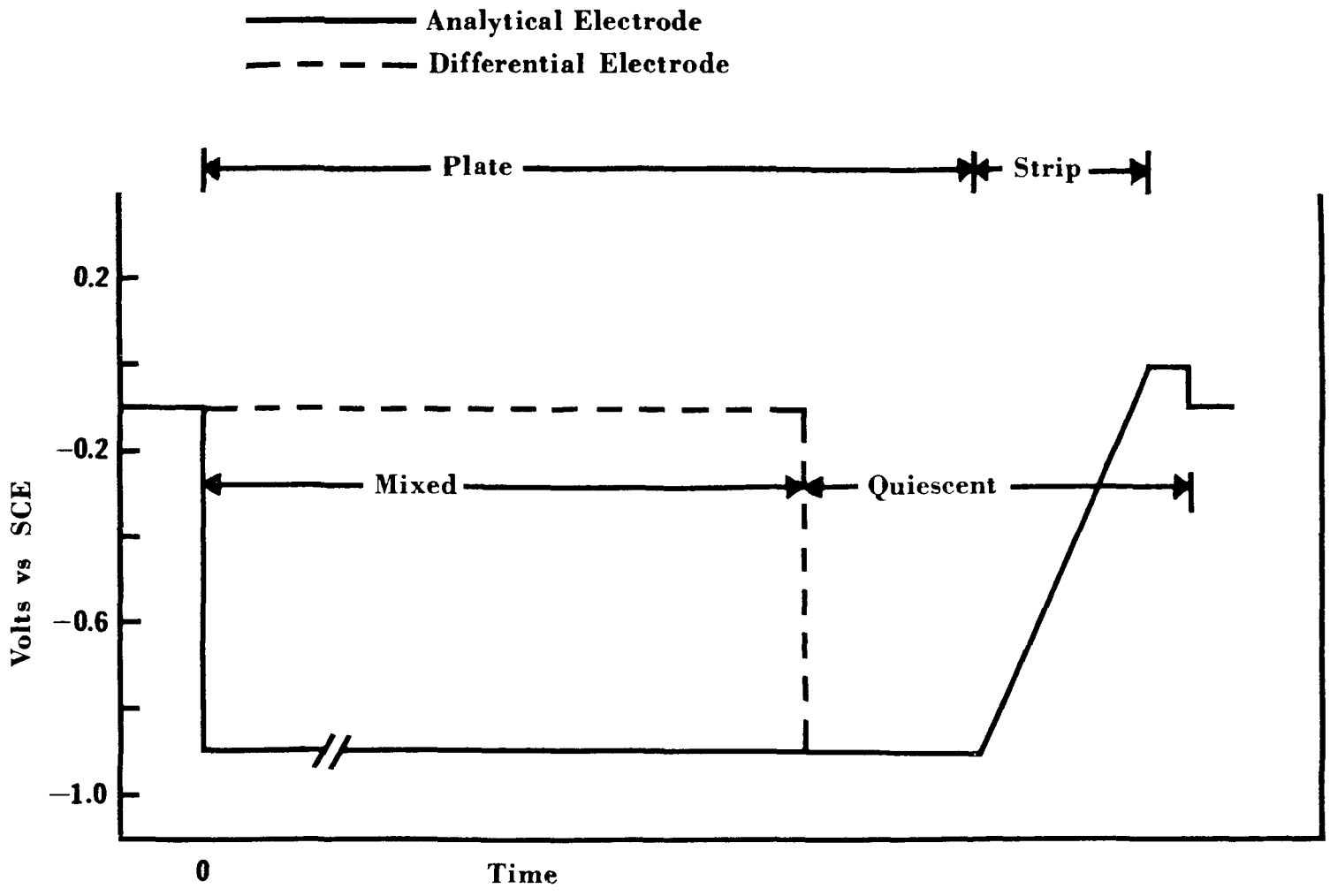

Figure 54. Plate-strip sequence for differential anodic stripping voltammetry.

where:

E_p = peak potential
δ = Nernst diffusion layer
D = diffusion constant
E_o = standard potential

E_p, then, is a function of scan rate, film thickness, and the Nernst diffusion layer. This theory does not apply for fast scan rates with very thick films. Peak width, which is important in resolution, varies only slightly with scan rate when the mercury thickness is small, and varies slightly with thickness with a slow scan rate.

Experimental

Equipment items in the trace metals monitor in the mobile laboratory include a custom built, four electrode potentiostat/timer (P/T) unit with automatic and manual modes; Technicon 16-channel proportioning pump and long jacketed mixing coil; Varian recorder, Model G2500; two Valcor miniature three-way valves; a customized Plexiglas flow cell; and four electrodes, Ag/AgCl reference, platinum (Pt) counter, and two graphite working electrodes.

In the automatic mode, all functions are controlled by the timer. There are six variable timed functions, five of which are necessary for one complete cycle:

1. Warm up (200 to 2,000 sec.)
   Allows time for system to warm up and sample to travel between its point of origin and the flow cell. (This function is used only when system is turned on.)
2. Plating primary electrode (100 to 1,000 sec.)
   Switches primary electrode to plating potential and initiates nitrogen mixing.
3. Plating differential electrode (10 to 100 sec.)
   Switches differential electrode to plating potential and stops nitrogen mixing.
4. Preelectrolysis procedures (1 to 10 sec.)
   Starts recorder and lowers pen.
5. Analytical step (2 to 20 sec.)
   Starts potential sweep on both electrodes simultaneously. (Sweep stops automatically.)
6. Wash period (30 to 300 sec.)
   Starts nitrogen mixing, allowing cell to be flushed with new sample prior to analysis. (System switches back to function 2.)

In the mobile laboratory, the time for one complete DASV cycle is 13 minutes. Plating potentials for each function are set at

a digital panel meter on the front panel of the control unit. A digital counter counts the number of analytical cycles which have occurred and, at some preset number of cycles, switches a valve at the beginning of function six, pumping standard instead of sample through the cell.

Sample is delivered to the flow cell, acid added, and standard pumped with the Technicon proportioning pump. Nitric acid is mixed with the test water in a ratio sufficient to produce a resultant pH of 2.5. (Metals exist in water in three forms: free ions, labile complexes, and nonlabile complexes. ASV does not measure the nonlabile complexes unless the sample is acidified to either break down the nonlabile metal complexes or exchange the H^+ for a metal ion. Total metals are measured only with acidification.)

A ten-inch Varian recorder with remote start/stop, remote pen lift, event marker, and a Z-fold paper tray is used with the DASV system. (An event marker is available and could be used to record the beginning and end of a standardization sequence.)

A water jacketed mixing coil maintains constant sample temperature and aids in the control of outgassing. Bubbles formed by outgassing are removed through a debubbler before the sample is acidified.

The flow of nitrogen is initiated by one of the Valcor valves in the system; the second valve switches from sample to standard in the standardization sequence.

A schematic illustration of the Plexiglas DASV flow cell in the mobile laboratory is shown in Figure 55. The internal volume of the cell is ten ml. Test electrodes are inserted through the sides of the cell, directly opposite each other, and mounted with epoxy to 1/4-inch hose conversion fittings for easy removal for servicing. Reference and counter electrodes, also directly opposite, are inserted through the front and back of the cell. The test solution is pumped in through the bottom and overflows through a port in the stopper at the top. Nitrogen enters through a small diameter polyethylene tube inserted in the bottom.

Working electrodes are made from 1-1/2 inch lengths of 5/16 inch diameter wax impregnated graphite rods. The end of each is polished for working electrode surface. Complete instructions for electrode preparation are included in the "Operation and Maintenance Manual," provided with the mobile laboratory (47).

A schematic illustration of the total DASV system is shown in Figure 56. Before plating is initiated, both working electrodes are at rest potential and the solution is mixed. To initiate plating, the analytical electrode is adjusted to plating potential; the differential electrode remains at rest potential. When

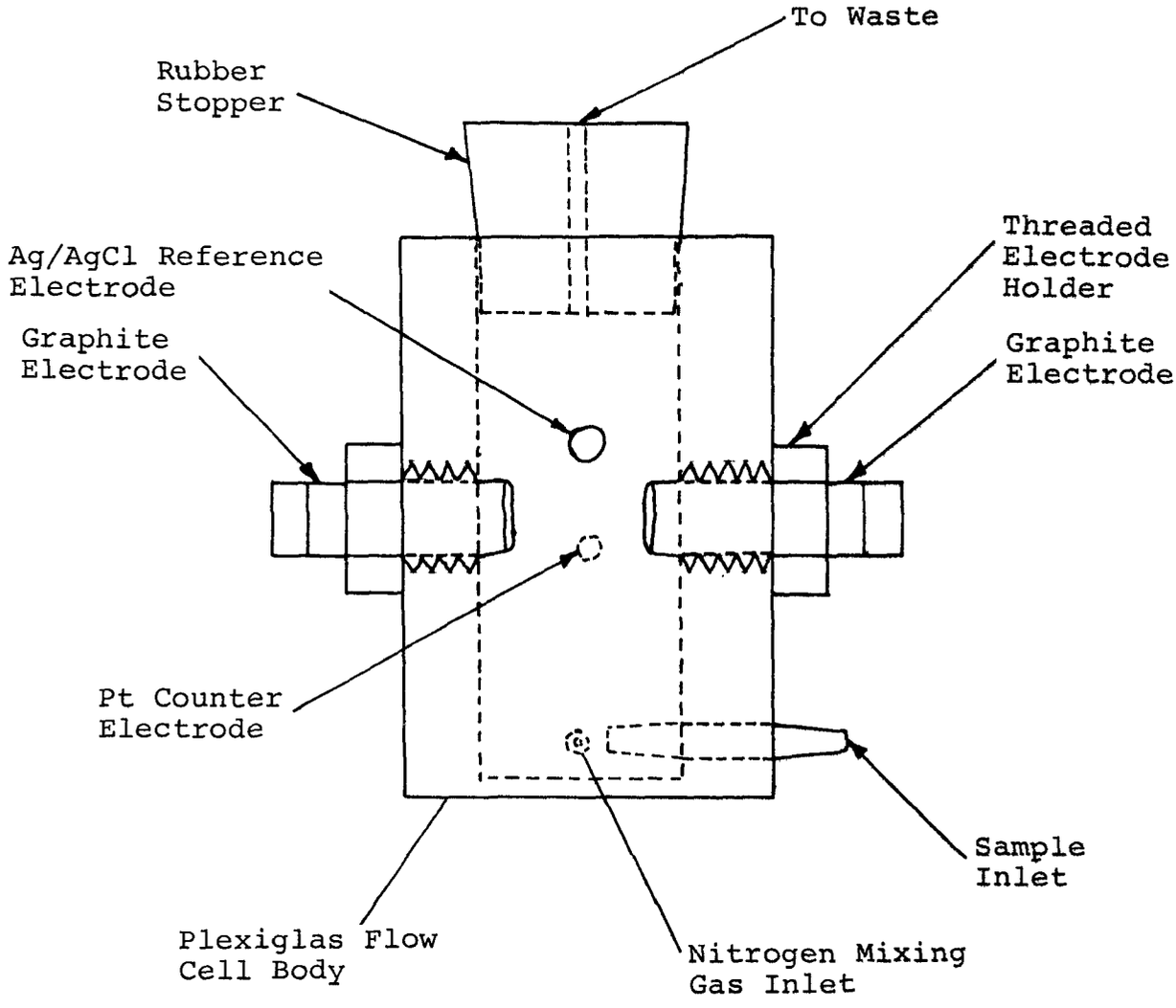

Figure 55. Schematic diagram of DASV flow cell used in the mobile laboratory.

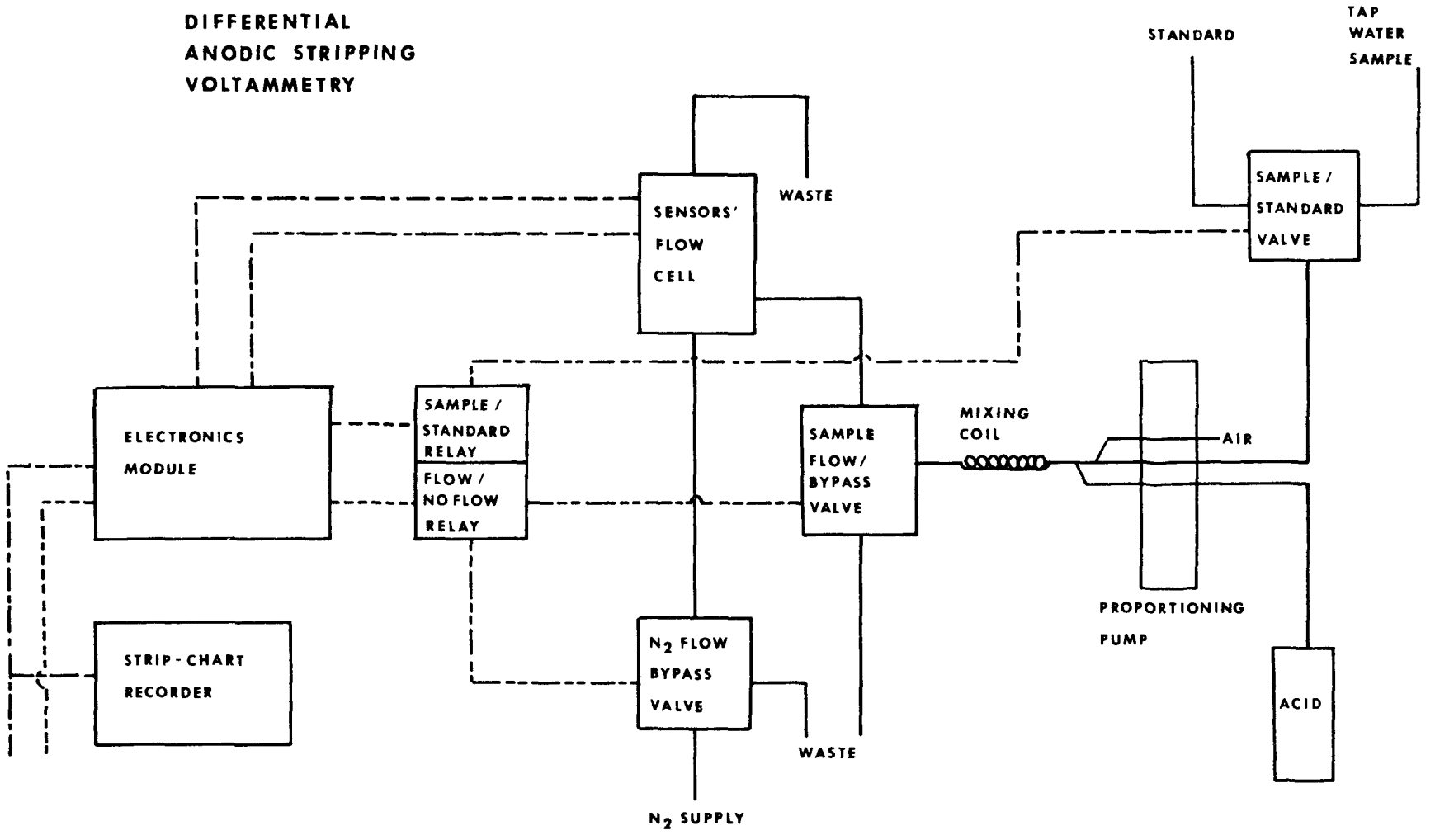

Figure 56. Schematic illustration of trace metals monitor in the mobile laboratory.

plating is completed, mixing is stopped and the differential electrode adjusted to plating potential. After a short waiting period (to attain solution quiescence and electrical stability), the stripping step is initiated by simultaneous application of the voltage sweep to both electrodes. The sweep is stopped at a predetermined potential and rest potential is again applied to both electrodes. Typical DASV voltammograms for standards and a tap water sample are shown in Figure 57. Preparation of reagents for DASV analyses is detailed in Appendix B.

Results and Discussion

Performance characteristics of the DASV system were determined experimentally. Calibration curves from standard solutions of 5, 10, and 15 ppb of each of the metals of interest (Cd, Pb, and Cu), run in triplicate, established a linear response for each of the metals. The plating time response curve for discrete samples is S-shaped with a limiting value representing total plating of a metal. In the continuous flow system, the plating time is linear as a result of the continuous flow of fresh sample; i.e., total plating cannot occur.

Continued use of working electrodes results in reduced signals for each of the measured metals. Periodic standardization is required to observe changes in electrode sensitivity. Data in Table 19 relate to a tap water sample spiked with five mg/l each of Cd, Pb, and Cu. The sample was cycled through the flow cell continuously for a period of 18 hours. Although electrode response decreases with time (Table 19), the rate of decrease is relatively constant; thus, results can be read from a calibration curve corrected for elapsed time. Periodic rejuvenation of the electrodes can be accomplished by a short period of plating additional mercury, as shown in Table 20. These data are from a pair of electrodes used continuously for alternate standard/sample cycling over a 48-hour period. The electrodes were rejuvenated by short mercury plating periods after each 24 hours of use.

Electrode response to variations in sweep rate is shown in Figure 58. Rapid sweep rates produce higher current response; thus, 162.5 mv/sec. was used for much of the DASV acquired data.

Special Study

A special study of the effect of residence times in household plumbing on metals uptake in drinking water was undertaken during this project. NSF employees were asked to bring two samples to the laboratory each day for five consecutive days. One sample was drawn from the tap immediately upon arising each morning; i.e., before any other water was drawn from the tap. The second

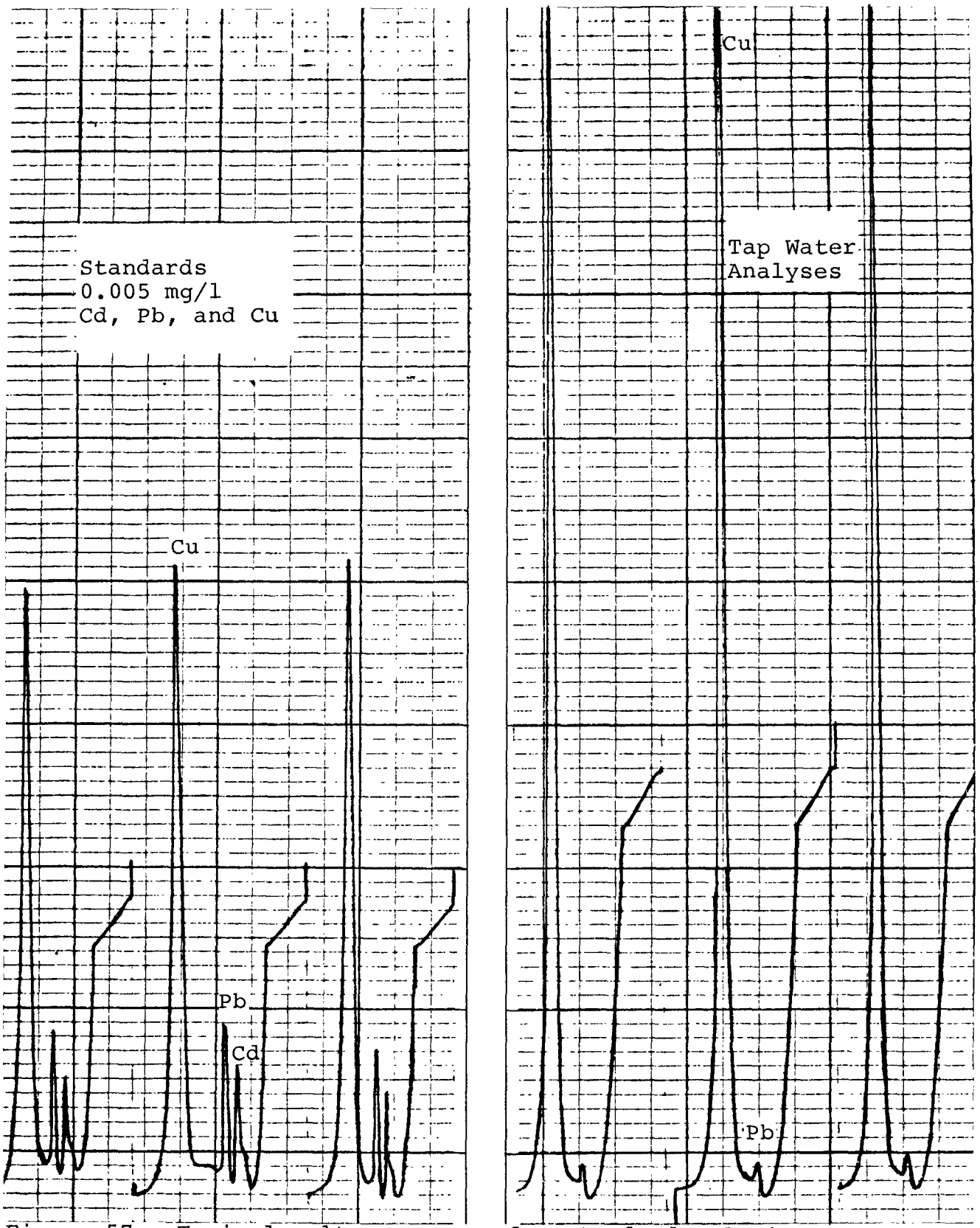

Figure 57. Typical voltammograms of a standard solution and tap water analyses.

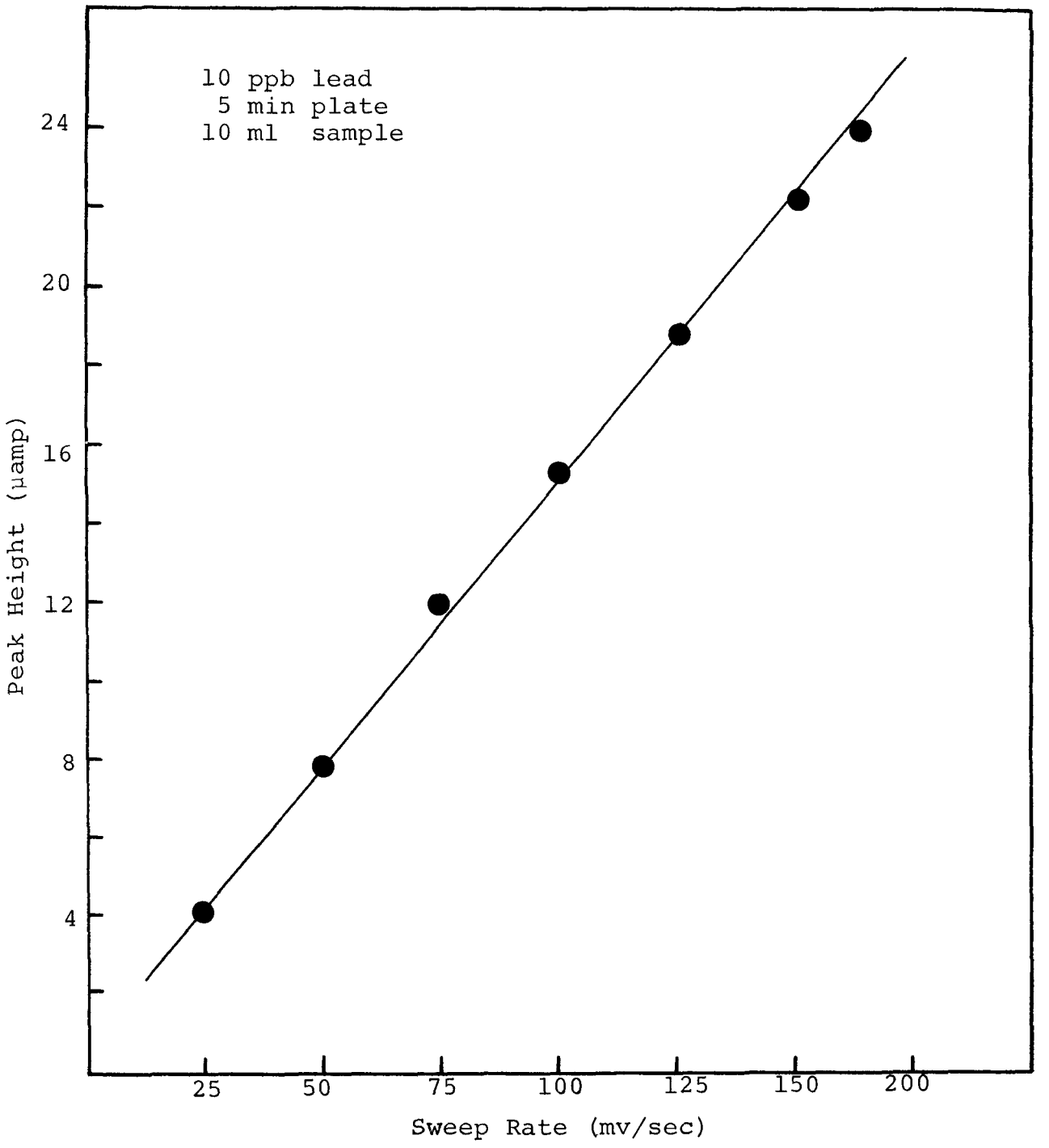

Figure 58. Sweep rate response.

Table 19. ELECTRODE DETERIORATION

Run	Cd	ΔCd	Pb	ΔPb	Cu	ΔCu
1	33.0		44.0		94.0	
		6.0		1.0		6.0
10	27.0		43.0		88.0	
		4.0		1.0		8.5
20	23.0		42.0		79.5	
		5.0		0.5		8.5
30	18.0		41.5		71.0	
		4.0		0.5		8.0
40	14.0		41.0		63.0	

Table 20. ELECTRODE RESPONSE AFTER REGENERATION (10 minute plating times; 10 ppb each metal)

	Cd	Pb	Cu
Start	23	22	50.5
24 hrs.	24.5	25.5	54.0
48 hrs.	27.0	27.0	55.0

sample was drawn from the same tap after the water had run continuously for three minutes. Samples were collected in acid-washed polyethylene bottles provided by the laboratory. For the analysis, ten ml of sample was placed in the flow cell and acidified to pH 2.5. Plating time was five minutes. Household systems included in the study are described in Table 21. Results are summarized in Table 22 and plotted in Figures 59, 60, and 61.

Regardless of the sample or characteristics of the system from which it was obtained, levels of Cd were insignificant (Figure 59). None of the metals was found at a significant level in samples from galvanized plumbing. Relatively high levels of both Pb and Cu were shown to accumulate with overnight residence in copper plumbing systems, but these levels were quickly reduced with flushing. (Figures 60 and 61.)

This study should be repeated in cities with more aggressive drinking water supplies. Ann Arbor water has an unusually high

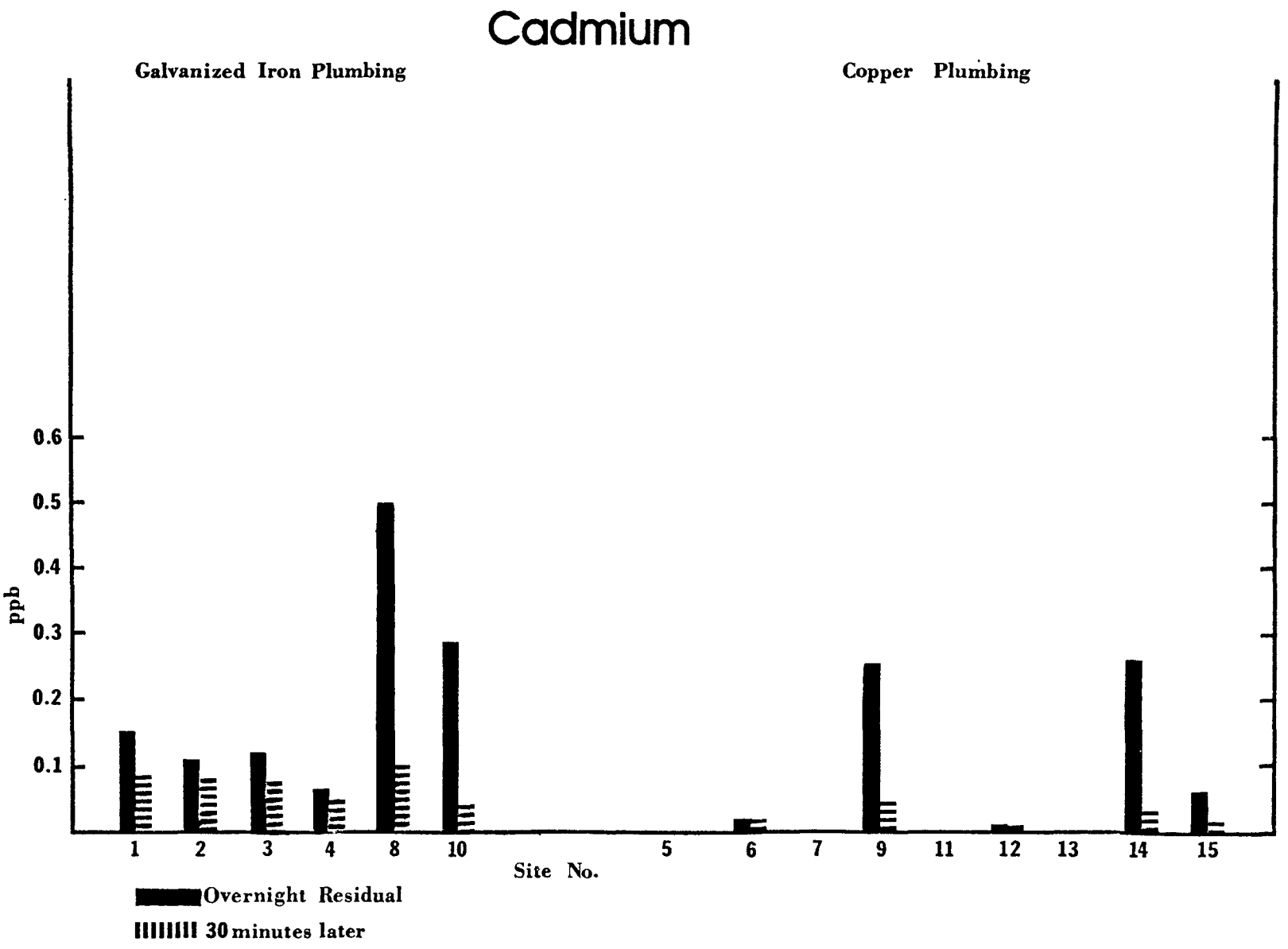

Figure 59. Household trace metals survey, cadmium.

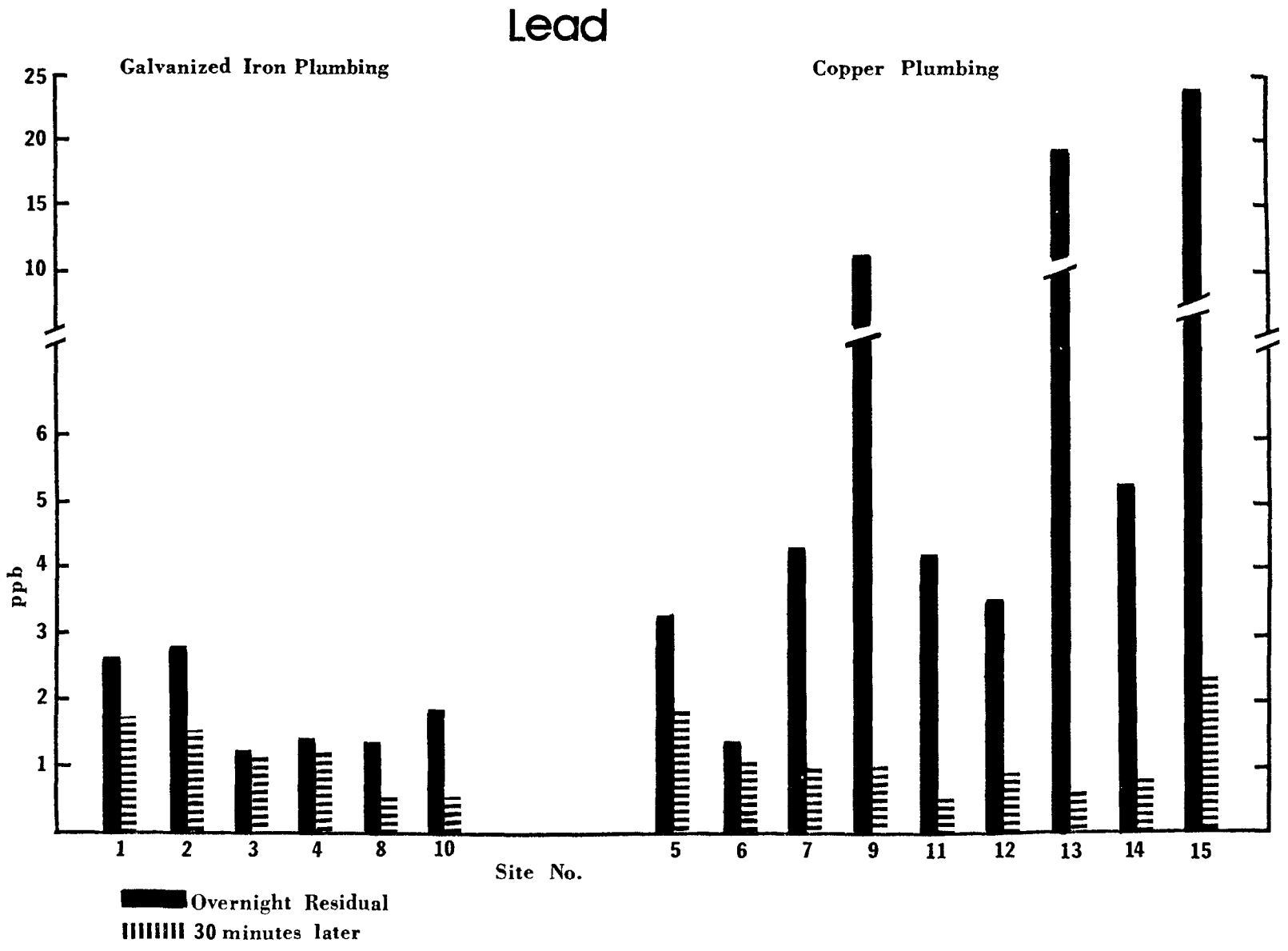

Figure 60. Household trace metals survey, lead.

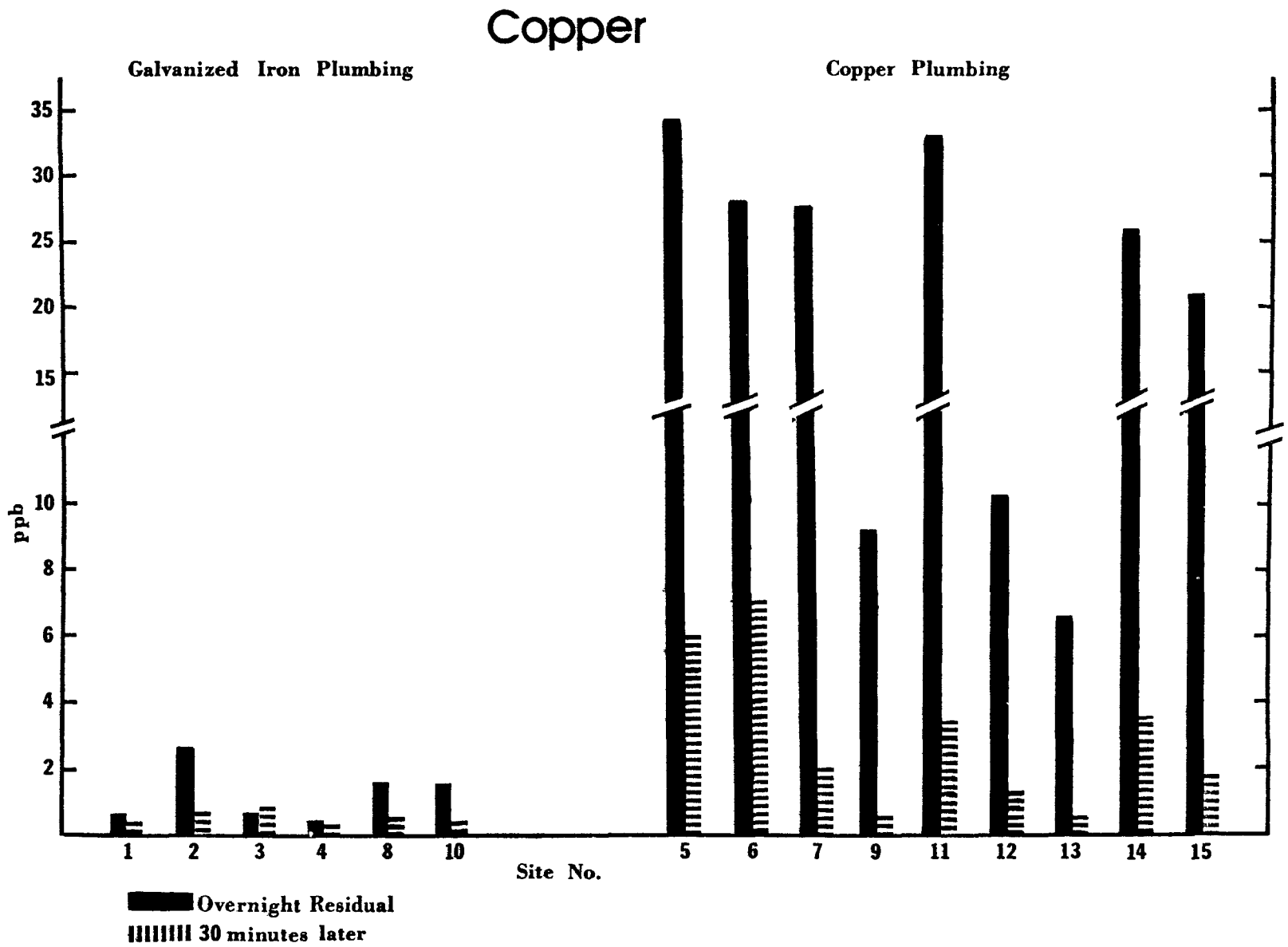

Figure 61. Household trace metals survey, copper.

Table 21. TRACE METALS SURVEY SITES

Site No.	Description	Approximate Building Age (yrs)	Plumbing
1	Single family home	10	Galvanized iron
2	Single family home	13	Galvanized iron
3	Single family home	17	Galvanized iron
4	2nd story apartment in 2 unit dwelling	35	Galvanized iron
5	2 story town house in new complex	2	Copper
6	Single family home	49	Copper installed 2 years ago
7	Commercial Building	10	Copper
8	Single family home	20	Galvanized iron
9	Single family home	12	Copper
10	Single family home	20	Galvanized iron
11	Single family home	1.5	Copper
12	2nd floor apartment in new apartment complex	1	Copper
13	Sub-basement in old University of MI laboratory	30	Galvanized iron-copper mixed
14	Basement in new University of MI laboratory	2	Copper
15	6th story in new University of MI laboratory	2	Copper

Table 22. SUMMARY OF RAW DATA FROM HOUSEHOLD TRACE METALS SURVEY

GALVANIZED IRON PLUMBING						
Site No.	Cd ppb		Pb ppb		Cu ppb	
	O.R.*	3+	O.R.	3	O.R.	3
1	0.16	0.08	2.68	1.75	0.64	0.42
2	0.11	0.08	2.84	1.46	2.78	0.39
3	0.12	0.08	1.24	1.15	0.35	0.45
4	0.06	0.05	1.4	1.2	0.22	0.14
8	0.5	0.11	1.35	0.5	1.65	0.54
10	0.29	0.04	1.84	0.48	1.58	0.26
Average	0.2	0.07	1.9	1.1	1.2	0.4

COPPER PLUMBING						
Site No.	Cd ppb		Pb ppb		Cu ppb	
	O.R.	3	O.R.	3	O.R.	3
5	–	–	3.22	1.86	33.9	5.9
6	0.02	0.02	1.35	1.08	28.0	7.0
7	–	–	4.28	0.92	27.5	1.97
9	0.25	0.04	11.5	1.0	9.2	0.62
11	–	–	4.18	0.47	32.7	3.4
12	0.01	0.01	3.5	0.83	10.2	1.2
13	–	–	18.9	0.58	6.64	0.38
14	0.26	0.03	5.25	0.78	25.6	3.6
15	–	–	23.4	2.3	21.0	1.8
Average	0.06	0.01	8.4	1.1	21.6	2.5

*O.R. = Overnight Residual
3+ = 3 minutes later

pH ($\geq$10.0 during the week of the study). A comparable study with tap water pH $\leq$ seven is recommended. Plastics piping systems should be included in the study.

SECTION V
MOBILE LABORATORY

General

In the final phase of the NSF water quality monitoring project, the prototype monitor; i.e., all instrumentation and ancillary equipment, was installed in a mobile laboratory and tested in actual field operation. Important design criteria included ruggedness of instrument mountings and overall laboratory portability. Ideally, the laboratory had to be easily and quickly movable and capable of being installed virtually anywhere on a potable water distribution network.

Physical Description

A heavy duty, intercity GMC delivery van with 4.9 meter long by two meter high load space was selected to house the NSF/EPA mobile water quality monitoring laboratory. The van is designed to carry heavy loads over long distances. It rides on six wheels (dual rear wheels) and includes heavy duty suspension to protect the delicate instruments against extreme road hazards. Its load space is sufficiently large to provide adequate benchtop work space, and sufficiently high to permit persons of average height to work in comfort. All cabinetry, electrical, and plumbing installations were customized to NSF specifications by a local general contractor. Cabinetry was constructed from plastic laminated heavy composition board, typical of that which is found in household kitchens and benchtops, covered with "matte white" formica.

The sink unit contains a closed cabinet and an electric heater with thermostatically controlled blower. An additional baseboard heater is provided on the opposite side, at the opposite end of the van. For cooling, a 12,000 BTU ARA mobile home airconditioner is mounted in the ceiling.

External power (100 amps, 220v, single phase) is brought to the van over a four conductor, 100 feet long by one inch diameter cable which weighs slightly over 100 pounds. When it is connected to the van, the cable splits at the circuit breaker box to two, 110v circuits. The two main circuits are further divided into nine smaller circuits for lights, airconditioner, left wall outlets, right wall front and right wall rear outlets, heaters,

hot water heater, computer, and Schneider Robot Monitor systems. No overloads were observed during six months of mobile laboratory operation.

NOTE: *A principal surge-type power requirement is exerted by the hot water heater. This item is not considered essential in any future projects of this kind. One hundred amp service would not be required if the hot water heater were omitted.*

Water is supplied to the van through a common one inch diameter garden hose, easily attached by hose connectors to both supply and laboratory. It is distributed to the various parametric systems through CPVC plastic piping. Drain lines are 2-1/2 inch plastic pipe which terminate at an opening in the right rear corner of the van. Connection to a sewer is made through flexible swimming pool drain tubing. Normal flow through the van with all systems operational is 24 to 30 liters per minute.

Instrumentation

Instruments used in the prototype monitor were not selected with mobile laboratory installation as an objective. Many unique problems developed in shock mounting and designing racks for the diverse sizes and shapes of equipment which had to be installed with optimized space economy.

Weight rated anti-shock/vibration mounting pads (Lord Manufacturing Company) are installed under every leg or corner of each piece of equipment to which they could be adapted, with racks constructed where required. The shock mount is screwed directly to a deck and the instrument bolted to the mount. Instruments which could not be adapted to shock mounts are attached to the walls with suitable vibration damping equipment fixed between the instrument and the wall. In traveling nearly 2,000 miles on field assignments, no instrument failure was detected which could be attributed to vibration.

Organization

In addition to the various sensors, 14 separate meters or other electronics packages, nine strip chart recorders, two proportioning pumps, a 24-bottle automatic sampler, seven reservoir reagent bottles, a cartridge type water deionizer, a rack mounted computer system, three boxes with relay switching mechanisms, a residual chlorine titrator, and miscellaneous tools and laboratory glassware are located in the mobile laboratory. Each piece of equipment was carefully positioned before being permanently mounted.

Figures 62 and 63 are schematic plan views of the equipped van interior. In Figure 62, "reagent reservoirs" contain, from left to right, alkalinity baseline solution, alkalinity buffer, free fluoride buffer, total fluoride buffer with masking agent, and fluoride baseline solution. Sensor flow cells and mixing coils for free and total fluoride and alkalinity are mounted on the platform to the left of the pump.

The flow cell, mixing coil, and run/by-pass switching values for DASV are mounted on the H-type rack near the center in Figure 63. The rotator, electronics module, and recorder for CCDT, and the corrosion rate monitor are not fixed in place. For travel, these instruments are stored on thick pads on the floor. A photograph showing an overview of the interior arrangement of the mobile laboratory is shown in Figure 64.

Computer System

All sensor systems in the mobile laboratory are controlled by an on-board mini computer system which includes a Texas Instruments digital computer, Model 960-A; Texas Instruments Silent 700/30 teleprinter; combination high speed paper tape reader perforator; and a Computer Products wide range analog to digital (A/D) converter, Model RTP7480. The computer contains 16K (16,384 words) of semiconductor memory, expandable internally to 32K and, with the addition of an external chassis, to 64K. An internal timer; 16 input/output digital switching board wired for interrupt; and an internal communications register unit (CRU) expansion chassis, required for five to 20 peripheral connections, are options used with the computer. Seven CRU connections are used in the mobile laboratory.

The gain of the wide range A/D converter is software programmable and output resolution is 13 bits (gain setting/4095) for full scale input voltage ranges of ± 2, 5, 10 mv ... ± 10.24v. Input from parametric systems to the converter, through Belden 8451 shielded twisted pairs plus ground cable, is made by connection to multiplexer boards mounted in the converter. Up to 16 eight-channel multiplexer cards can be installed internally - and 48 externally - to the converter chassis, for a total of 512 analog inputs. Two multiplexer cards (16 channels) are installed in the mobile laboratory.

The high speed paper tape reader/perforator reads 300 and punches 75 characters per minute. The Silent 700/30 teleprinter writes on heat sensitive paper, operating at printing speeds up to 30 characters per second. Its quiet operation makes it ideally suited for the mobile laboratory application.

The physical relationship of the Texas Instruments (TI) 960-A computer system to sensor equipment on the mobile water quality

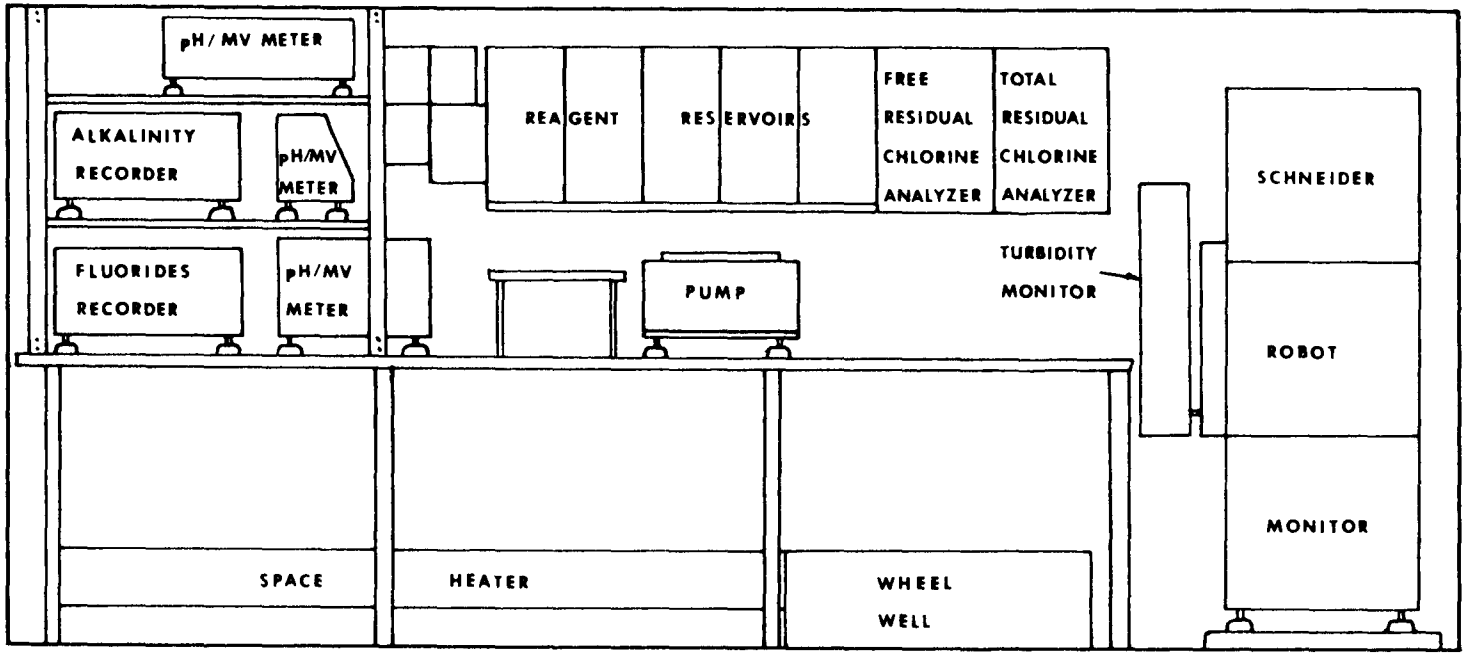

Figure 62. Schematic illustration of right side interior of mobile laboratory.

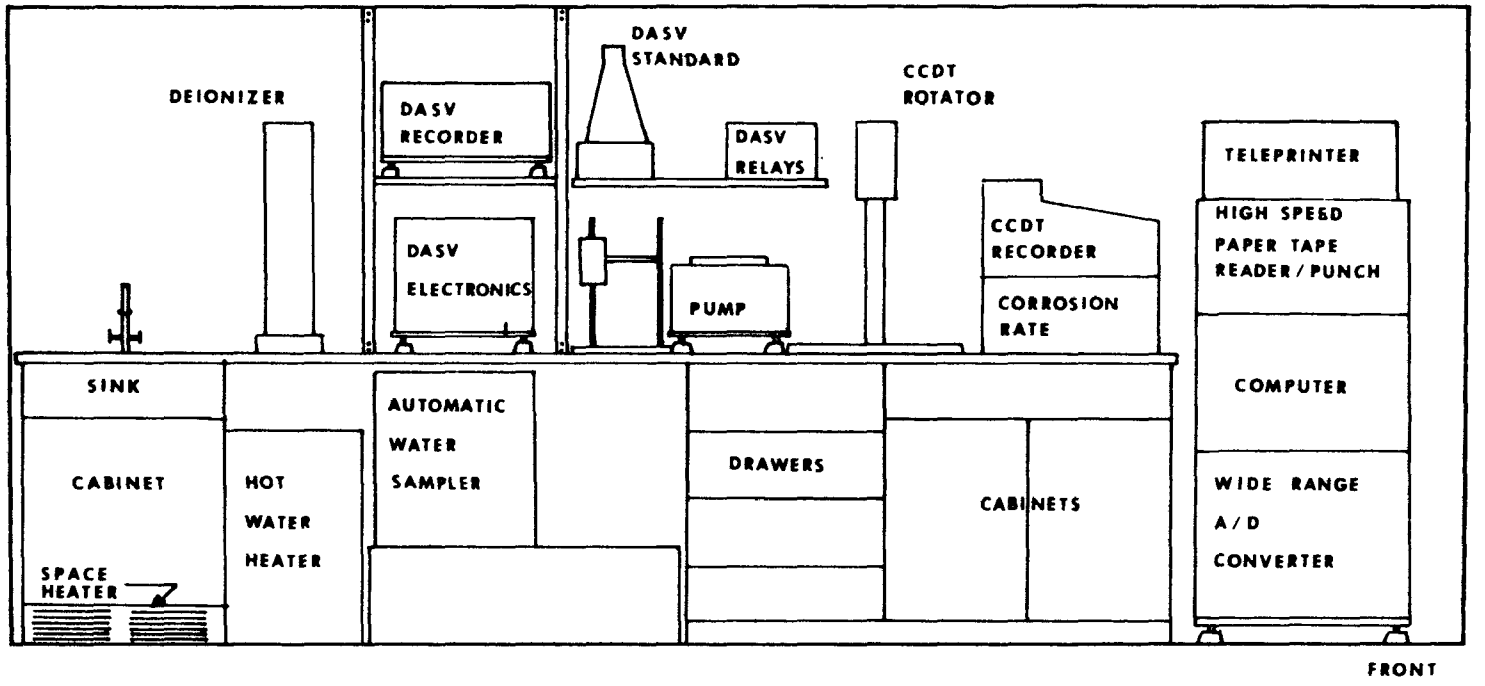

Figure 63. Schematic illustration of left side interior of mobile laboratory.

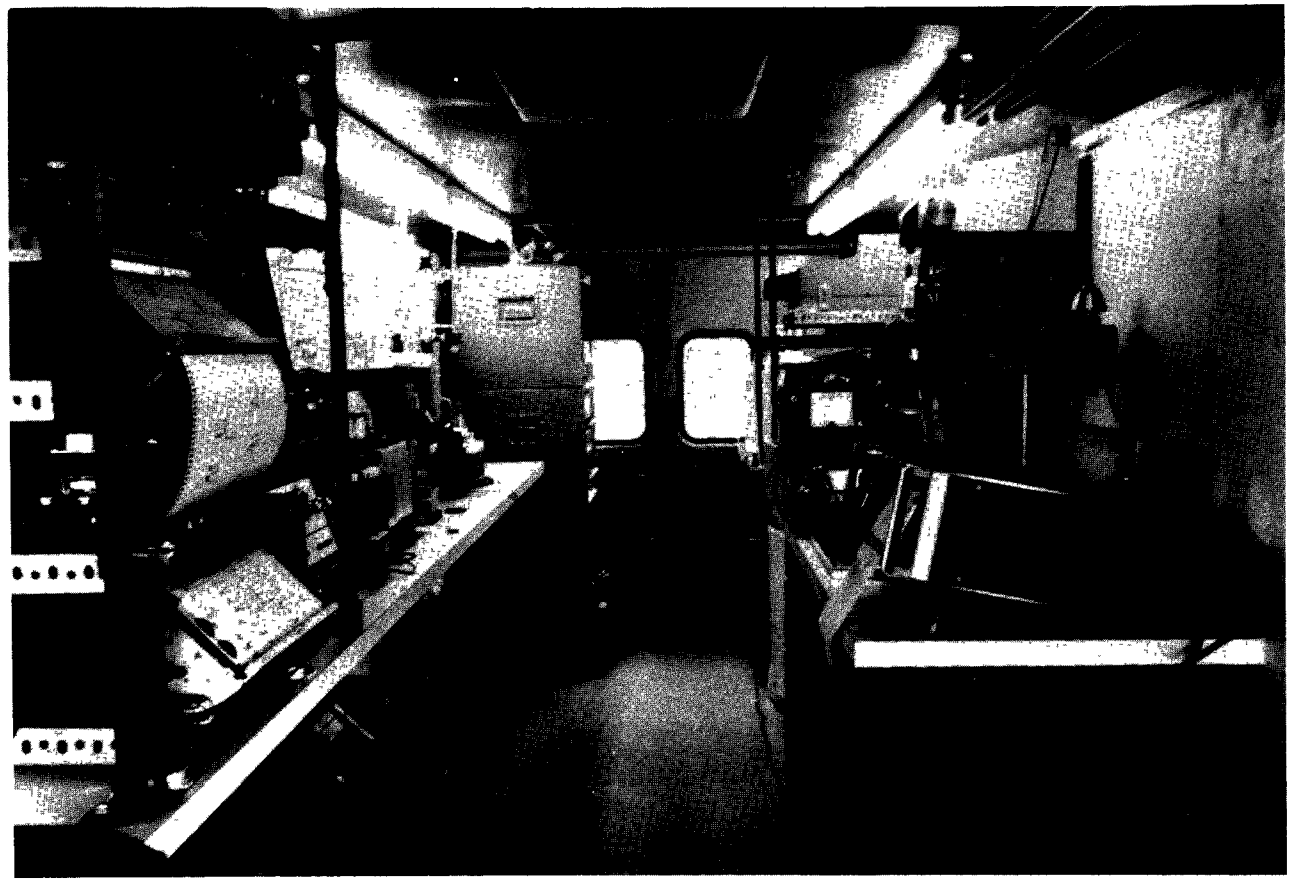

Figure 64. Photograph showing overview of mobile laboratory interior.

monitoring laboratory van is shown in overall view in Figure 65. Digital input from the anodic stripping voltammetry equipment is used to trigger the initiation of a data sampling cycle.

Within the data sampling cycle, appropriate digital outputs are sent to the corrosion, alkalinity, and free and total fluoride measuring equipment. Independent programs operating from the internal interval timer in the computer send digital output signals to the sampler and control the flow through the nitrate and hardness cells, located in the Schneider Robot Monitor.

In the data sampling cycle, the internal interval timer controls the timing for reading the analog signals from each of the different sensor instrumentation packages. The data acquisition program in the computer determines the gain to be used in the analog-to-digital converter (ADC) in reading each analog input channel.

Within the computer, all program operations are under the control of the Texas Instruments supervisor program PAM (Process Automation Monitor).

Eight worker tasks have been installed to operate in the computer under the control of PAM. Interrelations between the worker tasks, described as follows, are shown in Figure 66.

1. NSFC is a program containing utility routines, such as a decimal core dump routine. It is built to facilitate adding additional options. After NSFC is called into execution (either by Control-X or NSFC in response to OP?), a two-character code is used to select the option desired for execution. NSFC must be assigned Task ID 30.
2. BELL is a simple program which rings the bell on the teleprinter repeatedly until the operator halts the program. Its purpose is to attract the operator's attention.
3. INIT initializes output storage area, checks PUN, starts flow control, periodic sampling, and data acquisition. It is used for start-up when the system is initially loaded. (By changing the operation of the ST option in NSFC to bid task 32-INIT- instead of task 34-DAQ, the need to start system operation through job control can be eliminated.)
4. DAQ is the basic data acquisition program which reads the various analog input channels. It is initiated by an interrupt signal which indicates that DASV is ready to input data. During the next 13-minute interval, DAQ takes readings from each sensor system except alka-

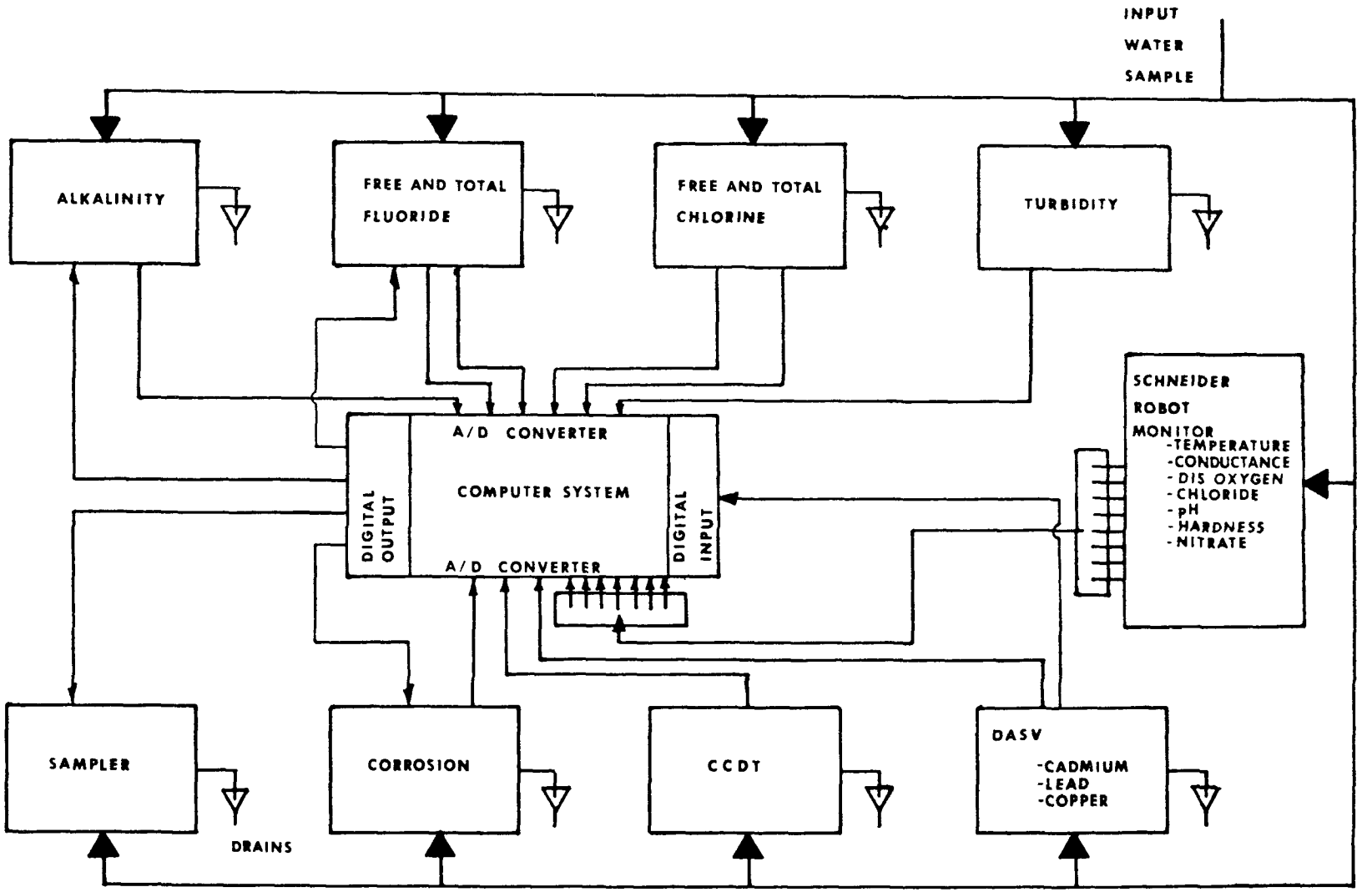

Figure 65. Relationship of computer system to analytical sensor systems.

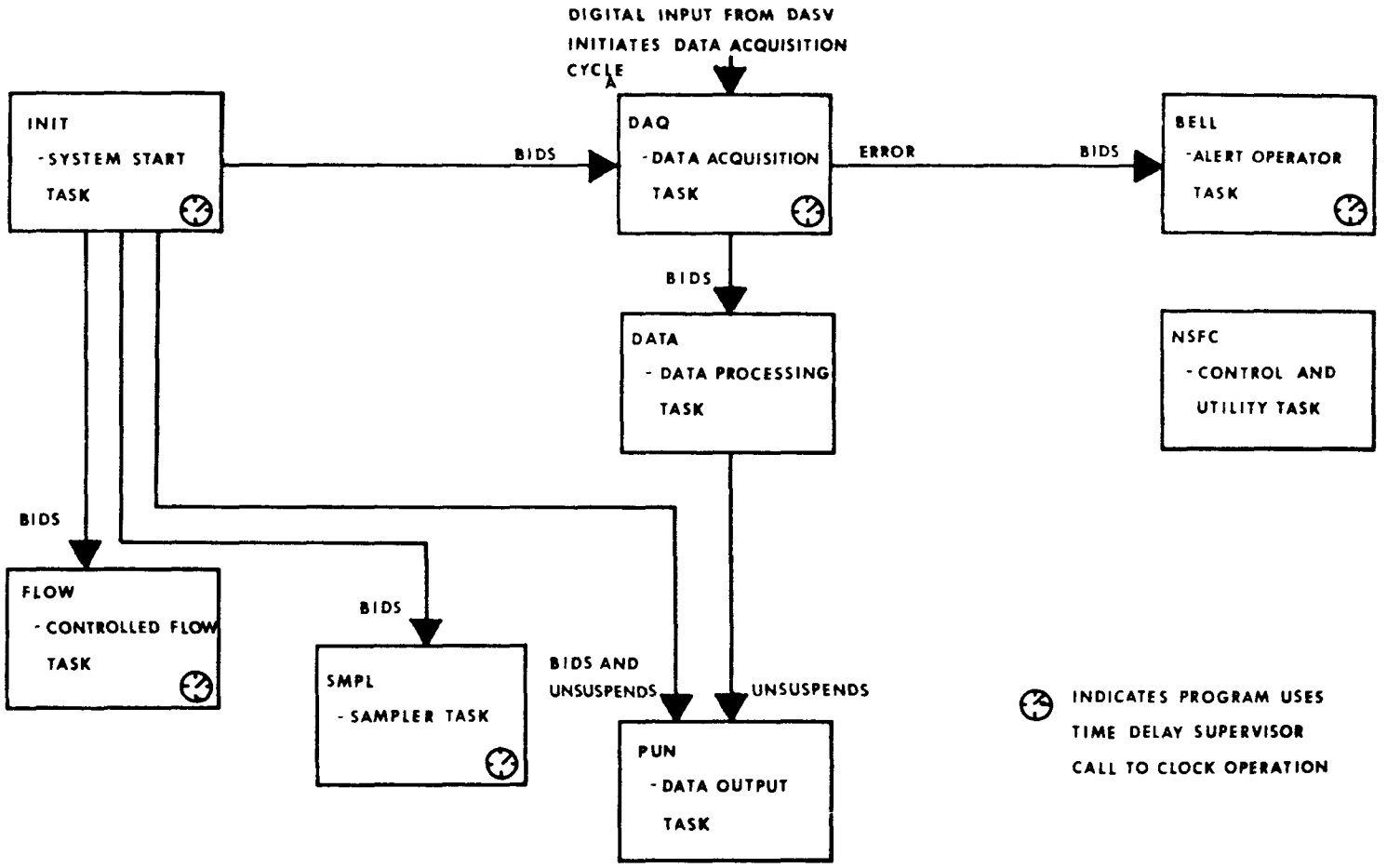

Figure 66. Computer system software relationships.

linity and corrosion rate, and switches the fluoride systems from baseline to sample. During the second 13-minute period, it takes readings from all sensors, including alkalinity and corrosion rate. At the end of the full 26-minute cycle, it waits for another interrupt signal from DASV to begin the cycle again.

5. DATA obtains data from the buffer area of DAQ, processes the data as needed, and stores the results in the output storage area.
6. FLOW controls the flow of water to the nitrate and hardness cells in the Schneider Robot Monitor.
7. SMPL controls the sampler to collect hourly samples of the water flowing through the mobile laboratory.
8. PUN outputs data from the output storage area and clears that area for fresh data. Sufficient space is available in the allocated storage area to retain up to two hours of data. DATA unsuspends PUN whenever more data is put into the output storage area. Currently, PUN outputs data and clears the area each time it is unsuspended; however, PUN can be modified to count the number of times it has been unsuspended since the last output of data, outputting data at greater intervals.

Flow charts of each of the worker tasks are shown in Figures 67 through 75. The flow of information through the system is described in Figure 76.

A detailed description of the operating system, DAQ, an operator manual for the computer system on-board the NSF mobile laboratory, and a paper entitled, "Computer Acquisition of Data from Paper Tape Output of the TI960-A," are included with the "Operation and Maintenance Manual" delivered to EPA with the mobile laboratory (47).

Field Studies

To evaluate the performance of all on-board systems under actual field conditions, the mobile laboratory was operated for one week in Ann Arbor (away from NSF), two months in the metropolitan Chicago area, and one week in Detroit, Michigan during April, May, June, and early July, 1973. It returned to NSF in July for installation and programming of the computer, then visited four sites in Philadelphia, Pennsylvania during the month of

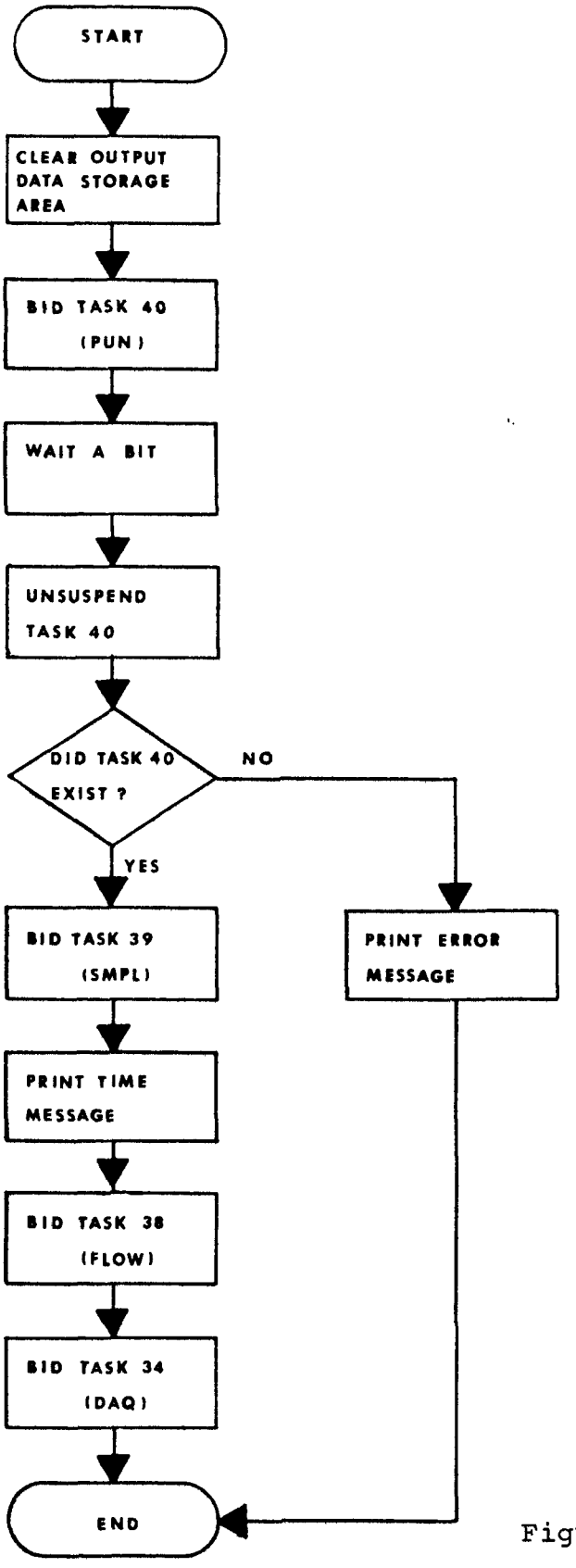

Figure 67. Flowchart of INIT.

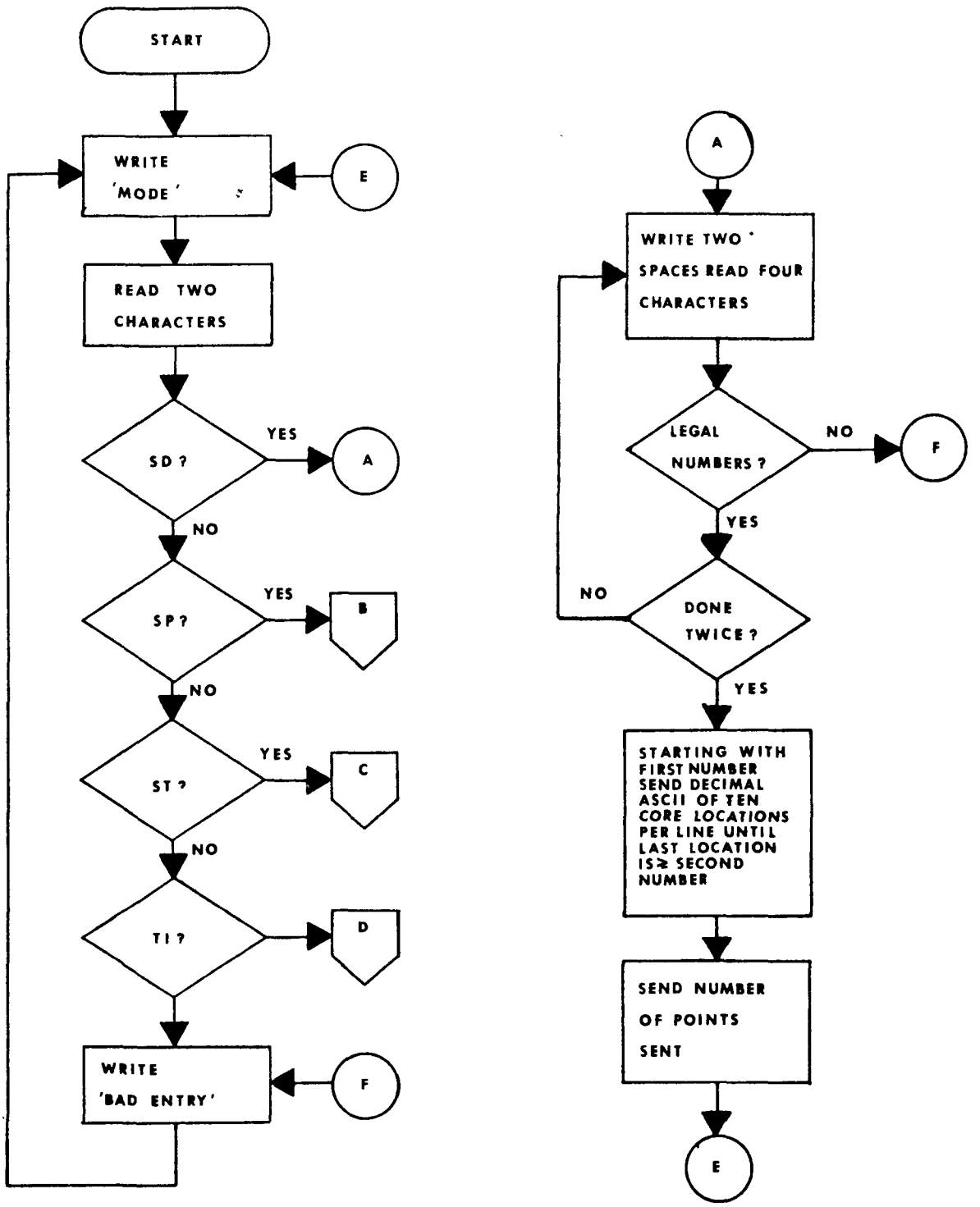

Figure 68.. Flowchart of NSFC.

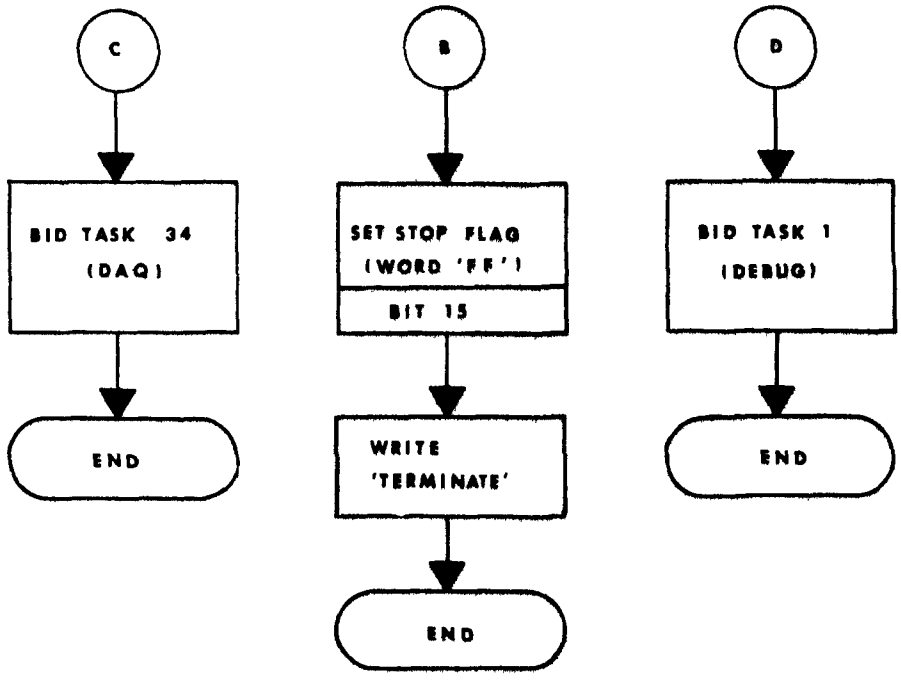

Figure 68 (Continued)

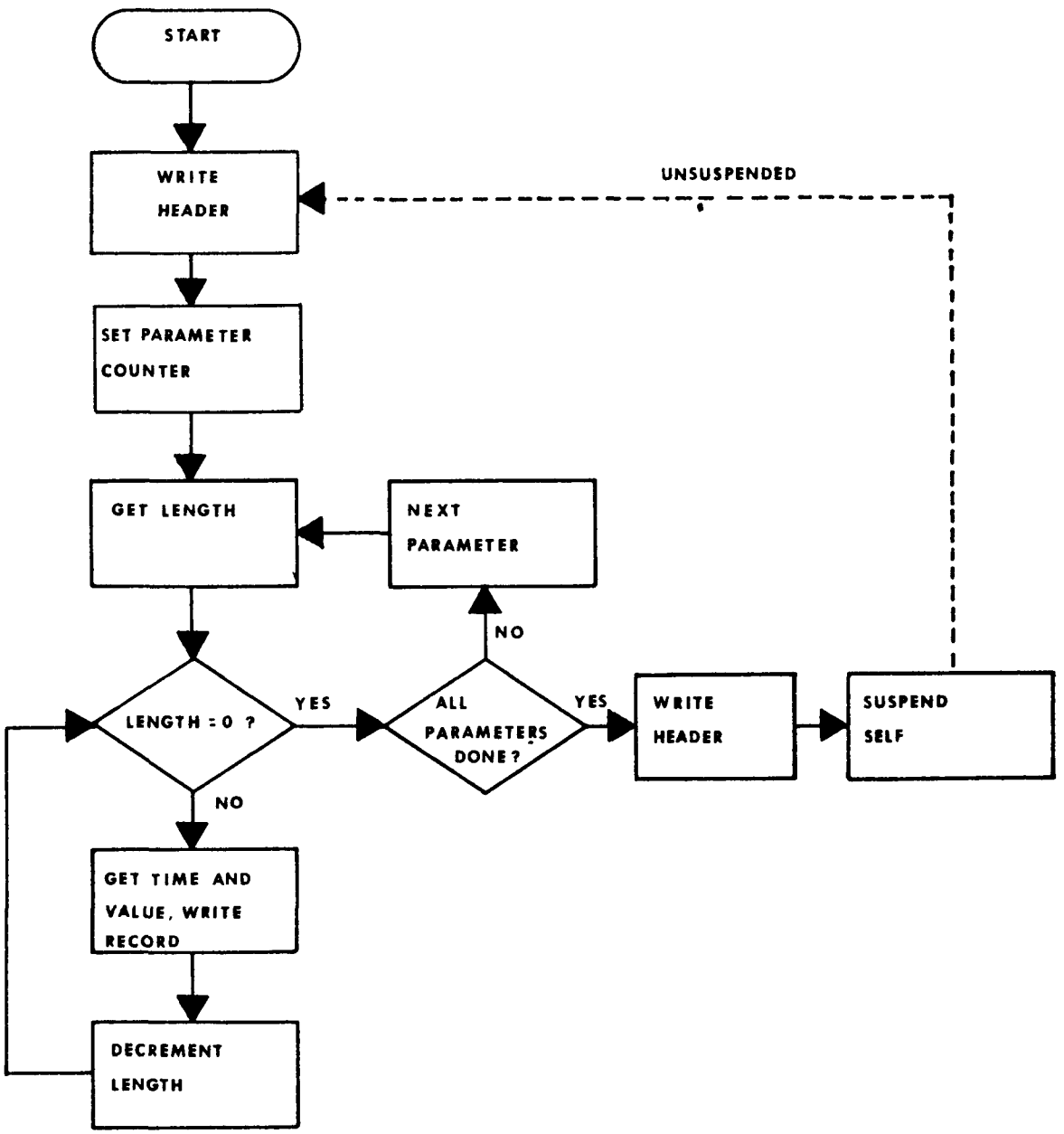

Figure 69. Flowchart of PUN.

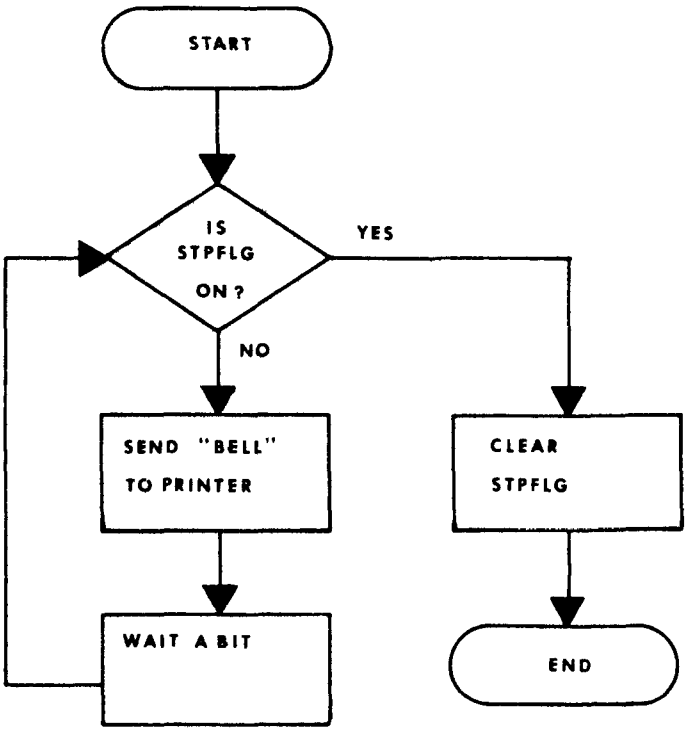

Figure 70. Flowchart of BELL.

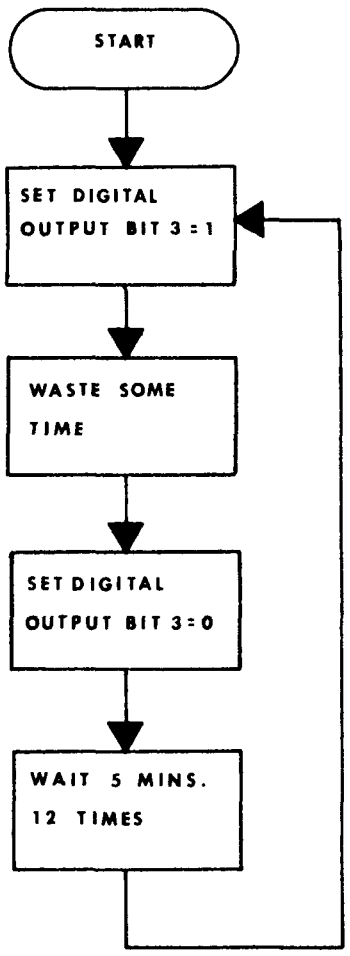

Figure 71. Flowchart of SMPL.

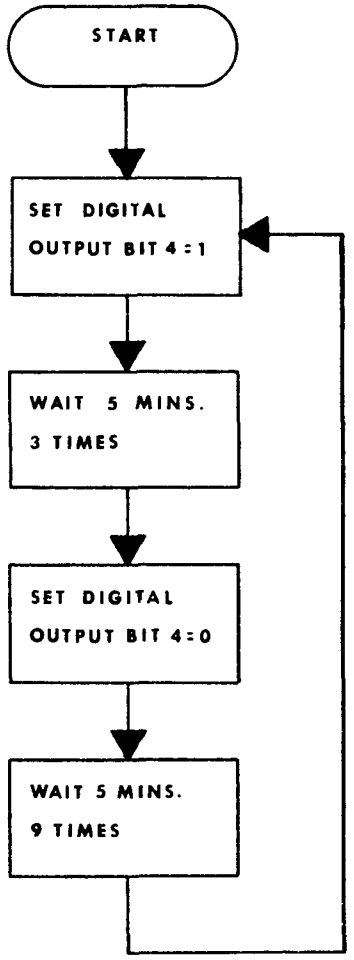

Figure 72. Flowchart of FLOW.

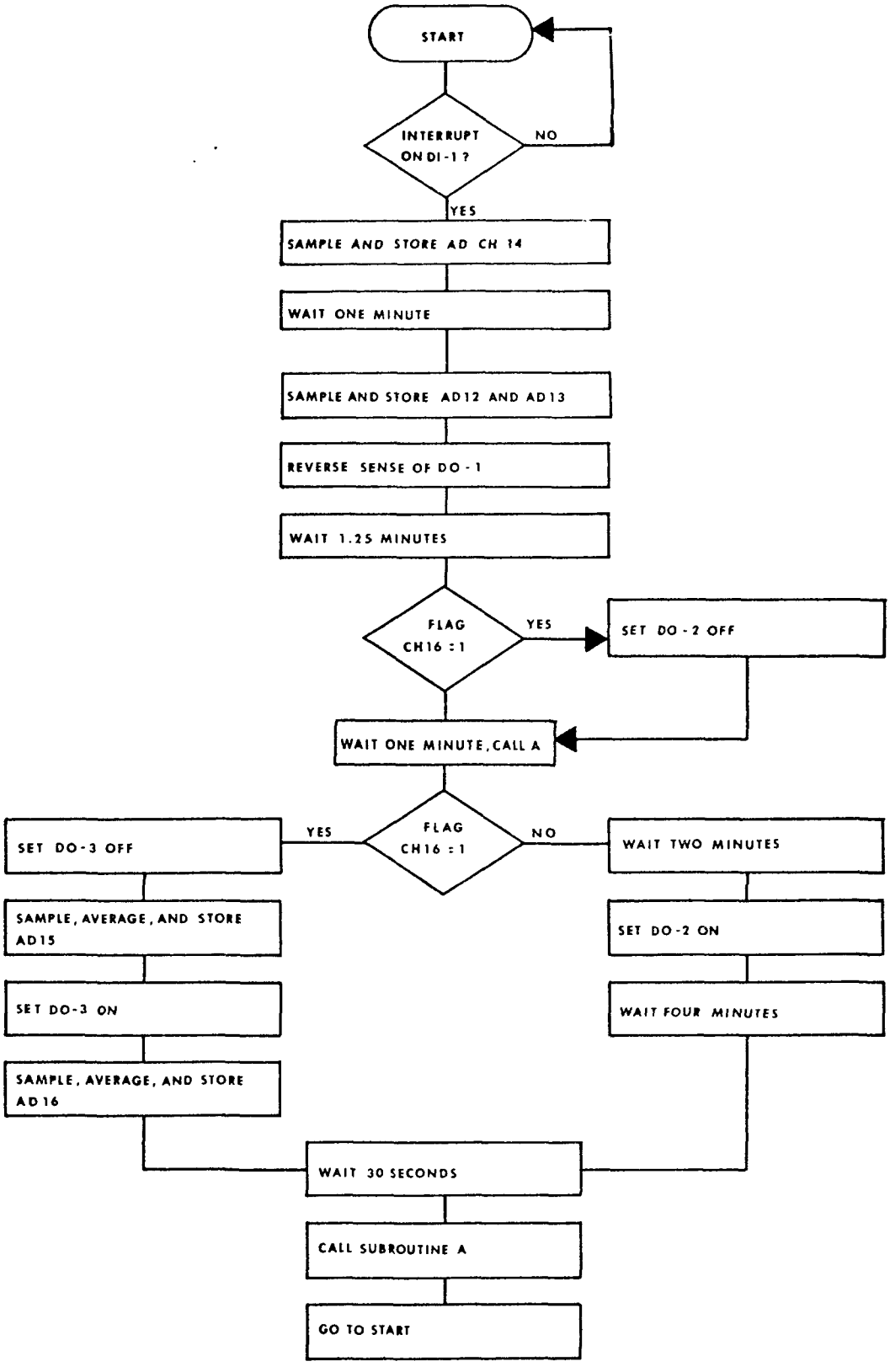

Figure 73. Flowchart of DAQ.

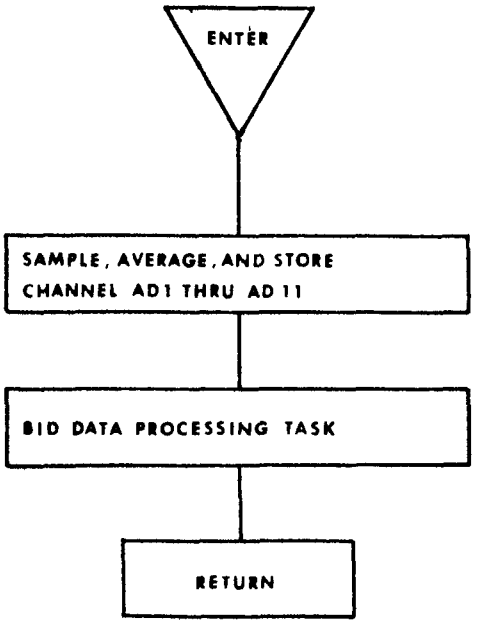

Figure 74. Flowchart of Subroutine A (DAQ).

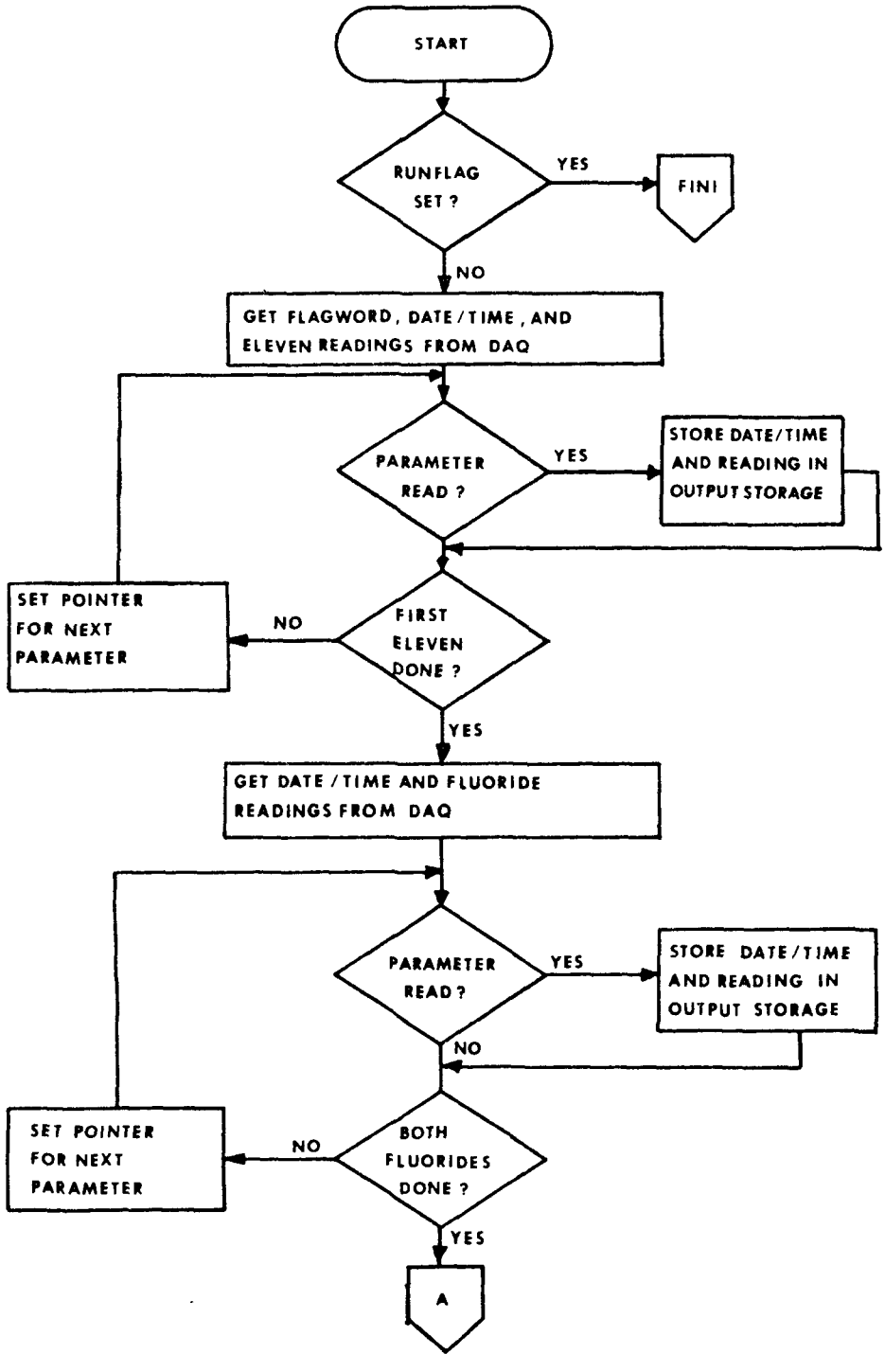

Figure 75. Flowchart of DATA.

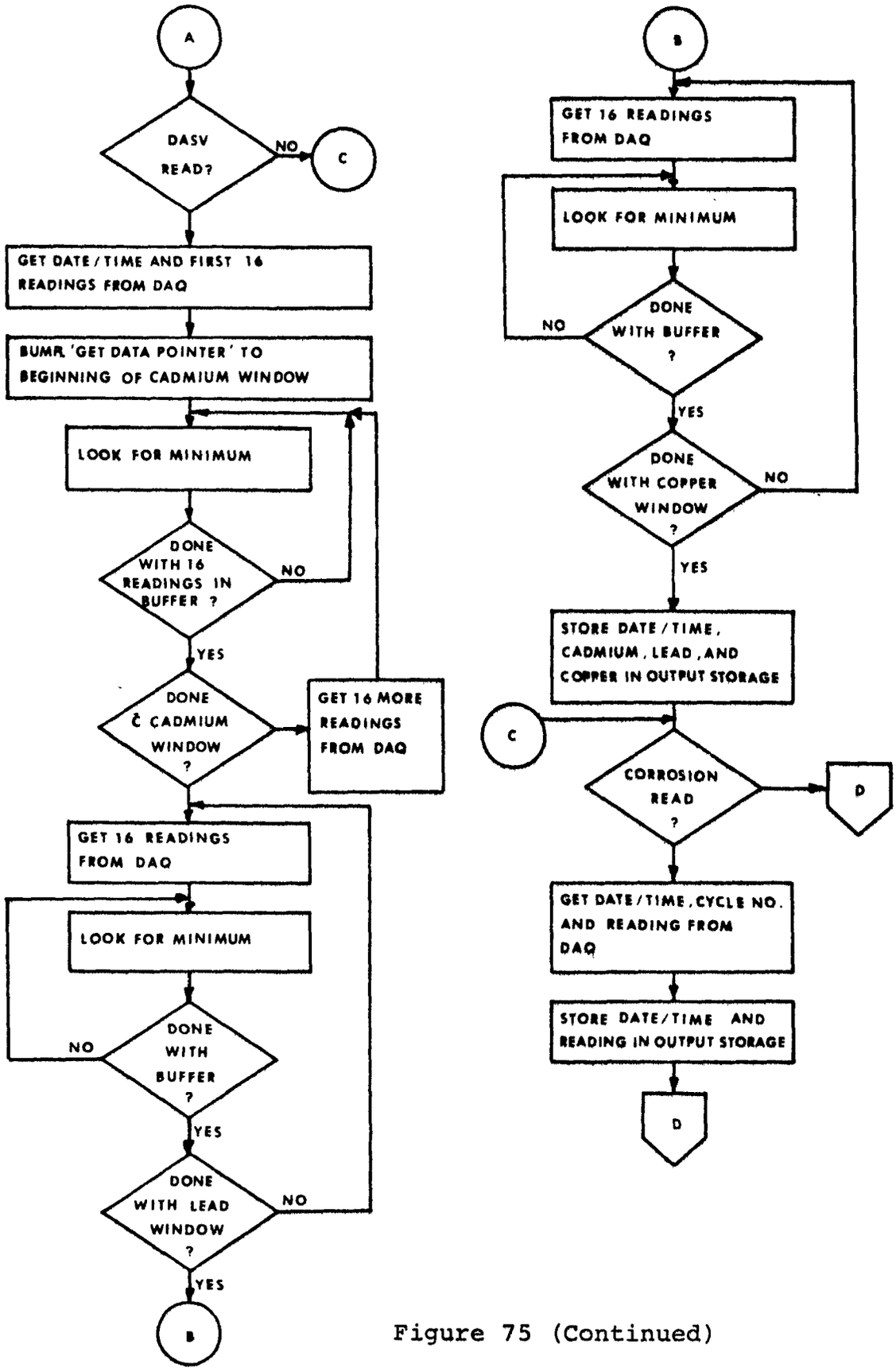

Figure 75 (Continued)

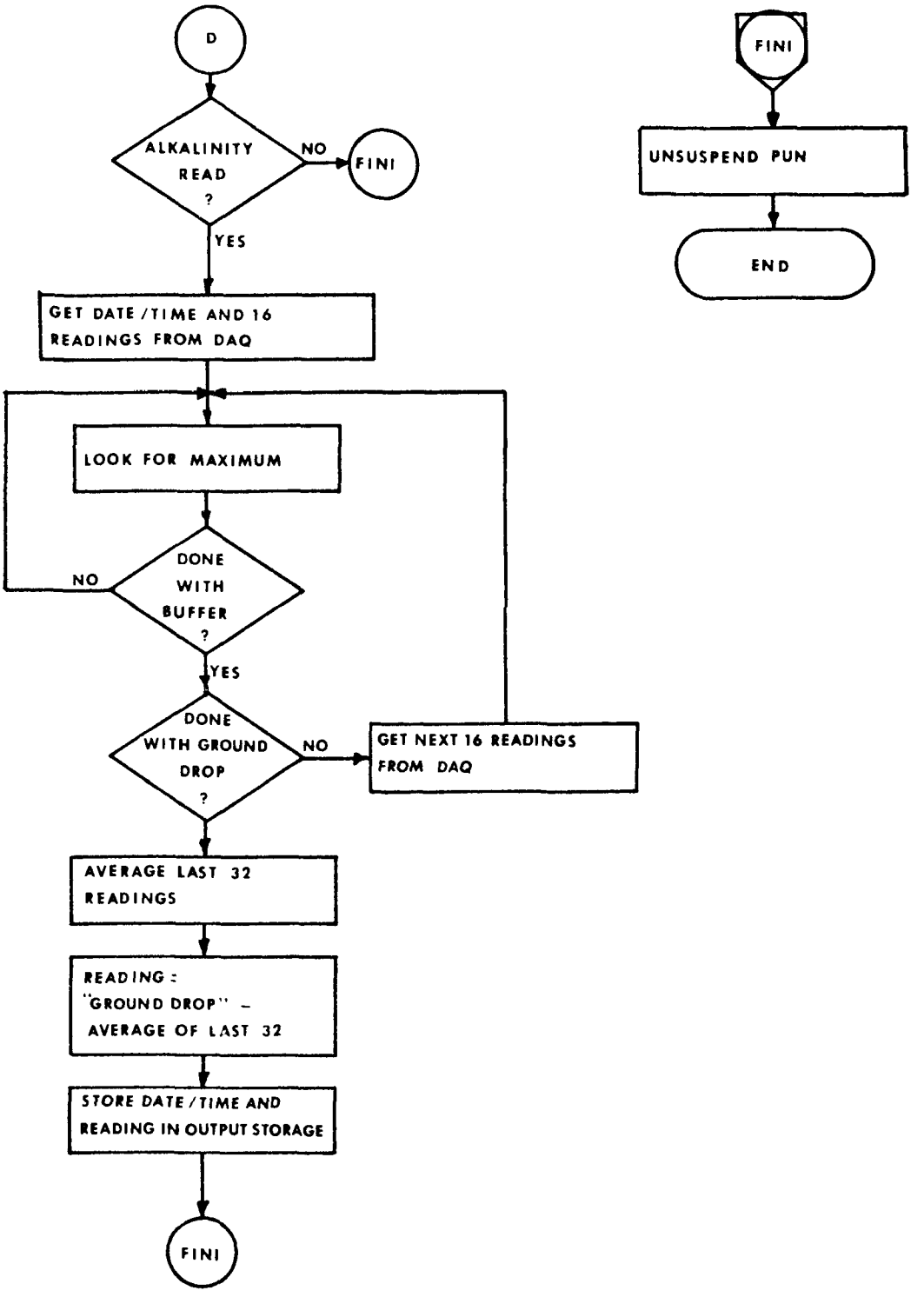

Figure 75 (Continued)

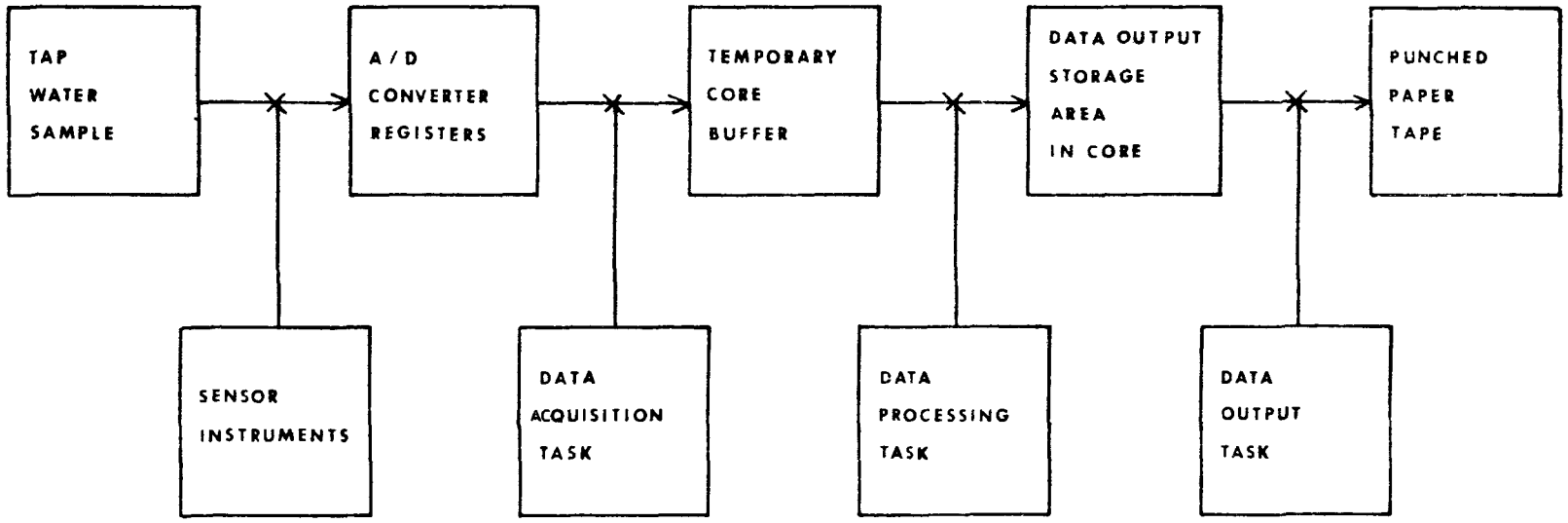

Figure 76. Normal data flow.

September. Acquisition of the computer was fully justified during the Chicago assignments. One man-day for every data-day is a conservative estimate of the time required to transpose parametric data from analog strip chart output to numbers which could be analyzed.

The first stop was the Ann Arbor municipal water treatment plant where the principal objective was to gain proficiency with getting the parametric systems on-line and calibrated, and disassembling for the next move. The van was parked outside, adjacent to the filter building. Although the visit was brief and operators inexperienced, some meaningful data were collected, and the troubleshooting experience was valuable.

The first field assignment away from Ann Arbor was in metropolitan Chicago. N. J. Davoust, Engineer, Chicago Division of Water Purification, and T. E. Larson, Head, Chemistry Section, Illinois State Water Survey, enthusiastically supported the project from its inception and served as members of the advisory committee. The entire Chicago assignment was coordinated through N. J. Davoust.

The trip from Ann Arbor to Chicago was made without incident. The van went directly to the first monitoring site, where it was parked inside a four year old fire station in the northwest part of the city. (Engine Company 79 at 6424 N. Lehigh), 10.5 miles from the Central Water Filtration Plant. All service lines to the van were copper. To evaluate long-term performance characteristics, especially sensor stability, the mobile laboratory remained at this site for one month.

NOTE: *Detailed reports of data collected at all locations were published separately and provided to the agency through which the field trips were coordinated. These reports are not available directly from NSF; however, a number of the special studies are included in pertinent sections of this report.*

The second Chicago location was a 60 year old fire station in the northeast section of the city (Engine Company 102 at 1723 West Greenleaf), approximately 8.5 miles from the Central Water Filtration Plant. Lead service connections brought water to the building from the street mains.

During this 48-hour period, June 11th and 12th (1973), the maximum level of lead in tap water was nine mg/l, well below the 50 mg/l level established by EPA as cause for rejection of a water supply (1), but high enough to be reliably monitored by the mobile laboratory. These data were confirmed by samples analyzed by atomic absorption spectrophotometry in the Chicago water filtration plant laboratory.

The third stop was in the City of Des Plaines, adjacent to northwest Chicago and O'Hare International Airport, within five miles of the Lehigh (first) location. The van was located at the Public Works Building (1111 Campground Road), where distributed water was normally a mixture of 75 percent purchased Chicago water (from the Central Filtration Plant) and 25 percent Des Plaines treated well water. The mix was altered to 1:1 to demonstrate the ability of on-board systems in the mobile laboratory to detect subtle changes in the distribution system. Their responsiveness was reliably demonstrated.

The fourth and final monitoring site on the Chicago trip was a nine year old fire station (Engine Company 80 at Doty Avenue and 127th Street) in the Calumet Harbor area, 41 miles from the previous location in Des Plaines, and 6.1 miles from the South Water Filtration Plant. Water arrived at this location through a one-mile section of six inch transmission line. The fire station was situated on the extreme dead end of the transmission line. The cast iron service line to the building was connected to the mobile laboratory through a few feet of galvanized pipe. Beginning at 1000 hours on June 29th, the main was flushed by opening all connections in the fire station. At 1115 hours, changes in measured levels of turbidity, free and total residual chlorine, temperature, and pH were appreciable, as shown in Figure 77. Relatively high levels of residual chlorine persisted throughout the remaining period of observation.

Each of the last three sites in the Chicago area was visited for just over a week. Moving between them was accomplished with a minimum of downtime. Water and wastewater connections at a new station were made by the laboratory operator; electric service was provided by a city electrician. With normal operation, all systems were on-line and calibrated in little more than two hours after arriving at a new location.

J. V. Radziul, Chief of Research and Development, Philadelphia Water Department and member of the project advisory committee, coordinated activities and planning for the Philadelphia trip. During the month of September, the mobile laboratory visited four sites in the City of Philadelphia, carefully selected to profile water quality from the various sources and treatment facilities providing water to Philadelphia. The locations, identified in Figure 78, include the Oak Lane Reservoir in the northern section of the city (site no. 1), Philadelphia International Airport in the southern section of the city (site no. 2), centrally located City Hall (site no. 3), and Gulf Oil Refinery, less than one mile from site no. 2, but with a different source of treated water (site no. 4).

Raw water for Philadelphia is entirely of surface origin but drawn from two sources, the Schuylkill River and the Delaware River. Water from the Delaware is treated at the Torresdale

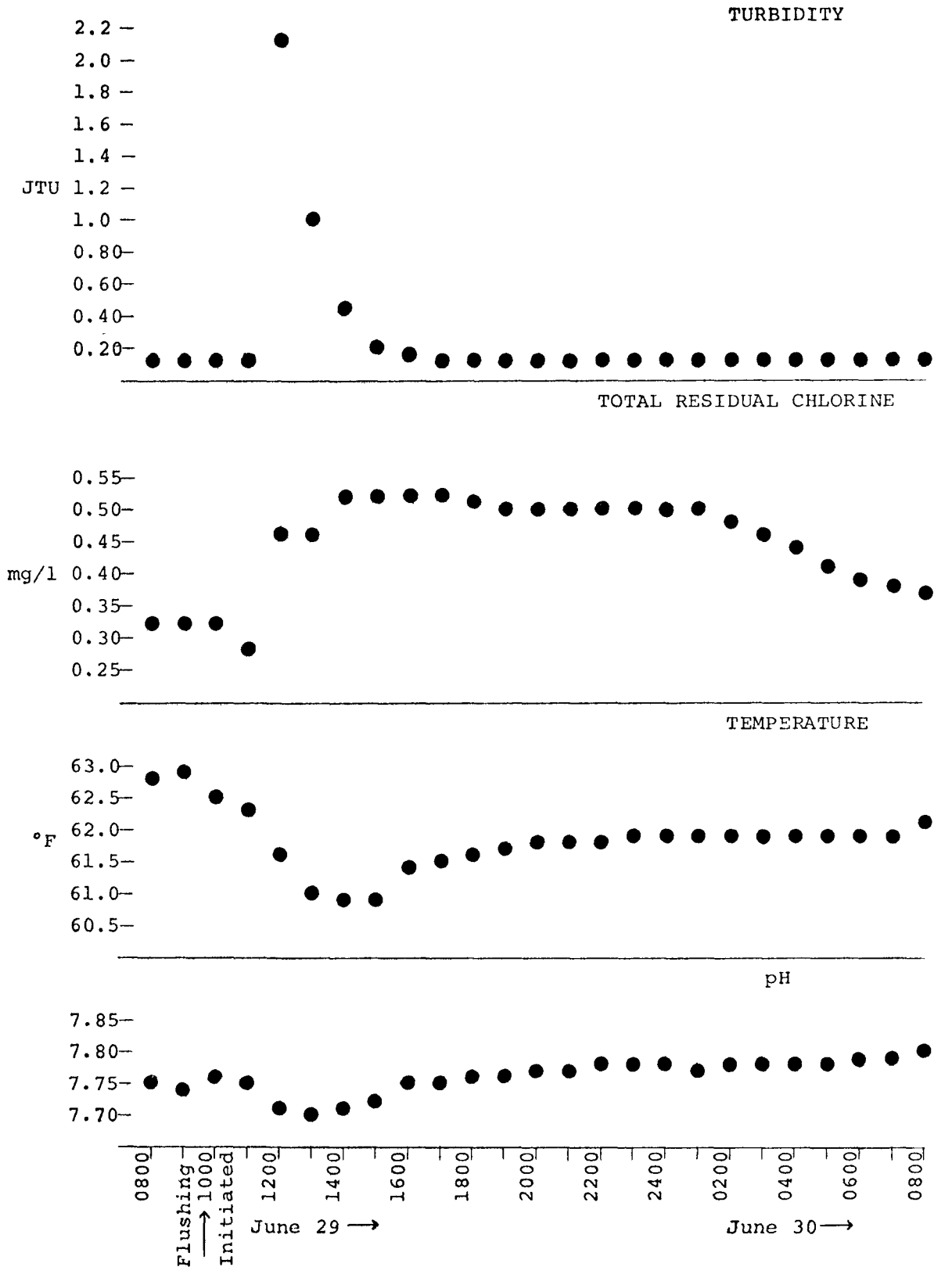

Figure 77. Data from main flushing at Chicago, Calumet Harbor.

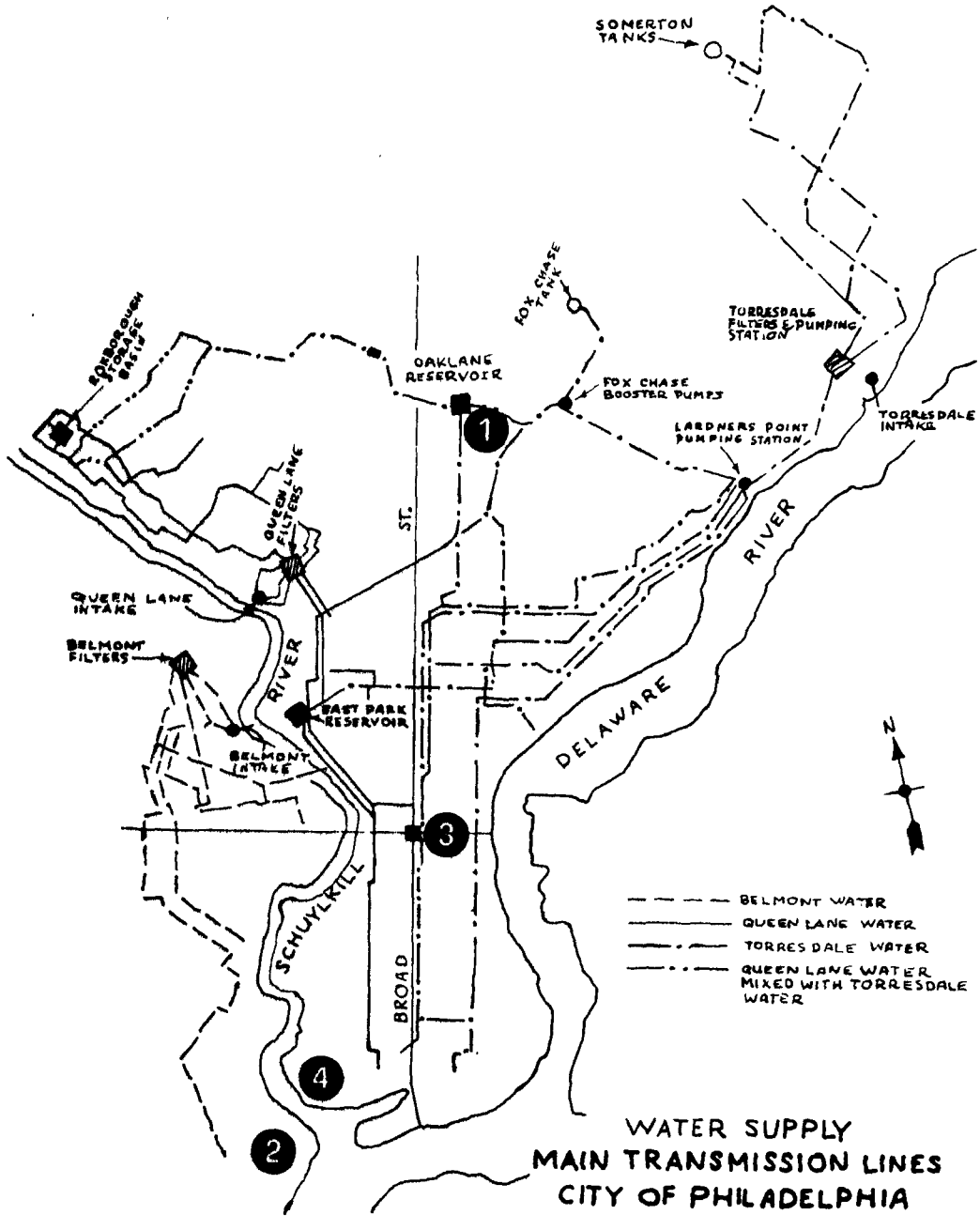

Figure 78. Relative locations of Philadelphia monitoring sites.

Filtration Plant, third largest in the world (282 mgd), and delivered to most of the eastern half of the city. Schuylkill water is treated at Queen Lane (120 mgd) or Belmont (78 mgd) Filtration Plants, and distributed principally to western sections of the city. Each of the treatment facilities is highly automated. Distribution is controlled by a "load control" facility, a central point to which all data related to demand are transmitted by microwave. All water is treated by prechlorination, presedimentation, alum-lime coagulation, rapid and slow mixing, sedimentation, rapid sand filtration, chlorination, and fluoridation. In addition, Belmont water is ammoniated to improve its taste and odor characteristics. Finished water is stored in three large reservoirs, Roxborough, Oak Lane (site no. 1), and East Park, and elevated tanks at various locations in the city.

The water at site no. 1 was treated at Torresdale and stored in the reservoir. Test water at the monitor was taken from the reservoir or from the main filling the reservoir. At the airport, site no. 2, water was from the Belmont filtration plant exclusively. Torresdale, or Queen Lane, or a mixture of the two waters was monitored at City Hall. At the Gulf Oil Refinery, water was delivered principally from Queen Lane, with some mixing from Torresdale possible.

During the first week in Philadelphia, little reliable data was collected. A record heat wave created virtually inoperable conditions for the operator and many of the sensor systems. Additional problems resulted from inadequate external grounding of the laboratory.

A malfunction in the computer power supply caused repeated but temporary "failures" throughout the Philadelphia assignment. Numerous calls by TI service personnel resulted in little satisfaction to the NSF staff. In fact, a general comment regarding failure of TI representatives to adequately diagnose and correct frequent problems with the on-board computer system is in order. A typical notation from the operator's log for site no. 3 cites a malfunction in one of the A/D multiplexer cards which was not replaced for three days after the TI field engineer was notified of the problem. In virtually every period of computer induced downtime, the NSF operator or an NSF computer specialist - not the TI field engineer - was responsible for diagnosing the failure. Although TI hardware offers many advantages for mobile laboratory application, it is unlikely that this computer system would be selected for any future NSF project applications.

SECTION VI
REFERENCES

1. Environmental Protection Agency. Interim Primary Drinking Water Standards. Federal Register. 40(51), March 14, 1975.

2. Fair, G. M., J. C. Geyer, and D. A. Okun. Water and Wastewater Engineering. John Wiley & Sons, Inc., New York, 1968. p. 17-31.

3. Standard Methods for the Examination of Water & Wastewater. 13th Edition. American Public Health Association, American Water Works Association, and Water Pollution Control Federation, New York, 1971.

4. McClelland, N. I. Water Quality Monitoring in Distribution Systems. National Sanitation Foundation, Ann Arbor, Michigan, May 1971. p. 169.

5. Turbidimeters. Second Revised Edition. Hach Chemical Company, Ames, 1973.

6. Quality Goals for Potable Water. Journal American Water Works Association, September 1973. p. 62.

7. Water Quality Monitoring in Metropolitan Chicago: Project Report. National Sanitation Foundation, Ann Arbor, Michigan, 1973.

8. Water Quality Monitoring in Detroit: Data Presentation. National Sanitation Foundation, Ann Arbor, Michigan, 1973.

9. Water Quality Monitoring in Metropolitan Philadelphia: Project Report. National Sanitation Foundation, Ann Arbor, Michigan, 1974.

10. Langelier, M. A. The Analytical Control of Anti-Corrosion Water Treatment. Journal American Water Works Association, 28:1500, 1936.

11. Larson, T. E. and A. M. Buswell. Calcium Carbonate Saturation Index and Alkalinity Interpretations. Journal American Water Works Association, 34:1664, 1942.

12. Ryzner, J. W. A New Index for Determining the Amount of Calcium Carbonate Scale Formed by a Water. Journal American Water Works Association, 36:472, 1944.

13. Pytkowicz, R. M. Rates of Inorganic Calcium Carbonate Nucleation. Journal Geology, 73:196, 1965.

14. Weyl, P. K. Solution Kinetics of Calcite. Journal Geology, 66:163, 1958.

15. Weyl, P. K. The Carbonate Saturometer. Journal Geology, 69:32, 1961.

16. McClanahan, M. A. Mechanism of Cast Iron Corrosion Inhibition by Calcium Carbonate Deposition in Water Distribution Systems. Doctoral dissertation, The University of Michigan, Ann Arbor, 1968.

17. Schlicting, H. Boundary Layer Theory. McGraw-Hill Book Co., 1960. p. 83.

18. Levich, V. G. Physicochemical Hydrodynamics. Prentice Hall, Inc., 1962.

19. Nernst, W. Z. Physical Chemistry, 47:52, 1904.

20. Riddiford, A. C. Advances in Electrochemistry and Electrochemical Engineering. 4:47, 1966.

21. Napp, D. T. Doctoral dissertation, University of Minnesota, Minneapolis, 1967.

22. Johnson, D. C. Doctoral dissertation, University of Minnesota, Minneapolis, 1967.

23. Enslow, L. H. The Continuous Stability Indicator. Water and Sewerage Works, 107, March 1939.

24. Enslow, L. H. The Continuous Stability Indicator and the Langelier Index. Water and Sewerage Works, 283, July 1939.

25. Durfor, C. N. and E. Becker. Public Water Supplies of the 100 Largest Cities in the United States. 1962. U.S. Geological Survey Water Supply Paper 1812. U.S. Government Printing Office, Washington, D.C., 1964.

26. Zipkin, I. and F. J. McClure. Fluoride Drinking Waters. U.S. Department of Education and Welfare Public Health Service Publication, 825:483, 1962.

27. Hein, J. W., D. E. Gardner, and G. B. Haydon. Preliminary Investigations of the Effect of Sodium Monofluorophosphate

on Salivary Acid Production and Hydroxyapatite Solubility. Journal Dentist Research, 30:466, 1951.

28. Cooley, W. E. Reaction of Tin (II) and Fluoride Ions with Etched Enamel. Journal Dentist Research, 40:1199, 1961.

29. Brudevold, F., et al. Uptake of Tin and Fluoride by Intact Enamel. Journal American Dentist Association, 53:159, 1956.

30. Cooley, W. E. Applied Research in the Development of Anti-caries Dentifrices. Journal Chemical Education, 47:177, 1970.

31. Frant, M. S. and J. W. Ross. Electrode for Sensing Fluoride Ion Activity in Solutions. Science, 154:1553, 1966.

32. Orion Instruction Manual, Fluoride Ion Activity Electrode, Model 94-09. Second Edition. Orion Research Inc., Cambridge, Massachusetts, 1967.

33. Bock, R. and F. Z. Strecker. Direkte Electrometrische Bestimmung des Fluorid-ions. Analytical Chemistry (Germany), 234:322, 1968.

34. Harwood, J. E. The Use of an Ion Selective Electrode for Routine Fluoride Analysis on Water Samples. Journal Water Research, 3:273, 1969.

35. Mesmer, R. E. Lanthanum Fluoride Electrode Response in Aqueous Chloride Media. Analytical Chemistry, 40:443, 1968.

36. Rechnitz, G. A. Ion Selective Electrodes. Chemistry and Engineering News, 45(25):146, 1967.

37. Scrinivasan, K. and G. A. Rechnitz. Activity Measurement with a Fluoride-Selective Membrane Electrode. Analytical Chemistry, 40:509, 1968.

38. Ciavatta, L. Hydrolysis of Fluoride Ion, F^-, in 3 M Na^+ $(ClO_4)^-$ and 3 M $K^+(Cl^-, F^-)$ Media. Arkiv Kemi (Sweden), 21:129, 1963.

39. Butler, J. N. Ionic Equilibrium, A Mathematical Approach. Addison-Wesley Publishing Co. Inc., 1964. Chapter 5-1, p. 115.

40. Frant, M. S. and J. W. Ross. Use of a Total Ionic Strength Adjustment Buffer for Electrode Determination of Fluoride in Water Supplies. Analytical Chemistry, 40:1169, 1968.

41. Crosby, N. T., A. L. Dennis, and J. G. Stevens. An Evaluation of Some Methods for the Determination of Fluoride in Potable Waters and Other Aqueous Solution. Analyst, 93:643, 1968.

42. Kelada, N. P. Electrochemical Characterization of Free & Complexed Fluorides in Drinking Water and Effects of Aluminum & Iron on Fluoride Incorporation into Tooth Enamel. Doctoral dissertation, University of Michigan, Ann Arbor, 1972.

43. Schwarzenback, G., R. Gut, and G. Anderegg, 117. Komplexone XXV. Die Polarographische untersuchung von austausch-gleichgewichten. Neue daten der piltungskonstanten von metall komplexen der Athylendiamin-tetraessigsaure und der 1,2-Diamin-cyclohexan-tetraessigsaure. Helv. Chim. Acta (Germany), 37:937, 1954.

44. Lacroix, S. Etude de quelques Complexes et Composes peu Solubles des Ions. Ann. Chim. (France), 4:5, 1949.

45. Bertin-Batsch, C. Etude par des Methodes variees de quelques Complexes Organiques de l'Ion Ferrique. Ann. Chim (France), 7:481, 1952.

46. Peterson, T. L., D. O. Brant, and K. H. Mancy. Characterization of Trace Metals in Municipal Water Supplies by Thin Layer Anodic Stripping Voltammetry. University of Michigan, Ann Arbor. (Presented at 160th National Meeting of the American Chemical Society. Chicago, September 1970.)

47. Operation and Maintenance Manual for Mobile Water Quality Monitoring Laboratory, National Sanitation Foundation, Ann Arbor, Michigan, 1973.

SECTION VII
PROJECT PUBLICATIONS

1. Committee Report, AWWA Corrosion and Stability Committee. "Water Quality Determination in Distribution Systems." (Presented at the 90th Annual Conference, American Water Works Association, Washington, D.C., 1970. Journal American Water Works Association, 795, 1972.

2. Kelada, N. P., N. I. McClelland, and K. H. Mancy. Characterization of Fluorides in Water Supplies by Selective Ion Electrodes. (Presented at 160th National Meeting, American Chemical Society, Chicago, Illinois, 1970.)

3. McClelland, N. I. and K. H. Mancy. Electrochemical Characterization of Drinking Water. (Presented at the 141st Meeting, Electrochemical Society, Houston, Texas, 1972.)

4. McClelland, N. I. and K. H. Mancy. Water Quality Monitoring in Distribution Systems. (Presented at the 92nd Annual Conference, American Water Works Association, Chicago, Illinois, 1972.)

5. Schimpff, W. K., N. I. McClelland, K. H. Mancy, and H. E. Allen. An Automated Differential Anodic Stripping Technique for Monitoring Trace Metals in Distribution Systems. (Presented at the 92nd Annual Conference, American Water Works Association, Chicago, Illinois, 1972.)

6. McClelland, N. I. Monitoring of Municipal Drinking Waters: Process to Consumer. (Presented at the 15th Eastern Analytical Symposium, New York, New York, 1973.)

7. McClelland, N. I. Monitoring of Drinking Water Quality in Distribution Systems. (Presented at the 2nd Joint Conference on Sensing of Environmental Pollutants, Washington, D.C., 1973.)

8. McClelland, N. I., J. R. Adams, R. R. Wood, and K. H. Mancy. Application of Monitoring Technology (for Assuring) Drinking Water Quality. (Presented at the 167th National Meeting, American Chemical Society, Los Angeles, California, 1974.)

9. Adams, J. R., R. R. Wood, and N. I. McClelland. Drinking Water Quality: Application of Monitoring Technology. (Presented at the 6th Central Regional Meeting, American Chemical Society, Detroit, Michigan, 1974.)

10. McClelland, N. I. and K. H. Mancy. Water Quality Surveillance in Distribution Systems. (Presented at 94th Annual Conference,

American Water Works Association, Boston, Massachusetts, 1974.)

11. Symons, J. M., M. C. Gardels, K. H. Mancy, and N. I. McClelland. Continuous Distribution System Monitoring to Study the Effects of Hardness and Other Water Quality Parameters. (Presented at 94th Annual Conference, American Water Works Association, Boston, Massachusetts, 1974.)

12. McClelland, N. I. Experiences in Monitoring Residual Chlorine. (Presented at 94th Annual Conference, American Water Works Association, Boston, Massachusetts, 1974.)

SECTION VIII
APPENDICES

		Page
A.	Technical Advisory Committee	175
B.	Preparation of Reagents	176
C.	Special Alkalinity Case Study	181

APPENDIX A

TECHNICAL ADVISORY COMMITTEE

Harry A. Faber, Chairman (1969-1972)
88 Main Street
Whitesboro, NY 13492

N. J. Davoust, Chairman (1973)
Engineer of Water Purification
Central Water Filtration Plant
1000 E. Ohio Street
Chicago, IL 60611

T. E. Larson
Head, Chemistry Section
Illinois State Water Survey
Box 232
Urbana, IL 61801

Blucher A. Poole
Consultant
5839 Brockton Drive
Indianapolis, IN 46220

Joseph V. Radziul
Chief, Research & Development
Water Department
1270 Municipal Services Bldg.
Philadelphia, PA 19107

Verdun Randolph
Associate Director
Consumer Health Protection
Illinois Department of Public Health
535 West Jefferson Street
Springfield, IL 62761

Gordon G. Robeck
Director
Water Supply Research Division
U.S. Environmental Protection Agency
Municipal Environmental Research Laboratory
Cincinnati, OH 45268

Elroy F. Spitzer
Director
American Water Works Assoc.
Research Foundation
6666 W. Quincy Avenue
Denver, CO 80235

James M. Symons
Chief, Physical and Chemical Removal Branch
Water Supply Research Division
U.S. Environmental Protection Agency
Municipal Environmental Research Laboratory
Cincinnati, OH 45268

T. L. VanderVelde
Deputy Chief
Bureau of Environmental and Occupational Health
Michigan Department of Public Health
Lansing, MI 48914

Richard Woodward
Vice President
Camp, Dresser, & McKee
One Center Plaza
Boston, MA 02108

APPENDIX B

PREPARATION OF REAGENTS

SRM-HOUSED SYSTEMS

Standard solutions are required for weekly calibration of SRM-housed sensor systems. No other reagents are used for routine operation of these systems. Standard solutions are prepared as follows:

HARDNESS

a. Calcium chloride stock solution

Dissolve 11.099 g $CaCl_2$ (anhydrous) in approximately one liter of distilled water. This solution should be standardized against EDTA and adjusted to contain $10^{(-1)}$M $CaCl_2$ concentration.

b. Standard solutions

To prepare standard solution, dilute 13.0 ml stock solution to 1,000 ml with distilled water, using a volummetric flask. This solution contains $10^{(-3)}$M Ca^{2+} activity. Dilute 1.075 ml stock solution to 1,000 ml. This solution contains $10^{(-4)}$M Ca^{2+} activity. Separate each of the standards into two 500 ml wide-mouth jars. Label one jar of each standard "wash," and the other, "standard."

NITRATE

a. Potassium nitrate stock solution

Dissolve 1.6308 g KNO_3 in exactly 1.0 liter of distilled water.

b. Standard solutions

To prepare standard solutions, dilute 104.2 ml stock solution to 1,000 ml with distilled water, using a volummetric flask. This solution contains 100 mg/l NO_3^- activity. Dilute 10.2 ml stock solution to 1,000 ml. This solution contains 10 mg/l NO_3^- activity.

Dilute 1.0 ml stock solution to 1,000 ml. This solution contains 1.0 mg/l NO_3^- activity. Separate each into "wash" and "standard" solutions.

CHLORIDE

a. Sodium chloride stock solution

Dissolve 1.6482 g NaCl (dried at 140°C) in chloride free water and dilute to 1.0 liter. This solution contains 1.0 mg Cl^-/ml.

b. Standard solutions

To prepare standard solutions, dilute 100 ml stock solution to 1,000 ml with chloride free water, using a volummetric flask. This solution contains 100 mg/l Cl^-. Dilute 10 ml stock solution to 1,000 ml. This solution contains 10 mg/l Cl^-. Separate each into "wash" and "standard" solutions.

CONDUCTIVITY

a. Standard reference potassium chloride solution

Dissolve 745.6 mg anhydrous KCl in freshly boiled distilled-deionized water and dilute to 1,000 ml at 25°C. This solution has a specific conductance of 1,413 μmhos/cm at 25°C. This solution is used to calibrate the laboratory conductivity meter, used to prepare standards of 1,000 and 100 μmhos/cm.

b. Standard solutions

Add KCl solution to distilled water at 25°C to prepare standard solutions of 1,000 and 100 μmhos/cm, respectively. Separate each into "wash" and "standard" solutions.

pH

a. pH 6.86 standard buffer
(0.025 M potassium dihydrogen phosphate +0.025 M disodium hydrogen phosphate)

Dissolve 1.179 g KH_2PO_4 and 4.30 g Na_2HPO_4 in distilled water and dilute to 1,000 ml. This solution is pH 6.86 at 25°C.

b. pH 9.18 standard buffer
(0.01 M borax)

Dissolve 3.80 g $Na_2B_4O_7 \cdot 10\ H_2O$ in distilled water and dilute to 1,000 ml. This solution is pH 9.18 at 25°C.

RESIDUAL CHLORINE

a. Buffer solution
(Sodium acetate-acetic acid buffer)

Fill the buffer dispensing bottle approximately one-fourth full with distilled water. Add 855 ml glacial HNO_3. Add 460 g $CH_3COONa \cdot 3\ H_2O$ with vigorous mixing and stir till completely dissolved. Fill bottle to top with distilled water. This solution is used with free- and total- residual chlorine analyzers.

b. Potassium iodide solution

Dissolve 20 g KI in distilled water and dilute to approximately two liters in the KI dispensing bottle (total chlorine analyzer only).

ALKALINITY

a. Buffer solution
(Potassium hydrogen phthalate buffer)

Dissolve 91.80 g potassium hydrogen phthalate ($HOCOC_6H_4COOK$) in approximately eight liters of distilled water. Dilute 13.4 ml concentrated hydrochloric acid (HCl) to 800 ml with distilled water. Mix the two solutions, add 0.0635 g sodium thiosulfate ($Na_2S_2O_3$), and bring up to nine liters. Adjust the pH to 3.1 using concentrated HCl.

b. Baseline solution

(1) Sodium carbonate stock solution
Dissolve 0.477 g Na_2CO_3 in CO_2 free distilled water and dilute to 1.0 liter.

(2) To prepare working baseline solution, dilute 200 ml stock solution to 9.0 liters with CO_2 free distilled water. This solution is equivalent to 10 mg/l $CaCO_3$.

c. Standard solutions

(1) Sodium carbonate stock solution
Dissolve 1.0590 g Na_2CO_3 in CO_2 free distilled water and dilute to 1.0 liter. Store in tightly stoppered glass bottle. Make up fresh stock solution monthly.

(2) To prepare standard solutions, dilute 1.0, 2.0, 3.0, ... 9.0 ml stock solution to 100 ml each. These solutions contain 10, 20, 30, ... 90 mg/l equivalent $CaCO_3$, respectively. Fresh standard solutions must be prepared for each calibration series.

FLUORIDES

a. Buffer solutions

(1) Free fluoride
Dissolve 850 g sodium nitrate ($NaNO_3$) in approximately nine liters distilled water. Add 57 ml glacial acetic acid (CH_3COOH) and mix. Bring volume up to 10.0 liters. Adjust to pH 5.2 with concentrated sodium hydroxide (NaOH) solution.

(2) Total fluoride
Dissolve 595 g $NaNO_3$ and 588 g sodium citrate ($Na_3C_6H_5O_7 \cdot 2\ H_2O$) in approximately nine liters distilled water. Add 115 ml CH_3COOH and mix. Bring volume up to 10.0 liters. Adjust to pH 5.2 with NaOH.

b. Baseline solution

Dilute 20.0 ml 100 mg/l F^- Harleco standard to 20.0 liters.

c. Standard solutions

Dilute 2.0, 5.0, and 10.0 ml 100 mg/l F^- Harleco standard to 1,000 ml each. These solutions contain 0.2, 0.5, and 1.0 mg/l F^-, respectively. Store in plastic bottles.

TRACE METALS ANALYZER (DASV for Cd, Pb, and Cu)

a. pH adjustment solution

The strength of the pH adjustment solution will vary with the pH of the test water. Add concentrated nitric acid (HNO_3) *dropwise* to distilled water to the predetermined level at which, when added to test water in the appropriate ratio, will result in a final pH of 2.5.

b. Standard solution

(1) Place 1.0 ml 1,000 mg/l Cd Harleco standard, 1.0 ml 1,000 mg/l Pb Harleco standard, and 1.0 ml 1,000 mg/l Cu Harleco standard in a 100 ml volummetric flask. Bring to volume

with distilled water and mix. This solution contains 10 mg/l each of Cd, Pb, and Cu. Transfer to plastic bottle for storage.

(2) Dilute 1.0 ml of stock solution to 2.0 liters in the quartz reservoir, using test water as the diluent. (The known addition technique is used for standardization in trace analysis.) This solution contains 0.05 mg each of Cd, Pb, and Cu.

c. Mercury plating solution

Dissolve one drop (approximately 0.05 ml) of reagent grade mercury (Hg) in concentrated HNO_3 (as little as possible). When solution is complete, dilute to approximately 100 ml with distilled water. Store in a glass stoppered bottle. Inject 2.0 ml of this solution into the flow cell filled with distilled water to plate (rejuvenate) the electrodes.

APPENDIX C

SPECIAL ALKALINITY CASE STUDY

Experimental Procedure

1. Prepare 0.050 F KHP and 0.019 F HCl standard phthalate buffer.
2. Prepare alkalinity standards from Na_2CO_3 in distilled water.
3. Prepare additional alkalinity standards using distilled with known concentrations of chlorine, prepared from gaseous chlorine.
4. Mix five parts of each alkalinity standard with one part buffer and determine resultant pH.
5. Plot H^+ versus alkalinity, developing a series of curves from the standards with varying concentrations of chlorine.

Theoretical Results

In the presence of free residual chlorine, initial formalities for the buffer are:

$$KHP = 0.050$$
$$HCl = 0.019$$

and for the test water:

$$Na_2CO_3 = 6/5\ C$$
$$Cl_2 = 6/5\ E$$

Final formalities at buffer:sample = 1:5 are:

$$HHP = 8.33(10)^{-3}$$
$$HCl = 3.17(10)^{-3}$$
$$Na_2CO_3 = C$$
$$Cl_2 = E$$

Known relationships are the same as those expressed in Equations 75 through 79 and 81 through 84. Equation 80 is rewritten as:

$$[Cl^-] = 3.17(10)^{-3} + [HOCl] + [OCl^-] \qquad (126)$$

and Equation 85:

$$[H^+] + [Na^+] + [K^+] = [OH^-] + [Cl^-] + [HP^-] + 2[P^{2-}] + [HCO_3^-] + 2[CO_3^{2-}] + [OCl^-] \quad (127)$$

Other known reactions include:

$$K_5 = \frac{[HOCl][H^+][Cl^-]}{[Cl_2]} = 4.2(10)^{-4} \quad (128)$$

$$K_6 = \frac{[H^+][OCl^-]}{[HOCl]} = 3.4(10)^{-8} \quad (129)$$

and

$$2[Cl_2] + [HOCl] + [OCl^-] + [Cl^-] = 2E + 3.17(10)^{-3} \quad (130)$$

Assuming $[CO_3^{2-}] = [P^{2-}] = [OH^-] = [Cl_2] = [OCl^-] = 0$, and that only the equilibria expressed in Equations 131 and 132 occur for free residual chlorine:

$$Cl_2 + H_2O \rightarrow HOCl + H^+ + Cl^- \quad (131)$$

$$HOCl + H_2O \rightarrow H_3O^+ + OCl^- \quad (132)$$

then derivations shown in Equations 86 through 98 and those in Equations 133 and 134 can be expressed:

$$[Cl^-] = 3.17(10)^{-3} + E \quad (133)$$

$$[HOCl] = E \quad (134)$$

Also, from Equations 80 and 86:

$$[Cl_2] = \frac{[H^+]}{K_5}\left\{3.17(10)^{-3} + [HOCl]\right\}[HOCl] \quad (135)$$

From Equations 79, 81, 82, 85, 95, and 98:

$$[H^+] + 2C + 8.33(10)^{-3} = 3.17(10)^{-3} + E + \frac{1.083(10)^{-5}}{[H^+]+1.3(10)^{-3}} + \frac{4.6(10)^{-3}C}{[H^+]+4.6(10)^{-3}} \quad (136)$$

$$L.C.D. = [H^+]^2 + 5.9(10)^{-3}[H^+] + 5.98(10)^{-6} \quad (137)$$

$$[H^+]+2C+5.16(10)^{-3} - E - \frac{1.083(10)^{-5}}{[H^+]+1.3(10)^{-3}} - \frac{4.6(10)^{-3}C}{[H^+]+4.6(10)^{-3}} = 0 \qquad (138)$$

$$\begin{aligned}[H^+]^3 &+ 2C[H^+]^2 + 5.16(10)^{-3}[H^+]^2 - E[H^+]^2 + 5.9(10)^{-3}[H^+]^2 \\ &+1.18(10)^{-2}C[H^+] + 3.044(10)^{-5}[H^+] - 5.9(10)^{-3}E[H^+] \\ &+5.98(10)^{-6}[H^+] + 1.196(10)^{-5}C + 3.086(10)^{-8} - 5.98(10)^{-6}E \\ &-1.083(10)^{-5}[H^+] - 4.982(10)^{-8} - 4.6(10)^{-3}C[H^+] \\ &-5.98(10)^{-6}C = 0 \end{aligned} \qquad (139)$$

$$\begin{aligned}[H^+]^3 &+ \{1.106(10)^{-2} + 2C - E\}[H^+]^2 + \{2.559(10)^{-5} + 7.2(10)^{-3}C \\ &- 5.9(10)^{-3}E\}[H^+] + \{-1.896(10)^{-8} + 5.98(10)^{-6}C - 5.98(10)^{-6}E\} = 0 \end{aligned} \qquad (140)$$

assuming $[H^+]^3 = 0$.

$$[H^+] = \frac{-2.559(10)^{-5} - 7.2(10)^{-3}C + 5.9(10)^{-3}E + \sqrt{\{2.559(10)^{-5}+7.2(10)^{-3}C - 5.9(10)^{-3}E\}^2 - 4\{1.106(10)^{-2}+2C-E\}\{-1.896(10)^{-8}+5.98(10)^{-6}C - 5.98(10)^{-6}E\}}}{2.212(10)^{-2} + 4C - 2E} \qquad (141)$$

$$[H^+] = \frac{-2.559(10)^{-5} - 7.2(10)^{-3}C + 5.9(10)^{-3}E + \sqrt{4(10)^{-6}C^2+2.556(10)^{-7}C +1.489(10)^{-9} +1.089(10)^{-5}E^2 -1.132(10)^{-7}E -1.32(10)^{-5}CE}}{2.212(10)^{-2} + 4C - 2E} \qquad (142)$$

The family of curves obtained by application of Equation 142 are shown in Table 23 and Figure 79.

Although alkalinity has been shown to be linear with respect to pH when no free chlorine is present, it is important to note that the alkalinity monitor reads potential in mv, not pH. To convert $[H^+]$ in the theoretical results to potential, the Nernst equation is applied:

$$E = E° + 0.059 \log [H^+] \tag{143}$$

or

$$E = E° - (0.059)pH \tag{144}$$

where:

E° = a function of reference electrode potential and E is the measured potential

E° cannot be predicted theoretically. If it is assumed to be equal to zero, then:

$$E = -(0.059)pH \tag{145}$$

Data from Table 23 are expressed as potentials in Table 24 and Figure 80. As shown in Figure 80, experimental and theoretical results for alkalinity solutions with no free chlorine residual vary only about three to seven mv at alkalinity equal to 30 to 70 mg/l as $CaCO_3$. This slight variation is likely attributable to experimental error and instrument limitations.

In Table 25, data from Table 23 for Cl_2 = 1.0 and $2.0(10)^{-5}$F (approximately 0.7 and 1.4 mg/l free residual chlorine) are expressed as potentials and compared with theoretical results for Cl_2 = 0. The greatest variation in potential associated with a specific level of alkalinity and a change from Cl_2 = 0 to Cl_2 = 1.4 mg/l is 0.3 mv. This small change in potential cannot be observed with the alkalinity monitor.

Experimental Results

Experimental data obtained by NSF closely approximated the theoretical results. NaOCl was substituted for gaseous Cl_2 in the procedure described on page 181. Alkalinity standards included 30, 40, 50, 60, 70, and 80 mg/l as $CaCO_3$, prepared from Na_2CO_3. Changes in volume with addition of NaOCl to the standards were negligible and disregarded. (The greatest addition was 0.1 ml to 60 ml of standard, or 0.167 percent change in volume.) The result of simple regression applied to the data is shown in Figure 81.

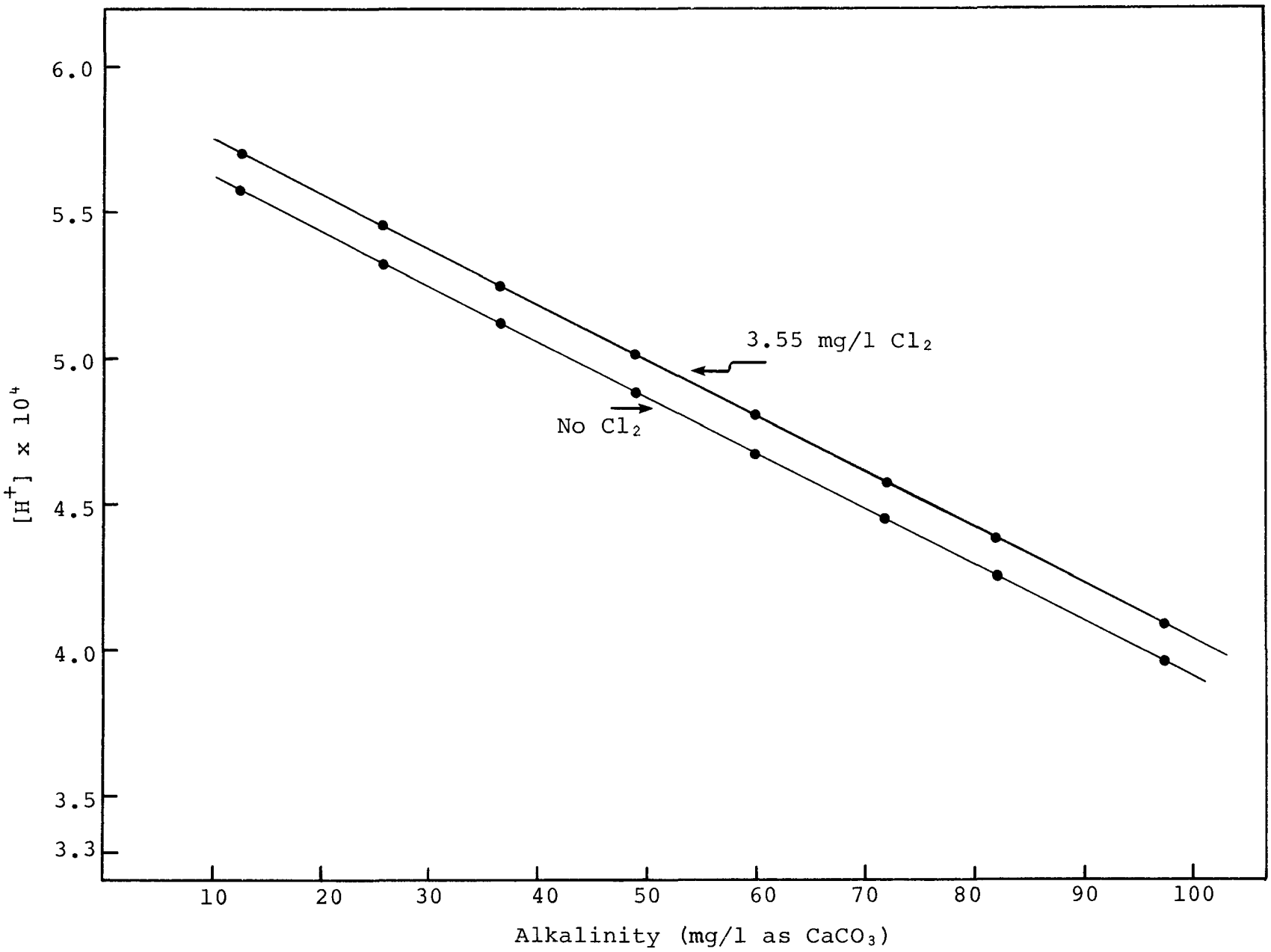

Figure 79. $[H^+]$ as a function of CO_3^{2-} and Cl_2 formality.

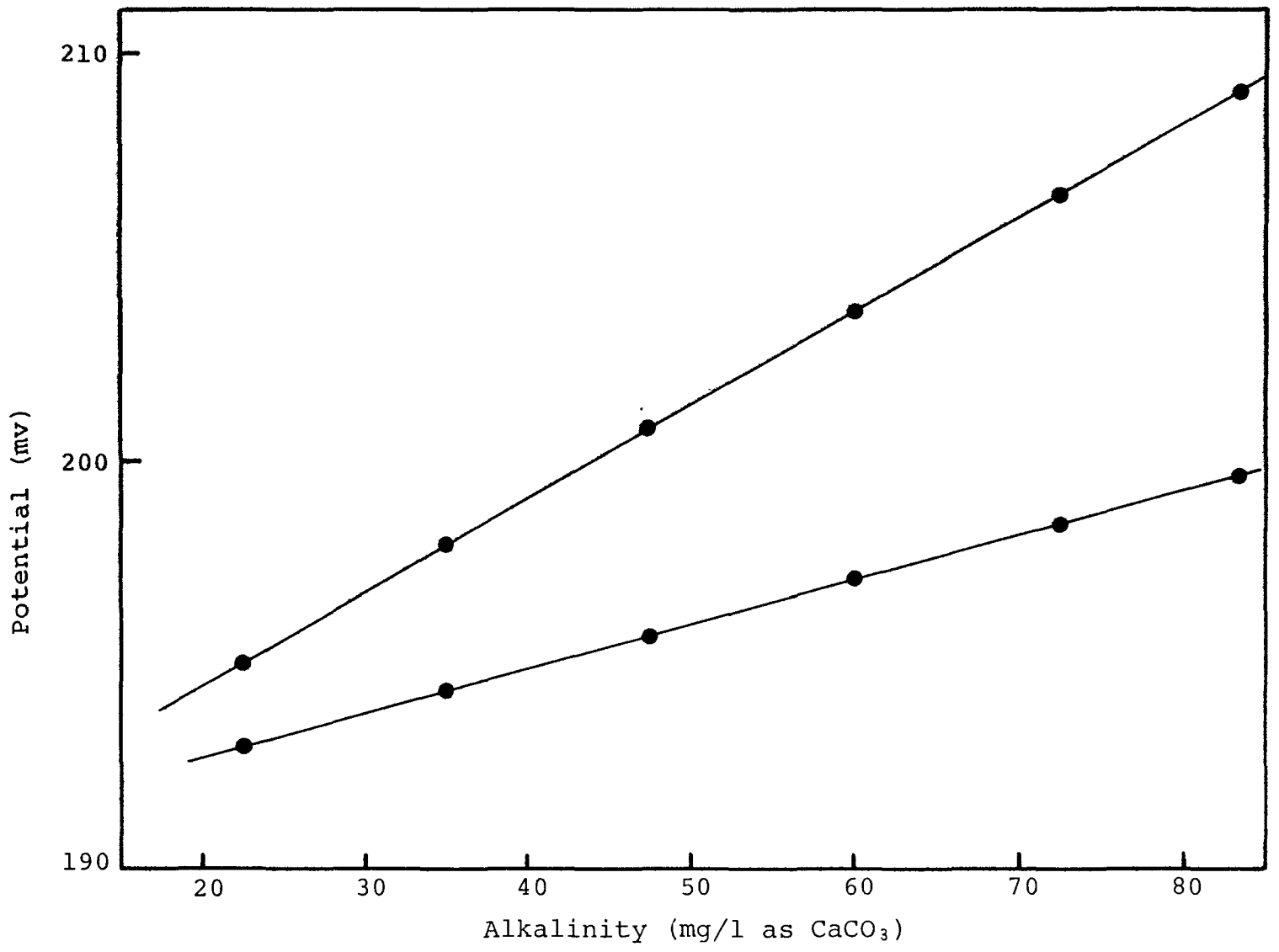

Figure 80. Experimental and theoretical relationships between alkalinity and potentials.

Table 23. $[H^+]$ AS A FUNCTION OF CO_3^{2-} AND Cl_2 FORMALITY

C (X 10↑-5)[2]	E (X 10↑-5)[1] 0.0	0.5	1.0	1.5	2.0	2.5	3.0	3.5	4.0	4.5	5.0
1.0	5.60	5.61	5.62	5.64	5.65	5.66	5.67	5.69	5.70	5.71	5.72
2.0	5.33	5.34	5.35	5.37	5.38	5.39	5.40	5.41	5.43	5.44	5.45
3.0	5.07	5.08	5.09	5.10	5.12	5.13	5.14	5.15	5.16	5.18	5.19
4.0	4.82	4.83	4.84	4.85	4.86	4.87	4.89	4.90	4.91	4.92	4.93
5.0	4.57	4.58	4.60	4.61	4.62	4.63	4.64	4.65	4.66	4.67	4.68
6.0	4.34	4.35	4.36	4.37	4.38	4.39	4.40	4.41	4.42	4.43	4.44
7.0	4.11	4.12	4.13	4.14	4.15	4.16	4.17	4.18	4.19	4.20	4.21
8.0	3.88	3.89	3.90	3.91	3.92	3.93	3.94	3.96	3.97	3.98	3.99
9.0	3.67	3.68	3.69	3.70	3.71	3.72	3.73	3.74	3.75	3.76	3.77
10.0	3.46	3.47	3.48	3.48	3.49	3.50	3.51	3.52	3.53	3.54	3.55

[1] Formality of Cl_2 in final solution
[2] Formality of Na_2CO_3 in final solution

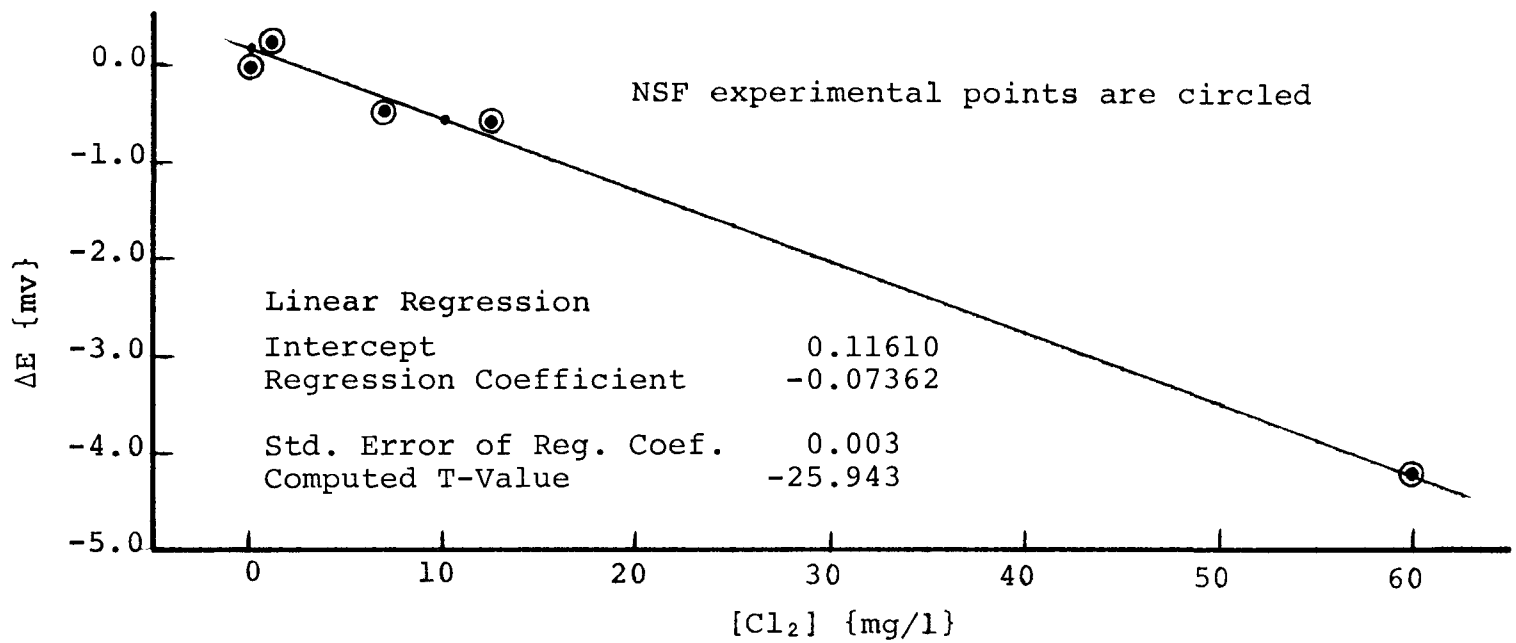

Figure 81. ΔE versus $[Cl_2]$ in alkalinity determination.

Table 24. EXPERIMENTAL AND THEORETICAL RELATIONSHIPS BETWEEN ALKALINITY AND POTENTIALS

Alkalinity (mg/l as $CaCO_3$)	Potentials (mv)	
	Experimental	Theoretical
24	-194.9	-193.1
36	-197.5	-194.4
48	-200.1	-195.7
60	-202.6	-197.1
72	-205.3	-198.4
84	-207.6	-199.8

Table 25. THEORETICAL RELATIONSHIP BETWEEN ALKALINITY AND POTENTIAL FOR SOLUTIONS WITH AND WITHOUT FREE RESIDUAL Cl_2

Alkalinity (mg/l as $CaCO_3$)	Potential (mv)		
	No Cl_2	0.7 mg/l	1.4 mg/l
24	-193.1	-193.0	-192.9
36	-194.4	-194.3	-194.2
48	-195.7	-195.6	-195.5
50	-197.1	-196.9	-196.8
72	-198.4	-198.3	-198.2
84	-199.8	-199.7	-199.5

Assuming that the NaOCl was made stoichiometrically according to the reaction:

$$2NaOH + Cl_2 \rightarrow 2Na^+ + Cl^- + OCl^- + H_2O \qquad (146)$$

i.e., there was no excess NaOH in the NaOCl, the net effect of substituting NaOCl for gaseous Cl_2 is a change in sign of the quantity representing Cl_2 in Equation 146; i.e., a cation (Na^+) is added in lieu of an anion (Cl^-). The predicted slope is approximately -0.18 mv per mg/l free Cl_2. This value is slightly larger than the experimental value obtained in the NSF laboratory (.07/.18), but it is 28 times smaller than the value obtained by EPA. (See Table 26.)

Table 26. CHANGES IN POTENTIAL FROM ADDITION OF 1.0 mg/l FREE RESIDUAL Cl_2

	Experimental		Theoretical
	NSF	EPA	
Slope =(as mv/mg/l)	-0.07	-5	-0.18

Despite the theoretical relationships which were established and closely related data acquired experimentally by NSF, anomalous results continued to occur with Cincinnati tap water monitoring. Although it does not seem likely that the observed effect can be attributed only to the presence of free chlorine residual, chlorine is very likely involved, perhaps synergistically with a complex organic material.

Additional experiments were undertaken to determine the effect of adding a reducing agent to the alkalinity system. Thiosulfate (five mg/l) added to the buffer solution did not interfere with potentiometric measurement of alkalinity and it eliminated the interference effect. (Data are shown in Table 27 and Figure 82.) As a result, it is now recommended as standard procedure that $S_2O_3^{2-}$ be added to pH 3.1 phthalate buffer solution used in all applications of the potentiometric alkalinity monitoring system.

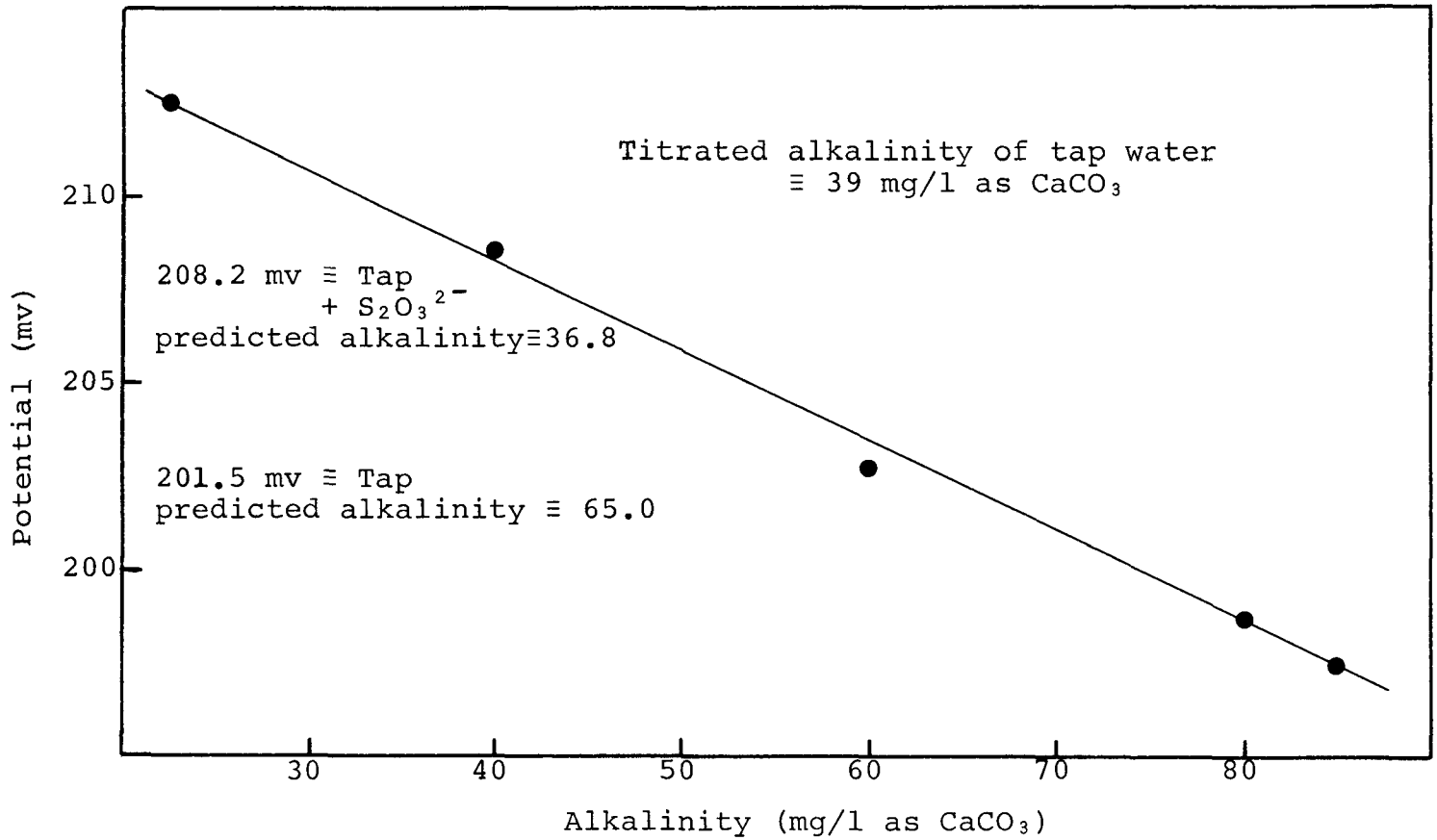

Figure 82. Potential versus alkalinity calibration series.

Table 27. EFFECT OF THIOSULFATE

Alkalinity (mg/l as C_aCO_3)	Potential (mv)			
	Sample	Sample + $S_2O_3^{2-}$	Sample + Cl_2 (1)	Sample +Cl_2 (1) + $S_2O_3^{2-}$(2)
20	212.2	212.6	–	–
40	208.0	208.0	206.0	208.5
60	202.2	–	–	–
80	198.0	–	–	–
Tap (39)	201.5	208.2	–	–

(1) $[Cl_2]$ = 0.94 mg/l

(2) $[S_2O_3^{2-}]$ = 5 mg/l

NOTE: Solutions prepared in deionized waters.

TECHNICAL REPORT DATA
(Please read Instructions on the reverse before completing)

1. REPORT NO. EPA-600/2-77-074	2.	3. RECIPIENT'S ACCESSION NO.
4. TITLE AND SUBTITLE WATER QUALITY MONITORING IN DISTRIBUTION SYSTEMS		5. REPORT DATE March 1977 (Issuing Date)
		6. PERFORMING ORGANIZATION CODE
7. AUTHOR(S) Nina I. McClelland K. H. Mancy		8. PERFORMING ORGANIZATION REPORT NO.
9. PERFORMING ORGANIZATION NAME AND ADDRESS National Sanitation Foundation Ann Arbor, Michigan 48106		10. PROGRAM ELEMENT NO. ICB047;ROAP 21AQB;TASK011
		11. CONTRACT/GRANT NO. 68-03-0043
12. SPONSORING AGENCY NAME AND ADDRESS Municipal Environmental Research Laboratory--Cin.,OH Office of Research and Development U.S. Environmental Protection Agency Cincinnati, Ohio 45268		13. TYPE OF REPORT AND PERIOD COVERED Final
		14. SPONSORING AGENCY CODE EPA/600/14

15. SUPPLEMENTARY NOTES

16. ABSTRACT

A mobile laboratory with 18 integrated, computer controlled parametric systems for monitoring potable water quality in distribution systems was developed and field evaluated at ten locations in four United States cities: Chicago, Illinois; Ann Arbor and Detroit, Michigan; and Philadelphia, Pennsylvania. Temperature, conductivity, pH, chloride, dissolved oxygen, free and total residual chlorine, turbidity, corrosion rate, free and total fluorides, alkalinity, hardness, nitrate, copper, cadmium, lead, and calcium carbonate deposition rate are measured using commercially available and newly developed sensor systems.

17. KEY WORDS AND DOCUMENT ANALYSIS

a. DESCRIPTORS	b. IDENTIFIERS/OPEN ENDED TERMS	c. COSATI Field/Group
Water quality Chemical analysis Monitors Data acquisition Distribution systems Potable Water		7 B 13 B

18. DISTRIBUTION STATEMENT RELEASE TO PUBLIC	19. SECURITY CLASS (This Report) UNCLASSIFIED	21. NO. OF PAGES 207
	20. SECURITY CLASS (This page) UNCLASSIFIED	22. PRICE

EPA Form 2220-1 (9-73)

☆U.S. GOVERNMENT PRINTING OFFICE 1977— 757-056/5576

U.S. ENVIRONMENTAL PROTECTION AGENCY
Office of Research and Development
Technical Information Staff
Cincinnati, Ohio 45268

OFFICIAL BUSINESS
PENALTY FOR PRIVATE USE, $300
AN EQUAL OPPORTUNITY EMPLOYER

POSTAGE AND FEES PAID
U S ENVIRONMENTAL PROTECTION AGENCY
EPA-335

Special Fourth-Class Rate
Book

[redacted]

[redacted]
REGION V USEPA
230 S DEARBORN
CHICAGO, IL 60604

[redacted]

MAY 1 1977

If your address is incorrect, please change on the above label; tear off; and return to the above address.
If you do not desire to continue receiving this technical report series, CHECK HERE ☐; tear off label, and return it to the above address.